

# Pumilio: A Novel Target for the Treatment of Epilepsy

A thesis submitted to The University of Manchester for the degree of Doctor of Philosophy in the Faculty of Biology, Medicine and Health.

2023

Fred P Mulroe

*School of Biological Sciences*

## Contents

Figures.....	4
Tables .....	7
Abbreviations.....	8
Abstract.....	9
Declaration and Copyright .....	10
Acknowledgements.....	11
1.0 Chapter 1- Introduction .....	12
1.2.1 Definitions of Seizure and Epilepsy .....	13
1.2 Causes of Epilepsy.....	14
1.2.2 Voltage Gated Sodium Channels ( $\text{Na}_v\text{s}$ ).....	14
1.2.3 $\text{K}^+$ Channels .....	15
1.2.4 Calcium Channels .....	17
1.2.5 Glutamatergic System.....	18
1.2.6 GABAergic System.....	20
1.2.7 Other Neurotransmitters .....	21
1.2.8 Environmental Factors .....	22
1.3 Current Anti-Epileptic Drugs .....	22
1.3.1 Sodium Channel Blockers.....	23
1.3.2 GABA Potentiators .....	24
1.3.3 Calcium Channels .....	25
1.3.4 Others.....	26
1.4 Models in epilepsy .....	27
1.4.1 Mammalian Models .....	28
1.4.2 <i>In Silico</i> and <i>in Vitro</i> Models of Epilepsy .....	30
1.4.3 Non Mammalian Organisms .....	31
1.4.4 <i>Drosophila</i> .....	32
1.5 Neuronal Homeostasis and Pumilio.....	36
1.5.1 Firing Rate Homeostasis.....	36
1.5.2 Function of Pumilio .....	38
1.5.3 Identification of Lead .....	41
1.6 Aims Of This Thesis .....	42
1.7 Bibliography .....	43
2.0 Chapter 2 – Identifying New Lead Compounds .....	61

2.1 Introduction- Identifying Lead Compounds.....	61
2.1.1 Avobenzone Breakdown Products.....	61
2.1.2 Considerations in Drug Design.....	63
2.2 Results.....	65
2.2.1 Design of Generation 1 Compounds.....	65
2.2.2 Synthesis of Generation 1 Compounds.....	71
2.2.3 Screening of Generation 1 Compounds.....	81
2.2.4 Design of Generation 2 Compounds.....	85
2.2.5 Synthesis of generation 2 compounds.....	89
2.2.6 Screening of Generation 2 Compounds.....	96
2.2.7 Establishment of Lead Compounds .....	99
2.2.8 Screening of Lead Analogues .....	103
2.3 Discussion.....	106
2.4 Materials and Methods.....	112
2.4.1 Chemistry .....	112
2.4.2 Fly Stocks.....	120
2.4.3 Larval Seizure Electroshock Assay.....	120
2.5 Bibliography .....	121
3.0 Chapter 3- Biological Characterisation of Lead Compounds .....	127
3.1 Introduction .....	127
3.2 Results.....	130
3.2.1 Mechanism of Action Studies .....	135
3.2.2 Rodent Seizure Models .....	145
3.3 Discussion.....	148
3.4 Experimental/Methods.....	151
3.4.1 Fly Stocks.....	151
3.4.2 L3 Seizure Electroshock Assay.....	151
3.4.3 Western Blot .....	152
3.4.4 PTZ Seizure-Induction .....	153
3.4.5 6 Hz Seizure-Induction .....	153
3.5 Bibliography .....	154
4.0 Chapter 4- Discussion.....	158
4.1 Bibliography .....	162

Word Count: 54964

## Figures

Figure 1.1- A) Structure of L-glutamate B) Structure of GABA.....	18
Figure 1.2 - Synthesis of GABA.....	20
Figure 1.3- Structures of phenytoin, carbamazepine and lamotrigine.....	23
Figure 1.4 - Structures of muscimol and guvacine.....	24
Figure 1.5- General structures of barbiturates and benzodiazepines.....	25
Figure 1.6- Structures of $\alpha 2\delta$ subunit calcium channel blockers pregablin and gabapentin.....	25
Figure 1.7- Structure of valproate .....	27
Figure 1.8 - The structures of 5-HT agonists clemizole (left) and lorcaserin.....	31
Figure 1.9 – Graphical representation of neuronal homeostasis.....	36
Figure 1.10- Crystal structure of the Pumilio-homology domain.....	39
Figure 1.11- Structure of original hit avobenzene.....	41
Figure 2.1- Structures of 2 potential leads 4TBB-ald (RAB102) and 4TBB-acid (RAB103).....	52
Figure 2.2- Difference in metabolism between ketone and aldehyde.....	60
Figure 2.3- Data from L3 seizure assay of initial leads.....	60
Figure 2.4- The 3 parts of the lead compound varied in drug screen 1.....	63
Figure 2.5- Ionisation of tetrazole.....	65
Figure 2.6 - H abstraction mechanism of CYP450 with primary alkanes.....	68
Figure 2.7 - Conditions used for synthesis of the tetrazole analogue RAB107.....	69
Figure 2.8- Mechanism of tetrazole formation.....	70
Figure 2.9- Synthetic route to amino acid analogue RAB106.....	70
Figure 2.10- Resonance stabilised forms of carbonyls and 1,3-dicarbonyls.....	70
Figure 2.11- Conditions for ester hydrolysis.....	71
Figure 2.12- Region of $^1\text{H}$ NMR spectra showing the 1:4 ratio of ester hydrolysis products.....	71
Figure 2.13- Initial conditions tried for the decarboxylation in RAB106 synthesis.....	71
Figure 2.14 - Conditions of successful decarboxylation and formation of product RAB106.....	72
Figure 2.15 - Conditions used for the synthesis of RAB114.....	72
Figure 2.16 - Synthetic route to the formation of RAB 114.....	73
Figure 2.17 - Mechanism for the reduction of double bonds with formic acid.....	73
Figure 2.18 - Reaction scheme for the synthesis of RAB116.....	73

Figure 2.19 - Attempted synthesis of RAB 128.....	74
Figure 2.20 - Mechanism for decarboxylation of $\beta$ -ketoacids.....	74
Figure 2.21 - Initial planned synthetic route of RAB124.....	75
Figure 2.22 - Mechanism of DMF catalysed acid chloride formation.....	76
Figure 2.23 - Attempted Synthesis of RAB122 intermediate.....	77
Figure 2.24 - Synthetic route for RAB 136.....	77
Figure 2.25 - Synthesis of RAB137.....	78
Figure 2.26 - Resonance canonical forms of the amide bond.....	79
Figure 2.27 - Mechanism of ester hydrolysis using $\text{AlCl}_3$ and DMA.....	79
Figure 2.28 – Ranking of generation 1 compounds based on the reduction of recovery time.....	80
Figure 2.29 – Structure of active generation 1 compounds.....	81
Figure 2.30 - Reaction scheme for the synthesis of RAB216.....	87
Figure 2.31- Possible routes for the mechanism of Ullmann couplings.....	88
Figure 2.32- Catalytic cycle of copper in the Hurtley reaction.....	88
Figure 2.33 - Mechanism of the Knorr pyrazole synthesis.....	89
Figure 2.34 - Scheme for the synthesis of RAB212.....	89
Figure 2.35 - Synthesis of RAB211.....	90
Figure 2.36 - Mechanism of the Suzuki coupling used to make RAB212.....	91
Figure 2.37 - Mechanism for a thermal Boc deprotection.....	92
Figure 2.38 – $^1\text{H}$ NMR spectrum of RAB 211.....	93
Figure 2.39 - Initial L3 seizure assay screen of generation 2 RAB compounds.....	94
Figure 2.40 - Structure of generation 1 compound RAB109.....	94
Figure 2.41 - Second L3 seizure assay screen of active RAB compounds (0.4 mM).....	97
Figure 2.42- 3D structures of various RAB compounds, indicating twist in RAB216.....	98
Figure 2.43 – L3 seizure assay of compounds found to be active in 0.4 Mm screen (0.1 Mm).....	99
Figure 2.44 – Structures of 2 analogues based on the structure of lead compound RAB216.....	100
Figure 2.45 - Relative charge densities of pyrazole and isoxazole.....	100
Figure 2.46 - L3 seizure assay of RAB 216 analogues RAB218 and RAB219.....	101
Figure 2.47 - Potential scheme of avobenzene photolysis leading to the formation of RAB103.....	105
Figure 2.48 - Properties of all compounds screened compared to CNS acting drugs.....	105
Figure 2.49 - Structures of 4-phenylbutyrate, ketoprofen and benzoic acid.....	108

Figure 3.1 - L3 seizure assay of RAB216 and valproate in different seizure mutants.....	127
Figure 3.2 – L3 seizure assay of ATP6VOC RNAi line.....	129
Figure 3.3 – L3 seizure assay of ATP6VOC RNAi line with AEDs.....	130
Figure 3.4 - Graphical representation of the construct used for the luciferase reporter assay.....	131
Figure 3.5 - Western blot analysis of the changes to Pum1 and Pum2 levels in mouse brains.....	132
Figure 3.6- Luciferase reporter assay investigating changes in transcription of pum in <i>Drosophila</i> ..	132
Figure 3.7 - L3 seizure assay of wild type CS flies with and without PTX.....	133
Figure 3.8 - Luciferase reporter assay, changes in dpumC expression with RAB102/216 and PTX....	134
Figure 3.9- L3 seizure assay of RAB216/102 and phenytoin in bss seizure mutants with pum RNAi.	136
Figure 3.10- L3 seizure assay of RAB102 and RAB216 in bss mutants overexpressing pum.....	137
Figure 3.11 - L3 seizure assay of RAB216/102 in seizure mutants ± overexpression of pum.....	138
Figure 3.12 - Western blot quantification of PUM1/2 mouse brain samples post-drug treatments.	140
Figure 3.13 – Data from the PTZ mouse seizure assay.....	142
Figure 3.14 -The effect of RAB216 on seizure duration as measured by the 6 Hz seizure model.....	143
Figure 4.1- Progression of lead compounds across the project.....	154

## Tables

Table 1.1- Different types of seizure and their description.....	13
Table 1.2 - Bang sensitive mutants identified in Drosophila.....	32
Table 2.1- Physiochemical properties in CNS drugs, non-CNS drugs and current lead compounds.....	62
Table 2.2- List of analogues with variation in acid/polar group.....	64
Table 2.3- List of analogues with variation in the lipophilic group para to the acid/aldehyde group..	66
Table 2.4- List of analogues with variation in aromatic ring.....	68
Table 2.5 - Structures and selected properties of active Gen 1 compounds.....	81
Table 2.6 - Structure and physical properties for the second generation of compounds.....	83
Table 2.7- Structure and selected properties of active compounds from the generation 2 screen.....	95
Table 2.8 - Comparison of the properties of RAB216 with CNS and non-CNS drugs.....	106

## Abbreviations

4TBBA	4-tert-butyl-benzoic acid
4TBB-ald	4-tert-butyl-benzaldehyde
5-HT	Serotonin (5-hydroxytryptamine)
ADMET	Adsorption, distribution, metabolism, excretion and toxicity
AEDs	Anti-epileptic drugs
AMPArs	A-amino-3-hydroxy-5-methyl-4-isoxazolepropionic acid receptors
BBB	Blood brain barrier
BDNF	Brain-derived neurotrophic factor
BFNIS	Benign familial neonatal infantile seizures
Boc	Tert-butyloxycarbonyl
bs	Bangsensitive
bss	Bangsenseless
Ca <sub>v</sub> s	Voltage gated calcium channels
D2R	Dopamine receptor
eas	Easily-shocked
ES	Electroshock
GABA	Γ-Aminobutyric acid
GAD	Glutamic acid decarboxylase
GDNF	Glial cell-derived neurotrophic factor
GFS	Giant fibre system
GPCRs	G-protein coupled receptors
H-bond	Hydrogen bond
iGluRs	Ionotropic glutamate receptors
iPSCs	Induced pluripotent stem cells
KARs	Kainic acid receptors
K <sub>v</sub> s	Voltage gated potassium channels
L3	Third instar larvae
LCMS	Liquid chromatography–mass spectrometry
LTD	Long term depression
LTP	Long term potentiation
MCT	Monocarboxylate transporters
Na <sub>v</sub> s	Voltage gated sodium channels
NMDARs	N-methyl-D-aspartate receptors
NRE	Nanos response element
para	Paralytic
PSA	Polar surface area
PTX	Picrotoxin
PTZ	Pentylentetrazol
Pum	Pumilio
RT	Recovery time
SAR	Structure activity relationship
TFA	Trifluoroacetic acid
TTX	Tetrodotoxin
UAS	Upstream activation system
V-ATPase	Vacuolar atpase
VPA	Valproate

## Abstract

Epilepsy is a condition characterised by recurrent seizures. The underlying mechanism of epileptic seizures is excessive and abnormal neuronal activity. Therefore, manipulating firing-rate neuronal homeostasis, mechanisms by which neurons regulate their intrinsic excitability, potentially offers an attractive opportunity to control seizures. Approximately one in three epilepsy cases cannot be controlled with the current option of medication. In order to reduce this number, the discovery of new druggable targets is required. In this project, a combination of both *Drosophila* and mouse models were used to evaluate the efficacy of a new class of compounds, based on the structure of 4-*tert*-butylbenzaldehyde. A drug library was created through a combination of purchases and organic synthesis techniques. Screening was performed using *Drosophila* larvae carrying the *para*<sup>bss</sup> mutation, a gain of function mutation in the voltage gated sodium channel of that causes seizure like behaviour. Results from the initial screen showed that the core benzoic acid structure was key to activity. These results were fed in to the design of a 2<sup>nd</sup> generation of compounds, which resulted in the discovery of a more potent analogue 4-(3,5-dimethyl-1H-pyrazol-4-yl)benzoic acid, which was referred to as RAB216 in the library. This compound was tested in various *Drosophila* seizure mutants and was found to be effective at reducing seizure recovery times in all those that were tested. In the initial 2 mM screen it reduced recovery times by over 50% and was found to be at least 4x more potent than any other analogue. RAB216 was then taken forward to mouse models, where it was tested in both the PTZ and 6 Hz psychomotor models of seizure. In both models, the compound was found to be efficacious at reducing the severity or time of onset of seizures. Additionally, western blot analysis of mouse brains treated with RAB216, found the levels of the homeostatic regulator, Pum2 were significantly increased by 70%. This study provides proof of principle that targeting neuronal homeostasis is a viable anticonvulsant strategy and identifies a lead compound, which could possibly act as a starting point for future development.

## Declaration and Copyright

No portion of the work referred to in the thesis has been submitted in support of an application for another degree or qualification of this or any other university or other institute of learning.

- i. The author of this thesis (including any appendices and/or schedules to this thesis) owns certain copyright or related rights in it (the "Copyright") and they have given the University of Manchester certain rights to use such Copyright, including for administrative purposes.
- ii. Copies of this thesis, either in full or in extracts and whether in hard or electronic copy, may be made only in accordance with the Copyright, Designs and Patents Act 1988 (as amended) and regulations issued under it or, where appropriate, in accordance with licensing agreements which the University has from time to time. This page must form part of any such copies made.

The ownership of certain Copyright, patents, designs, trademarks and other intellectual property (the "Intellectual Property") and any reproductions of copyright works in the thesis, for example graphs and tables ("Reproductions"), which may be described in this thesis, may not be owned by the author and may be owned by third parties. Such Intellectual Property and Reproductions cannot and must not be made available for use without the prior written permission of the owner(s) of the relevant Intellectual Property and/or Reproductions.

iv. Further information on the conditions under which disclosure, publication and commercialisation of this thesis, the Copyright and any Intellectual Property and/or Reproductions described in it may take place is available in the University IP Policy (see <http://documents.manchester.ac.uk/DocuInfo.aspx?DocID=24420>), in any relevant Thesis restriction declarations deposited in the University Library, the University Library's regulations (see <http://www.library.manchester.ac.uk/about/regulations/>) and in the University's policy on Presentation of Theses.

## Acknowledgements

Foremost, I would like to thank Prof Richard Baines and Dr Sally Freeman for their expert supervision throughout the project. The knowledge, advice, support, and patience they have provided me has been invaluable and I count myself lucky to have had them as my PhD supervisors.

I would also like to thank everyone who directly contributed to the work in this thesis. Namely, Prof Stuart Allan and Dr Graham Coutts for their work on the PTZ mouse seizure model; Dr Najat Aourz and Prof Ilse Smolders for the 6 Hz seizure model data; Dr Carol Fan, Aoibhinn Kelly, Iona Hayes, Thomas Humphreys and Ceri Hughes for their contributions to the L3 seizure assays.

Thank you to all those involved in running and upkeep of the University of Manchester fly facility, in particular Sanjai Patel for keeping the facility running and providing great chat to make the time flipping flies fly by. Additionally, I would like to thank all other university staff that have supported me, in particular Alison Cox for her patience and support in helping to get me over the line.

I would like to thank every member of the Baines and Freeman labs I have worked with over these past years. Anna Munro, Jurga Mituzaitė, Adam Bradlaugh, Alex Dyson, Fiona He, Bramwell Coulson, Iain Hunter, Sarah Ryan, James Beswick, Rachael Magwaza, Lina Elsharkawy and Manikandan Kadirvel for the laughs and making such an enjoyable environment to work in. I would like to send the same thanks to Dr Carol Fan (again) and Dr Carlo Giachello for their help and wisdom that it made it possible for a chemist to do so much biology work.

A big thanks to all of the other friends who have helped me through some very difficult times over the last few years. Without the support and good times to keep me sane none of this would have been possible.

Lastly, I would like to give a special thanks to my partner Lauren for putting up with me at my lowest points and always being there. I have no idea how I would ever have got through any of the last few years without the patience, laughter and care she has given.

## 1.0 Chapter 1- Introduction

Epilepsy is a common brain condition characterised by spontaneous and reoccurring seizures (Fisher et al. 2017). Approximately 1 in 20 people will have a seizure in their lifetime and around 3 in 100 will develop an epilepsy-related disorder (Ngugi et al. 2010). For the brain to enter an epileptic state, the brain undergoes irreversible change known as epileptogenesis, after which patients experience recurrent seizures (McNamara, Huang, and Leonard 2006). This can include changes in gene expression, neural network connectivity and/or alterations in synaptic transmission.

Approximately a third of epilepsy patients are drug resistant and drugs released within the last 20 years have done little to reduce this number (Kwan, Schachter, and Brodie 2011). This may be because many of the drugs developed act on the same/similar targets as older drugs: these targets include voltage gated sodium channels ( $Na_v$ s) and the GABAergic system. It seems likely that to reduce the number of pharmaco-resistant cases, compounds with novel mechanisms of actions are required (Patel, Wilcox, and Metcalf 2017).

In order to discover novel anti-epileptic drugs (AEDs) animal models are required for both identifying targets and screening compounds. There are a variety of epilepsy and seizure models currently in use, each of which has its specific advantages and disadvantages. One of these model organisms, the fruit fly *Drosophila melanogaster*, was used recently by the Baines group to screen for genes whose transcription is affected by seizures. This screen and corresponding work thereafter identified *pumilio* (gene), Pumilio (protein) to be upregulated during seizure. Additionally, this transgenic upregulation has been shown to be anticonvulsant (Lin, Giachello, and Baines 2017b). Screening approved drugs/chemicals identified that the sunscreen blocker avobenzone is seemingly able to increase *pum* expression and also, when ingested by *Drosophila*, to reduce recovery time in *Drosophila* seizure mutants. This project therefore has the overarching aim to use the principles of drug design in order to develop a potential drug or chemical tool that boosts Pum activity and that is anticonvulsant.

### 1.2.1 Definitions of Seizure and Epilepsy

For a disorder to be classed as epilepsy it must show three essential elements:

- History of at least one seizure (preferable multiple seizures)
- Enduring alteration in the brain meaning likelihood of future seizures is increased (epileptogenesis)
- Associated neurobiological, cognitive, social and/or psychological disturbances.

Seizures are caused by neurons firing in an excessive synchronous and abnormal manner (Fisher et al. 2005). This results in symptoms that vary depending on the type of seizure and the part of the brain in which the seizure originates. Symptoms of the various types of seizure are described in Table 1.1 (Fisher et al. 2017). In patients with epilepsy these seizures are recurrent due to various changes within the brain which ultimately cause an imbalance between excitation and inhibition.

*Table 1.1- Different types of seizure and their description.*

Type of seizure	Description
<b>Simple focal (partial) seizures</b>	Seizure starts in, and affects one part of the brain.
<b>Complex focal seizures</b>	Seizure starts in, and affects one part of the brain and awareness is impaired.
<b>Generalised seizure</b>	Seizure effects the whole brain.
<b>Absence seizure</b>	Form of generalised seizure where the patient is unconscious for a short amount of time.
<b>Tonic seizure</b>	Form of generalised seizure where muscles suddenly become stiff.
<b>Atonic seizure</b>	Form of generalised seizure where muscles suddenly become limp.
<b>Myoclonic seizure</b>	Form of generalised seizure involving muscle jerking.
<b>Tonic-clonic (convulsive) seizure</b>	Form of generalised seizure where the muscles first stiffen and then relax and tighten repeatedly.
<b>Clonic seizure</b>	Form of generalised seizure similar to tonic-clonic but the body does not stiffen to begin with.

There are over 500 gene loci associated with epilepsy. As well as these, causes of epilepsy can include brain trauma, infection, and stroke (Moshé et al. 2015). This, plus the fact that in 60% of cases the causes are unknown, makes epilepsy a difficult condition to treat. Only 1-2% of cases are caused by single genetic defects. In most cases the cause is due to polygenic and environmental factors. For example, a study found that in monozygotic twins if one has epilepsy there is a 50% chance the other will be affected, compared to 15% for dizygotic twins (Pandolfo 2011).

The underlying neurophysiology of seizures involves either excessive excitation, or insufficient inhibition. These issues can be present at the single cell level or all the way up to large networks of neurons (Scharfman, 2007).

## 1.2 Causes of Epilepsy

### 1.2.2 Voltage Gated Sodium Channels ( $Na_v$ s)

Signalling in the nervous system relies on a finely tuned electrical balance between excitation and inhibition (E:I balance). Disruptions to the mechanisms that maintain this balance have been linked to epilepsy. Genetic studies of patients with epilepsy have identified a large array of mutations, most of which were found in genes that code for ion channels (EPi4K Consortium, 2013).

$Na_v$ s are responsible for the generation and propagation of action potentials and are involved in many types of epilepsy.  $Na_v$ s are membrane proteins that change conformation, allowing an increase in membrane permeability to sodium. Sodium diffuses down its electrochemical gradient causing depolarisation and the upstroke of the action potential (Fouda and Ruben 2020). The human genome contains 10  $Na_v$   $\alpha$ -subunits (pore-forming). Each isoform, encoded by a different gene, has unique properties and any changes to the function or expression of these channels has the potential to have a large effect on the balance between excitation and inhibition (Wengert and Patel 2021).

Of the sodium channel genes *SCN1A*, which codes for  $Na_v1.1$ , has the most known variants linked to epilepsy (Schutte et al. 2016). Mutations of *SCN1A* that lead to loss of function are known to cause an extreme form of epilepsy known as Dravet syndrome (Dravet, 2011). Mutations that only impair the function of  $Na_v1.1$  often cause generalised epilepsy with febrile seizures. It is thought that this is due to reduced sodium current ( $I_{Na}$ ) in GABAergic interneurons, lowering inhibition which varies depending on the severity of the mutation (Cheah et al. 2012). Sodium channel blockers cannot be prescribed for Dravet syndrome as they further reduce this current, further reducing inhibition.

*SCN2A*, which encodes the  $\alpha$ -subunit of  $Na_v1.2$ , was typically linked to benign familial neonatal infantile seizures (BFNIS) but recent evidence has linked the gene to more debilitating forms of

epilepsy. BFNIS is a rare form of childhood epilepsy which is self-limiting and relatively mild, with cases usually remitting by the age of 12 months (Berkovic et al. 2004). This is due to the fact that Nav1.2 channels are expressed as two different splice forms, adult and neonatal (Thompson et al. 2020). The neonatal form is less excitable meaning a more excitable mutant channel can lead to seizures, whereas the effect in adults is negligible. More recent studies have linked *SCN2A* to developmental and epileptic encephalopathies, whereby seizures begin in childhood and are associated with poor developmental outcomes and comorbidities including autism spectral disorder, microcephaly, cerebral and/or cerebellar atrophy, and cortical visual impairment (Wolff et al. 2017; Sanders et al. 2018).

Mutations in the gene *SCN8A* (Nav1.6) were originally linked to motoneuron dysfunction and ataxia, due to evidence from rodent models with hypomorphic or null alleles (Estacion et al. 2014). However, since the first Nav1.6 epilepsy causing mutation was identified in 2012 there has been a significant number of pathogenic *SCN8A* variants identified in epilepsy patients (Kaplan, Isom, and Petrou 2016). This channel is known to have a role in maintaining the persistent sodium current, setting the action potential threshold for a given neuron and facilitating repetitive firing (Y. Chen et al. 2008). Therefore, mutations that result in a gain-of-function for Nav1.6 increase the likelihood of uncontrolled action potential firing. However, another study, in a single patient, showed that a loss-of-function mutation in *SCN8A* can also be causative of epilepsy (De Kovel et al., 2014). Additionally, the channel has also been linked to absence seizures. A mutagenesis rodent study in which mice with an *SCN8A* mutation, showed a clear spontaneous absence seizure phenotype with distinct spike-wave discharges (Papale et al., 2009). Recently, a novel pathogenic mutation was discovered in *SCN8A* that contributes to an epileptic phenotype, despite being outside of the gene and promoter regions or translational or transcriptional sites (Johannesen et al. 2019). The severity of seizure varied with the strain of mouse, additionally highlighting how the genetic causes of many epilepsies can be due to a number of combined factors rather than single gene mutations.

### 1.2.3 K<sup>+</sup> Channels

Voltage gated potassium channels (K<sub>v</sub>s) regulate the efflux of K<sup>+</sup> from a cell contributing to membrane repolarisation/ hyperpolarisation and limit neuronal excitability. K<sub>v</sub>s are also involved in molecular and cell signalling pathways as well as modulation of neurotransmitter release (Shah and Aizenman 2014). The *KCNA1* gene encodes for the K<sub>v</sub>1.1 subunit, which like other K1-family subunits, plays an important role in the initiation and regulation of action potential firing. Heterozygous

mutations of this gene have typically been related to episodic ataxia (Browne et al. 1994). Interestingly, patients exhibited epileptic seizures suggesting  $K_v1.1$  may contribute to an epileptic phenotype (Browne et al. 1994; Eunson et al. 2000). Loss-of-function in *KCNA1* results in reduced current amplitude and an increase in the chance of seizures (Imbrici et al. 2006). This evidence is supported by knock-out mouse models which show loss of  $K_v1.1$  leads to epileptic behaviour (Smart et al. 1998).

$K_v4$  channels are predominantly expressed in the brain and are mainly involved in the regulation of action potential back-propagation and certain forms of synaptic plasticity (Birnbaum et al. 2004). The first  $K_v4$  channel associated with epilepsy was  $K_v4.2$ , encoded by *KCND2*. A patient with temporal lobe epilepsy was found to possess a mutation in this gene causing a frame shift, leading to a premature termination codon and ultimately  $K_v4.2$  channel haploinsufficiency (B. Singh et al. 2006). More recently, a *de novo* mutation to the *KCND3* has been discovered (Smets et al. 2015) which was found to cause a severe channel dysfunction, leading to a range of conditions including epilepsy. The symptoms were likely to be due to a strong depolarising shift in the voltage of both the activation and deactivation of the channel.

The genes *KCNQ2* and *KCNQ3* encode the  $K_v7.2$  and  $K_v7.3$  proteins respectively. Between them, these proteins form the M channel, which has a critical role in controlling neuronal excitability through raising the threshold for firing an action potential (Passmore et al. 2012). Mutation in *KCNQ2* and *KCNQ3* genes are known to cause benign neonatal familial convulsions (Cooper et al. 2000). The M channel has been targeted in the past by the anticonvulsant retigabine, but this was discontinued due to side effects involving changes in retinal pigmentation and discolouring of the skin (Groseclose and Castellino 2019).

Voltage gated potassium channels  $K_{Na}$ , contribute to slow afterhyperpolarisation that follows the action potential in several neuronal population of the brain (Budelli et al. 2009). They are activated by increased cytoplasmic  $Na^+$  concentration. Mutations in the gene *KCNT1*, which codes for the subunit  $K_{Na}1.1$ , has been linked to several different epileptic disorders, but has a particularly strong link to malignant migrating focal seizures of infancy (MMFSI) (Lim et al. 2016). This condition is characterised by onset before 6 months of age, migrating focal seizures and developmental delay (Coppola et al. 1995). More recently, another  $K_{Na}$  subunit  $K_{Na}1.2$  have also been shown to cause MMFSI, with both gain of function and loss of function mutation reported (Gong et al. 2021).

#### 1.2.4 Calcium Channels

Upon depolarisation, voltage gated calcium channels ( $\text{Ca}_v\text{s}$ ) open to allow an influx of calcium into the cell, which regulates calcium sensitive signalling pathways (Zamponi et al. 2015). Even small alterations in channel properties or expression can cause significant changes to the brain due to the wide range of calcium effects. This includes processes such as neurotransmitter release, gene expression and enzyme activity, all of which may contribute to the development of seizures and epilepsy (Flavell and Greenberg 2008). Additionally, calcium influx can also open other channels such as  $\text{Ca}^{2+}$ -activated K channels, which play a key role in neuronal excitability and neurotransmitter release (Kshatri, Gonzalez-Hernandez, and Giraldez 2018).

T-type calcium channels require smaller depolarisation than sodium and potassium channels in order to activate. Gain-of-function mutations or increased expression of these channels can lead to a low threshold spike (Cain, Hildebrand, and Snutch 2014). This can depolarise the membrane, causing sodium and potassium channels to open and initiate high frequency action potential firing, known as a 'burst', often seen on an EEG recording from epilepsy patients (Blumenfeld 2005). Animal models of temporal lobe epilepsy have shown that the T-type channel subunit  $\text{Ca}_v3.2$  is upregulated following a seizure, but it is unknown whether increased expression causes neuronal damage or if damage increases expression (Becker et al. 2008).

*CACNA1A* encodes for both Q-type and P-type channels through different splicing mechanisms (Bourinet et al. 1999). These channels are expressed presynaptically and are involved in neurotransmission and therefore have influence over neuronal excitability (R. M. Evans and Zamponi 2006). Mutations to this gene have been identified in patients inflicted with severe neurological disorders. Loss-of-function mutations, in particular, have been shown to cause epilepsy and ataxia due to reduced current density in cerebellar granule cells and an alteration to glutamate release in cortical cells (Ayata et al. 1999).

Many of the causes mentioned related to ion channels are caused by a single mutation in a single ion channel. However, it is now clear that a large majority of cases are due to the combined effect of multiple factors. This was highlighted in a study performed by Klassen and colleagues (Klassen et al. 2011) who sequenced 237 ion channel genes in patients with epilepsy vs. a control group. The study found thousands of single nucleotide polymorphisms equally spread between both groups. Interestingly when the comparison was limited to just genes associated with epilepsy, a significant number of missense genes were also found in the control. These results suggest that many types of epilepsy are due to the accumulation of specific ion channel mutations that affect the homeostasis

of excitability within the brain. Excitability is not only affected by ion channels, but also by the release of neurotransmitters: glutamate and GABA being the most relevant for this thesis.

### 1.2.5 Glutamatergic System

Synaptic transmission plays a key role in maintaining the excitatory balance of neuronal networks and has therefore been researched extensively with respect to epilepsy. As  $\gamma$ -aminobutyric acid (GABA) and glutamate (Figure 1.1) are the major inhibitory and excitatory neurotransmitters in the CNS, respectively, they have most commonly been linked with epilepsy. Glutamate concentration has been found to be increased in the cerebrospinal fluid (CSF) of epilepsy patients, whereas the concentration of GABA is unaffected (Stover et al. 1997). Additionally, it has also been shown that glutamate levels are elevated in the CSF prior to seizure events (During and Spencer 1993). Recent advancements in imaging have also allowed the localised concentration of glutamate within the brain to be studied. One study by Davis and colleagues (Davis et al. 2015), found that glutamate concentration is elevated in the hippocampus ipsilateral to the seizure onset site. Furthermore, a study of glioma patients found that increased glutamate concentration is associated with seizures and drug resistant epilepsy (Neal et al. 2019). Although the underlying mechanisms vary, evidence suggests that an increase in glutamate concentration is common amongst different epilepsies.

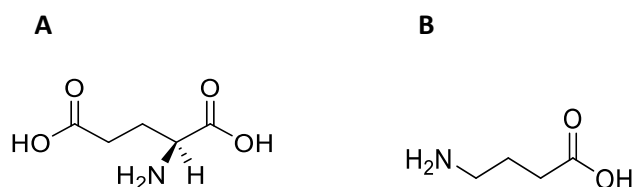


**Figure 1.1- A) Structure of L-glutamate, the principal excitatory neurotransmitter in the mammalian CNS B) Structure of GABA, the main inhibitory neurotransmitter in the CNS. Increased concentrations of glutamate and/or decreased concentration of GABA are associated with epilepsy, due to an excitation-inhibition imbalance.**

Ionotropic glutamate receptors (iGluRs) are ligand gated ion channels that bind glutamate. There are three subtypes:  $\alpha$ -amino-3-hydroxy-5-methyl-4-isoxazolepropionic acid receptors (AMPA), N-methyl-D-aspartate receptors (NMDARs) and kainic acid receptors (KARs), all named after ligands they bind (Collingridge et al. 2009). All have different functions but all mediate excitatory synaptic transmission and are key players in synaptic plasticity.

AMPA receptors are the most abundant iGluRs in the mammalian brain and mediate the majority of the synaptic response to glutamate. When AMPARs are repeatedly activated it causes long term potentiation, whereby changes in NMDA  $\text{Ca}^{2+}$  permeability leads to a cascade that results in the

increased trafficking of AMPARs to the synapse, strengthening synaptic signalling (Collingridge, Isaac, and Wang 2004). AMPARs play a more central role than NMDA receptors in excitatory synaptic transmission and seem more effective targets in preventing the spread of seizures (Rogawski 2011). In 2012 the drug perampanel was released, which is a negative allosteric modulator of AMPARs. This reduces the activity of the receptor by binding away from the active site and decreases the amount of glutamate that can bind to these receptors, reducing overall excitation (Krauss et al. 2013).

It is also believed that AMPARs play a leading role in synchronised firing, one of the hallmarks of epilepsy. Soon after the discovery of selective non-NMDA glutamate receptor antagonists, experiments showed that these compounds were more effective in reducing epileptiform activity *in vitro*, when compared to selective NMDA blockers (Neuman, Cherubini, and Ben-Ari 1988). Additionally, computer models have suggested that blockage of AMPARs prevents synchronous firing, whereas NMDA blockage only shortened bursts (Ekeberg et al. 1991). Mutations in AMPARs are heavily linked to autism and cognitive impairment, but evidence linking them to epilepsy is more limited (Hanada 2020).

KARs can be expressed both postsynaptically, where they mediate slow excitatory post synaptic currents, and presynaptically, where they facilitate or inhibit neurotransmitter release (Vignes and Collingridge 1997). The ligand after which the receptors are named is a known convulsant and is still used in animal models of temporal lobe epilepsy. This effect is at least partially due to kainite binding to KARs although it does also have an affinity for AMPARs. Although there is currently no drug on the market that specifically targets KARs, they are seen as a promising anti-epileptic strategy because it has been shown that blocking these receptors reduces chronic seizures without affecting AMPAR transmission (Pinheiro and Mulle 2006). A rodent study by Epsztein and colleagues (Epsztein et al. 2005) found the mossy fibres that sprout in the epileptogenesis process establish kainite receptor operated synapses on granule cells. They could then deduce that KARs contribute to the enhanced synchronised network seen in the dentate gyrus of the rats.

Of the iGluRs, NMDARs have been historically most linked to CNS diseases, including epilepsy (Newcomer, Farber, and Olney 2000). These receptors are found on most CNS neurons and are responsible for  $\text{Ca}^{2+}$  influx upon binding of glutamate and glycine. Meldrum discovered that NMDA antagonists protect against seizure induced by excitotoxic cell death (Meldrum 1993). Cell death occurs as excessive binding of glutamate to NMDARs allows toxic amounts of  $\text{Ca}^{2+}$  into a cell. This generates reactive oxygen species, uncouples oxidative phosphorylation in mitochondria causing oxidative stress, and activates various enzymes, all of which negatively affect cell function and lead to cell death (De Keyser, Sulter, and Luiten 1999). The damage can then lead to the activation of

hundreds of genes that cause a change in brain structure through the sprouting of granule cell axons, known as mossy fibres (Represa and Ben-Ari 1997). Glutamate is the neurotransmitter of the synapses in these axons, so it is likely that sprouting results in excessive excitation (T. Sutula et al. 1996). This is an example of how an imbalance of neurotransmitters at the molecular level can lead to changes in neuronal networks. Despite their role in epilepsy, NMDARs are a poor drug target, as antagonists often have hallucinogenic properties (Rogawski 1993).

In more recent years, evidence has suggested that anti-NMDAR encephalitis may also contribute to the excitation-inhibition balance (Dalmau and Graus 2018). Anti-NMDAR encephalitis refers to inflammation of the brain caused by an autoimmune response to NMDARs. Anti-NMDAR receptor antibodies cause surface NMDA receptors to be internalised, resulting in reduced receptor density at the cell surface (Moscatto et al. 2014). There is evidence to suggest that NMDA antagonists can exacerbate seizures (Sveinbjornsdottir et al. 1993). However, due to the involvement of NMDARs in epileptogenesis and excitatory synaptic transmission, it is counter-intuitive to think that a lower density of these receptors could contribute to increased excitability. GABAergic interneurons utilise NMDARs for neuronal excitation and therefore, if the density of NMDARs is lowered, GABAergic transmission may well be affected leading to reduced inhibition. This is an example of the complexity involved in the excitation-inhibition balance. This paradox with NMDARs is similar to the one highlighted with sodium channel blockers and Dravet syndrome. Targeting one class of receptor may lower excitation, but if excitation is lowered in inhibitory pathways, then overall network becomes more excitable. Due to the high number of different genes that contribute to the epileptic phenotype, a drug target that works for one patient may not only be ineffectual in another but may actively make seizures worse. Targeting the overall excitation-inhibition balance through homeostatic mechanisms, rather than a single class of receptor, may prevent this from occurring and act on a wide range of different epilepsies.

#### 1.2.6 GABAergic System

GABA (Figure 1.1) acts as the primary inhibitory neurotransmitter by binding to receptors both pre- and post-synaptically. Binding to GABA<sub>A</sub> receptors causes a negative change in transmembrane potential by increasing chloride conductance into cells. GABA<sub>B</sub> receptors are G-protein linked receptors that hyperpolarise a cell by increasing potassium conductance out of the cell and reducing calcium entry, lowering the chance of a neuron firing. GABA is mainly located in the axon terminals of intermediate neurons, where it is formed *via* the transamination of  $\alpha$ -ketoglutarate into glutamic acid, which is then converted to GABA by glutamic acid decarboxylase (GAD) (Figure 1.2). *GAD1* is crucial for the synthesis of GABA and therefore it is thought that *GAD1* mutations may lead to a GABA imbalance within the brain and ultimately hyperexcitability. A recent study discovered

biallelic mutations to *GAD1* that resulted in early infantile onset epilepsy and developmental delay (Neuray et al. 2020). Another recent study which measured the changes to the transcriptome associated with epileptogenesis, found that *GAD1* was downregulated in epilepsy patients (Pfisterer et al. 2020). However, it is not known whether this is causative of seizures or a homeostatic response to changes in excitation. Further human genetic studies are required to elucidate how *GAD1* mutations relate to GABA synthesis and to better understand how it relates to epilepsy (Akyuz et al. 2020).

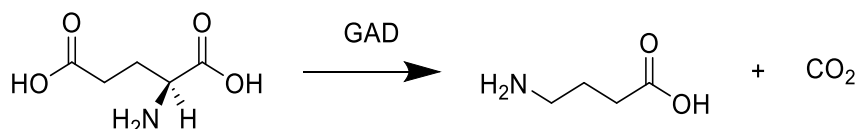


*Figure 1.2 - Synthesis of GABA, the main inhibitory neurotransmitter in the mammalian CNS. GABA is synthesised from glutamate in a decarboxylation reaction catalysed by glutamic acid decarboxylase (GAD).*

GABA<sub>A</sub> receptors, in particular, have been heavily linked with epilepsy (M. S. Evans et al. 1994; Kapur and Macdonald 1997; P. K. Banerjee et al. 1998). However, more recent evidence suggests that GABA<sub>B</sub>Rs may also be linked to absence seizures, which occur in experimental models with GABA<sub>B</sub> antagonists (Stewart et al. 2009). It has been established for decades that GABA<sub>A</sub> receptor function is required for limiting network synchrony (Miles and Wong 1983). High frequency synchronous neuronal firing that spreads through the brain often precedes seizures. Therefore, drugs that potentiate GABA activity can prevent this synchronisation as well as reducing overall excitability. Various mutations have been documented that affect GABA receptor expression or activity (Baulac et al. 2001; Wallace et al. 2001; Harkin et al. 2002). In human patients many show an epileptic phenotype; however as with other epilepsy related genes the severity of the phenotype depends on other genetic and environmental factors.

#### 1.2.7 Other Neurotransmitters

Although glutamate and GABA have been most heavily linked with epilepsy, other neurotransmitters may also play a more subtle role. Neuromodulators including serotonin (5-HT) and dopamine can affect the ratio of excitation and inhibition by inducing changes in the activity of glutamatergic and/or GABAergic neurons (Yagüe et al. 2013). Studies have shown significant change can occur to the dopaminergic system following seizures. Dopamine receptor (D2R) signalling may contribute to epileptogenesis by activation of neuronal cell death cascades (Bozzi and Borrelli 2013).

Whilst studies have shown agonists of D2Rs can prevent seizures and associated brain damage, systemic investigation into D2R as a potential target are lacking (Micale et al. 2006; Deepak et al.

2007). This is likely due to the fact that drugs that act on the dopaminergic system often have severe side effects and challenging withdrawal symptoms (Bozzi and Borrelli 2013).

Serotonin (5-HT) is a neuromodulator thought to be involved in virtually all human behavioural processes. Reduced 5-HT activity is generally associated with seizure genesis whereas increased activity is anticonvulsant (Epps and Weinshenker, 2013; Hamid and Kanner, 2013). In particular, patients with temporal lobe epilepsy have been shown to have small alterations in 5-HT neurotransmission (Martinez *et al.*, 2013). Multiple rodent models of seizure have also shown activation of 5-HT<sub>1A</sub> receptors to be anticonvulsant (Salgado and Alkadhi, 1995; Gariboldi *et al.*, 1996; Lu and Gean, 1998). The serotonin system is complex and how it exerts effects on excitability within the CNS is poorly understood. There are 14 different sub-types of 5-HT receptor which may exert opposing control on cell membrane potential and act on different neuronal circuits involved in various types of epilepsy. This is likely why, despite an array of evidence linking 5-HT to epilepsy, there are no AEDs which specifically target the serotonin system. However, the 5-HT<sub>2C</sub> agonist lorcaserin has recently been shown to reduce seizure occurrence by 48% for some severe forms of epilepsy, such as Dravet syndrome (Tolete *et al.*, 2018).

#### 1.2.8 Environmental Factors

Whilst some forms of epilepsy are purely down to genetic factors, many cases also have a contribution from environmental factors. For example, 25% of epilepsy cases are associated with antecedent CNS injuries such as head trauma, stroke or infection (Hauser, Annegers and Kurland, 1991). However, the chance of someone developing epilepsy after such an injury varies with genetic factors. The fact that epilepsy is a group of different conditions with a long list of causes and risk factors makes it very hard to treat. This is exacerbated by 60% of cases being due to unknown causes.

### 1.3 Current Anti-Epileptic Drugs

Because epilepsy has a variety of different causes, a diverse array of drugs is needed to treat different patients. Indeed, many patients may require treatment through drug cocktails (Hochbaum *et al.*, 2022). There are more than 20 currently clinically approved drugs, however despite this a third of epilepsy cases are pharmacoresistant. Furthermore, around half of patients on anti-epileptic drugs (AEDs) will experience severe adverse effects (Schmidt and Schachter, 2014). Additionally, treating children poses further problems due to effects on brain development (Goldenberg, 2010).

For patients with drug-resistant focal epilepsy, surgery can be highly effective, leading to seizure freedom of 60-80% (Spencer and Huh, 2008). However, drug resistant focal epilepsy only accounts

for a small number of epilepsy cases. A medium chain fatty acid ketogenic (low carbohydrate) diet is a proven, non-pharmaceutical, method of seizure control that can be beneficial for those with drug resistant epilepsy. It was identified as a treatment 50 years ago but suffered from high attrition rates as patients find it difficult to tolerate the diet (Huttenlocher, Wilbourn and Signore, 1971). More recent evidence suggests that the active molecule in this diet is decanoic acid (Chang *et al.*, 2016). This may lead to an easier to follow diet plan, and/or the development of decanoic acid as an AED. Currently though, the ketogenic diet is seen as a way of potentially reducing seizure incidence in certain patients, rather than as a way of fully preventing seizures. Both of these non-pharmaceutical methods are effective for certain groups of patients, but overall AEDs are the most common tool employed to control seizures.

AEDs aim to restore balance between inhibition and excitation. There are three main classes of drugs that achieve this via different mode of action: sodium channel blockers, GABA potentiators and calcium channel blockers; however, calcium channel blockers are generally only used in adjunctive therapy (Schmidt and Schachter, 2014). Since the release of Valproate in 1962, 5 AEDs have been released that act on a completely novel target. Perampanel, (AMPA receptors) (Greenwood and Valdes, 2016), levetiracetam (synaptic vesicle protein SV2A) (Abou-Khalil, 2008), cannabidiol (various targets) (Chayasirisobhon, 2020), fenfluramine (serotonin release) (Schoonjans, Lagae and Ceulemans, 2015) and topiramate (carbonic anhydrase inhibitor) (White, 2005). More novel mechanisms of action are needed to reduce the number of drug resistant patients.

Ideally, AEDs should be convenient to take for patients (tablet 1-3 times daily), have limited adverse effects and preferably not be an enzyme inducer (e.g CYP450) to minimise the chance of drug-drug interactions (Trinka, 2012).

### 1.3.1 Sodium Channel Blockers

Phenytoin, carbamazepine and lamotrigine (Figure 1.3) are commonly prescribed AEDs that block sodium channels as their primary mechanism of action (Kyle and Ilyin, 2007). These three compounds all bind to a common site within the channel and all bind favourably to inactivated states of sodium channels (Ragsdale *et al.*, 1994). This allows the drugs to preferentially block sodium channels involved in 'burst activity' seen after a low threshold spike (Macdonald and Kelly, 1995).

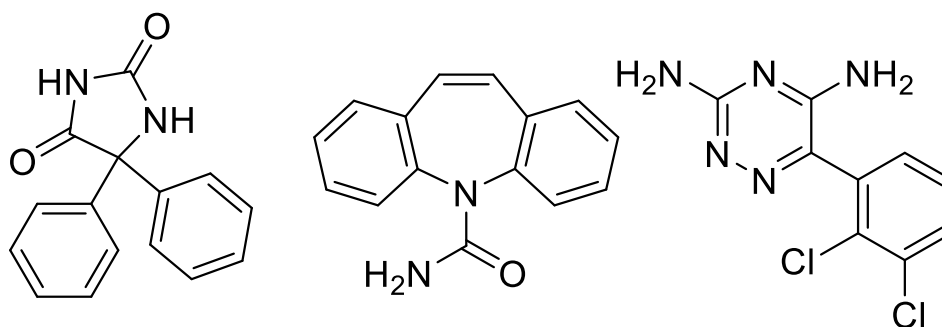


**Figure 1.3- Structures of phenytoin, carbamazepine and lamotrigine (left to right), three commonly prescribed sodium channel blocker AEDs**

Generally, sodium channel blockers are unselective towards the different subtypes ( $\text{Na}_v1.1-1.7$ ) which is thought to contribute to their side effect profile (Catterall, 2014). The three drugs mentioned have all been associated with hypersensitivity syndrome, a rare but potentially life-threatening side effect (Knowles, Shapiro and Shear, 1999). In particular, carbamazepine and phenytoin have undesirable side effect profiles, including cognitive impairment, leukopenia and aplastic anaemia (Schmidt and Schachter, 2014).

As mentioned previously, in some cases sodium channel blockers can aggravate seizures in loss-of-function  $\text{Na}_v1.1$  mutants as they further block sodium channel function in inhibitory neurons (Catterall, 2014). Furthermore, sodium channel blockers are ineffective in the treatment of absence seizures (Macdonald and Kelly, 1995). It is thought selectively blocking the  $\text{Na}_v1.6$  subtype could be more efficacious with less side effects as they seem to drive repetitive firing in neurons (Chen *et al.*, 2008).

### 1.3.2 GABA Potentiators

Drugs that enhance GABAergic inhibition are anticonvulsant, whereas GABA antagonists are proconvulsant. Anticonvulsants activate GABA receptors or increase levels of GABA which leads to activation of chloride channels and increased inhibition (Treiman, 2001).

Due to the three rotatable bonds within the structure of GABA, the molecule is conformationally very flexible. This is important for the function of GABA, as it allows it to bind to a diverse range of receptors in different conformations. This also allows the pharmacology of the GABAergic system to be highly selective and variable. Several GABA analogues have been developed with more rigid structures, in order to control their binding and increase their selectivity (Majumdar and Guha, 1988). For example, the psychoactive component of *Amanita muscaria* muscimol, selectively binds to  $\text{GABA}_A$  receptors and entered phase 1 clinical trials for epilepsy (Heiss *et al.*, 2012). Guvacine is

another GABA analogue with similar conformational restriction as it contains only 1 rotatable bond. Muscimol binds selectively to GABA<sub>A</sub> receptors whereas guvacine inhibits GABA reuptake with no significant binding to any GABA receptors. Both structures are shown in Figure 1.4.

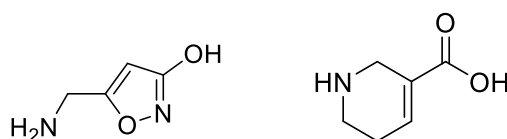


*Figure 1.4 - Structures of muscimol (left) and guvacine (right). Both are structural analogues of GABA. Similarly to GABA, both compounds are zwitterions at neutral pH, with the OH group of muscimol acting as an acid. GABA is conformationally flexible due to the 3 rotational bonds which allows it to bind to a variety of receptors. These compounds contain 1 or 0 rotational bonds and as a result are more selective for specific GABA binding partners.*

There are two main classes of AEDs that potentiate GABA, barbiturates (phenobarbital, primidone) and benzodiazepines (diazepam, Clobazam) (Figure 1.5) (Kwan, Sills and Brodie, 2001). Both activate GABA<sub>A</sub> receptors as their main mode of action but bind to distinctly different sites. Vigabatrin and tiagabine also potentiate GABAergic activity, but through inhibition of GABA reuptake and catabolic enzymes increasing synaptic GABA concentration (Kwan, Sills and Brodie, 2001). However, vigabatrin is rarely prescribed due to harmful side effects including teratogenicity. Barbiturates and benzodiazepines can often cause side effects including sedation, cognitive impairment and withdrawal (Schmidt and Schachter, 2014).

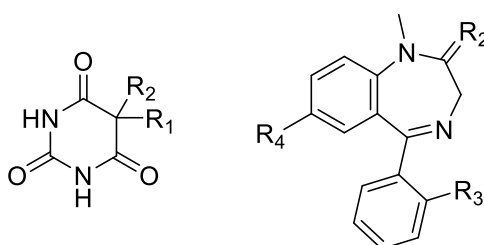


*Figure 1.5- General structures of barbiturates (left) and benzodiazepines (right), both are AEDs that potentiate GABA.*

Whilst other drugs mentioned are generally only used for adjunctive therapy, phenobarbital is an effective treatment for a range of epileptic conditions and is one of the most widely prescribed AEDs (Johannessen Landmark *et al.*, 2009). This drug was released on to the market in 1912 and is still the most effective AED that acts on GABA, highlighting the need for new targets in AED development.

### 1.3.3 Calcium Channels

Gabapentin and pregabalin (Figure 1.6) are calcium channel blockers that both act on the  $\alpha 2\delta$  receptor subunit (Ben-Menachem, 2004). Both have an improved side effect profile compared to the other AEDs mentioned, however both are generally only used in conjunction with other drugs (Johannessen Landmark *et al.*, 2009). This class of compound is referred to as a gabapentinoid, due

to their structural similarity to GABA. Both were initially designed to be conformationally restricted, lipophilic GABA analogues, similar those mentioned above, but both were found to act as calcium channel blockers. However, recent evidence suggests that gabapentin may exert at least some of its action through potentiating GABA (Yu *et al.*, 2019).

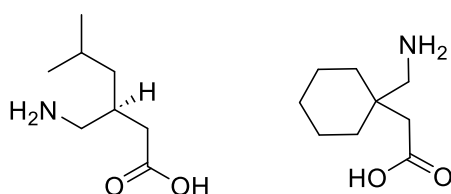


*Figure 1.6- Structures of  $\alpha 2\delta$  subunit calcium channel blockers pregabalin (left) gabapentin (right).*

Succinimides act as T-type calcium channel blockers and can generally have some severe psychoactive effects (Ijff and Aldenkamp, 2013). Ethosuximide is the best tolerated of this class of compounds and is widely prescribed as a treatment for absence epilepsy (Glauser *et al.*, 2013). Other T-type channel blockers are currently in clinical trials, which may be more potent than current AEDs without the side effects associated with succinimides (Richard *et al.*, 2019).

Levetiracetam acts on calcium channels indirectly by blocking the synaptic vesicle protein SV2A (Lynch *et al.*, 2004). SV2A regulates the expression and trafficking of synaptotagmin, a protein required for the calcium mediated exocytosis of neurotransmitters from synaptic vesicles (Bai and Chapman, 2004). SV2A has also been shown to be involved in the endocytosis and priming vesicles for exocytosis, independent of synaptotagmin (Chang and Südhof, 2009). By blocking SV2A levetiracetam reduces neurotransmitter release and lowers overall excitation. However, similarly to AEDs previously mentioned, there can be cases whereby taking levetiracetam can increase the likelihood of seizures, particularly in children (Nakken *et al.*, 2003). The cause of this paradoxical effect is unknown, but aside from this levetiracetam has a good side effect profile when compared to other AEDs.

#### 1.3.4 Others

For most AEDs their mechanism of action was only discovered after clinical approval, and some are still not fully understood today. Target based approaches over the last 40 years have concentrated on GABAergic and glutamatergic systems with limited success. The gabapentinoids came from this approach, as did the GABA-potentiators tiagabine and vigabatrin. However, despite much research, perampanel is the only AED thought to act mainly through iGluRs. Perampanel is a non-competitive AMPA antagonist released on to the market in 2012 that is used as an adjunctive therapy. It has no effect on NMDA currents, which is thought to be the cause of many of the psychotic side effects associated with targeting iGluRs. However, the side effects can still be quite severe, including

behavioural and psychotic changes such as increased agitation, anger, and anxiety (Rugg-Gunn, 2014). Whilst iGluRs and GABARs would seem like obvious targets for the treatment of epilepsy, it has been claimed that concentrating too much on these oversimplifies the alterations within these neurotransmitter systems in an epileptic brain (Löscher *et al.*, 2013). Additionally, focussing on a limited number of targets is unlikely to decrease the number of pharmacoresistant resistant cases and is less likely to produce novel drugs when compared to a novel target. AEDs from new targets may also have a less severe side effect profile, particularly when compared to drugs that target glutamate.

Valproate (Figure 1.7) and topiramate are AEDs with unknown mechanisms of action. Both are thought to act in some way on most of the targets mentioned above and are two of the broadest AEDs on the market in terms of effectiveness (Schmidt and Schachter, 2014). Topiramate is commonly prescribed despite its wide range of common side effects including depression, cognitive impairment and sedation (Sommer, Mitchell and Wroolie, 2013). Valproate is also one of the most widely prescribed AEDs available (Johannessen Landmark *et al.*, 2009) mainly due to its broad spectrum of anticonvulsant activity. This is despite valproate being a known teratogen, and in some cases hepatotoxic (Jeavons, 1984). Although it is not clear how valproate works, models suggest that sodium channel blockade is a large part of its action (Romoli *et al.*, 2019).

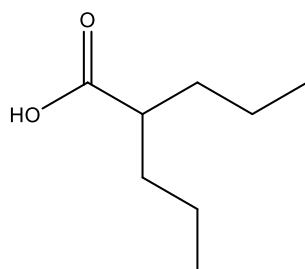


*Figure 1.7- Structure of valproate, a regularly prescribed AED with an unknown mode of action. It is thought part of its effect may come through blocking  $Na_v$ s*

## 1.4 Models in epilepsy

Up until the 1990s (White, 1997) drug induced seizure assays in rodents have been used successfully to develop new AEDs. However, after this point it was realised that in order to detect the therapeutic potential of new AEDs additional model systems with more aetiologies are required

(Stables *et al.*, 2003). For example, the pilocarpine induced status epilepticus rodent model causes hippocampal sclerosis to model the human condition, but also leads to extra widespread brain damage with no link to epilepsy (Cavalheiro, Santos and Priel, 1996). Whilst this assay is still informative, when screening for new AEDs many *in vitro*, *in silico* and non-mammalian models are often able to provide more selective behavioural and molecular features of a given epilepsy syndrome. Having the ability to study the aetiology of specific epilepsy syndromes, combined with genetic screening of patients, should pave the way for epilepsy syndrome-specific medicines and, hopefully, less pharmacoresistant cases.

#### 1.4.1 Mammalian Models

Over the last few decades there has been a sharp increase in the number of rodent models, which has facilitated new kinds of epilepsy research and a better understanding of the mechanisms behind epilepsy syndromes (Nissinen *et al.*, 2000). Chemoconvulsants are some of the most commonly used tools to model seizures and epilepsy, and for screening for novel AEDs (Velíšková, Shakarjian and Velíšek, 2017). Kainic acid was one of the first chemoconvulsants used to study temporal lobe epilepsy, the most common epilepsy syndrome seen in adults (Sharma *et al.*, 2007). It is an agonist of kainate and AMPA iGluRs, mimicking the role of glutamate and increasing excitability.

In order to mimic temporal lobe epilepsy rodents must display similar clinical history of adults, including an initial injury affecting temporal lobe (e.g., status epilepticus) and a latent period where the brain undergoes structural changes which eventually lead to spontaneous seizures (Lothman and Bertram, 1993). This occurs after injection of kainic acid, resulting in similar changes to the hippocampus as those seen in temporal lobe epilepsy (Raedt *et al.*, 2009). Although an ability to specifically target the hippocampus is a useful tool for some studies, extrahippocampal areas are also damaged in temporal lobe epilepsy (Bonilha *et al.*, 2010). Pilocarpine is another chemoconvulsant that causes similar effects to kainic acid but with more extrahippocampal damage and behavioural changes seen in temporal lobe epilepsy patients (Faure *et al.*, 2014). However, these chronic epilepsy models are rarely used due to costs, time restraints and high mortality rates (Kandratavicius *et al.*, 2014).

Compounds such as N-methyl-D-aspartate (NMDA), pentylenetetrazol (PTZ) and penicillin are used to model acute seizures rather than models of epilepsy (Kandratavicius *et al.*, 2014). Different proconvulsants can be used depending on the desired seizure type. For example, NMDA produces generalised tonic-clonic seizures whereas PTZ can be used to generate myoclonic seizures (Löscher, 1997). Drugs which are thought to act *via* ion channels (e.g., valproate and ethosuximide) were discovered with these types of acute seizure models, whereas drugs with different mechanisms of

action (e.g. tiagabine and vigabatrin) were discovered using chronic epilepsy models (Löscher, 2002). This highlights how a variation in model is a critical choice in order to find new classes of AEDs.

Electrical stimulation in rodents is another commonly used model of epilepsy (Gorter and van Vliet, 2017). Electroshock (ES) induced seizures can be separated into maximal and minimal seizures depending on the conditions (Frankel *et al.*, 2001). Minimal ES induces myoclonic seizures whereas maximal ES is used to model generalised tonic-clonic seizures (Browning and Nelson, 1985). Maximal ES and PTZ have largely been used to screen for AEDs, however drugs that protect against non-convulsive and partial seizures fail in these models. ES has also been applied to research into how epileptiform activities cause changes to brain structure (Tsankova, Kumar and Nestler, 2004).

Perhaps the most powerful electrostimulation tool to study epileptogenesis is kindling (Sutula, 2004). Kindling is a phenomenon that occurs from repeated stimulation (often electrical but can be chemical) that causes a gradual enhancement of seizure susceptibility, ultimately leading to a permanent epileptic state (Goddard, McIntyre and Leech, 1969). Chronic epilepsy models that rely on drug induced status epilepticus result in the rapid emergence of seizures, whereas kindling is a controlled gradual process better mirroring epileptogenesis (Sayin *et al.*, 2003). This difference allows opportunities to study both slow and rapid epileptogenic processes, which is representative of the variation seen in human temporal lobe epilepsy (Sutula, 2004). Combinations of the kindling and pharmacological approaches can also be used in a model of pharmacoresistant epilepsies, a critical tool in the development of new AEDs (Srivastava *et al.*, 2013).

Although a useful tool, kindling is expensive, time consuming and difficult, due to the fact that chronic implanted electrodes or repeated injections need to be maintained (Bertram, 2007). Additionally, there is uncertainty with regards to its relevance to human epilepsy. Kindling does, however, provide useful neurobiological observations relevant to epilepsy and is now being used in conjunction with transgenic studies to discover genes that increase disposition to kindling (Liu *et al.*, 2017).

Since the first targeted gene deletion producing epilepsy in 1994, (Van der Lugt *et al.*, 1994) genetically engineered mice have been a valuable tool in the identification of candidate gene families and uncovering biological pathways in epileptogenesis (Maheshwari and Noebels, 2014). There are now many genetically modified mice strains with seizure phenotypes and with advances in genetic engineering, this number will continue to grow (Maheshwari and Noebels, 2014) (Taniguchi *et al.*, 2011). Thus, there are now examples of transgenic mice with specific conditions including Dravet syndrome (Yu *et al.*, 2006) and tuberous sclerosis complex (Wang and Cohen, 2007). This has aided research into precision medicine for epileptic conditions, such as the use of rapamycin to

target specific signalling pathways associated with tuberous sclerosis complex (Zeng *et al.*, 2008). However, it should not be assumed that orthologous gene models show the same molecular or cellular lesions seen in humans. Reasons include variations in splicing (Colombo *et al.*, 2000) and fundamental biological differences (Noebels, 2017).

#### 1.4.2 *In Silico* and *in Vitro* Models of Epilepsy

Within the last 20 years *in silico* models have considerably improved and gained acceptance (Lytton, 2008). They are based on computations that predict brain activity and seek to provide mechanistic details and generate testable hypotheses (Wendling *et al.*, 2016). The first model of a single neuron was developed by Hodgkin and Huxley in 1952 (HODGKIN and HUXLEY, 1952) and this model has been consistently improved to include detailed dynamics of channels, pumps, buffers and ion concentrations (Wei, Ullah and Schiff, 2014). Although they are always improving, *in silico* models can still be limited, mainly due to the complexity of both the human brain and epilepsy syndromes, however it is hoped that with increasing computer power and understanding of the human brain, *in silico* models will be able to provide new predictions and aide the discovery of new treatments (Stefanescu, Shivakeshavan and Talathi, 2012) (Wendling, Bartolomei and Modolo, 2017). The use of electrical stimulation for seizure controls, which is currently in clinical trials (Sohal and Sun, 2011) (Morrell, 2011), requires accurate models in order to detect abnormal brain activity (Stefanescu, Shivakeshavan and Talathi, 2012).

The advancement of human induced pluripotent stem cells (iPSCs) and their derivation into tissues has provided a convenient source of human neurons (Tidball and Parent, 2016). 2D-neuronal cell cultures form functional synapses and neuronal networks (Lancaster and Knoblich, 2014); however, the development in 3D cultures such as brain organoids, has permitted models to better resemble the architecture of the human brain (Qian *et al.*, 2016). This has allowed neuronal function in developmental epilepsies to be better studied using optical imaging and/or electrophysiological recordings (Dang and Parent, 2017). iPSC models also have benefits for studying genetic epilepsies, whilst acquired epilepsies are better modelled with animals (Dang and Parent, 2017). This is mainly due to different mouse strains may having different seizure thresholds and therefore varying phenotypes (Mistry *et al.*, 2014). However, it is much more difficult to characterise an epileptic phenotype in iPSCs, due to the fact that the induction of seizures and drug application are still emerging areas of research (Steinberg et al. 2021). Therefore, characteristics including synchrony and burst activity must be used as *in vitro* correlates of epilepsy. Although as iPSC models are developed this will lead to a better understanding of *in vitro* epileptic phenotypes (Dang and Parent, 2017). The development of brain organoids has improved the area of *in vitro* models, as they have

the potential to establish different brain regions in a single organoid, allowing the study of cell-cell interactions (Quadrato et al., 2017).

#### 1.4.3 Non Mammalian Organisms

Although there are greater similarities in the nervous systems of different mammalian species, non-mammalian models offer a cheaper and higher throughput alternative to rodent models. Simpler models can often be advantageous when studying the biological processes of seizure generation and mechanisms of drug action due to their tractability. Furthermore, in higher non-mammalian species such as *Drosophila melanogaster* (fruit flies) and *Danio rerio* (Zebrafish), seizure mechanisms show many similarities to mammals (Jirsa et al., 2014). The use of a variety of models when screening for AEDs is key, as what may show up in one species may not in another.

*Caenorhabditis elegans* has been one of the major models in biology since studies performed in the early 1970's by Brenner (Brenner, 1974). Additionally, *C. elegans* was the first metazoan genome to be fully sequenced in 1998 (Fire et al., 1998). They are a non-parasitic nematode worm with a nervous system that comprises only 302 neurons (Tsalik and Hobert, 2003). As they primarily reproduce rapidly as self-fertilizing hermaphrodites *C. elegans* are especially suited to high throughput chemical screening (Sulston, 1983). There are drawbacks to using *C. elegans* as a model, mainly due to the differences in neuron morphology. For example, electrophysiology is very challenging with the worm and this animal lacks voltage gated sodium channels preventing certain lines of research (Bargmann, 1998). However, given that new generation AEDs should interact with novel targets, this can be seen as an advantage. Above all else, their facile genetics and short generation time makes the nematode a useful tool in studying certain aspects of seizures such as epileptogenic processes and AED mechanisms of action as well as high throughput drug screening (Wong et al., 2018).

In the last decade, Baraban and colleagues (Baraban, Dinday and Hortopan, 2013) have exploited *Danio rerio* (zebrafish) to screen for novel treatments of Dravet syndrome. By using fish with a mutation in the *SCN1A* homologue, they were able to replicate convulsions seen in patients with Dravet syndrome. With this screen, they were able to identify that the 5-HT receptor agonist clemizole (structure in Figure 1.8) reduced seizure severity in zebrafish (Baraban, Dinday and Hortopan, 2013). Further investigation led to a small clinical trial of 5 children with drug resistant Dravet syndrome with a different 5-HT agonist, lorcaserin (Griffin et al., 2017). All 5 patients exhibited a reduction in the number of seizures with minimal side effects, although this improvement did taper off for most patients. Interestingly clemizole, the initial hit which led to the

lorcaserin trial, is rapidly metabolised with a half-life of 10 minutes (in mice) compared to 3.4 hours in humans (Nishimura *et al.*, 2013). If this screen were performed in rats clemizole would likely show as a false negative, exemplifying why a variety of models are needed in epilepsy research. This is the first example of a potential therapy discovered in a fish model taken directly into a human clinical trial. As new drugs are currently being screened in models of some of the 70 childhood epilepsies, more AEDs are likely to be discovered (Griffin *et al.*, 2017).

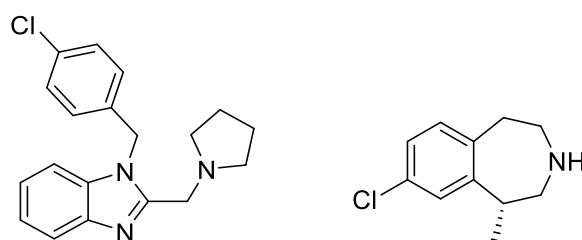


**Figure 1.8 - The structures of 5-HT agonists clemizole (left) and lorcaserin (right). Clemizole had been marketed previously as an antihistamine but was found to be active in a zebrafish model of epilepsy due to its binding to serotonin receptors. This led to the screening of more 5-HT agonists including lorcaserin, which became the first compound to be taken from screening in zebrafish straight to human trials.**

Zebrafish are now seen as an established model of human disease in areas including neurodegeneration, inflammation, and epilepsy (Copmans, Siekierska and de Witte, 2017). The fact that they are vertebrates and have homologues of at least 82% of genes involved in human genetic disorders, gives them an advantage over other non-mammalian species as the vertebrate CNS is highly conserved. Their transparent embryo allows developmental studies to be conducted simply by light microscopy (Kimmel *et al.*, 1995). Additionally, as zebrafish larvae only have a body length of 3.5-4.5 mm, they can easily be added to microtiter plates, aiding high-throughput screens. However, the compounds that can be tested in zebrafish are limited. Drugs that are added to their water must be sufficiently soluble to dissolve, but lipophilic enough ( $\text{LogP} > 1$ ), in order to be absorbed (Milan *et al.*, 2003). Injection during development can be used to get around this problem, however this results in lower throughput (Tiedeken and Ramsdell, 2009).

#### 1.4.4 *Drosophila*

Since the identification of the first seizure mutant in the early 1970s (Konopka and Benzer, 1971) *Drosophila Melanogaster* (fruit flies) have been a common model used to study seizure like activity. The first identified mutant was referred to 'bang sensitive (bs)' after it was discovered that mechanical shocks or 'bangs' cause them to exhibit seizure like behaviour. This mutation was localised to the sole  $\text{Na}_v$  in the fly genome. There are now 14 known bs mutants and at least 20 more are known to affect seizure susceptibility in some way (Parker *et al.*, 2011a). Furthermore, certain mutations provide a direct link to specific forms of epilepsy. For example, *para*<sup>bs</sup> encodes for voltage

gated sodium channels and therefore can be used to study Nav channelopathies such as Dravet syndrome and generalised epilepsy with febrile seizures plus (GEFS+) (Guillerm *et al.*, 2014).

*Table 1.2 - Bang sensitive mutants identified in Drosophila.*

Allele	Gene	Function
<i>Bangsenseless (bss)</i>	Paralytic (Nav)	Ion channel/neural signalling
<i>Easily-shocked (eas)</i>	Ethanolamine kinase	Glycerophospholipid metabolism
<i>Bangsensitive (bas)</i>	Unknown	Unknown
<i>Julius seizure (jus)</i>	<i>CG14509</i>	Unknown
<i>Technical knockout (tko)</i>	Ribosomal protein S12	Mitochondria/ATP
<i>Jitterbug (jbug)</i>	Flamin	Actin-binding protein
<i>Couch potato (cpo)</i>	RNA-binding protein	Neural signalling
<i>Kazachoc (kcc)</i>	KCC2 transporter	Neural signalling
<i>Knockdown (kdn)</i>	Citrate synthase	Mitochondria/ATP
<i>Prickle (pk)</i>	LIM domain protein	Microtubule polarity
<i>Stress sensitive B (sesB)</i>	Adenine nucleotide translocator	Mitochondria/ATP
<i>Rock-n-roll (rnr)</i>	Unknown	Unknown

There are many similarities between seizure behaviour in *Drosophila* and humans. For example, upon induction of seizures fruit flies exhibit convulsion like behaviours (wing flapping, leg shaking etc.) before losing standing posture. This is then followed by a period of paralysis due to synaptic failure, followed finally by a recovery seizure similar, all of which is also witnessed in certain human epilepsies (Song and Cronin, 2008). Other similarities include defined seizure thresholds and the spread of seizures throughout the CNS occurring via defined neuronal tracts (Baines, Giachello and Lin, 2017). Additionally, mutations in orthologous genes cause seizures in both humans and flies and both respond to the same AEDs (Marley and Baines, 2011) (Kuebler and Tanouye, 2002).

Both adults and larvae can be used to induce seizure like activity. The most straightforward assay begins by transferring flies to a plastic vial and then subjecting them to a mechanical shock, using a lab vortexer for 10 seconds. The recovery time is then calculated by taking the average time for all the flies to return to a standing position. Another, more informative seizure inducing method utilises

electrostimulation to the giant fibre system (GFS). Tungsten electrodes are placed on the brain of immobilised flies and following stimulation, a response can be measured with an intracellular electrode in the leg or flight muscle (Tanouye and Wyman, 1980). High frequency stimulation of the GFS induces seizure like activity that is characterised by prolonged bursting of muscle potentials (Baines, Giachello and Lin, 2017). This technique can also be used to determine seizure thresholds, which varies considerably depending on genotype.

To characterise seizure like activity in larvae an established electroshock assay can be utilised (Marley and Baines, 2011). Once larvae reach the wandering third instar (L3) phase, they begin to climb out of the food within their vial. These larvae are transferred to a plastic dish to be washed and are then dried. Once recovered, a conductive probe is placed over the CNS and an electric shock is applied for 2 seconds. The time it takes for the larvae to return to normal crawling behaviour is then recorded. To determine the voltage applied the probe must be calibrated to produce a paralysis of ~30 seconds in wild type and ~200 seconds in a standard BS mutant - *para<sup>bss</sup>*.

In order to screen for new AEDs, test compounds can easily be applied to the food of both larvae and adults by simply melting the food and adding the compound of interest. *Drosophila* are much more tolerant to the potential toxicity of drugs in comparison to zebrafish. Fly larvae in particular will additionally eat almost any substance added to their food without the concern of the drug being insufficiently soluble or lipophilic. Furthermore, starving adult flies for 12 hours increases ingestion of unpalatable compounds (Reynolds *et al.*, 2004). Although the CNS of *D. Melanogaster* has more differences to humans when compared to other vertebrates, the extra simplicity has allowed neurons in the CNS to be uniquely identified and are accessible by recording electrodes (Baines and Bate, 1998). Larval motoneurons have been especially well characterised both electrically and morphologically (Baines *et al.*, 2002). Larval locomotor circuits are repeated within each segment to facilitate the passing of motoneuron activity from one segment to another in a wave like fashion (Pulver *et al.*, 2015). Using calcium indicators such as GCaMP it can be demonstrated that peaks of calcium activity usually occur with a separation of more than 200 ms between adjacent segments (Streit *et al.*, 2016). This timing is significantly reduced in BS mutants, indicative of synchronized activity; a hallmark of mammalian epilepsy.

Even if no seizure like activity is observed, electrophysiological recordings show that bs mutants exhibit increased synaptic excitation (Marley and Baines, 2011). Furthermore, analysis of ionic conductances in larval motoneurons show that the persistent voltage gated sodium current ( $I_{NaP}$ ) is of higher amplitude in bs mutants, which may explain the mechanism behind their increased

neuronal excitability (Lin *et al.*, 2012). Again, an increased  $I_{NaP}$  is often observed in mutations affecting mammalian SCN genes (REFS).

The similarities in the mechanisms that underlie seizures, along with the tractability of *D. Melanogaster*, make them a useful model in both target identification and AED screening. Seizure suppressor genes provide a useful tool for studying seizure mechanisms and identifying possible drug targets. The sheer number of seizure suppressor mutants and the ease with which they are identified, make the approach particularly promising (Song and Tanouye, 2008). Using reverse genetic searches that focus on known excitability mutations, it was found that potassium channel (*sh*), gap junction (*shakb*) and sodium channel (*para*) mutations all effectively suppress seizures (Kuebler *et al.*, 2001; Song and Tanouye, 2006). Forward genetic approaches, which employ mutagenesis screens of *Drosophila*, have been able to uncover more unexpected seizure suppressor genes. The meiotic gene *mei-p2G<sup>EG</sup>*, zinc finger transcription factor *escargot* (*esg*), and DNA topoisomerase 1 enzyme (*top1<sup>JS1</sup>*) have all been found to possess seizure suppressing alleles using this method (Glasscock and Tanouye, 2005; Hekmat-Scafe, Dang and Tanouye, 2005; Song, Hu and Tanouye, 2007). This is consistent with molecular studies that have shown many epilepsy causing syndromes are not acting directly on electrical excitability (Royden, 1987; Pavlidis, Ramaswami and Tanouye, 1994; Puranam and McNamara, 1999). Once the target has been identified, flies can then be used as a high-throughput model system to screen for AEDs. This is exemplified in a study by Song and colleagues (Song, Hu and Tanouye, 2007) in which they first identified TOP1 as a target using a forward genetic approach, before confirming TOP1 inhibitors were effective in reducing seizure like behaviour in bs mutants.

A similar approach was recently adopted in the Baines laboratory, where *Drosophila* was used to identify changes in gene transcription that occur following seizure (Lin, Giachello and Baines, 2017b). Both a genetic model (*para<sup>bss</sup>*) and chemical model with picrotoxin (PTX) were used in conjunction with RNA sequencing which identified 743 common transcriptional changes. This included *pum*, a translational repressor of *Drosophila* Na<sub>v</sub> that has previously been linked to epilepsy.

*Drosophila* is a powerful tool for investigating seizure mechanisms and treatments, however there are limitations. There are many differences between the human and fruit fly CNS. For example, *Drosophila* use acetylcholine as a primary excitatory neurotransmitter instead of glutamate. Additionally, there are big variances in CNS structure. *Drosophila* have a ganglionic structure whereas mammals have a layered system, which may explain why there is a lack of spontaneous fruit fly mutants. Also, differences in both metabolism and the blood-brain barrier mean it is not easily possible to measure drug bioavailability and distribution in flies (Baines, Giachello and Lin,

2017). Despite this, the tractability of *Drosophila*, the fact that their genome contains 75% of known human disease-related genes and their tolerance to different pharmaceuticals makes this insect an extremely useful model in the screening of new drugs (Pandey and Nichols, 2011). This is especially true when it comes to AEDs, due to the many similarities of the mechanisms and behaviours associated with seizures.

## 1.5 Neuronal Homeostasis and Pumilio

### 1.5.1 Firing Rate Homeostasis

Homeostatic control is the term used to describe the maintenance of a system output despite changes in input. Many diverse biological systems utilise homeostasis, such as temperature and pH, to ensure that these do not deviate significantly from a physiologically relevant set point in response to changes in the environment. Homeostatic control is also applied to neuronal firing rates, but in a slightly different way. Neuronal function is dependent on a variation in the firing rate of individual neurons, which is responsible for conveying information, meaning a strict homeostatic system that does not allow neurons to deviate from the set point would render the CNS ineffective (O’Leary and Wyllie, 2011). Therefore, the homeostatic controller must ensure the neuron’s firing rate is maintained within a particular range and allow for large, but transient, deviations from the mean. This is not the case with typical homeostatic controllers such as body temperature, where a large deviation from the mean could be potentially fatal for warm blooded animals. Figure 1.9 describes the concept of firing rate homeostasis, but the means how neural networks keep within these parameters, without affecting the storage of information, is overall much more complex.

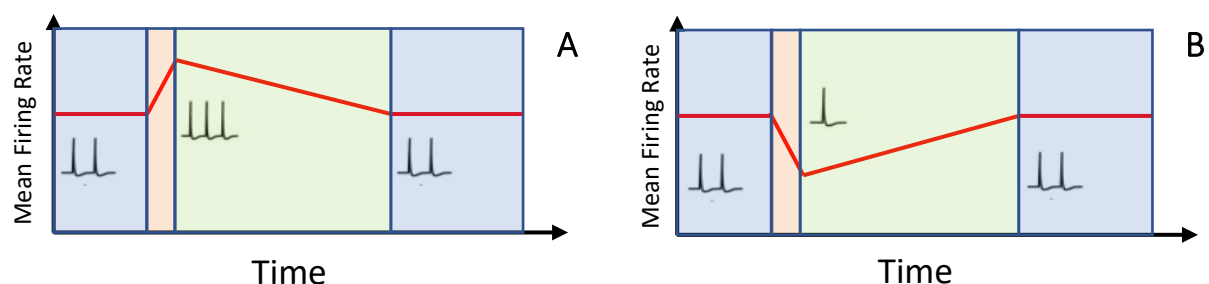


*Figure 1.9 – Graphical representation of neuronal homeostasis. When a constant perturbation (A - hyperactivity, B - inactivity) is applied to a neural network, homeostatic mechanisms respond by altering the mean firing rate back towards the set point. Compensatory mechanisms are introduced that return the firing rate back to normal, despite constant interference. The different phases of mean firing rate homeostasis are represented by different colours – baseline stability (blue), perturbation to the system (orange) and action by effectors (green).*

Hebbian plasticity is thought to be a mechanism by which information can be stored and coded in the brain. Since first being proposed in 1949 by Donald Hebb, a large amount of experimental evidence has since supported the idea that synaptic connections are strengthened between neurons when a presynaptic neuron persistently causes a postsynaptic partner to fire (Hebb, 1949). This occurs through a process known as long term potentiation (LTP). In contrast, if there is little transmission between these two cells the strength of the synapse weakens, which is known as long term depression (LTD). In the hippocampus LTP and LTD are dictated by the ionotropic glutamate receptor NMDA, as well as the relative timing of action potentials in the presynaptic and postsynaptic cells (Malenka, 1994). LTP/LTD can also be elicited if action potentials occur with appropriate timing in both the pre and post synaptic neuron. The influx of calcium through NMDA receptors is at its largest when the backpropagating action potential in the dendrite arrives shortly after the synapse is active (Linden, 1999). Therefore, if a presynaptic spike occurs just before (5-20 ms) the postsynaptic cell fires, the generated excitatory postsynaptic potential precedes the backpropagating action potential. As this pre-post firing maximises  $\text{Ca}^{2+}$  influx, repeated firing of this nature can generate LTP. Conversely, if the backpropagating action potential repeatedly occurs before the synapse is active LTD occurs. This phenomenon is named spike-dependent-timing-plasticity and is thought to be a more physiological method of inducing LTP/LTD. Other forms of LTP exist including those that act independently of NMDA (Harris and Cotman, 1986) and others which do not follow Hebbian theory (Kullmann and Lamsa, 2008). However, NMDAR dependant LTP in the CA1 hippocampus is the most widely studied form due to the ease with which LTP can be induced.

The plasticity allowed by these mechanisms is integral to the brain's function as it provides a way for the brain to respond to retain new information and adapt to external stimuli. However, if left unchecked these positive feedback mechanisms are likely to be destabilizing to the CNS. If LTP was allowed to occur with no overt control, it would ultimately lead to hyperexcitability, which not only increases the risk of a seizure but also reduces the coding ability of the neuron as it reaches activity-saturation. Conversely, if LTD had no overt control it could render neurons quiescent and prevent information transfer in a network. To prevent this, neurons employ a variety of homeostatic mechanisms, all working together, to ensure action potential firing is kept in a functionally relevant range.

Currently, synaptic scaling is the most understood form of neuronal homeostatic control. It was first identified in neocortical neurons by measuring the strength of a large number of synapses on to one neuron. It was shown that changes in activity had an inverse effect on the amplitude of miniature excitatory postsynaptic currents, suggesting that in response to prolonged increased activity, postsynaptic synaptic strength is reduced (Turrigiano *et al.*, 1998). Further chronic inactivity experiments found that deprivation in neuronal cell cultures leads to changes in post synaptic receptor density (Turrigiano and Nelson, 2004). Importantly, synaptic strength at all the synapses was scaled up or down by a multiplicative factor. This ensures that the relative strength of synapses (formed through LTD and LTP) is unaffected, whilst the global activity rate can be controlled homeostatically. However, subsequent *in vivo* experiments have shown since that the overall picture is more complicated. For example, one experiment by Echevoyen and colleagues, found that mouse CA1 hippocampal cells behaved differently in response to activity-deprivation compared to culture systems (Echevoyen *et al.*, 2007). Inactivity was induced using a slow release of the highly potent sodium channel blocker tetrodotoxin (TTX). Whilst this experiment showed activity-deprivation generally enhanced synaptic input from both glutamatergic and GABAergic terminals in CA1 cells, no overall synaptic scaling effect was observed. There is considerable evidence that shows other localised mechanisms of neuronal homeostasis exist, without severely disrupting Hebbian plasticity (Rabinowitch and Segev, 2006). Potential mechanisms include changes in AMPAR subtypes (postsynaptic) and alterations to neurotransmitter release probability (presynaptic) (Sutton *et al.*, 2007; Branco *et al.*, 2008). However, it is not clear how more localised mechanisms of homeostasis are compatible with Hebbian plasticity.

Computational studies looking at individual neurons and small networks suggest there is a variety of ways in which ion channel densities can restore neurons to an appropriate firing rate. One study by Prinz and colleagues evaluated 20 million simulations of varying channel densities and synaptic conductances between 3 cells (Prinz, Bucher and Marder, 2004). The simulation found hundreds of thousands of different combinations that produced the correct patterned output. This highlights just how complex the relationship between Hebbian plasticity and firing rate homeostasis is, with multiple mechanisms working at different timescales and sometimes even opposing each other, to produce a stable, yet malleable, network.

### 1.5.2 Function of Pumilio

In mammals, the RNA binding proteins, Pumilio 1 (PUM1) and Pumilio 2 (PUM2), are an integral part of the machinery involved in maintaining neuronal homeostasis (Goldstrohm, Hall and McKenney, 2018). The *Drosophila* homolog Pumilio (Pum) is very similar in both structure and function. Studies

in *Drosophila* reveal that Pum is a translational repressor that binds mRNA transcripts, usually those that contain a binding motif consisting of 8 nucleotides in their 3'UTR, known as a Nanos response element (NRE) (Gerber et al., 2006). The *pum* gene was first identified as a maternal effect gene involved in embryo posterior patterning (Lehmann and Nüsslein-Volhard, 1987). Pum, with cofactors Nanos (Nos) and brain tumour (Brat) repress *hunchback (hb)* mRNA in the posterior of the embryo, which is key for formation of the abdomen. Pum represses translation by first binding with the 8 nucleotide NRE (UGUA(A/C/U)AUA) before recruiting Nos and Brat to form a quaternary RNA-protein complex that promotes deadenylation (Gerber et al., 2006). However, there is also recent evidence to suggest that deadenylation is not crucial for regulation as it has been shown that Pum and other PUF proteins repress translation by antagonising poly(A) binding protein, a protein that binds to poly(A) tails promoting translation (Weidmann et al., 2014). The RNA binding domain of Puf proteins, termed the Pum-homology domain (Pum HD), is highly structurally conserved (Wang et al., 2002). The Pum HD is composed of 36 amino acids repeated 8 times. Binding to the NRE occurs through three residues of each repeat making contact with a different mRNA base, meaning that each repeat binds to one of the 8 residues within the NRE (Wang et al., 2002). This is shown in the crystal structure (Figure 1.10) taken from work by Wang and colleagues (Wang et al., 2002).



**Figure 1.10- Crystal structure of the Pumilio-homology domain from human Pumilio 1 in complex with NRE1-19 RNA (X. Wang et al., 2002).**

With respect to seizure, Navs are a particularly relevant Pum target. It has been shown that *Drosophila* Nav *para* is translationally regulated by Pum and also that rodent Nav1.6 is regulated in a similar fashion by *PUM2*, the closest mammalian homologue to Pum (Muraro et al., 2008; Driscoll et al., 2013). mRNA encoding Navs 1.1, 1.2 and 1.7 also contain an NRE highlighting possible wide

scale Pum2 regulation (Driscoll *et al.*, 2013). Translational repression of Navs is part of a homeostatic response that modulates action potential firing depending on the synaptic excitation neurons are exposed to (Lin, Giachello and Baines, 2017b). Pum is also able to influence synaptic and dendritic structure as well as neuronal excitability and contributes to the formation of long-term memories in *Drosophila* (Baines, 2005). This was exemplified in a study by Dubnau and colleagues (Dubnau *et al.*, 2003) they isolated genes with altered regulation during learning. By using a combination of forward and reverse genetics they discovered that loss of Pum resulted in behavioural tests with low memory scores. This suggests that Pum may translationally regulate a wide range of mRNAs.

With reference to homeostasis, a study which focussed on the microRNA-134 (miR-134), suggested that Pum2 is integral to synaptic downscaling (Fiore *et al.*, 2014). Fiore and colleagues discovered that Pum2 is a target of miR-134, which when bound, suppresses translation of Pum2. As expected, treatment of cell lines with the proconvulsant PTX lead to overall increase in the expression of Pum2 in neurons. Interestingly, when they looked at the expression levels in dendrites specifically, it was found that the amount of Pum2 protein had in fact decreased due to increased activity of miR-134. Further investigation found that downregulation of Pum2 is necessary for synapse elimination, a key facet of homeostatic synaptic downscaling. Furthermore, overexpression or knockdown of Pum2 both resulted in a loss of synapse elimination suggesting that Pum2 levels must be maintained within a particular range for synaptic elimination to occur effectively. This process is likely aided by the fact that Pum2 regulates its own transcript. Pum2 suppression by miR-134 in dendrites is required for synapse elimination due to Pum2's regulation of the Plk2 transcript, a protein which promotes the internalisation of the AMPA subunit GluA2.

Recent work has shown that Pum2 may also be important for the regulation of GABAergic transmission. By studying the effects of Pum2 knockdown on the neuronal proteome, it was found that various proteins associated with GABAergic transmission were downregulated (Schieweck *et al.*, 2021). This is likely due to Pum2 repressing the translation of other gene(s) that inhibit their synthesis, either directly or indirectly. The downregulated proteins include Gad1, which as previously mentioned promotes the synthesis of GABA from glutamate and Gephyrin, a key scaffold protein for the GABA<sub>A</sub> receptor. This results in an increased decay time for inhibitory postsynaptic currents, which in turn influences the excitability of the postsynaptic cell (Aradi *et al.*, 2002). Whilst the effects of PUM2 on reducing excitability are established, this study also shows that it may also promote inhibitory transmission. This further strengthens the case for the Pum proteins being a key part of neuronal homeostatic mechanisms.

It is thus perhaps not surprising that evidence from a range of studies links Pum to epilepsy. Firstly, *pum2* knockout mice exhibit spontaneous seizures, which suggests *pum2* is required for the homeostatic control of excitability (Siemen *et al.*, 2011). Secondly, *Pum2* expression is lower in human TLE patients (Wu *et al.*, 2015a). Interestingly, a published model predicts *Pum2* should actually increase during a seizure (Mee *et al.*, 2004). It is thought this decrease is seen as *Pum* mRNA also contains the NRE transcript and can therefore auto-regulate. Therefore, seizures may first increase the levels *Pum* which then feeds back downregulating its own transcript (Gerber *et al.*, 2006). Finally, overexpression of *pum* in *para<sup>bss</sup>* flies is extremely anticonvulsant, which is likely due to a reduction in  $I_{NaP}$  (Lin, Giachello and Baines, 2017b). Together this evidence suggests that prevention of this feedback and increasing levels of *Pum* is a promising anticonvulsant strategy.

### 1.5.3 Identification of Lead

Using a luciferase reporter of *Pum* activity, the Baines group screened 785 FDA-approved compounds to see if any could potentiate *Pum* expression/stability. This screen identified 12 compounds that increase *Pum* activity. Of these, avobenzone (Figure 1.11) was the most promising as unlike the other hits it did not have significant effect on basal transcription rate (Lin, Giachello and Baines, 2017b). This same study showed that there is no acute effect on the seizure phenotype but raising larvae on food containing avobenzone lowers seizure recovery times in *Drosophila* through reduction of  $I_{NaP}$ . These results are consistent with a chronic (and not acute) mode of action, consistent with a mechanism that affects *pum* transcription/transcript stability. Additionally, avobenzone was equally as effective at reducing recovery times in a wide range of *Drosophila* *bs* mutants, suggesting that increasing *Pum* activity might be effective for a broad range of epilepsies. However, it should be noted that although it seems that avobenzone's anticonvulsant activity is due to increased *Pum* action, the exact mechanism of action is unknown.

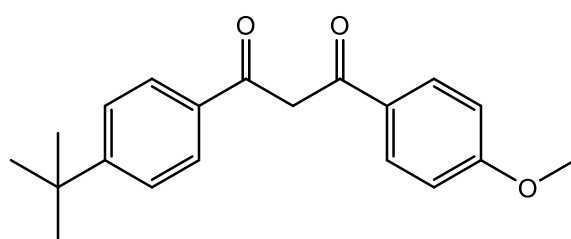


**Figure 1.11- Structure of original hit avobenzone, which has been shown to reduce the recovery time of seizures in *Drosophila* larvae.**

Avobenzone is a chemical UV absorber used in sun cream to provide protection against UVA1 rays (340-400 nm) (Mturi and Martincigh, 2008). It is able to absorb UV rays due to its highly conjugated system; however, this also contributes to its photoinstability. Deep UV (230 nm), when absorbed by avobenzone leads to the formation of a reactive triplet state, which in turn can react with oxygen to

give free radicals and photoisomeration products (Cantrell and McGarvey, 2001). Due to this potential toxicity and other properties of the compound, avobenzone cannot be seen as a potential drug treatment. It can, however, be used as a starting point in the potential development of an AED targeting Pum.

## 1.6 Aims Of This Thesis

Epileptic phenotypes are usually the result of numerous genetic and environmental factors. Because there are so many different causes and mechanisms that underlie seizures, epilepsy is particularly difficult to treat. As a result, despite a number of potential new drugs within the last 20 years, 30% of cases of epilepsy are still resistant to drugs. To improve this situation, new targets need to be identified using the plethora of animal models available. It is important to use a variety of models when screening for targets and potential drugs as what may show as a hit in one model may not translate to another. Pum appears to be an attractive target for the potential treatment of a wide range of epilepsies. It targets homeostatic balance rather than a specific receptor or ion channel. However, even if targeting Pum proves not to be a viable antiepileptic strategy, finding a compound that increases Pum activity and is tolerated in animal models, would be of significant value in future research.

The specific aims of this PhD thesis are:

1. To design a library of compounds, based on the structure of avobenzone, to improve the physiochemical and ADME-Tox properties of the lead compound in line with current neurological drugs.
2. To establish a suitable screening process for compounds identified in aim 1 to test their ability to increase Pum and/or are anticonvulsant in both *Drosophila* and rodent models of seizure.
3. Determine, based on the outcome of aims 1 and 2, whether Pum is a viable target for the design of improved AEDs.

The main overall objectives are to design and test a compound that is effective at reducing seizure severity in a variety of both rodent and *Drosophila* models, and to highlight the effectiveness of *Drosophila* as a model organism for screening AEDs that translates into similar results in rodent models. A compound that successfully increases Pum activity would have the potential to be used as a tool compound in future research, or lead to the development of more compounds which target Pum to treat epilepsy.

## 1.7 Bibliography

- Abou-Khalil, Bassel. 2008. 'Levetiracetam in the Treatment of Epilepsy'. *Neuropsychiatric Disease and Treatment* 4 (3): 507.
- Akyuz, Enes, Ayse Kristina Polat, Ece Eroglu, Irem Kullu, Efthalia Angelopoulou, and Yam Nath Paudel. 2020. 'Revisiting the Role of Neurotransmitters in Epilepsy: An Updated Review'. *Life Sciences*, 118826.
- Aradi, Ildiko, Vijayalakshmi Santhakumar, Kang Chen, and Ivan Soltesz. 2002. 'Postsynaptic Effects of GABAergic Synaptic Diversity: Regulation of Neuronal Excitability by Changes in IPSC Variance'. *Neuropharmacology* 43 (4): 511–22.
- Ayata, C, M Shimizu-Sasamata, E H Lo, J L Noebels, and M A Moskowitz. 1999. 'Impaired Neurotransmitter Release and Elevated Threshold for Cortical Spreading Depression in Mice with Mutations in the A1A Subunit of P/Q Type Calcium Channels'. *Neuroscience* 95 (3): 639–45.
- Bai, Jihong, and Edwin R Chapman. 2004. 'The C2 Domains of Synaptotagmin—Partners in Exocytosis'. *Trends in Biochemical Sciences* 29 (3): 143–51.
- Baines, R A, and M Bate. 1998. 'Electrophysiological Development of Central Neurons in the Drosophila Embryo.' *The Journal of Neuroscience : The Official Journal of the Society for Neuroscience* 18 (12): 4673–83.
- Baines, Richard A. 2005. 'Neuronal Homeostasis through Translational Control'. *Molecular Neurobiology* 32 (2): 113–21.
- Baines, Richard A., Carlo N.G. Giachello, and Wei-Hsiang Lin. 2017. 'Drosophila'. In *Models of Seizures and Epilepsy*, 345–58. Elsevier. <https://doi.org/10.1016/B978-0-12-804066-9.00024-9>.
- Baines, Richard A, Laurent Seugnet, Annemarie Thompson, Paul M Salvaterra, and Michael Bate. 2002. 'Regulation of Synaptic Connectivity: Levels of Fasciclin II Influence Synaptic Growth in the Drosophila CNS.' *The Journal of Neuroscience : The Official Journal of the Society for Neuroscience* 22 (15): 6587–95. <https://doi.org/20026681>.
- Banerjee, Pradeep K, Niranjala J K Tillakaratne, Simon Brailowsky, Richard W Olsen, Allan J Tobin, and O Carter Snead. 1998. 'Alterations in GABA A Receptor A1 and A4 Subunit mRNA Levels in Thalamic Relay Nuclei Following Absence-like Seizures in Rats'. *Experimental Neurology* 154 (1): 213–23.
- Baraban, Scott C., Matthew T. Dinday, and Gabriela A. Hortopan. 2013. 'Drug Screening in Scn1a Zebrafish Mutant Identifies Clemizole as a Potential Dravet Syndrome Treatment'. *Nature Communications* 4 (September): 2410. <https://doi.org/10.1038/ncomms3410>.
- Bargmann, C. I. 1998. 'Neurobiology of the Caenorhabditis Elegans Genome'. *Science* 282 (5396): 2028–33. <https://doi.org/10.1126/science.282.5396.2028>.
- Baulac, Stéphanie, Gilles Huberfeld, Isabelle Gourfinkel-An, Georgia Mitropoulou, Alexandre Beranger, Jean-François Prud'homme, Michel Baulac, Alexis Brice, Roberto Bruzzone, and Eric LeGuern. 2001. 'First Genetic Evidence of GABAA Receptor Dysfunction in Epilepsy: A Mutation in the  $\gamma 2$ -Subunit Gene'. *Nature Genetics* 28 (1): 46–48.

- Becker, Albert J, Julika Pitsch, Dmitry Sochivko, Thoralf Opitz, Matthäus Staniek, Chien-Chang Chen, Kevin P Campbell, Susanne Schoch, Yoel Yaari, and Heinz Beck. 2008. 'Transcriptional Upregulation of Cav3. 2 Mediates Epileptogenesis in the Pilocarpine Model of Epilepsy'. *Journal of Neuroscience* 28 (49): 13341–53.
- Ben-Menachem, Elinor. 2004. 'Pregabalin Pharmacology and Its Relevance to Clinical Practice'. *Epilepsia* 45 (s6): 13–18. <https://doi.org/10.1111/j.0013-9580.2004.455003.x>.
- Berkovic, Samuel F., Sarah E. Heron, Lucio Giordano, Carla Marini, Renzo Guerrini, Robert E. Kaplan, Antonio Gambardella, et al. 2004. 'Benign Familial Neonatal-Infantile Seizures: Characterization of a New Sodium Channelopathy'. *Annals of Neurology* 55 (4): 550–57. <https://doi.org/10.1002/ana.20029>.
- Bertram, Edward. 2007. 'The Relevance of Kindling for Human Epilepsy'. *Epilepsia* 48 (s2): 65–74. <https://doi.org/10.1111/j.1528-1167.2007.01068.x>.
- Birnbaum, Shari G, Andrew W Varga, Li-Lian Yuan, Anne E Anderson, J David Sweatt, and Laura A Schrader. 2004. 'Structure and Function of Kv4-Family Transient Potassium Channels'. *Physiological Reviews* 84 (3): 803–33.
- Blumenfeld, Hal. 2005. 'Cellular and Network Mechanisms of Spike-wave Seizures'. *Epilepsia* 46 (s9): 21–33.
- Bonilha, Leonardo, Jordan J. Elm, Jonathan C. Edwards, Paul S. Morgan, Christian Hicks, Carl Lozar, Zoran Rumboldt, Donna R. Roberts, Chris Rorden, and Mark A. Eckert. 2010. 'How Common Is Brain Atrophy in Patients with Medial Temporal Lobe Epilepsy?' *Epilepsia* 51 (9): 1774–79. <https://doi.org/10.1111/j.1528-1167.2010.02576.x>.
- Bourinet, Emmanuel, Tuck W Soong, Kathy Sutton, Sarah Slaymaker, Eleanor Mathews, Arnaud Monteil, Gerald W Zamponi, Joel Nargeot, and Terry P Snutch. 1999. 'Splicing of A1A Subunit Gene Generates Phenotypic Variants of P-and Q-Type Calcium Channels'. *Nature Neuroscience* 2 (5): 407–15.
- Bozzi, Yuri, and Emiliana Borrelli. 2013. 'The Role of Dopamine Signaling in Epileptogenesis'. *Frontiers in Cellular Neuroscience* 7.
- Branco, Tiago, Kevin Staras, Kevin J Darcy, and Yukiko Goda. 2008. 'Local Dendritic Activity Sets Release Probability at Hippocampal Synapses'. *Neuron* 59 (3): 475–85.
- Brenner, S. 1974. 'The Genetics of *Caenorhabditis Elegans*.' 77 (1): 71–94.
- Browne, David L, Stephen T Gancher, John G Nutt, Ewout R P Brunt, Eric A Smith, Patricia Kramer, and Michael Litt. 1994. 'Episodic Ataxia/Myokymia Syndrome Is Associated with Point Mutations in the Human Potassium Channel Gene, KCNA1'. *Nature Genetics* 8 (2): 136–40.
- Browning, R A, and D K Nelson. 1985. 'Variation in Threshold and Pattern of Electroshock-Induced Seizures in Rats Depending on Site of Stimulation.' *Life Sciences* 37 (23): 2205–11.
- Budelli, Gonzalo, Travis A Hage, Aguan Wei, Patricio Rojas, Yuh-Jiin Ivy Jong, Karen O'malley, and Lawrence Salkoff. 2009. 'Na+-Activated K+ Channels Express a Large Delayed Outward Current in Neurons during Normal Physiology'. *Nature Neuroscience* 12 (6): 745–50.
- Cain, Stuart M, Michael E Hildebrand, and Terrance P Snutch. 2014. 'T-Type Calcium Channels and Epilepsy'. In *Pathologies of Calcium Channels*, 77–96. Springer.

- Cantrell, Ann, and David J McGarvey. 2001. 'Photochemical Studies of 4-Tert-Butyl-4'-Methoxydibenzoylmethane (BM-DBM)'. *Journal of Photochemistry and Photobiology B: Biology* 64 (2–3): 117–22. [https://doi.org/10.1016/S1011-1344\(01\)00226-3](https://doi.org/10.1016/S1011-1344(01)00226-3).
- Catterall, William A. 2014. 'Sodium Channels, Inherited Epilepsy, and Antiepileptic Drugs'. *Annual Review of Pharmacology and Toxicology* 54 (1): 317–38. <https://doi.org/10.1146/annurev-pharmtox-011112-140232>.
- Cavalheiro, E A, N F Santos, and M R Priel. 1996. 'The Pilocarpine Model of Epilepsy in Mice'. *Epilepsia* 37 (10): 1015–19.
- Chang, Pishan, Katrin Augustin, Kim Boddum, Sophie Williams, Min Sun, John A Terschak, Jörg D Hardege, Philip E Chen, Matthew C Walker, and Robin S B Williams. 2016. 'Seizure Control by Decanoic Acid through Direct AMPA Receptor Inhibition'. *Brain* 139 (2): 431–43.
- Chang, Wen-Pin, and Thomas C Südhof. 2009. 'SV2 Renders Primed Synaptic Vesicles Competent for Ca<sup>2+</sup>-Induced Exocytosis'. *Journal of Neuroscience* 29 (4): 883–97.
- Chayasirisobhon, Sirichai. 2020. 'Mechanisms of Action and Pharmacokinetics of Cannabis.' *The Permanente Journal* 25: 1–3.
- Cheah, Christine S, Frank H Yu, Ruth E Westenbroek, Franck K Kalume, John C Oakley, Gregory B Potter, John L Rubenstein, and William A Catterall. 2012. 'Specific Deletion of NaV1.1 Sodium Channels in Inhibitory Interneurons Causes Seizures and Premature Death in a Mouse Model of Dravet Syndrome.' *Proceedings of the National Academy of Sciences of the United States of America* 109 (36): 14646–51. <https://doi.org/10.1073/pnas.1211591109>.
- Chen, Yuan, H Yu Frank, Elizabeth M Sharp, Daniel Beacham, Todd Scheuer, and William A Catterall. 2008. 'Functional Properties and Differential Neuromodulation of Na V 1.6 Channels'. *Molecular and Cellular Neuroscience* 38 (4): 607–15.
- Collingridge, Graham L, John T R Isaac, and Yu Tian Wang. 2004. 'Receptor Trafficking and Synaptic Plasticity'. *Nature Reviews Neuroscience* 5 (12): 952–62.
- Collingridge, Graham L., Richard W. Olsen, John Peters, and Michael Spedding. 2009. 'A Nomenclature for Ligand-Gated Ion Channels'. *Neuropharmacology* 56 (1): 2–5. <https://doi.org/10.1016/j.neuropharm.2008.06.063>.
- Colombo, J. A., E. Fuchs, W. Härtig, L. R. Marotte, and V. Puissant. 2000. "'Rodent-like" and "primate-like" Types of Astroglial Architecture in the Adult Cerebral Cortex of Mammals: A Comparative Study'. *Anatomy and Embryology* 201 (2): 111–20. <https://doi.org/10.1007/PL00008231>.
- Cooper, Edward C, Kenneth D Aldape, Aviva Abosch, Nicholas M Barbaro, Mitchel S Berger, Warwick S Peacock, Yuh Nung Jan, and Lily Yeh Jan. 2000. 'Colocalization and Coassembly of Two Human Brain M-Type Potassium Channel Subunits That Are Mutated in Epilepsy'. *Proceedings of the National Academy of Sciences* 97 (9): 4914–19.
- Copmans, Daniëlle, Aleksandra Siekierska, and Peter A.M. de Witte. 2017. 'Zebrafish Models of Epilepsy and Epileptic Seizures'. In *Models of Seizures and Epilepsy*, 369–84. Elsevier. <https://doi.org/10.1016/B978-0-12-804066-9.00026-2>.
- Coppola, G, P Plouin, C Chiron, O Robain, and O Dulac. 1995. 'Migrating Partial Seizures in Infancy: A Malignant Disorder with Developmental Arrest'. *Epilepsia* 36 (10): 1017–24.

- Dalmau, Josep, and Francesc Graus. 2018. 'Antibody-Mediated Encephalitis'. *New England Journal of Medicine* 378 (9): 840–51. <https://doi.org/10.1056/nejmra1708712>.
- Dang, Louis T., and Jack M. Parent. 2017. 'Genetic Epilepsy Modeling With Human Pluripotent Stem Cells'. In *Models of Seizures and Epilepsy*, 247–60. Elsevier. <https://doi.org/10.1016/B978-0-12-804066-9.00017-1>.
- Davis, Kathryn Adamiak, Ravi Prakash Reddy Nanga, Sandhitsu Das, Stephanie H. Chen, Peter N. Hadar, John R. Pollard, Timothy H. Lucas, et al. 2015. 'Glutamate Imaging (GluCEST) Lateralizes Epileptic Foci in Nonlesional Temporal Lobe Epilepsy'. *Science Translational Medicine* 7 (309). <https://doi.org/10.1126/scitranslmed.aaa7095>.
- Deepak, Doddabele, Christina Daousi, Mohsen Javadpour, and Ian A MacFarlane. 2007. 'Macroprolactinomas and Epilepsy'. *Clinical Endocrinology* 66 (4): 503–7.
- Dravet, Charlotte. 2011. 'The Core Dravet Syndrome Phenotype'. *Epilepsia* 52 (s2): 3–9. <https://doi.org/10.1111/j.1528-1167.2011.02994.x>.
- Driscoll, H. E., N. I. Muraro, M. He, and R. A. Baines. 2013. 'Pumilio-2 Regulates Translation of Nav1.6 to Mediate Homeostasis of Membrane Excitability'. *Journal of Neuroscience* 33 (23): 9644–54. <https://doi.org/10.1523/JNEUROSCI.0921-13.2013>.
- Dubnau, Josh, Ann-Shyn Chiang, Lori Grady, Jody Barditch, Scott Gossweiler, John McNeil, Patrick Smith, et al. 2003. 'The Staufén/Pumilio Pathway Is Involved in Drosophila Long-Term Memory'. *Current Biology : CB* 13 (4): 286–96. [https://doi.org/10.1016/S0960-9822\(03\)00064-2](https://doi.org/10.1016/S0960-9822(03)00064-2).
- During, M. J., and D. D. Spencer. 1993. 'Extracellular Hippocampal Glutamate and Spontaneous Seizure in the Conscious Human Brain'. *The Lancet* 341 (8861): 1607–10. [https://doi.org/10.1016/0140-6736\(93\)90754-5](https://doi.org/10.1016/0140-6736(93)90754-5).
- Echegoyen, Julio, Axel Neu, Kevin D Graber, and Ivan Soltesz. 2007. 'Homeostatic Plasticity Studied Using in Vivo Hippocampal Activity-Blockade: Synaptic Scaling, Intrinsic Plasticity and Age-Dependence'. *PLoS One* 2 (8): e700.
- Ekeberg, Örjan, Peter Wallén, Anders Lansner, Hans Tråvén, Lennart Brodin, and Sten Grillner. 1991. 'A Computer Based Model for Realistic Simulations of Neural Networks'. *Biological Cybernetics* 65 (2): 81–90.
- Epi4K, Andrew S. Allen, Samuel F. Berkovic, Patrick Cossette, Norman Delanty, Dennis Dlugos, Evan E. Eichler, et al. 2013. 'De Novo Mutations in Epileptic Encephalopathies'. *Nature* 501 (7466): 217–21. <https://doi.org/10.1038/nature12439>.
- Epps, S Alisha, and David Weinshenker. 2013. 'Rhythm and Blues: Animal Models of Epilepsy and Depression Comorbidity'. *Biochemical Pharmacology* 85 (2): 135–46.
- Epsztein, Jérôme, Alfonso Represa, Isabel Jorquera, Yehezkel Ben-Ari, and Valérie Crépel. 2005. 'Recurrent Mossy Fibers Establish Aberrant Kainate Receptor-Operated Synapses on Granule Cells from Epileptic Rats'. *Journal of Neuroscience* 25 (36): 8229–39.
- Estacion, Mark, Janelle E O'Brien, Allison Conravey, Michael F Hammer, Stephen G Waxman, Sulayman D Dib-Hajj, and Miriam H Meisler. 2014. 'A Novel de Novo Mutation of SCN8A (Nav1.6) with Enhanced Channel Activation in a Child with Epileptic Encephalopathy'. *Neurobiology of Disease* 69 (Supplement C): 117–23. <https://doi.org/https://doi.org/10.1016/j.nbd.2014.05.017>.

- Eunson, L H, R Rea, S M Zuberi, S Youroukos, C P Panayiotopoulos, R Liguori, P Avoni, R C McWilliam, J B P Stephenson, and M G Hanna. 2000. 'Clinical, Genetic, and Expression Studies of Mutations in the Potassium Channel Gene KCNA 1 Reveal New Phenotypic Variability'. *Annals of Neurology* 48 (4): 647–56.
- Evans, M Steven, Kimberly E Viola-McCabe, Donald M Caspary, and Carl L Faingold. 1994. 'Loss of Synaptic Inhibition during Repetitive Stimulation in Genetically Epilepsy-Prone Rats (GEPR)'. *Epilepsy Research* 18 (2): 97–105.
- Evans, Rhian M, and Gerald W Zamponi. 2006. 'Presynaptic Ca<sup>2+</sup> Channels—Integration Centers for Neuronal Signaling Pathways'. *Trends in Neurosciences* 29 (11): 617–24.
- Faure, Jean-Baptiste, José E. Marques-Carneiro, Gladys Akimana, Brigitte Cosquer, Arielle Ferrandon, Karine Herbeaux, Estelle Koning, Alexandra Barbelivien, Astrid Nehlig, and Jean-Christophe Cassel. 2014. 'Attention and Executive Functions in a Rat Model of Chronic Epilepsy'. *Epilepsia* 55 (5): 644–53. <https://doi.org/10.1111/epi.12549>.
- Fiore, Roberto, Marek Rajman, Chrysovalandis Schwale, Silvia Bicker, Anna Antoniou, Claus Bruehl, Andreas Draguhn, and Gerhard Schratt. 2014. 'MiR-134-dependent Regulation of Pumilio-2 Is Necessary for Homeostatic Synaptic Depression'. *The EMBO Journal* 33 (19): 2231 LP – 2246.
- Fire, Andrew, SiQun Xu, Mary K. Montgomery, Steven A. Kostas, Samuel E. Driver, and Craig C. Mello. 1998. 'Potent and Specific Genetic Interference by Double-Stranded RNA in *Caenorhabditis Elegans*'. *Nature* 391 (6669): 806–11. <https://doi.org/10.1038/35888>.
- Fisher, Robert S, Walter van Emde Boas, Warren Blume, Christian Elger, Pierre Genton, Phillip Lee, and Jerome Engel. 2005. 'Epileptic Seizures and Epilepsy: Definitions Proposed by the International League Against Epilepsy (ILAE) and the International Bureau for Epilepsy (IBE)'. *Epilepsia* 46 (4): 470–72. <https://doi.org/10.1111/j.0013-9580.2005.66104.x>.
- Fisher, Robert S., J. Helen Cross, Carol D'Souza, Jacqueline A. French, Sheryl R. Haut, Norimichi Higurashi, Edouard Hirsch, et al. 2017. 'Instruction Manual for the ILAE 2017 Operational Classification of Seizure Types'. *Epilepsia* 58 (4): 531–42. <https://doi.org/10.1111/epi.13671>.
- Flavell, Steven W., and Michael E. Greenberg. 2008. 'Signaling Mechanisms Linking Neuronal Activity to Gene Expression and Plasticity of the Nervous System'. *Annual Review of Neuroscience*. Annual Reviews . <https://doi.org/10.1146/annurev.neuro.31.060407.125631>.
- Fouda, Mohamed A, and Peter C Ruben. 2020. 'Action Potentials: Generation and Propagation'. In *ELS*, 1–8. <https://doi.org/https://doi.org/10.1002/9780470015902.a0000278.pub3>.
- Frankel, Wayne N., Laura Taylor, Barbara Beyer, Bruce L. Tempel, and H.Steve White. 2001. 'Electroconvulsive Thresholds of Inbred Mouse Strains'. *Genomics* 74 (3): 306–12. <https://doi.org/10.1006/geno.2001.6564>.
- Gariboldi, Marco, Piotr Tutka, Rosario Samanin, and Annamaria Vezzani. 1996. 'Stimulation of 5-HT<sub>1A</sub> Receptors in the Dorsal Hippocampus and Inhibition of Limbic Seizures Induced by Kainic Acid in Rats'. *British Journal of Pharmacology* 119 (5): 813–18.
- Gerber, A. P., S. Luschnig, M. A. Krasnow, P. O. Brown, and D. Herschlag. 2006. 'Genome-Wide Identification of MRNAs Associated with the Translational Regulator PUMILIO in *Drosophila Melanogaster*'. *Proceedings of the National Academy of Sciences* 103 (12): 4487–92. <https://doi.org/10.1073/pnas.0509260103>.

- Glasscock, Edward, and Mark A Tanouye. 2005. 'Drosophila Couch Potato Mutants Exhibit Complex Neurological Abnormalities Including Epilepsy Phenotypes.' *Genetics* 169 (4): 2137–49. <https://doi.org/10.1534/genetics.104.028357>.
- Glauser, Tracy A, Avital Cnaan, Shlomo Shinnar, Deborah G Hirtz, Dennis Dlugos, David Masur, Peggy O Clark, Peter C Adamson, and Childhood Absence Epilepsy Study Team. 2013. 'Ethosuximide, Valproic Acid, and Lamotrigine in Childhood Absence Epilepsy: Initial Monotherapy Outcomes at 12 Months'. *Epilepsia* 54 (1): 141–55.
- Goddard, G V, D C McIntyre, and C K Leech. 1969. 'A Permanent Change in Brain Function Resulting from Daily Electrical Stimulation.' *Experimental Neurology* 25 (3): 295–330.
- Goldenberg, Marvin M. 2010. 'Overview of Drugs Used For Epilepsy and Seizures: Etiology, Diagnosis, and Treatment'. *Pharmacy and Therapeutics* 35 (7): 392–415.
- Goldstrohm, Aaron C, Traci M Tanaka Hall, and Katherine M McKenney. 2018. 'Post-Transcriptional Regulatory Functions of Mammalian Pumilio Proteins'. *Trends in Genetics* 34 (12): 972–90.
- Gong, Pan, Xianru Jiao, Dan Yu, and Zhixian Yang. 2021. 'Case Report: Causative De Novo Variants of KCNT2 for Developmental and Epileptic Encephalopathy'. *Frontiers in Genetics* 12: 649556.
- Gorter, Jan A., and Erwin A. van Vliet. 2017. 'Post-Status Epilepticus Models: Electrical Stimulation'. In *Models of Seizures and Epilepsy*, 637–50. Elsevier. <https://doi.org/10.1016/B978-0-12-804066-9.00044-4>.
- Greenwood, Jessica, and Jose Valdes. 2016. 'Perampanel (Fycompa): A Review of Clinical Efficacy and Safety in Epilepsy'. *Pharmacy and Therapeutics* 41 (11): 683.
- Griffin, Aliesha, Kyla R. Hamling, Kelly Knupp, SoonGweon Hong, Luke P. Lee, and Scott C. Baraban. 2017. 'Clemizole and Modulators of Serotonin Signalling Suppress Seizures in Dravet Syndrome'. *Brain* 140 (3): aww342. <https://doi.org/10.1093/brain/aww342>.
- Groseclose, M Reid, and Stephen Castellino. 2019. 'An Investigation into Retigabine (Ezogabine) Associated Dyspigmentation in Rat Eyes by MALDI Imaging Mass Spectrometry'. *Chemical Research in Toxicology* 32 (2): 294–303.
- Guillerm, Vincent, Dongwook Kim, Jarrod F. Eubank, Ryan Luebke, Xinfang Liu, Karim Adil, Myoung Soo Lah, and Mohamed Eddaoudi. 2014. 'A Supramolecular Building Approach for the Design and Construction of Metal–Organic Frameworks'. *Chem. Soc. Rev.* 43 (16): 6141–72. <https://doi.org/10.1039/C4CS00135D>.
- Hamid, Hamada, and Andres M Kanner. 2013. 'Should Antidepressant Drugs of the Selective Serotonin Reuptake Inhibitor Family Be Tested as Antiepileptic Drugs?' *Epilepsy & Behavior* 26 (3): 261–65.
- Hanada, Takahisa. 2020. 'Ionotropic Glutamate Receptors in Epilepsy: A Review Focusing on Ampa and Nmda Receptors'. *Biomolecules*. MDPI AG. <https://doi.org/10.3390/biom10030464>.
- Harkin, Louise A, David N Bowser, Leanne M Dibbens, Rita Singh, Fiona Phillips, Robyn H Wallace, Michaela C Richards, David A Williams, John C Mulley, and Samuel F Berkovic. 2002. 'Truncation of the GABA A-Receptor  $\Gamma 2$  Subunit in a Family with Generalized Epilepsy with Febrile Seizures Plus'. *The American Journal of Human Genetics* 70 (2): 530–36.
- Harris, Eric W, and Carl W Cotman. 1986. 'Long-Term Potentiation of Guinea Pig Mossy Fiber Responses Is Not Blocked by N-Methyl D-Aspartate Antagonists'. *Neuroscience Letters* 70 (1): 132–37.

- Hauser, W Allen, John F Annegers, and Leonard T Kurland. 1991. 'Prevalence of Epilepsy in Rochester, Minnesota: 1940–1980'. *Epilepsia* 32 (4): 429–45.
- Hebb, Donald Olding. 1949. *The Organisation of Behaviour: A Neuropsychological Theory*. Science Editions New York.
- Heiss, John D, Stuart Walbridge, R N Rene'Smith, Susumu Sato, Edward H Oldfield, and Russell R Lonser. 2012. '174; Convection-Enhanced Delivery of Muscimol to the Epileptic Focus'. *Neurosurgery* 71 (2): E568.
- Hekmat-Scafe, Daria S., Kim N. Dang, and Mark A. Tanouye. 2005. 'Seizure Suppression by Gain-of-Function *Escargot* Mutations'. *Genetics* 169 (3): 1477–93. <https://doi.org/10.1534/genetics.104.036558>.
- Hochbaum, Maja, Ricardo Kienitz, Felix Rosenow, Juliane Schulz, Lena Habermehl, Lisa Langenbruch, Stjepana Kovac, Susanne Knake, Felix von Podewils, and Sophie von Brauchitsch. 2022. 'Trends in Antiseizure Medication Prescription Patterns among All Adults, Women, and Older Adults with Epilepsy: A German Longitudinal Analysis from 2008 to 2020'. *Epilepsy & Behavior* 130: 108666.
- HODGKIN, A L, and A F HUXLEY. 1952. 'A Quantitative Description of Membrane Current and Its Application to Conduction and Excitation in Nerve.' *The Journal of Physiology* 117 (4): 500–544.
- Huttenlocher, P R, A J Wilbourn, and J M Signore. 1971. 'Medium-Chain Triglycerides as a Therapy for Intractable Childhood Epilepsy.' *Neurology* 21 (11): 1097–1103.
- Ijff, Dominique M, and Albert P Aldenkamp. 2013. 'Cognitive Side-Effects of Antiepileptic Drugs in Children.' *Handbook of Clinical Neurology* 111: 707–18. <https://doi.org/10.1016/B978-0-444-52891-9.00073-7>.
- Imbrici, Paola, Maria Cristina D'adamo, Dimitri M Kullmann, and Mauro Pessia. 2006. 'Episodic Ataxia Type 1 Mutations in the KCNA1 Gene Impair the Fast Inactivation Properties of the Human Potassium Channels Kv1. 4-1.1/Kvβ1. 1 and Kv1. 4-1.1/Kvβ1. 2'. *European Journal of Neuroscience* 24 (11): 3073–83.
- Jeavons, P. M. 1984. 'Non-Dose-Related Side Effects of Valproate'. *Epilepsia* 25 (s1): S50–55. <https://doi.org/10.1111/j.1528-1157.1984.tb05638.x>.
- Jirsa, Viktor K., William C. Stacey, Pascale P. Quilichini, Anton I. Ivanov, and Christophe Bernard. 2014. 'On the Nature of Seizure Dynamics'. *Brain* 137 (8): 2210–30. <https://doi.org/10.1093/brain/awu133>.
- Johannesen, Katrine M., Elena Gardella, Alejandra C. Encinas, Anna Elina Lehesjoki, Tarja Linnankivi, Michael B. Petersen, Ida Charlotte Bay Lund, et al. 2019. 'The Spectrum of Intermediate SCN8A-Related Epilepsy'. *Epilepsia* 60 (5): 830–44. <https://doi.org/10.1111/epi.14705>.
- Johannessen Landmark, Cecilie, Pål G. Larsson, Elisif Rytter, and Svein I. Johannessen. 2009. 'Antiepileptic Drugs in Epilepsy and Other Disorders—A Population-Based Study of Prescriptions'. *Epilepsy Research* 87 (1): 31–39. <https://doi.org/10.1016/J.EPILEPSYRES.2009.07.005>.
- Kandratavicius, Ludmyla, Priscila Alves Balista, Cleiton Lopes-Aguiar, Rafael Naime Ruggiero, Eduardo Henrique Umeoka, Norberto Garcia-Cairasco, Lezio Soares Bueno-Junior, and Joao Pereira Leite. 2014. 'Animal Models of Epilepsy: Use and Limitations.' *Neuropsychiatric Disease and Treatment* 10: 1693–1705. <https://doi.org/10.2147/NDT.S50371>.

- Kaplan, David I, Lori Isom, and Steven Petrou. 2016. '17. Role of Sodium Channels in Epilepsy'. *Cold Spring Harbor Perspectives in Medicine* 6 (6): a022814. <https://doi.org/10.1101/cshperspect.a022814>.
- Kapur, Jaideep, and Robert L Macdonald. 1997. 'Rapid Seizure-Induced Reduction of Benzodiazepine and Zn<sup>2+</sup> Sensitivity of Hippocampal Dentate Granule Cell GABA<sub>A</sub> Receptors'. *Journal of Neuroscience* 17 (19): 7532–40.
- Keyser, Jacques De, Geert Sulter, and Paul G. Luiten. 1999. 'Clinical Trials with Neuroprotective Drugs in Acute Ischaemic Stroke: Are We Doing the Right Thing?' *Trends in Neurosciences* 22 (12): 535–40. [https://doi.org/10.1016/S0166-2236\(99\)01463-0](https://doi.org/10.1016/S0166-2236(99)01463-0).
- Kimmel, Charles B., William W. Ballard, Seth R. Kimmel, Bonnie Ullmann, and Thomas F. Schilling. 1995. 'Stages of Embryonic Development of the Zebrafish'. *Developmental Dynamics* 203 (3): 253–310. <https://doi.org/10.1002/aja.1002030302>.
- Klassen, Tara, Caleb Davis, Alica Goldman, Dan Burgess, Tim Chen, David Wheeler, John McPherson, Traci Bourquin, Lora Lewis, and Donna Villasana. 2011. 'Exome Sequencing of Ion Channel Genes Reveals Complex Profiles Confounding Personal Risk Assessment in Epilepsy'. *Cell* 145 (7): 1036–48.
- Knowles, Sandra R, Lori E Shapiro, and Neil H Shear. 1999. 'Anticonvulsant Hypersensitivity Syndrome'. *Drug Safety* 21 (6): 489–501.
- Konopka, R J, and S Benzer. 1971. 'Clock Mutants of *Drosophila Melanogaster*'. *Proceedings of the National Academy of Sciences of the United States of America* 68 (9): 2112–16.
- Kovel, Carolien G F De, Miriam H Meisler, Eva H Brilstra, Frederique M C van Berkestijn, Ruben van't Slot, Stef van Lieshout, Isaac J Nijman, Janelle E O'Brien, Michael F Hammer, and Mark Estacion. 2014. 'Characterization of a de Novo SCN8A Mutation in a Patient with Epileptic Encephalopathy'. *Epilepsy Research* 108 (9): 1511–18.
- Krauss, Gregory L, Emilio Perucca, Elinor Ben-Menachem, Patrick Kwan, Jerry J Shih, David Squillacote, Haichen Yang, Michelle Gee, Jin Zhu, and Antonio Laurenza. 2013. 'Perampanel, a Selective, Noncompetitive A-amino-3-hydroxy-5-methyl-4-isoxazolepropionic Acid Receptor Antagonist, as Adjunctive Therapy for Refractory Partial-onset Seizures: Interim Results from Phase III, Extension Study 307'. *Epilepsia* 54 (1): 126–34.
- Kshatri, Aravind S, Alberto Gonzalez-Hernandez, and Teresa Giraldez. 2018. 'Physiological Roles and Therapeutic Potential of Ca<sup>2+</sup> Activated Potassium Channels in the Nervous System'. *Frontiers in Molecular Neuroscience* 11: 258.
- Kuebler, Daniel, and Mark Tanouye. 2002. 'Anticonvulsant Valproate Reduces Seizure-Susceptibility in Mutant *Drosophila*'. *Brain Research* 958 (1): 36–42.
- Kuebler, Daniel, Haiguang Zhang, Xiaoyun Ren, and Mark A. Tanouye. 2001. 'Genetic Suppression of Seizure Susceptibility in *Drosophila*'. *Journal of Neurophysiology* 86 (3): 1211–25. <https://doi.org/10.1152/jn.2001.86.3.1211>.
- Kullmann, Dimitri M, and Karri Lamsa. 2008. 'Roles of Distinct Glutamate Receptors in Induction of Anti-Hebbian Long-term Potentiation'. *The Journal of Physiology* 586 (6): 1481–86.
- Kwan, Patrick, Steven C Schachter, and Martin J Brodie. 2011. 'Drug-Resistant Epilepsy'. *New England Journal of Medicine* 365 (10): 919–26.

- Kwan, Patrick, Graeme J Sills, and Martin J Brodie. 2001. 'The Mechanisms of Action of Commonly Used Antiepileptic Drugs'. *Pharmacology & Therapeutics* 90 (1): 21–34.
- Kyle, Donald J, and Victor I Ilyin. 2007. 'Sodium Channel Blockers'. *Journal of Medicinal Chemistry* 50 (11): 2583–88.
- Lancaster, Madeline A, and Juergen A Knoblich. 2014. 'Generation of Cerebral Organoids from Human Pluripotent Stem Cells'. *Nature Protocols* 9 (10): 2329–40. <https://doi.org/10.1038/nprot.2014.158>.
- Lehmann, Ruth, and Christiane Nüsslein-Volhard. 1987. 'Involvement of the Pumilio Gene in the Transport of an Abdominal Signal in the Drosophila Embryo'. *Nature* 329 (September): 167.
- Lim, Chiao Xin, Michael G Ricos, Leanne M Dibbens, and Sarah E Heron. 2016. 'KCNT1 Mutations in Seizure Disorders: The Phenotypic Spectrum and Functional Effects'. *Journal of Medical Genetics* 53 (4): 217–25.
- Lin, Wei-Hsiang, Carlo N G Giachello, and Richard A Baines. 2017. 'Seizure Control through Genetic and Pharmacological Manipulation of Pumilio in <Em>Drosophila</Em>; A Key Component of Neuronal Homeostasis'. *Disease Models & Mechanisms* 10 (2): 141 LP – 150.
- Lin, Wei-Hsiang, Cengiz Günay, Richard Marley, Astrid A Prinz, and Richard A Baines. 2012. 'Activity-Dependent Alternative Splicing Increases Persistent Sodium Current and Promotes Seizure.' *The Journal of Neuroscience : The Official Journal of the Society for Neuroscience* 32 (21): 7267–77. <https://doi.org/10.1523/JNEUROSCI.6042-11.2012>.
- Linden, David J. 1999. 'The Return of the Spike: Postsynaptic Action Potentials and the Induction of LTP and LTD'. *Neuron* 22 (4): 661–66.
- Liu, Shijie, Yu Shen, Sandy R. Shultz, Anne Nguyen, Christopher Hovens, Paul A. Adlard, Ashley I. Bush, et al. 2017. 'Accelerated Kindling Epileptogenesis in Tg4510 Tau Transgenic Mice, but Not in Tau Knockout Mice'. *Epilepsia* 58 (9): e136–41. <https://doi.org/10.1111/epi.13847>.
- Löscher, W. 1997. 'Animal Models of Intractable Epilepsy.' *Progress in Neurobiology* 53 (2): 239–58.
- Löscher, Wolfgang. 2002. 'Animal Models of Epilepsy for the Development of Antiepileptogenic and Disease-Modifying Drugs. A Comparison of the Pharmacology of Kindling and Post-Status Epilepticus Models of Temporal Lobe Epilepsy.' *Epilepsy Research* 50 (1–2): 105–23.
- Löscher, Wolfgang, Henrik Klitgaard, Roy E Twyman, and Dieter Schmidt. 2013. 'New Avenues for Anti-Epileptic Drug Discovery and Development'. *Nature Reviews Drug Discovery* 12 (10): 757–76.
- Lothman, E W, and E H Bertram. 1993. 'Epileptogenic Effects of Status Epilepticus.' *Epilepsia* 34 Suppl 1: S59–70.
- Lu, K-T, and P-W Gean. 1998. 'Endogenous Serotonin Inhibits Epileptiform Activity in Rat Hippocampal CA1 Neurons via 5-Hydroxytryptamine1A Receptor Activation'. *Neuroscience* 86 (3): 729–37.
- Lugt, N M Van der, Jos Domen, Koert Linders, M Van Roon, Els Robanus-Maandag, H Te Riele, M Van der Valk, Jacqueline Deschamps, Michael Sofroniew, and M Van Lohuizen. 1994. 'Posterior Transformation, Neurological Abnormalities, and Severe Hematopoietic Defects in Mice with a Targeted Deletion of the Bmi-1 Proto-Oncogene.' *Genes & Development* 8 (7): 757–69.
- Lynch, Berkley A, Nathalie Lambeng, Karl Nocka, Patricia Kensel-Hammes, Sandra M Bajjalieh, Alain Matagne, and Bruno Fuks. 2004. 'The Synaptic Vesicle Protein SV2A Is the Binding Site for the

- Antiepileptic Drug Levetiracetam'. *Proceedings of the National Academy of Sciences* 101 (26): 9861–66.
- Lytton, William W. 2008. 'Computer Modelling of Epilepsy'. *Nature Reviews Neuroscience* 9 (8): 626–37. <https://doi.org/10.1038/nrn2416>.
- Macdonald, Robert L, and Kevin M Kelly. 1995. 'Antiepileptic Drug Mechanisms of Action'. *Epilepsia* 36 (s2).
- Maheshwari, Atul, and Jeffrey L. Noebels. 2014. 'Monogenic Models of Absence Epilepsy'. In *Progress in Brain Research*, 213:223–52. <https://doi.org/10.1016/B978-0-444-63326-2.00012-0>.
- Majumdar, Devashis, and Sephali Guha. 1988. 'Conformation, Electrostatic Potential and Pharmacophoric Pattern of GABA (Gamma-Aminobutyric Acid) and Several GABA Inhibitors'. *Journal of Molecular Structure: THEOCHEM* 180: 125–40.
- Malenka, Robert C. 1994. 'Synaptic Plasticity in the Hippocampus: LTP and LTD'. *Cell* 78 (4): 535–38.
- Marley, Richard, and Richard A. Baines. 2011. 'Increased Persistent Na<sup>+</sup> Current Contributes to Seizure in the Slamdance Bang-Sensitive *Drosophila* Mutant'. *Journal of Neurophysiology* 106 (1): 18–29. <https://doi.org/10.1152/jn.00808.2010>.
- Martinez, Ashley, Andrey Finegersh, Dara M Cannon, Irene Dustin, Alison Nugent, Peter Herscovitch, and William H Theodore. 2013. 'The 5-HT<sub>1A</sub> Receptor and 5-HT Transporter in Temporal Lobe Epilepsy'. *Neurology* 80 (16): 1465–71.
- McNamara, James O, Yang Zhong Huang, and A Soren Leonard. 2006. 'Molecular Signaling Mechanisms Underlying Epileptogenesis'. *Science Signaling* 2006 (356): re12–re12.
- Mee, C. J., Edward C G Pym, Kevin G Moffat, and Richard A Baines. 2004. 'Regulation of Neuronal Excitability through Pumilio-Dependent Control of a Sodium Channel Gene'. *Journal of Neuroscience* 24 (40): 8695–8703. <https://doi.org/10.1523/JNEUROSCI.2282-04.2004>.
- Meldrum, B S. 1993. 'Excitotoxicity and Selective Neuronal Loss in Epilepsy.' *Brain Pathology (Zurich, Switzerland)* 3 (4): 405–12.
- Micale, V, T Incognito, A Ignoto, L Rampello, M Sparta, and F Drago. 2006. 'Dopaminergic Drugs May Counteract Behavioral and Biochemical Changes Induced by Models of Brain Injury'. *European Neuropsychopharmacology* 16 (3): 195–203.
- Milan, David J, Travis A Peterson, Jeremy N Ruskin, Randall T Peterson, and Calum A MacRae. 2003. 'Drugs That Induce Repolarization Abnormalities Cause Bradycardia in Zebrafish.' *Circulation* 107 (10): 1355–58.
- Miles, Richard, and Robert K S Wong. 1983. 'Single Neurones Can Initiate Synchronized Population Discharge in the Hippocampus'. *Nature* 306 (5941): 371–73.
- Mistry, Akshitkumar M., Christopher H. Thompson, Alison R. Miller, Carlos G. Vanoye, Alfred L. George, and Jennifer A. Kearney. 2014. 'Strain- and Age-Dependent Hippocampal Neuron Sodium Currents Correlate with Epilepsy Severity in Dravet Syndrome Mice'. *Neurobiology of Disease* 65 (May): 1–11. <https://doi.org/10.1016/j.nbd.2014.01.006>.
- Morrell, M. J. 2011. 'Responsive Cortical Stimulation for the Treatment of Medically Intractable Partial Epilepsy'. *Neurology* 77 (13): 1295–1304. <https://doi.org/10.1212/WNL.0b013e3182302056>.

- Moscato, Emilia H., Xiaoyu Peng, Ankit Jain, Thomas D. Parsons, Josep Dalmau, and Rita J. Balice-Gordon. 2014. 'Acute Mechanisms Underlying Antibody Effects in Anti-N-Methyl-D-Aspartate Receptor Encephalitis'. *Annals of Neurology* 76 (1): 108–19. <https://doi.org/10.1002/ana.24195>.
- Moshé, Solomon L, Emilio Perucca, Philippe Ryvlin, and Torbjörn Tomson. 2015. 'Epilepsy: New Advances'. *The Lancet* 385 (9971): 884–98. [https://doi.org/10.1016/S0140-6736\(14\)60456-6](https://doi.org/10.1016/S0140-6736(14)60456-6).
- Mturi, Georges J., and Bice S. Martincigh. 2008. 'Photostability of the Sunscreening Agent 4-Tert-Butyl-4'-Methoxydibenzoylmethane (Avobenzone) in Solvents of Different Polarity and Proticity'. *Journal of Photochemistry and Photobiology A: Chemistry* 200 (2–3): 410–20. <https://doi.org/10.1016/J.JPHOTOCHEM.2008.09.007>.
- Muraro, N. I., A. J. Weston, A. P. Gerber, S. Luschnig, K. G. Moffat, and R. A. Baines. 2008. 'Pumilio Binds Para MRNA and Requires Nanos and Brat to Regulate Sodium Current in Drosophila Motoneurons'. *Journal of Neuroscience* 28 (9): 2099–2109. <https://doi.org/10.1523/JNEUROSCI.5092-07.2008>.
- Nakken, Karl O, Ann-Sofie Eriksson, Rasmus Lossius, and Svein I Johannessen. 2003. 'A Paradoxical Effect of Levetiracetam May Be Seen in Both Children and Adults with Refractory Epilepsy'. *Seizure* 12 (1): 42–46.
- Neal, Andrew, Bradford A. Moffat, Joel M. Stein, Ravi Prakash Reddy Nanga, Patricia Desmond, Russell T. Shinohara, Hari Hariharan, et al. 2019. 'Glutamate Weighted Imaging Contrast in Gliomas with 7 Tesla Magnetic Resonance Imaging'. *NeuroImage: Clinical* 22 (January): 101694. <https://doi.org/10.1016/j.nicl.2019.101694>.
- Neuman, R, E Cherubini, and Y Ben-Ari. 1988. 'Epileptiform Bursts Elicited in CA 3 Hippocampal Neurons by a Variety of Convulsants Are Not Blocked by N-Methyl-D-Aspartate Antagonists'. *Brain Research* 459 (2): 265–74.
- Neuray, Caroline, Reza Maroofian, Marcello Scala, Tipu Sultan, Gurpur S Pai, Majid Mojarrad, Heba El Khashab, Leigh deHoll, Wyatt Yue, and Hessa S Alsaif. 2020. 'Early-Infantile Onset Epilepsy and Developmental Delay Caused by Bi-Allelic GAD1 Variants'. *Brain* 143 (8): 2388–97.
- Newcomer, J W, N B Farber, and J W Olney. 2000. 'NMDA Receptor Function, Memory, and Brain Aging'. *Dialogues in Clinical Neuroscience* 2 (3): 219–32.
- Ngugi, Anthony K, Christian Bottomley, Immo Kleinschmidt, Josemir W Sander, and Charles R Newton. 2010. 'Estimation of the Burden of Active and Life-time Epilepsy: A Meta-analytic Approach'. *Epilepsia* 51 (5): 883–90.
- Nishimura, T., Y. Hu, M. Wu, E. Pham, H. Suemizu, M. Elazar, M. Liu, et al. 2013. 'Using Chimeric Mice with Humanized Livers to Predict Human Drug Metabolism and a Drug-Drug Interaction'. *Journal of Pharmacology and Experimental Therapeutics* 344 (2): 388–96. <https://doi.org/10.1124/jpet.112.198697>.
- Nissinen, Jari, Toivo Halonen, Esa Koivisto, and Asla Pitkänen. 2000. 'A New Model of Chronic Temporal Lobe Epilepsy Induced by Electrical Stimulation of the Amygdala in Rat'. *Epilepsy Research* 38 (2): 177–205. [https://doi.org/10.1016/S0920-1211\(99\)00088-1](https://doi.org/10.1016/S0920-1211(99)00088-1).
- Noebels, Jeffrey L. 2017. 'Spontaneous and Gene-Directed Epilepsy Mutations in the Mouse'. In *Models of Seizures and Epilepsy*, 763–76. Elsevier. <https://doi.org/10.1016/B978-0-12-804066-9.00052-3>.
- O'Leary, Timothy, and David J A Wyllie. 2011. 'Neuronal Homeostasis: Time for a Change?' *The Journal of Physiology* 589 (20): 4811–26.

- Pandey, U. B., and C. D. Nichols. 2011. 'Human Disease Models in *Drosophila Melanogaster* and the Role of the Fly in Therapeutic Drug Discovery'. *Pharmacological Reviews* 63 (2): 411–36. <https://doi.org/10.1124/pr.110.003293>.
- Pandolfo, Massimo. 2011. 'Genetics of Epilepsy'. *Seminars in Neurology* 31 (05): 506–18. <https://doi.org/10.1055/s-0031-1299789>.
- Papale, Ligia A, Barbara Beyer, Julie M Jones, Lisa M Sharkey, Sergio Tufik, Michael Epstein, Verity A Letts, Miriam H Meisler, Wayne N Frankel, and Andrew Escayg. 2009. 'Heterozygous Mutations of the Voltage-Gated Sodium Channel SCN8A Are Associated with Spike-Wave Discharges and Absence Epilepsy in Mice'. *Human Molecular Genetics* 18 (9): 1633–41.
- Parker, Louise, Miguel Padilla, Yuzhe Du, Ke Dong, and Mark A Tanouye. 2011. 'Drosophila as a Model for Epilepsy: Bss Is a Gain-of-Function Mutation in the Para Sodium Channel Gene That Leads to Seizures'. *Genetics* 187 (2): 523–34. <https://doi.org/10.1534/genetics.110.123299>.
- Passmore, Gayle M, Joanne M Reilly, Matthew Thakur, Vanessa N Keasberry, Stephen J Marsh, Anthony H Dickenson, and David A Brown. 2012. 'Functional Significance of M-Type Potassium Channels in Nociceptive Cutaneous Sensory Endings'. *Frontiers in Molecular Neuroscience* 5: 63.
- Patel, Dipan C, Karen S Wilcox, and Cameron S Metcalf. 2017. 'Novel Targets for Developing Antiseizure and, Potentially, Antiepileptogenic Drugs'. *Epilepsy Currents* 17 (5): 293–98. <https://doi.org/10.5698/1535-7597.17.5.293>.
- Pavlidis, Paul, Mani Ramaswami, and Mark A. Tanouye. 1994. 'The *Drosophila* Easily Shocked Gene: A Mutation in a Phospholipid Synthetic Pathway Causes Seizure, Neuronal Failure, and Paralysis'. *Cell* 79 (1): 23–33. [https://doi.org/10.1016/0092-8674\(94\)90397-2](https://doi.org/10.1016/0092-8674(94)90397-2).
- Pfisterer, Ulrich, Viktor Petukhov, Samuel Demharter, Johanna Meichsner, Jonatan J. Thompson, Mykhailo Y. Batiuk, Andrea Asenjo-Martinez, et al. 2020. 'Identification of Epilepsy-Associated Neuronal Subtypes and Gene Expression Underlying Epileptogenesis'. *Nature Communications* 2020 11:1 11 (1): 1–19. <https://doi.org/10.1038/s41467-020-18752-7>.
- Pinheiro, Paulo, and Christophe Mulle. 2006. 'Kainate Receptors'. *Cell and Tissue Research* 326 (2): 457–82.
- Prinz, Astrid A, Dirk Bucher, and Eve Marder. 2004. 'Similar Network Activity from Disparate Circuit Parameters'. *Nature Neuroscience* 7 (12): 1345–52.
- Pulver, Stefan R., Timothy G. Bayley, Adam L. Taylor, Jimena Berni, Michael Bate, and Berthold Hedwig. 2015. 'Imaging Fictive Locomotor Patterns in Larval *Drosophila*'. *Journal of Neurophysiology* 114 (5): 2564–77. <https://doi.org/10.1152/jn.00731.2015>.
- Puranam, Ram S, and James O McNamara. 1999. 'Seizure Disorders in Mutant Mice: Relevance to Human Epilepsies'. *Current Opinion in Neurobiology* 9 (3): 281–87. [https://doi.org/10.1016/S0959-4388\(99\)80041-5](https://doi.org/10.1016/S0959-4388(99)80041-5).
- Qian, Xuyu, Ha Nam Nguyen, Mingxi M. Song, Christopher Hadiono, Sarah C. Ogden, Christy Hammack, Bing Yao, et al. 2016. 'Brain-Region-Specific Organoids Using Mini-Bioreactors for Modeling ZIKV Exposure'. *Cell* 165 (5): 1238–54. <https://doi.org/10.1016/j.cell.2016.04.032>.
- Quadrato, Giorgia, Tuan Nguyen, Evan Z Macosko, John L Sherwood, Sung Min Yang, Daniel R Berger, Natalie Maria, Jorg Scholvin, Melissa Goldman, and Justin P Kinney. 2017. 'Cell Diversity and Network Dynamics in Photosensitive Human Brain Organoids'. *Nature* 545 (7652): 48–53.

- Rabinowitch, Ithai, and Idan Segev. 2006. 'The Interplay between Homeostatic Synaptic Plasticity and Functional Dendritic Compartments'. *Journal of Neurophysiology* 96 (1): 276–83.
- Raedt, R, A Van Dycke, D Van Melkebeke, T De Smedt, P Claeys, T Wyckhuys, K Vonck, W Wadman, and P Boon. 2009. 'Seizures in the Intrahippocampal Kainic Acid Epilepsy Model: Characterization Using Long-Term Video-EEG Monitoring in the Rat.' *Acta Neurologica Scandinavica* 119 (5): 293–303.
- Ragsdale, David S, Jancy C McPhee, Todd Scheuer, and William A Catterall. 1994. 'Molecular Determinants of State-Dependent Block of Na<sup>+</sup> Channels by Local Anesthetics'. *Science* 265 (5179): 1724–29.
- Represa, A, and Y Ben-Ari. 1997. 'Molecular and Cellular Cascades in Seizure-Induced Neosynapse Formation.' *Advances in Neurology* 72: 25–34.
- Reynolds, Elaine R., Eric A. Stauffer, Laura Feeney, Elizabeth Rojahn, Benjamin Jacobs, and Carol McKeever. 2004. 'Treatment with the Antiepileptic Drugs Phenytoin and Gabapentin Ameliorates Seizure and Paralysis Of *Drosophila* Bang-Sensitive Mutants'. *Journal of Neurobiology* 58 (4): 503–13. <https://doi.org/10.1002/neu.10297>.
- Richard, Muriel, Priska Kaufmann, Rüdiger Kornberger, and Jasper Dingemanse. 2019. 'First-in-man Study of ACT-709478, a Novel Selective Triple T-type Calcium Channel Blocker'. *Epilepsia* 60 (5): 968–78.
- Rogawski, Michael A. 1993. 'Therapeutic Potential of Excitatory Amino Acid Antagonists: Channel Blockers and 2,3-Benzodiazepines'. *Trends in Pharmacological Sciences* 14 (9): 325–31. [https://doi.org/10.1016/0165-6147\(93\)90005-5](https://doi.org/10.1016/0165-6147(93)90005-5).
- Rogawski, Michael A. 2011. 'Revisiting AMPA Receptors as an Antiepileptic Drug Target'. *Epilepsy Currents* 11 (2): 56–63.
- Romoli, Michele, Petra Mazzocchetti, Renato D'Alonzo, Sabrina Siliquini, Victoria E Rinaldi, Alberto Verrotti, Paolo Calabresi, and Cinzia Costa. 2019. 'Valproic Acid and Epilepsy: From Molecular Mechanisms to Clinical Evidences'. *Current Neuropharmacology* 17 (10): 926–46.
- Royden, Constance S., Vincenzo Pirrotta, and Lily Y. Jan. 1987. 'The *Tko* Locus, Site of a Behavioral Mutation in *D. Melanogaster*, Codes for a Protein Homologous to Prokaryotic Ribosomal Protein S12'. *Cell* 51 (2): 165–73. [https://doi.org/10.1016/0092-8674\(87\)90144-9](https://doi.org/10.1016/0092-8674(87)90144-9).
- Rugg-Gunn, Fergus. 2014. 'Adverse Effects and Safety Profile of Perampanel: A Review of Pooled Data'. *Epilepsia* 55 (January): 13–15. <https://doi.org/10.1111/epi.12504>.
- Salgado, Delanthi, and Karim A Alkadhi. 1995. 'Inhibition of Epileptiform Activity by Serotonin in Rat CA1 Neurons'. *Brain Research* 669 (2): 176–82.
- Sanders, Stephan J, Arthur J Campbell, Jeffrey R Cottrell, Rikke S Moller, Florence F Wagner, Angie L Auldridge, Raphael A Bernier, William A Catterall, Wendy K Chung, and James R Empfield. 2018. 'Progress in Understanding and Treating SCN2A-Mediated Disorders'. *Trends in Neurosciences* 41 (7): 442–56.
- Sayin, Umit, Susan Osting, Joshua Hagen, Paul Rutecki, and Thomas Sutula. 2003. 'Spontaneous Seizures and Loss of Axo-Axonic and Axo-Somatic Inhibition Induced by Repeated Brief Seizures in Kindled Rats' 23 (7): 2759–68.
- Scharfman, Helen E. 2007. 'The Neurobiology of Epilepsy.' *Current Neurology and Neuroscience Reports* 7 (4): 348–54.

- Schieweck, Rico, Therese Riedemann, Ignasi Forné, Max Harner, Karl E Bauer, Daniela Rieger, Foong yee Ang, Saskia Hutten, Antonia F Demleitner, and Bastian Popper. 2021. 'Pumilio2 and Staufe2 Selectively Balance the Synaptic Proteome'. *Cell Reports* 35 (12): 109279.
- Schmidt, Dieter, and Steven C Schachter. 2014. 'Drug Treatment of Epilepsy in Adults.' *BMJ (Clinical Research Ed.)* 348 (February): g254. <https://doi.org/10.1136/BMJ.G254>.
- Schoonjans, An-Sofie, Lieven Lagae, and Berten Ceulemans. 2015. 'Low-Dose Fenfluramine in the Treatment of Neurologic Disorders: Experience in Dravet Syndrome'. *Therapeutic Advances in Neurological Disorders* 8 (6): 328–38.
- Schutte, Soleil S., Ryan J. Schutte, Eden V. Barragan, and Diane K. O'Dowd. 2016. 'Model Systems for Studying Cellular Mechanisms of SCN1A -Related Epilepsy'. *Journal of Neurophysiology* 115 (4): 1755–66. <https://doi.org/10.1152/jn.00824.2015>.
- Shah, Niyathi Hegde, and Elias Aizenman. 2014. 'Voltage-Gated Potassium Channels at the Crossroads of Neuronal Function, Ischemic Tolerance, and Neurodegeneration'. *Translational Stroke Research* 5 (1): 38–58.
- Sharma, Alok K., Rachel Y. Reams, William H. Jordan, Margaret A. Miller, H. Leon Thacker, and Paul W. Snyder. 2007. 'Mesial Temporal Lobe Epilepsy: Pathogenesis, Induced Rodent Models and Lesions'. *Toxicologic Pathology* 35 (7): 984–99. <https://doi.org/10.1080/01926230701748305>.
- Siemen, Henrike, Damien Colas, H. Craig Heller, Oliver Brüstle, and Renee A. Reijo Pera. 2011. 'Pumilio-2 Function in the Mouse Nervous System'. Edited by Xiaoxi Zhuang. *PLoS ONE* 6 (10): e25932. <https://doi.org/10.1371/journal.pone.0025932>.
- Singh, Baljinder, Ikuo Ogiwara, Makoto Kaneda, Natsuko Tokonami, Emi Mazaki, Koichi Baba, Kazumi Matsuda, Yushi Inoue, and Kazuhiro Yamakawa. 2006. 'AK v 4.2 Truncation Mutation in a Patient with Temporal Lobe Epilepsy'. *Neurobiology of Disease* 24 (2): 245–53.
- Smart, Sharon L, Valeri Lopantsev, C L Zhang, Carol A Robbins, Hao Wang, S Y Chiu, Philip A Schwartzkroin, Albee Messing, and Bruce L Tempel. 1998. 'Deletion of the K V 1.1 Potassium Channel Causes Epilepsy in Mice'. *Neuron* 20 (4): 809–19.
- Smets, Katrien, Anna Duarri, Tine Deconinck, Berten Ceulemans, Bart P van de Warrenburg, Stephan Züchner, Michael Anthony Gonzalez, Rebecca Schüle, Matthias Synofzik, and Nathalie Van der Aa. 2015. 'First de Novo KCND3 Mutation Causes Severe Kv4. 3 Channel Dysfunction Leading to Early Onset Cerebellar Ataxia, Intellectual Disability, Oral Apraxia and Epilepsy'. *BMC Medical Genetics* 16 (1): 51.
- Sohal, Vikaas S., and Felice T. Sun. 2011. 'Responsive Neurostimulation Suppresses Synchronized Cortical Rhythms in Patients with Epilepsy'. *Neurosurgery Clinics of North America* 22 (4): 481–88. <https://doi.org/10.1016/j.nec.2011.07.007>.
- Sommer, Barbara R, Erica L Mitchell, and Tonita E Wroolie. 2013. 'Topiramate: Effects on Cognition in Patients with Epilepsy, Migraine Headache and Obesity.' *Therapeutic Advances in Neurological Disorders* 6 (4): 211–27. <https://doi.org/10.1177/1756285613481257>.
- Song, Juan, Joyce Hu, and Mark Tanouye. 2007. 'Seizure Suppression by Top1 Mutations in Drosophila.' *The Journal of Neuroscience : The Official Journal of the Society for Neuroscience* 27 (11): 2927–37. <https://doi.org/10.1523/JNEUROSCI.3944-06.2007>.

- Song, Juan, and Mark A. Tanouye. 2006. 'Seizure Suppression by *ShakB*<sup>2</sup>, a Gap Junction Mutation in *Drosophila*'. *Journal of Neurophysiology* 95 (2): 627–35. <https://doi.org/10.1152/jn.01059.2004>.
- Song, Juan, and Mark A. Tanouye. 2008. 'From Bench to Drug: Human Seizure Modeling Using *Drosophila*'. *Progress in Neurobiology* 84 (2): 182–91. <https://doi.org/10.1016/J.PNEUROBIO.2007.10.006>.
- Song, Yu-Fei, and Leroy Cronin. 2008. 'Postsynthetic Covalent Modification of Metal–Organic Framework (MOF) Materials'. *Angewandte Chemie International Edition* 47 (25): 4635–37.
- Spencer, Susan, and Linda Huh. 2008. 'Outcomes of Epilepsy Surgery in Adults and Children'. *The Lancet Neurology* 7 (6): 525–37.
- Srivastava, Ajay K., Anitha B. Alex, Karen S. Wilcox, and H. Steve White. 2013. 'Rapid Loss of Efficacy to the Antiseizure Drugs Lamotrigine and Carbamazepine: A Novel Experimental Model of Pharmacoresistant Epilepsy'. *Epilepsia* 54 (7): 1186–94. <https://doi.org/10.1111/epi.12234>.
- Stables, James P, Ed Bertram, F E Dudek, Greg Holmes, Gary Mathern, Asla Pitkanen, and H S White. 2003. 'Therapy Discovery for Pharmacoresistant Epilepsy and for Disease-Modifying Therapeutics: Summary of the NIH/NINDS/AES Models II Workshop'. *Epilepsia* 44 (12): 1472–78. <https://doi.org/10.1111/j.0013-9580.2003.32803.x>.
- Stefanescu, Roxana A., R.G. Shivakeshavan, and Sachin S. Talathi. 2012. 'Computational Models of Epilepsy'. *Seizure* 21 (10): 748–59. <https://doi.org/10.1016/J.SEIZURE.2012.08.012>.
- Steinberg, Daniel J, Srinivasarao Repudi, Afifa Saleem, Irina Kustanovich, Sergey Viukov, Baraa Abudiab, Ehud Banne, Muhammad Mahajnah, Jacob H Hanna, and Shani Stern. 2021. 'Modeling Genetic Epileptic Encephalopathies Using Brain Organoids'. *EMBO Molecular Medicine* 13 (8): e13610.
- Stewart, Lee S, Ying Wu, James H Eubanks, Hua Han, Yevgen Leschenko, Jose L Perez Velazquez, Miguel A Cortez, and O Carter Snead. 2009. 'Severity of Atypical Absence Phenotype in GABA B Transgenic Mice Is Subunit Specific'. *Epilepsy & Behavior* 14 (4): 577–81.
- Stover, J. F., U. E. Pleinesf, M. C. Morganti-Kossmannf, T. Kossmannf, K. Lowitzschj, and O. S. Kempfski. 1997. 'Neurotransmitters in Cerebrospinal Fluid Reflect Pathological Activity'. *European Journal of Clinical Investigation* 27 (12): 1038–43. <https://doi.org/10.1046/j.1365-2362.1997.2250774.x>.
- Streit, Anne K., Yuen Ngan Fan, Laura Masullo, and Richard A. Baines. 2016. 'Calcium Imaging of Neuronal Activity in *Drosophila* Can Identify Anticonvulsive Compounds'. Edited by Brian D. McCabe. *PLOS ONE* 11 (2): e0148461. <https://doi.org/10.1371/journal.pone.0148461>.
- Sulston, J. E. 1983. 'Neuronal Cell Lineages in the Nematode *Caenorhabditis Elegans*.' 48 Pt 2: 443–52.
- Sutton, Michael A, Anne M Taylor, Hiroshi T Ito, Anh Pham, and Erin M Schuman. 2007. 'Postsynaptic Decoding of Neural Activity: EEF2 as a Biochemical Sensor Coupling Miniature Synaptic Transmission to Local Protein Synthesis'. *Neuron* 55 (4): 648–61.
- Sutula, T, J Koch, G Golarai, Y Watanabe, and J O McNamara. 1996. 'NMDA Receptor Dependence of Kindling and Mossy Fiber Sprouting: Evidence That the NMDA Receptor Regulates Patterning of Hippocampal Circuits in the Adult Brain.' *The Journal of Neuroscience : The Official Journal of the Society for Neuroscience* 16 (22): 7398–7406.
- Sutula, Thomas P. 2004. 'Mechanisms of Epilepsy Progression: Current Theories and Perspectives from Neuroplasticity in Adulthood and Development'. *Epilepsy Research* 60 (2–3): 161–71. <https://doi.org/10.1016/j.eplepsyres.2004.07.001>.

- Sveinbjornsdottir, S., J. W.A.S. Sander, D. Upton, P. J. Thompson, P. N. Patsalos, D. Hirt, M. Emre, D. Lowe, and J. S. Duncan. 1993. 'The Excitatory Amino Acid Antagonist D-CPP-Ene (SDZ EAA-494) in Patients with Epilepsy'. *Epilepsy Research* 16 (2): 165–74. [https://doi.org/10.1016/0920-1211\(93\)90031-2](https://doi.org/10.1016/0920-1211(93)90031-2).
- Taniguchi, Hiroki, Miao He, Priscilla Wu, Sangyong Kim, Raehum Paik, Ken Sugino, Duda Kvitsiani, et al. 2011. 'A Resource of Cre Driver Lines for Genetic Targeting of GABAergic Neurons in Cerebral Cortex'. *Neuron* 71 (6): 995–1013. <https://doi.org/10.1016/j.neuron.2011.07.026>.
- Tanouye, M A, and R J Wyman. 1980. 'Motor Outputs of Giant Nerve Fiber in Drosophila'. *Journal of Neurophysiology* 44 (2): 405–21. <https://doi.org/10.1152/jn.1980.44.2.405>.
- Thompson, Christopher H., Roy Ben-Shalom, Kevin J. Bender, and Alfred L. George. 2020. 'Alternative Splicing Potentiates Dysfunction of Early-Onset Epileptic Encephalopathy SCN2A Variants'. *Journal of General Physiology* 152 (3). <https://doi.org/10.1085/JGP.201912442>.
- Tidball, Andrew M., and Jack M. Parent. 2016. 'Concise Review: Exciting Cells: Modeling Genetic Epilepsies with Patient-Derived Induced Pluripotent Stem Cells'. *STEM CELLS* 34 (1): 27–33. <https://doi.org/10.1002/stem.2203>.
- Tiedeken, Jessica A., and John S. Ramsdell. 2009. 'DDT Exposure of Zebrafish Embryos Enhances Seizure Susceptibility: Relationship to Fetal p,p'-DDE Burden and Domoic Acid Exposure of California Sea Lions'. *Environmental Health Perspectives* 117 (1): 68–73. <https://doi.org/10.1289/ehp.11685>.
- Tolete, Patricia, Kelly Knupp, Michael Karlovich, Elaine DeCarlo, Judith Bluvstein, Erin Conway, Daniel Friedman, Patricia Dugan, and Orrin Devinsky. 2018. 'Lorcaserin Therapy for Severe Epilepsy of Childhood Onset: A Case Series'. *Neurology* 91 (18): 837–39.
- Treiman, D M. 2001. 'GABAergic Mechanisms in Epilepsy'. *Epilepsia* 42 Suppl 3: 8–12.
- Trinka, E. 2012. 'Ideal Characteristics of an Antiepileptic Drug: How Do These Impact Treatment Decisions for Individual Patients?'. *Acta Neurologica Scandinavica* 126 (December): 10–18. <https://doi.org/10.1111/ane.12015>.
- Tsalik, Ephraim L., and Oliver Hobert. 2003. 'Functional Mapping of Neurons That Control Locomotory Behavior In *Caenorhabditis Elegans*'. *Journal of Neurobiology* 56 (2): 178–97. <https://doi.org/10.1002/neu.10245>.
- Tsankova, N. M., Arvind Kumar, and Eric J Nestler. 2004. 'Histone Modifications at Gene Promoter Regions in Rat Hippocampus after Acute and Chronic Electroconvulsive Seizures'. *Journal of Neuroscience* 24 (24): 5603–10. <https://doi.org/10.1523/JNEUROSCI.0589-04.2004>.
- Turrigiano, Gina G, Kenneth R Leslie, Niraj S Desai, Lana C Rutherford, and Sacha B Nelson. 1998. 'Activity-Dependent Scaling of Quantal Amplitude in Neocortical Neurons'. *Nature* 391 (6670): 892–96.
- Turrigiano, Gina G, and Sacha B Nelson. 2004. 'Homeostatic Plasticity in the Developing Nervous System'. *Nature Reviews Neuroscience* 5 (2): 97–107.
- Velíšková, Jana, Michael P. Shakarjian, and Libor Velíšek. 2017. 'Systemic Chemoconvulsants Producing Acute Seizures in Adult Rodents'. In *Models of Seizures and Epilepsy*, 491–512. Elsevier. <https://doi.org/10.1016/B978-0-12-804066-9.00035-3>.
- Vignes, Michel, and Graham L Collingridge. 1997. 'The Synaptic Activation of Kainate Receptors'. *Nature* 388 (6638): 179–82.

- Wallace, Robyn H, Carla Marini, Steven Petrou, Louise A Harkin, David N Bowser, Rekha G Panchal, David A Williams, Grant R Sutherland, John C Mulley, and Ingrid E Scheffer. 2001. 'Mutant GABAA Receptor  $\Gamma$ 2-Subunit in Childhood Absence Epilepsy and Febrile Seizures'. *Nature Genetics* 28 (1): 49–52.
- Wang, Xiaoqiang, Juanita McLachlan, Phillip D Zamore, and Traci M. Tanaka Hall. 2002. 'Modular Recognition of RNA by a Human Pumilio-Homology Domain'. *Cell* 110 (4): 501–12. [https://doi.org/10.1016/S0092-8674\(02\)00873-5](https://doi.org/10.1016/S0092-8674(02)00873-5).
- Wang, Zhenqiang, and Seth M Cohen. 2007. 'Postsynthetic Covalent Modification of a Neutral Metal-Organic Framework'. *Journal of the American Chemical Society* 129 (41): 12368–69.
- Wei, Yina, Ghanim Ullah, and Steven J Schiff. 2014. 'Unification of Neuronal Spikes, Seizures, and Spreading Depression.' *The Journal of Neuroscience : The Official Journal of the Society for Neuroscience* 34 (35): 11733–43. <https://doi.org/10.1523/JNEUROSCI.0516-14.2014>.
- Weidmann, Chase A., Nathan A. Raynard, Nathan H. Blewett, Jamie Van Etten, and Aaron C. Goldstrohm. 2014. 'The RNA Binding Domain of Pumilio Antagonizes Poly-Adenosine Binding Protein and Accelerates Deadenylation'. *RNA* 20 (8): 1298–1319. <https://doi.org/10.1261/rna.046029.114>.
- Wendling, Fabrice, Fabrice Bartolomei, and Julien Modolo. 2017. 'Neocortical/Thalamic In Silico Models of Seizures and Epilepsy'. In *Models of Seizures and Epilepsy*, 233–46. Elsevier. <https://doi.org/10.1016/B978-0-12-804066-9.00016-X>.
- Wendling, Fabrice, Pascal Benquet, Fabrice Bartolomei, and Viktor Jirsa. 2016. 'Computational Models of Epileptiform Activity'. *Journal of Neuroscience Methods* 260 (February): 233–51. <https://doi.org/10.1016/J.JNEUMETH.2015.03.027>.
- Wengert, Eric R., and Manoj K. Patel. 2021. 'The Role of the Persistent Sodium Current in Epilepsy'. *Epilepsy Currents* 21 (1): 40–47. <https://doi.org/10.1177/1535759720973978>.
- White, H. Steve. 1997. 'Clinical Significance of Animal Seizure Models and Mechanism of Action Studies of Potential Antiepileptic Drugs'. *Epilepsia* 38 (s1): S9–17. <https://doi.org/10.1111/j.1528-1157.1997.tb04523.x>.
- White, H Steve. 2005. 'Molecular Pharmacology of Topiramate: Managing Seizures and Preventing Migraine'. *Headache: The Journal of Head and Face Pain* 45: S48–56.
- Wolff, Markus, Katrine M Johannesen, Ulrike B S Hedrich, Silvia Masnada, Guido Rubboli, Elena Gardella, Gaetan Lesca, Dorothée Ville, Mathieu Milh, and Laurent Villard. 2017. 'Genetic and Phenotypic Heterogeneity Suggest Therapeutic Implications in SCN2A-Related Disorders'. *Brain* 140 (5): 1316–36.
- Wong, Shi Quan, Alistair Jones, Steven Dodd, Douglas Grimes, Jeff W Barclay, Anthony G Marson, Vincent T Cunliffe, Robert D Burgoyne, Graeme J Sills, and Alan Morgan. 2018. 'A Caenorhabditis Elegans Assay of Seizure-like Activity Optimised for Identifying Antiepileptic Drugs and Their Mechanisms of Action'. *Journal of Neuroscience Methods* 309: 132–42.
- Wu, Xu-Ling, Hao Huang, Yun-Yi Huang, Jin-Xian Yuan, Xin Zhou, and Yang-Mei Chen. 2015. 'Reduced Pumilio-2 Expression in Patients with Temporal Lobe Epilepsy and in the Lithium–Pilocarpine Induced Epilepsy Rat Model'. *Epilepsy & Behavior* 50 (September): 31–39. <https://doi.org/10.1016/j.yebeh.2015.05.017>.

- Yagüe, Josue G, Anna Cavaccini, Adam C Errington, Vincenzo Crunelli, and Giuseppe Di Giovanni. 2013. 'Dopaminergic Modulation of Tonic but Not Phasic GABA A-Receptor-Mediated Current in the Ventrobasal Thalamus of Wistar and GAERS Rats'. *Experimental Neurology* 247: 1–7.
- Yu, Frank H, Massimo Mantegazza, Ruth E Westenbroek, Carol A Robbins, Franck Kalume, Kimberly A Burton, William J Spain, G Stanley McKnight, Todd Scheuer, and William A Catterall. 2006. 'Reduced Sodium Current in GABAergic Interneurons in a Mouse Model of Severe Myoclonic Epilepsy in Infancy'. *Nature Neuroscience* 9 (9): 1142–49. <https://doi.org/10.1038/nn1754>.
- Yu, Jieying, Dian-Shi Wang, Robert P Bonin, Antonello Penna, Ali Alavian-Ghavanini, Agnieszka A Zurek, Gail Rauw, Glen B Baker, and Beverley A Orser. 2019. 'Gabapentin Increases Expression of  $\delta$  Subunit-Containing GABAA Receptors'. *EBioMedicine* 42: 203–13.
- Zamponi, Gerald W, Joerg Striessnig, Alexandra Koschak, and Annette C Dolphin. 2015. 'The Physiology, Pathology, and Pharmacology of Voltage-Gated Calcium Channels and Their Future Therapeutic Potential'. *Pharmacological Reviews* 67 (4): 821–70.
- Zeng, Ling-Hui, Lin Xu, David H. Gutmann, and Michael Wong. 2008. 'Rapamycin Prevents Epilepsy in a Mouse Model of Tuberous Sclerosis Complex'. *Annals of Neurology* 63 (4): 444–53. <https://doi.org/10.1002/ana.21331>.

## 2.0 Chapter 2 – Identifying New Lead Compounds

### 2.1 Introduction- Identifying Lead Compounds

#### 2.1.1 Avobenzone Breakdown Products

Data from a *Drosophila* seizure assay showed that avobenzone is more effective at reducing recovery times in *para<sup>bss</sup>* mutants after being exposed to UV light (Wei-Hsiang Lin, personal observation), suggesting a UV breakdown product is more effective, or may in fact be, the active compound.

A study into the breakdown products of avobenzone by Karlsson and colleagues (Karlsson *et al.*, 2009) shows there are 7 major photodegradation products of avobenzone in polar solvents. Using this information some of the breakdown products were screened in a preliminary L3 seizure assay. This identified 4-*tert*-butyl-benzaldehyde (4TBB-ald) as a potential new lead, being more effective than avobenzone with no UV exposure. Furthermore, in preliminary data, 4TBB-ald was shown to increase Pum2 levels in the brain, whereas no increase was observed with avobenzone (Wei-Hsiang Lin, personal observation).

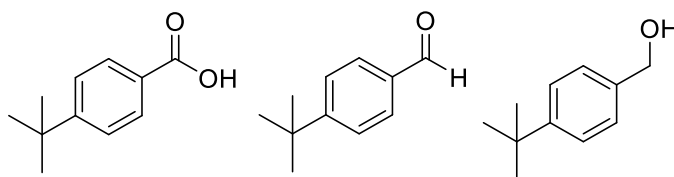


**Figure 2.1- Structures of 2 potential leads 4TBB-acid (left) and 4TBB-ald (centre). Both are products of avobenzone photolysis. 4TBB-alc (right) was also included in this screen to cover all potential oxidation states of the oxygen bonded carbon.**

Interestingly, data from an earlier screen, conducted before this project began (He, unpublished data) showed that the analogous ketone to 4TBB-ald (Figure 2.2) had no anticonvulsant activity, suggesting the acid analogue that was the active metabolite. Both mammals and *Drosophila* possess enzymes that metabolise toxic aldehydes to carboxylic acids in order to increase solubility and aid excretion however, ketones cannot be metabolised in this way (Moxon *et al.*, 1985). For completion, the alcohol analogue (4TBB-alc) was also screened as there are enzymes which catalyse the reduction of aldehydes to alcohols, such as the aldose reductase family (Doan *et al.*, 2002).

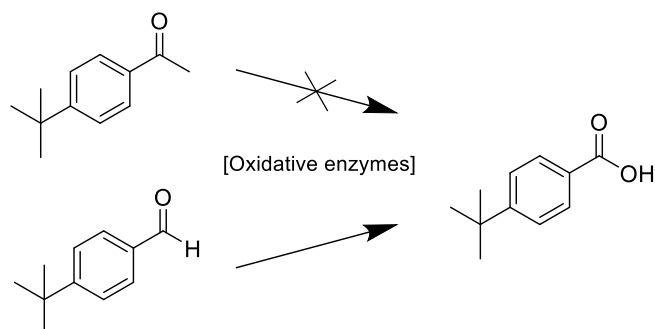


*Figure 2.2- Difference in metabolism between ketone (top left) and aldehyde (bottom left). Aldehydes are readily oxidized to carboxylic acids in both humans and *Drosophila*, whereas ketones are not. Metabolism of ketones is more difficult than aldehydes as it requires the breaking of a C-C bond.*

Exposure of larvae to these drugs and a resultant seizure assay (Figure 2.3) supported this hypothesis because it was shown that 4-*tert*-butyl-benzoic acid (4TBBA) is equally as effective as 4TBB-ald in suppressing seizure like behaviour. However, it is unknown whether 4TBBA has the same effect of increasing Pum2 levels in rodents which has yet to be tested. Differences may occur due to their variance in adsorption, distribution, metabolism and excretion (ADME) properties, especially as 4TBBA would be ionised at physiological pH. However, 4TBBA is less likely to cause toxicity and irreversible inhibition than 4TBB-ald due to aldehydes possessing a highly reactive electrophilic centre.

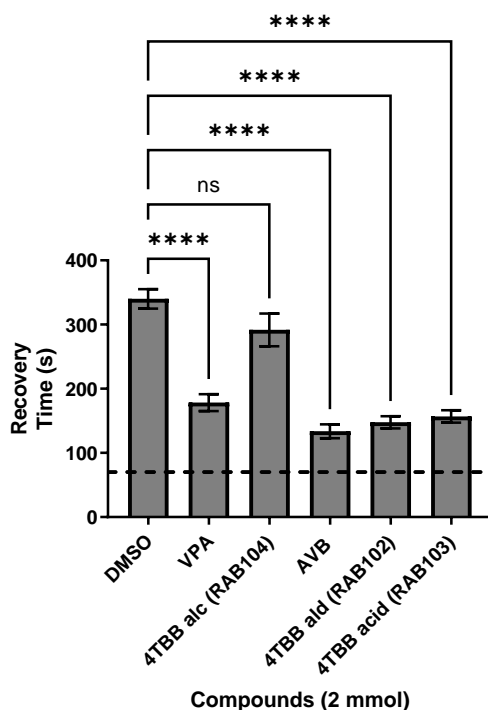


*Figure 2.3- Data from L3 seizure assay looking at how different compounds affect larval recovery time. Dashed line indicates average wild type recovery time. Valproate (VPA) is included as a positive control (established antiepileptic drug). AVB = avobenzene. Results were analysed via a one-way ANOVA. N = 24, refers to number of larvae shocked. Values given are mean  $\pm$  SEM. \* =  $p < 0.05$ , \*\* =  $p < 0.01$ , \*\*\* =  $p < 0.001$ , \*\*\*\* =  $p < 0.0001$*

### 2.1.2 Considerations in Drug Design

In drug design, Lipinski's rule of 5 is commonly used to determine whether a compound is "drug like" or not, depending on physiochemical properties. These guidelines are:

- No more than 5 hydrogen bond donors (OH, NH)
- No more than 10 hydrogen bond acceptors (sum of all O and N)
- Molecular mass less than 500 Daltons
- Octanol-water partition coefficient (cLogP) less than 5

There are many exceptions to these rules and as a result they are, at best, only to be used as a guideline (Lipinski *et al.*, 2001). However, most clinically available orally active small molecule drugs do fit within most of these parameters and these compounds generally have better ADME properties (Lipinski, 2016).

When designing CNS active compounds other guidelines and properties need to be also considered due to the blood brain barrier (BBB). Organs possess a layer of endothelial cells that control the transfer of compounds in and out of the cell from the blood. As the CNS is particularly sensitive to many compounds within the blood, the BBB forms tight junctions meaning transfer into the CNS must enter the brain *via* transcellular diffusion or active transport. (Pajouhesh and Lenz, 2005) Active transport only occurs for privileged structures such as amino acids, so nearly all CNS acting drugs must get to the brains by transcellular diffusion. As a result, polar molecules struggle to get access to the brain and CNS active drugs tend to be more lipophilic with a lower polar surface area (PSA) (Table 2.1) (Manallack, 2007; Wager *et al.*, 2010).

*Table 2.1- Comparison of physiochemical properties in CNS drugs, non-CNS drugs and current lead compounds 4TBB-ald and 4TBBA. Red indicates large differences, amber moderate differences and green within a nominal desired range. Data on drugs taken from (Doan et al., 2002). 48 CNS and 43 non-CNS drugs were analysed. Selection was based on molecular weight 150-800 and stability/state (gasses and solids excluded).*

Chemical properties	CNS Drugs	Non-CNS Drugs	4TBB-ald	4TBBA
Molecular weight	319	330	162	178
cLogP	3.43	2.78	3.32	3.71
Polar surface area (PSA)	44.8	56.1	17.07	37.3
H-bond donors	0.85	1.56	0	0
H-bond acceptors	3.56	4.51	1	2
Rotatable bonds	1.27	2.18	2	2
Aromatic rings	1.92	1.93	1	1
pKa	6.1-10	3.5-11.5	N/A	4.4

Currently the 2 lead compounds, 4TBBA-ald and 4TBBA, have a lower molecular weight and PSA when compared to other CNS active drugs. Additionally, 4TBBA has an acidic pKa of 4.4, when generally CNS drugs are weak bases or neutral due to the difficulty of getting negatively charged species through the BBB. There are a limited number of CNS acting drugs that contain a carboxylic acid group, including valproate. Passive diffusion of negatively charged molecules across the BBB is difficult due to unfavourable electrostatic interactions, however valproate is seemingly taken into the CNS via a medium-chain fatty acid transporter (Adkison and Shen, 1996). Other transporters that carry carboxylic acids across the BBB include the monocarboxylate transporters (MCTs), that transport key nutrients such as pyruvate and lactate, and Large Amino Acid Transporter 1 (LAT1) which is utilised by essential amino acids including phenylalanine (Mac and Nałęcz, 2003; Singh and Ecker, 2018).

Although not ideal for clinical compounds, low molecular weight and PSA is beneficial for a lead compound as it gives the opportunity to make additions to the structure without exceeding the guideline limits. However, low PSA is often associated with toxicity and promiscuity, especially when combined with a cLogP > 3 (Meanwell, 2011). Similarly, a low number of H-bond donors/acceptors is advantageous, as this allows for the inclusion of more electronegative atoms in different regions of the molecule. Hydrogen bonds are a strong form of electrostatic interaction a compound can form with its binding partner, whereby partially positively charged hydrogen atoms interact with

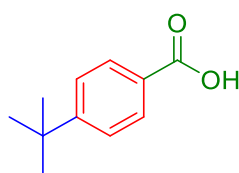
heteroatoms that are negatively charged, either partially or formally. In order for compounds to form these interactions they require H-bond donors/acceptors; however, inclusion of these groups also tends to increase PSA and lower cLogP.

Throughout the first part of this project the aim was to use the principles of drug design and structure-activity relationships (SAR) to design compound analogues based on the initial leads 4TBB-ald and 4TBBA. By screening one set of analogues and designing another set using a SAR the aim was to make the lead compound more drug-like, whilst retaining or improving potency.

## 2.2 Results

### 2.2.1 Design of Generation 1 Compounds

After establishing the acid 4TBBA as the lead compound, the next step was to design a series of analogues and test their activity against the current lead (4TBBA, aka RAB102). Because the target(s) of these compounds is unknown, it was not possible to use modelling techniques to aid design. Instead, bioisosteric replacements were deployed for different parts of the compound with the intention to establish a structure activity relationship (SAR). The compound was split into 3 parts, highlighted by different colours in Figure 2.4; the acid group, the aromatic ring and the lipophilic *tert*-butyl group, located in the para position.

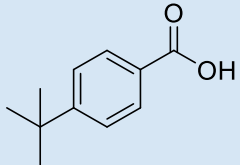
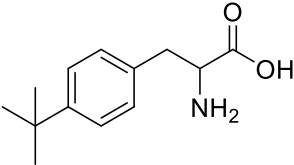
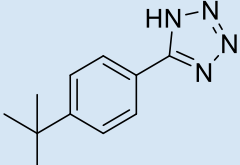
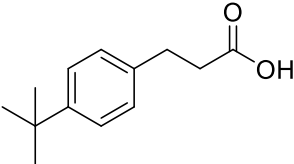
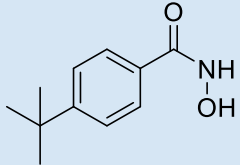
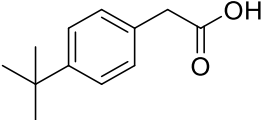
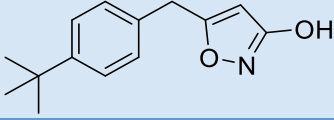


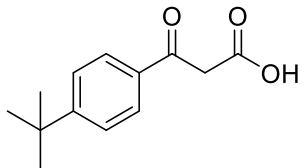
*Figure 2.4- The 3 parts of the lead compound (4TBBA, RAB103). When designing analogues one variation was made at each of these positions. Acid/ polar group (green), aromatic ring (red) and lipophilic group para to acid (blue).*

Each compound was designed by making a change to only one of these 3 parts and replacing them with a group that has a similar electronic structure. By making one small change, with each compound, the most efficacious group in the 3 different parts of the molecule can hopefully be identified, to potentially make a more potent next-generation compound. Once the most potent compound from this series is discovered, the process can begin again by making analogues based on that new lead compound etc.

When selecting a suitable replacement for the acid/aldehyde group, it is integral that hydrogen bond donors (any OH or NH) and hydrogen bond acceptors (any N or O) are included. This is because it is highly likely that this part of the compound is important for binding to the target because it is the only part containing a charge or electronegative atoms (Kunde *et al.*, 2021). This allows the compound to form stronger intermolecular bonds with the target, which are based on electrostatic interactions, and are significantly stronger than induced dipole-dipole (Van der Waal) forces (Vuignier *et al.*, 2010). With this in mind, the analogues in Table 2.2 were designed.

**Table 2.2- List of analogues with variation in acid/polar group.**

Compound # (RAB #)	Structure	MW (g/mol)	Clog P	Polar surface area Å <sup>2</sup>	pKa	Purchased/synthesised/ Synthesis unsuccessful
103		178.23	3.71	37.30	4.4	Purchased Fluorochem
106		222.1	0.27	64.94	OH, 2.2 NH <sub>2</sub> , 9.9	Synthesised
109		201.1	3.46	51.18	4.3	Synthesised
114		206.1	3.73	37.30	4.5	synthesised
116		192.1	1.96	52.16	9.8	Synthesised
123		191.1	3.24	40.13	4.3	Purchased Fluorochem
124		216.1	4.27	44.65	6.4	Synthesis unsuccessful

128		219.1	2.90	57.2	3.5	Synthesis unsuccessful
-----	---	-------	------	------	-----	------------------------

The amino acid analogue (RAB106) was designed for 3 reasons. Firstly, it contains an acid group with a formal negative charge analogous to the lead. Secondly, unpublished data from a screen done before this project started, showed that both enantiomers of phenylalanine are effective at reducing seizure RT in the L3 seizure electroshock assay (Fiona He, unpublished data). Finally, due to the structural similarity to phenylalanine, it may be a substrate for the LAT1 transporter across the blood brain barrier, as occurs for L-dopa in the treatment of the Parkinson's disease (Kageyama *et al.*, 2000).

The purpose of RAB114 and RAB123 is to determine the ideal methylene chain length between the aromatic ring and the acidic group. This chain length will be extended by a single carbon each time until the optimal length is discovered.

RAB109, RAB116 and RAB124 all contain isosteric replacements of carboxylic acid groups. The hydroxamic acid (RAB116), however, could be seen more analogous to the aldehyde, because it has no formal charge at physiological pH (7.4). The tetrazole (RAB109) and isoxazole (RAB124) analogues both carry a net negative charge; there is a less profound effect on lipophilicity compared to carboxylic acids, which in both cases the charge is delocalised around the aromatic ring (e.g. the tetrazole shown in Figure 2.5). Interestingly, the pKa of RAB124 is 6.2, relatively close to physiological pH, meaning 89% of the compound will be ionised at pH 7.4 in what is a dynamic process. This may allow the compound to pass through cell membranes as a neutral species before ionising when it reaches the target, possibly increasing affinity and distribution. RAB128 was also included because it contains a 1,3-dicarbonyl moiety seen in the original hit avobenzone, whilst still possessing an acid group.

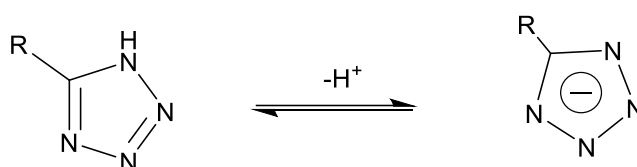
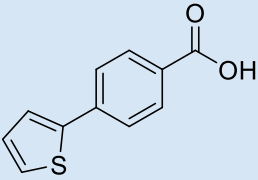
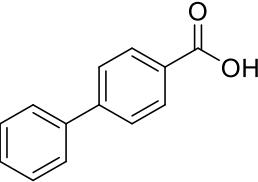
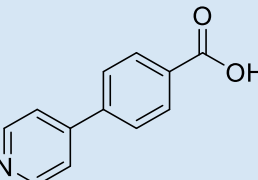
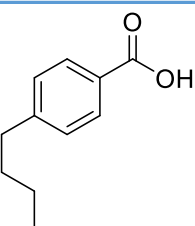
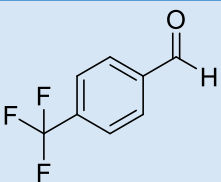
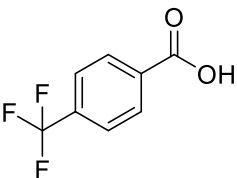


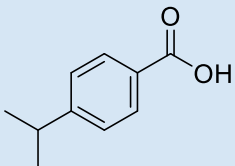
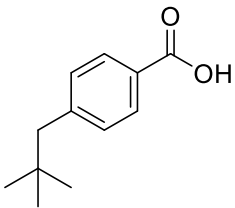
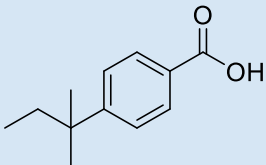
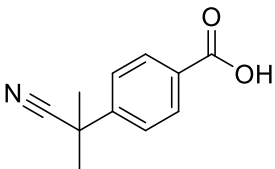
Figure 2.5- Ionisation of tetrazole. Negative charge is delocalised around the aromatic ring system.

The *tert*-butyl group in the *para* position is likely to be involved in the formation of van der Waal forces within a non-polar part of the binding pocket of the target (Westphal *et al.*, 2015).

Additionally, this side group adds lipophilicity to the compound, which is important when the compound needs to pass through the BBB and possesses a formal charge. Analogues with variants in this position are shown in Table 2.3.

**Table 2.3-** List of analogues with variation in the lipophilic group *para* to the acid/aldehyde group.

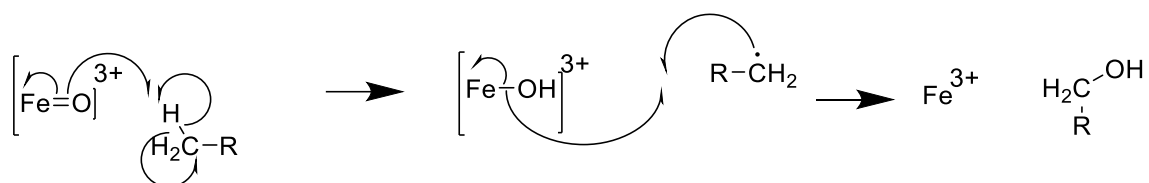
Compound # (RAB)	Structure	MW (g/mol)	clog P	Polar surface area Å <sup>2</sup>	pKa	Purchased/ synthesised/ to be synthesised
108		203.0	3.65	40.13	4.2	Purchased
118		197.0	3.77	40.13	4.3	Purchased Fluorochem
119		198.0	2.35	53.02	4.2	Purchased Merck
120		177.0	3.97	40.13	4.3	Purchased Fluorochem
130		174.03	2.59	17.07	N/A	Purchased Fluorochem
131		189.0	2.94	40.13	3.9	Purchased Fluorochem

132		164.08	3.31	37.3	4.3	Purchased Fluorochem
133		191.11	4.24	40.13	4.2	Purchased Merck
134		191.11	4.24	40.13	4.2	Purchased Merck
135		188.07	2.02	63.92	4.1	Purchased Fluorochem

Compounds RAB108, RAB118 and RAB119 were designed, not only because they are isosteric replacements for a *tert*-butyl, but because they can also act as ‘tool compounds’. By testing these compounds, it may be shown whether the target is able to tolerate a group of this size, in this position. These compounds additionally probe for  $\pi$ - $\pi$  stacking interactions. The pyridine analogue (RAB119) has a H-bond acceptor. Additionally, if a group this large can be accommodated, then this creates another part of the molecule that can be edited, with the addition of groups around an aromatic ring. RAB120 is an isomer of the original acid analogue but with an *n*-butyl group instead of the *tert*-butyl. If this group proved to be more potent than the original *tert*-butyl group, then the chain length could be adjusted to find an optimum length.

In terms of size and shape, the lipophilic groups in RAB131, RAB132, RAB133, RAB134 and RAB135 are more direct replacements of *tert*-butyl. RAB131 contains a trifluoromethyl group which is comparable in shape and size to a *tert*-butyl but has fluorine atoms in place of the methyl groups. Fluorine is used in drugs for a variety of reasons including increased lipophilicity due to its electron withdrawing property, which is responsible for the reduction in pKa seen for RAB131 when compared to RAB 103. This inductive effect is caused by electronegative fluorine atoms pulling electron density away from the benzene ring. This makes the negative charge of the acid more stable, lowering pKa and increasing acidity. The addition of fluorine is also able to block certain forms of metabolism: in this instance it prevents a possible oxidation mediated by cytochrome p450 shown in Figure 2.6 (Posner and O’Neill, 2004). In some cases, fluorine atoms increase ligand binding

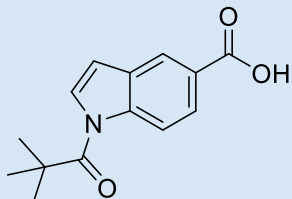
to proteins (DiMagno and Sun, 2006). The polarity of the C-F bond causes a dipole moment with the negative charge on the fluorine which can act as a hydrogen bond acceptor, adding an extra possible interaction when compared to the corresponding hydrogen analogue.



**Figure 2.6 - H abstraction mechanism of CYP450 with primary alkanes.** In a radical mechanism the H is removed from the alkane. In a radical mechanism the 2 electrons required to form a bond each come from different sources. The resulting carbon radical extracts the OH from the Fe within the enzyme to form an alcohol from an alkane. This aids with excretion due to the addition of a polar group, increasing water solubility.

**Table 2.4- List of analogues with variation in aromatic ring**

Compound # (RAB)	Structure	MW (g/mol)	Clog P	Polar surface area Å <sup>2</sup>	pKa	Purchased/synthesised/ Synthesis unsuccessful
107		178.0	2.62	53.02	4.2	Purchased Flurochem
112		216.1	3.70	45.06	4.0	Synthesis unsuccessful
125		177.0	3.71	40.13	4.2	Purchased Merck
136		202.1	3.31	43.37	4.0	Synthesised

137		244.1	3.37	60.44	3.7	Synthesised
-----	---	-------	------	-------	-----	-------------

The final part of the compound that was varied was the core aromatic ring. For RAB107 and RAB112 the benzene ring was substituted with alternative aromatic ring systems. The advantage of adding a pyridine ring is to increase solubility (providing a lone pair to H-bond to water), however, as shown in Table 2.3 this can also have an adverse effect on lipophilicity. The indole analogues were chosen because they add size and additional sites to modify, whilst keeping the groups which are involved in bonding at similar orientations. Additionally, an indole scaffold features regularly in marketed drugs, which is due to the fact that many alkaloids contain indoles. As a result, many G-protein coupled receptors (GPCRs) possess a conserved binding pocket that recognises the indole structure (Alves and Fraga, 2009). RAB125 was designed to determine whether the acid group is more effective in the *para* or *meta* position. If there is little difference found between RAB125 and RAB103 analogues, both orientations will be considered in future designs.

The intention of this first round of screening was to ask a different question with each analogue, in order to decide where to go next with future compound designs. Once the efficacy of each compound was known, parts of the more active compounds could be combined to generate a new series of, hopefully even more potent, analogues.

### 2.2.2 Synthesis of Generation 1 Compounds

The first compound synthesised was the tetrazole analogue RAB109. Tetrazoles are a common isostere of carboxylic acids due to their similar pKa. The acidity is due to the delocalisation of negative charge around the heteroaromatic ring, making the ionic state stable. This delocalisation also results in a less profound effect of the change on cLogP when compared to an acid group. The tetrazole was synthesised by the reaction shown in Figure 2.5.

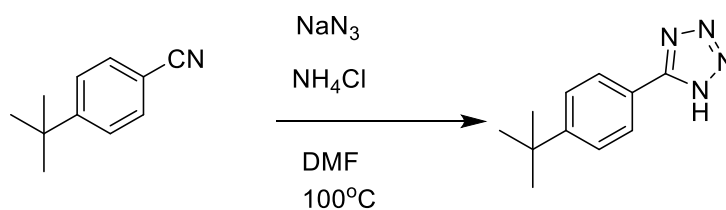
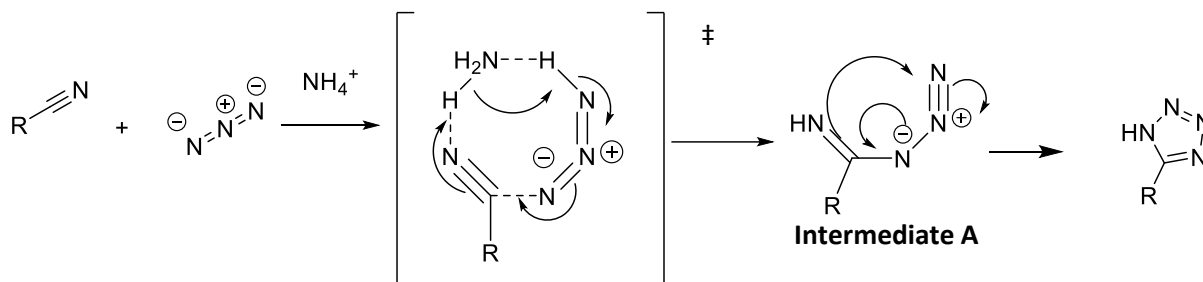
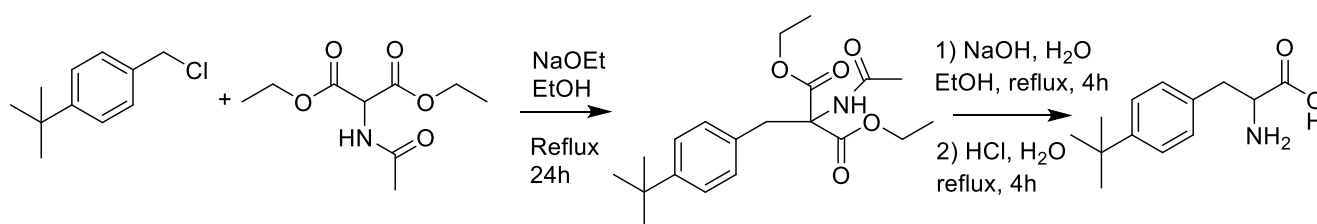


Figure 2.7 - Conditions used for synthesis of the tetrazole analogue RAB107.

The nitrile group was converted to the tetrazole using sodium azide and ammonium chloride in DMF, resulting in a 20% yield. Figure 2.8 shows the mechanism of the reaction. The mechanism was originally thought to be a [2+3] cycloaddition, but it is now thought to go *via* intermediate A in Figure 2.8, after it was noted that a proton source is required from the ammonium salt for the reaction to proceed. Calculations show the mechanism in Figure 2.8 is the route with the lowest energy barrier (Himo *et al.*, 2002). The second compound synthesised was the amino acid analogue RAB106, utilising the method shown in Figure 2.9.



**Figure 2.8- Mechanism of tetrazole formation.** An 8-membered cyclic transition state is formed with the nitrile, azide and ammonium cation. This leads to the formation of intermediate A which undergoes a 1,5 cyclisation to form the tetrazole.



**Figure 2.9- Synthetic route to amino acid analogue RAB106.**

The first step is a nucleophilic substitution with the enolate ion acting as a nucleophile. Hydrogen atoms located alpha to a carbonyl group are slightly acidic due to the resonance stabilisation of negative charge. When a hydrogen atom is located between 2 carbonyls, it becomes more acidic, because the charge can delocalise onto 2 groups as shown in Figure 2.10 (Rahimi and Fattahi, 2021). This reaction proceeded in a 76% yield with no need for further purification of the intermediate.

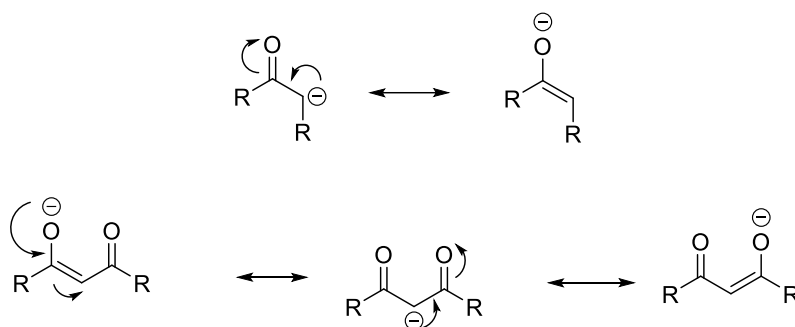


**Figure 2.10- Resonance stabilised forms of carbonyls and 1,3-dicarbonyls. 1,3-Dicarbonyls are more acidic due to the extra resonance stabilisation of the negative charge.**

Taken from work by Kienzle and colleagues (Kienzle, Reischl and Machulla, 2005), the next step was hydrolysis of the ester groups using sodium hydroxide under reflux. This reaction proceeded to create a mixture of the desired product and hydrolysed amide to give the amine. Amide hydrolysis was a desired result of the next reaction, and the amine would be unlikely to disrupt the mechanism of the reaction. The product was therefore taken forward to the next step as a mixture.

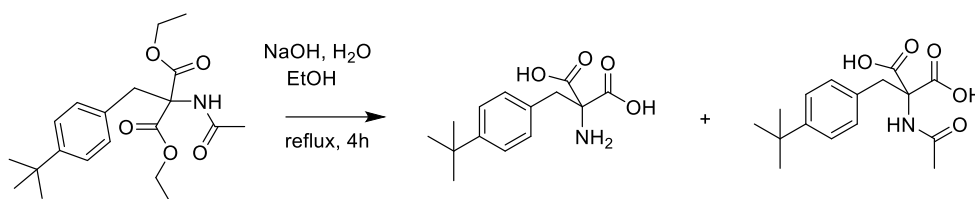


**Figure 2.11- Conditions for ester hydrolysis. Reaction also resulted in partial hydrolysis of the amide and the mixture was taken forward in the next reaction.**

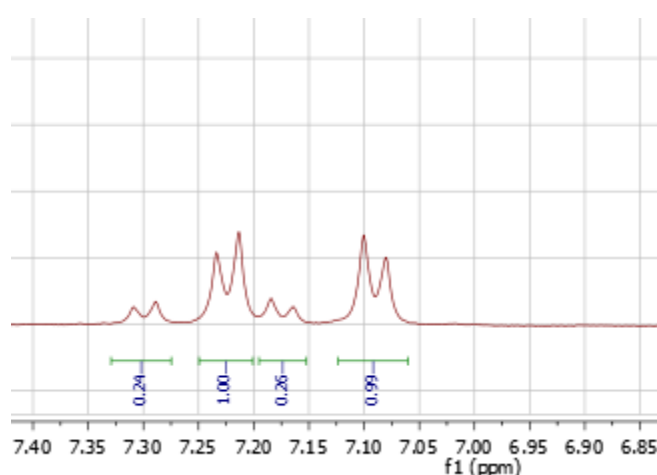


**Figure 2.12-Aromatic region of  $^1\text{H}$  NMR spectra showing the 1:4 ratio of products shown in Figure 2.11 as determined by comparing the integrations.**

The LCMS (not shown) and  $^1\text{H}$  NMR spectra (Figure 2.12) both suggest that the expected product was formed in a 4:1 ratio with the amine formed through hydrolysis. The spectrum shown in Figure 2.12 represents the aromatic region of the two compounds. Analysis of the masses and spectra of the 2 compounds made it clear that the 2 products were the desired intermediate shown in Figure 2.9 and the hydrolysed amine shown in Figure 2.11. As a result, the crude mixture was taken through to the next step. The reported conditions used 1,4 dioxane (Varnavas *et al.*, 2005), but toluene was tried as a replacement because it is also a non-polar high boiling point solvent (111 °C) and decarboxylation reactions often require high temperatures to proceed.

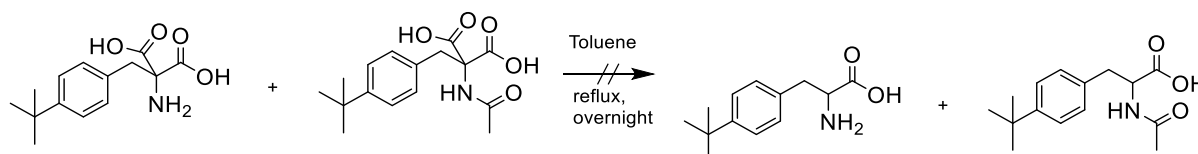


**Figure 2.13- Initial conditions tried for the decarboxylation step, using toluene as a solvent. No product formation was observed.**

When the reaction in Figure 2.13 was attempted, no conversion was noted. It is possible this was due to the boiling point of toluene being lower than the petroleum ether in the reported method. The next set of conditions tried 6 M hydrochloric acid instead of petroleum ether. Although the boiling point of water is lower than toluene, a decarboxylation can still occur as the addition of acid means more of the neutral acid species is present. Additionally, the presence of water is thought to lower the activation barrier by providing an alternative route that includes solvent activation (Brown, 1951). Not only did this reaction in Figure 2.14 result in a successful decarboxylation it also hydrolysed the amide, converting both species in the mixture to the desired product. After trituration with ether the product RAB106 was made with a final step yield of 20%.

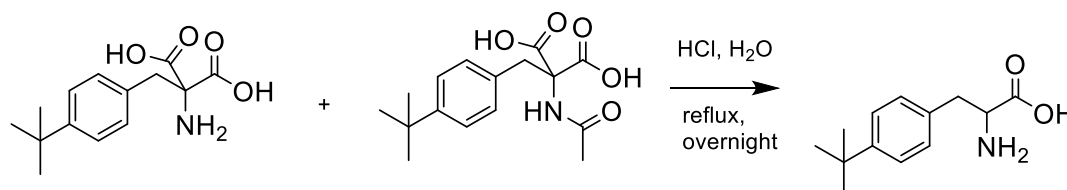


**Figure 2.14 - Conditions which resulted in successful decarboxylation and formation of product RAB106. Conditions also led to hydrolysis of the amide, converting both precursors in the mixture to the desired product.**

Synthesis of analogue RAB114 was achieved using a one-pot method that proceeds *via* an arylidene intermediate, formed through a condensation reaction of benzaldehyde with Meldrum's acid (Figure 2.15) (Mudhar and Witty, 2010). Meldrum's acid is a 6-membered heterocycle made through a condensation reaction of acetone with malonic acid. Meldrum's acid contains a 1,3-diketone similar

to the one employed in the synthesis of RAB106. However, Meldrum's acid is 8 orders of magnitude more acidic when compared to the closely related dimethyl malonate (Byun, Mo and Gao, 2001). The cause of this was unknown until calculations revealed the lowest energy conformation aligns the alpha proton's  $\sigma_{\text{CH}}$  orbital with the  $\pi^*_{\text{CO}}$ , meaning in the ground state, the C-H bond is destabilised, which increases acidity (Nakamura, Hirao and Ohwada, 2004).

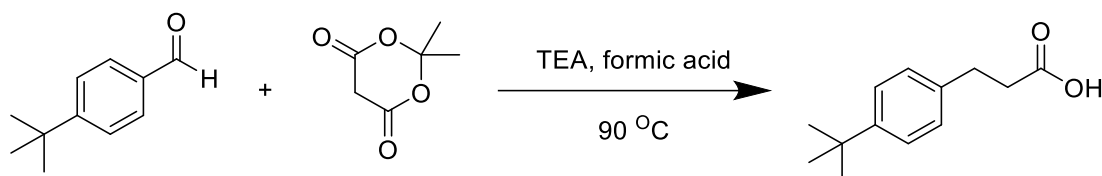


**Figure 2.15 - Conditions used for the synthesis of RAB114.**

This method employed a 2.5:1 mixture of formic acid and triethylamine (TEA) as both a solvent and a reducing agent. First, intermediate 1 (I1) from Figure 2.16 is formed through a condensation reaction between the aldehyde and Meldrum's acid before it is reduced to intermediate 2 (I2). Upon deprotonation, formic acid readily splits into  $\text{CO}_2$  and hydride, where it acts as a reducing agent, hydrogenating the double bond as shown in Figure 2.17. At room temperature the reaction halts at I2, however heating to 80-100 °C allows the hydrolysis step and subsequent decarboxylation to occur, yielding the propanoic acid analogue RAB114.

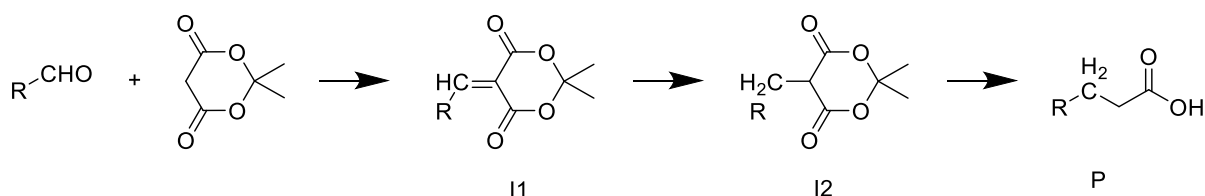


**Figure 2.16 - Synthetic route to the formation of RAB 114 (P). I1 is formed through an aldol condensation between the aldehyde and Meldrum's acid. Reduction of the double bond via the mechanism shown in fFigure 2.20 leads to the formation of I2. P is formed through hydrolysis of the ester bonds followed by a decarboxylation.**

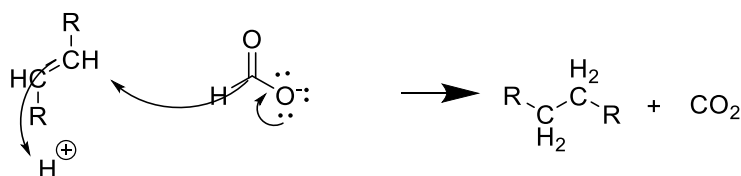


**Figure 2.17 - Mechanism for the reduction of double bonds with formic acid. Upon deprotonation, formic acid readily forms  $\text{CO}_2$  and a hydride ( $\text{H}^-$ ). Hydride acts as a reducing agent on the  $\text{C}=\text{C}$  double bond.**

The hydroxamic acid analogue RAB116, was made through a 2-step synthesis shown in Figure 2.18. The acid must first be converted to the ethyl ester as carboxylic acids are not usually reactive towards nucleophiles (Nguyen and Bekensir, 2014). Therefore, an esterification was performed first using ethanol and sulphuric acid. This then allows the 'good nucleophile' hydroxylamine to attack the carbonyl group in the next step, leading to a substitution reaction via an addition-elimination mechanism, with the formation of the hydroxamic acid RAB116.

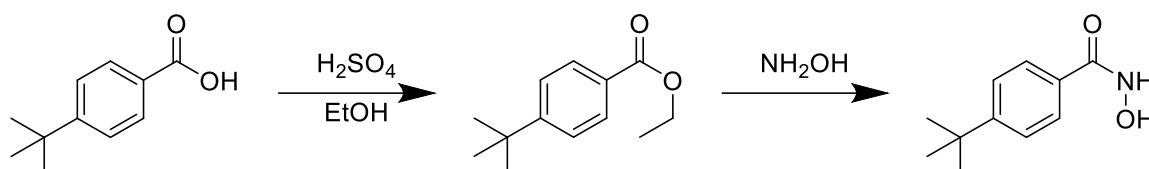


*Figure 2.18 - Reaction scheme for the synthesis of RAB116.*

RAB128 was designed to emulate the 1,3-diketone structure of the original hit avobenzone whilst retaining the acid functionality seen for other compounds. The attempted synthesis shown in Figure 2.19 comprised of 2 steps. The first was an addition-elimination reaction between the enolate and dimethyl carbonate ester to give the  $\beta$ -keto ester followed by a hydrolysis to give the acid. However, the acid product was found to be unstable.

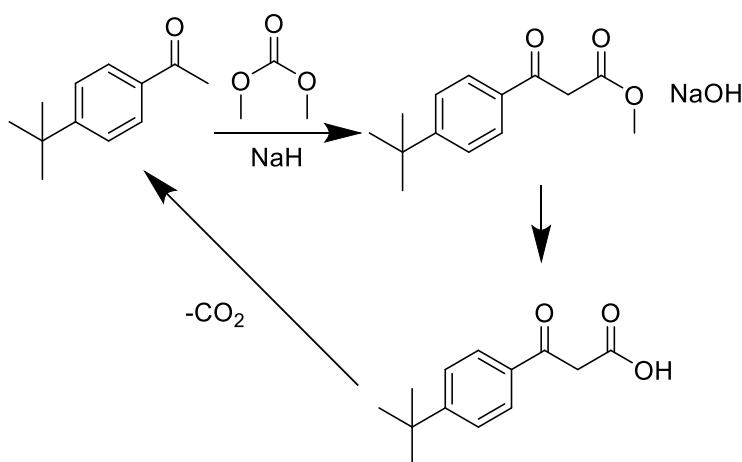


*Figure 2.19 - Attempted synthesis of RAB 128. The desired product spontaneously decarboxylates back to the original starting material.*

$\beta$ -Keto acids can readily undergo decarboxylation even under relatively mild conditions to give  $\text{CO}_2$  and an enol (Hay and Bond, 1967). This is because the relative positions of the 2 carbons allows for the formation of the 6 membered transition state in Figure 2.20, providing a route for the pericyclic reaction to occur. This mechanism is known as a *syn*-elimination and requires a 6 membered transition state to facilitate the concerted movement of 3 electron pairs, which results in the loss of

CO<sub>2</sub> and formation of an enol (Bach, Badger and Lang, 1979). The stability of the enol also aids the reaction as it lowers the activation energy barrier. Additionally, the reaction is also entropically favourable due to the formation of a gaseous product. As the compound was found to be unstable it was deleted from the library.

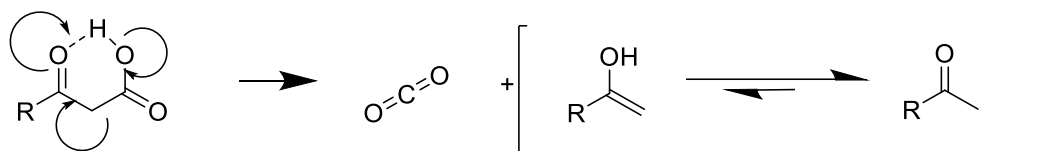


**Figure 2.20 - Mechanism for decarboxylation of  $\beta$ -ketoacids.** The acid proton interacts with the ketone oxygen to create a 6 membered transition state. This allows the pericyclic syn-elimination to occur to give CO<sub>2</sub> and an enol. The enol is converted to the ketone through tautomerisation.

The attempted synthesis of RAB124 was a 4-step synthesis (Figure 2.21) starting with the conversion of a carboxylic acid to an acid chloride. Acid chlorides are highly reactive carbonyl compounds, usually formed through conversion of a carboxylic acid with chlorine containing reagents. For this synthesis, SOCl<sub>2</sub> was used, with DMF acting as a catalyst. SOCl<sub>2</sub> only gives the gaseous by products HCl and SO<sub>2</sub> meaning the purification is simplified.

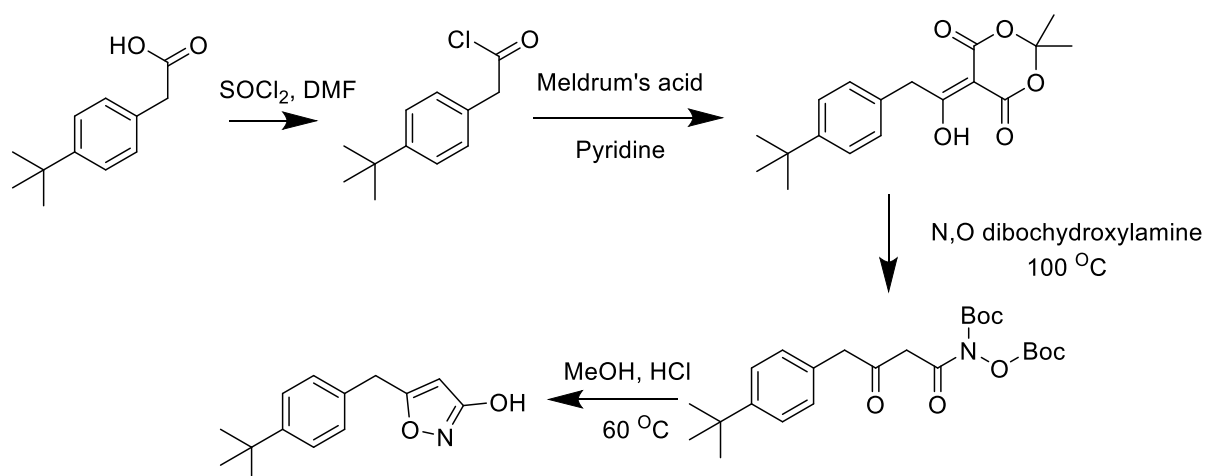


**Figure 2.21 - Initial planned synthetic route of RAB124.** The di-boc protected hydroxylamine was synthesised successfully but the final product was never reached despite trying a variety of different conditions.

The reaction still proceeds without the DMF catalyst but at a lower rate. Reagent A from Figure 2.22 is formed first through a reaction between DMF and SOCl<sub>2</sub> (Hempel *et al.*, 1999). The iminium carbon of this reagent is highly electrophilic due to the chlorine positively charged nitrogen drawing away

electron density and lowering the activation energy when compared to the mechanism with no DMF. This allows the oxygen of the carboxylic acid to attack the iminium carbon initiating in an addition-elimination reaction. Another addition elimination reaction then occurs as the chlorine attacks the carbonyl group, leading to the formation of the acyl chloride and regeneration of DMF.

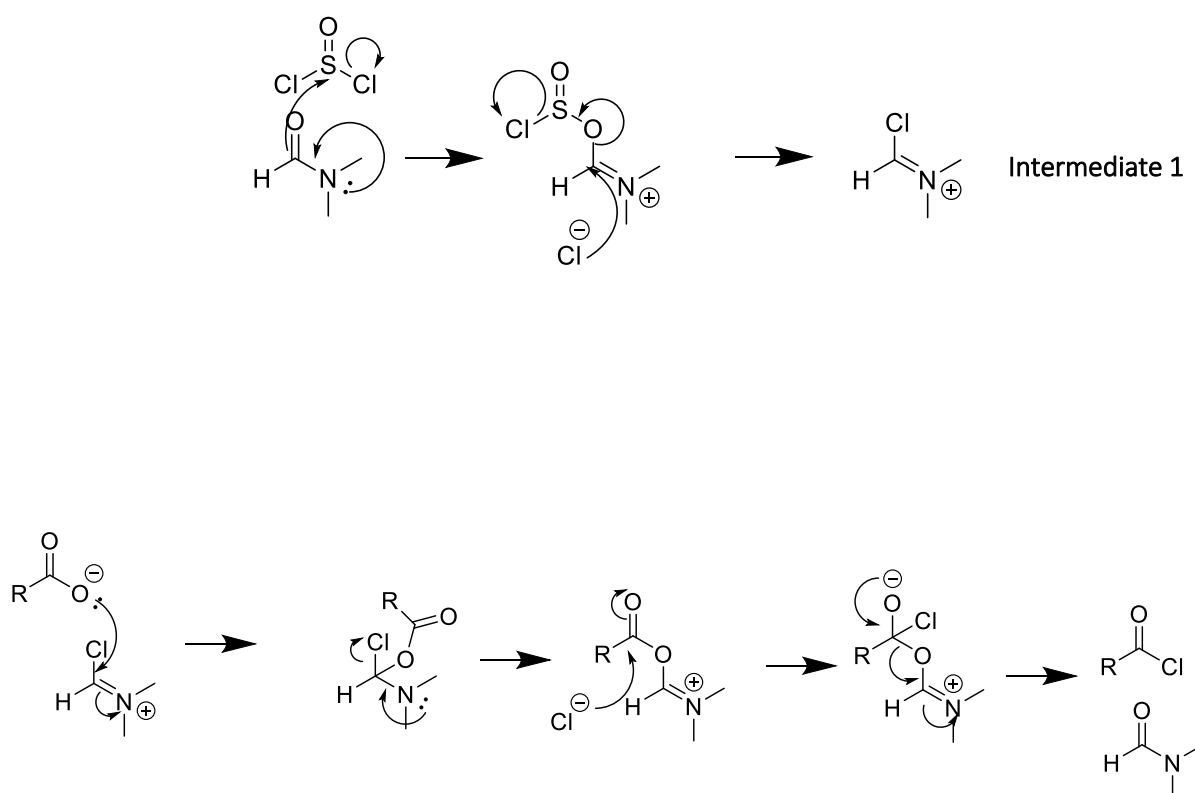


**Figure 2.22 - Mechanism of DMF catalysed acid chloride formation.**

The reactivity of acyl chlorides is due to the high electrophilicity of the carbonyl carbon and the strength of chloride as a leaving group (Palling and Jencks, 1984). Additionally, they do not contain the same resonance stabilisation seen in carboxylic acids making them highly reactive towards nucleophiles (Hardee, Kovalchuke and Lambert, 2010). This includes water which converts it back to the carboxylic acid therefore, dry conditions were used throughout the first 2 steps.

For the second step Meldrum's acid was employed. The step required only the weak base pyridine to ionise Meldrum's acid due to the high acidity explained in the synthesis of RAB114 (Figure 2.22). Deprotonation of the  $\alpha$ -proton creates a nucleophile which attacks the carbonyl carbon of the acid

chloride to give Intermediate 1 from Figure 2.22 and HCl. This step usually proceeded when efforts were made at the synthesis of RAB124, and on optimisation occurred in a 70% yield, with only one purification step required.

In the 2 steps that followed, difficulties were encountered in the synthesis. The first of these steps was the formation of a di-Boc-protected hydroxamic acid. The mechanism here begins with a nucleophilic attack of one of the carbonyl groups in the Meldrum's acid segment of the compound and an addition-elimination reaction to form the amide bond. Following this acetone is lost, as the ester is hydrolysed, before a decarboxylation occurs to give the desired product. However, during the cyclisation step, an unknown undesired product formed instead. Further investigation and synthesis of RAB124 was not pursued.

The first indole analogue designed was RAB122 which possess a *tert*-butyl group on the indole nitrogen. To ensure that the acid functionality did not interfere with the reaction, methyl 1*H*-indole-5-carboxylate was used instead of the corresponding acid, as it can easily be converted through hydrolysis after the first step. For this reaction, shown in Figure 2.23, the indole was first deprotonated at a low temperature using sodium hydride. Then, after 20-30 min, the electrophile *tert*-butyl iodide was added, and the temperature raised to 20 °C. However, in this case, no reaction was observed even after changing conditions such as the base used (LDA), or increased temperature following deprotonation. This is likely due to the steric hindrance of the bulky *tert*-butyl group (Marcelin and Brooks, 1975).

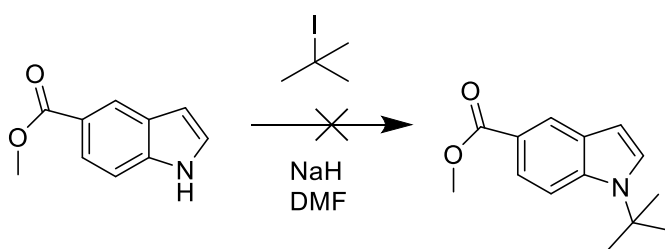


**Figure 2.23 - Attempted Synthesis of RAB122 intermediate. The reaction did not work, which is likely due to steric hindrance.**

Analogues RAB 136 and RAB 137 were designed in an attempt to mimic the structure RAB 122, whilst being suitable for synthesis through the above method. By replacing *tert*-butyl iodide with isopropyl iodide, RAB 136 was made through this method of alkylation at the nitrogen, followed by hydrolysis of the ester with sodium hydroxide at room temperature overnight (Figure 2.24). The yield was 28% over 2 steps, with column chromatography required to purify the final compound.

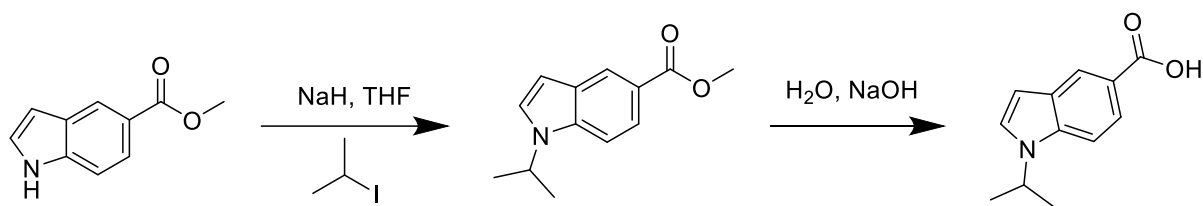


*Figure 2.24 - Synthetic route for RAB 136. The indole is alkylated with 2 iodopropane following deprotonation with sodium hydride. The ester is then hydrolysed with hydroxide.*

The first step in the synthesis of RAB137 in Figure 2.25, required acylation of the indole nitrogen. The conditions employed for the first step were similar to the alkylation, but the indole was instead reacted with acetyl chloride and LDA as the base. This step proceeded in an excellent yield of 88%. Initially, for the ester hydrolysis, again the same conditions were used for those seen in the synthesis of RAB136. However, this resulted in both cleavage of the amide group and the ester.

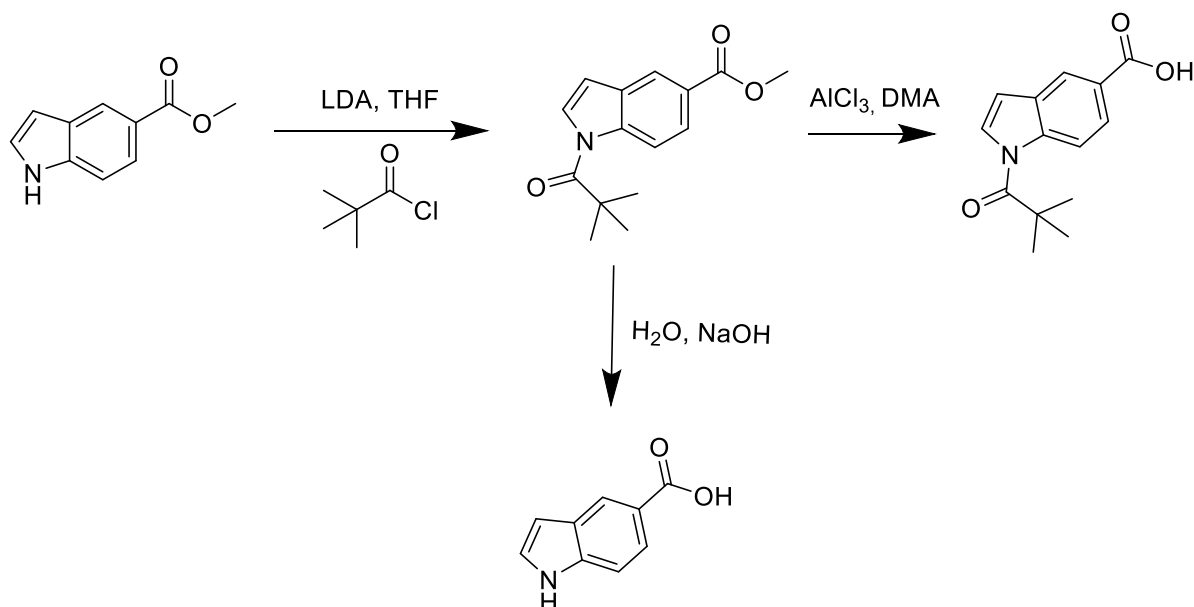


*Figure 2.25 - Synthesis of RAB137. The first step is an acylation at the indole nitrogen with t-butyl chloride. The initial attempt at an ester hydrolysis using hydroxide was unsuccessful but the  $\text{AlCl}_3$ , DMA system was able to give the desired product.*

The strength of the C-N bond in this case is not as strong as a usual amide bond seen in Figure 2.26. This is because usually, the lone pair of the nitrogen is available to be involved in the resonance stabilisation of this bond (Kemnitz and Loewen, 2007). However, in indoles the nitrogen is involved in the formation of the aromatic  $\pi$  system weakening the amide bond. This allows this bond to be hydrolysed under relatively mild conditions where amides would remain stable.

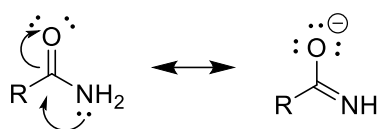


**Figure 2.26 - Resonance canonical forms of the amide bond.** Resonance structures increase stability of compounds as electrons are delocalised and occupy a greater volume. For indoles, the nitrogen lone pair is delocalised into the aromatic system, so any amide-like bonds here, such as the one in RAB 137, do not have this stabilisation and are therefore weaker.

Instead, selective hydrolysis of the ester was achieved using aluminium chloride ( $\text{AlCl}_3$ ).  $\text{AlCl}_3$  is a Lewis acid, meaning it readily accepts electron pairs (Fringuelli, Pizzo and Vaccaro, 2001). This leaves an orbital in the outer shell of aluminium empty, allowing electron pairs from Lewis bases to donate into this orbital forming a Lewis acid-base pair.

In this case  $\text{AlCl}_3$  interacts with an electron pair on the carbonyl oxygen. This causes electron density to be drawn away from the carbonyl oxygen and in turn, the carbonyl carbon. As a result, the C-O ester bond is strengthened due to an increase in polarity, whereas the second C-O bond is weakened (Fringuelli, Pizzo and Vaccaro, 2001). This allows the methyl carbon to act as an electrophile, where it is attacked by dimethyl aniline (DMA). This leads to the formation of a new C=O bond and loss of the methyl ester. The resulting Lewis acid-carboxylate pair can then be converted to the carboxylic acid via treatment with HCl. The mechanism is shown in Figure 2.27. Following purification through column chromatography, the acid RAB137 was isolated in a yield of 40%.

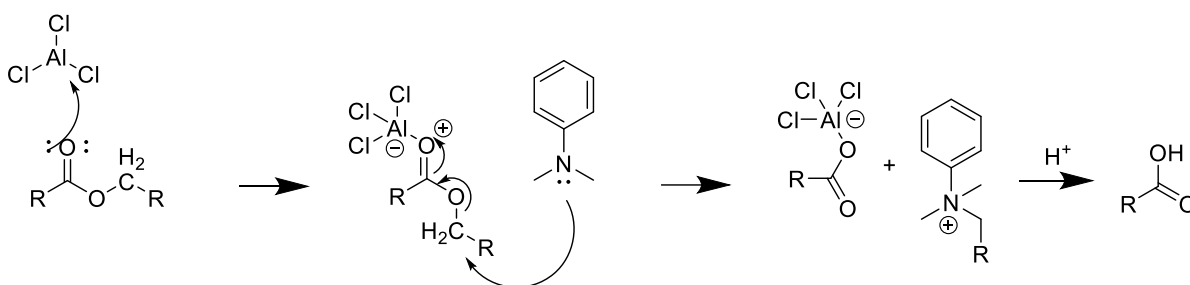


**Figure 2.27 - Mechanism of ester hydrolysis using  $\text{AlCl}_3$  and DMA.**

### 2.2.3 Screening of Generation 1 Compounds

Once the compound library had been collated, compounds were first screened in order to test potency to suppress seizures. The initial screen utilised the same electroshock assay which was used to compare the effects of RAB102 intermediates. *Drosophila* larvae carrying the *para*<sup>bss</sup> mutation

were raised on food containing the compounds. This gain of function mutation is the result of a hyperactive  $\text{Na}_v$  channel, which results in *Drosophila* displaying seizure like behaviour (Parker *et al.*, 2011b).

The results are shown in Figure 2.28 and are an aggregate result of work performed by 2 undergraduate project students (Aoibhinn Kelly, Iona Hayes, supervised by the author). Experiments were set up by the author and given to the students blinded, who then performed the electroshock assay detailed in the methods. Experiments were performed by both students at the same time to minimise risk of false negatives. Analysis shown in this thesis was performed by the author. Of the 22 compounds described above, 17 were screened. RAB124 and RAB128 were excluded due to problems with synthesis. RAB108 wasn't able to be screened due to suspected toxicity. RAB109 wasn't included because not enough was available as the material (this compound is, however, shown in the next round of testing). RAB114 was excluded as RAB123 was inactive, which suggests that the addition of methylene groups between the acid group and the benzene ring eradicates any activity. RAB113, RAB130, RAB133 and RAB137 were only tested by one project student due to time constraints and therefore have an  $n=12$  rather than  $n=24$ .

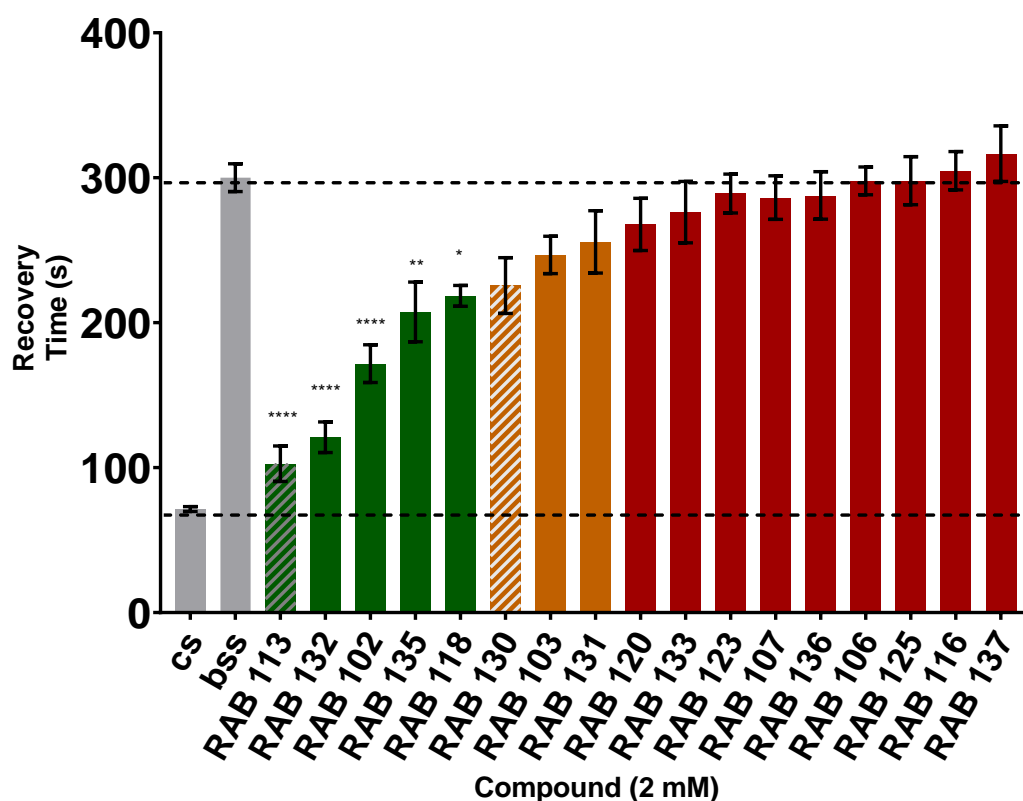


Figure 2.28 – Ranking of generation 1 compounds based on the reduction of recovery time. Cs flies represent canton-s wild type and bss bang-senseless seizure mutant. Green represents compounds which on average significantly reduced

recovery time. Orange represents compounds which were shown to be active in one of the 2 screens but did not significantly reduce the recovery time on average. Red represents compounds that showed no signs of being anticonvulsant. N refers to number of larvae shocked. n=24 unless striped where n=12. Results were analysed via a one-way ANOVA [ $F(18, 381) = 18.00$   $P < 0.0001$ ] with correction for multiple comparison (Dunnett's). Values given are mean  $\pm$  SEM. \* =  $p < 0.05$ , \*\* =  $p < 0.01$ , \*\*\* =  $p < 0.001$ , \*\*\*\* =  $p < 0.0001$

Of the compounds screened, 5 were shown to reduce seizure duration in the *para*<sup>bss</sup> mutant, evidenced by a reduced recovery time. A further 3 (130, 103 and 131) shown signs of activity by significantly reducing recovery times in just one of the 2 data sets. Therefore, these compounds will also be taken forward for further testing giving a total of 8 compounds shown in Table 2.5, including details of their physicochemical properties.

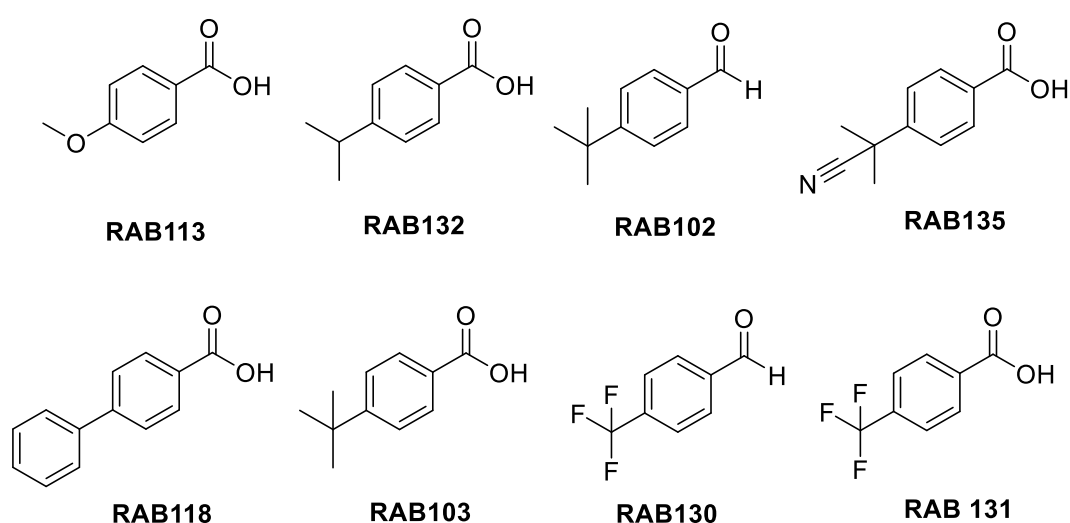
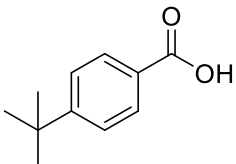
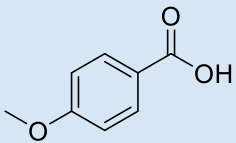
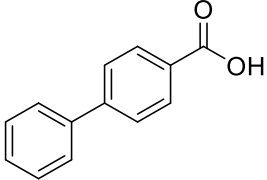
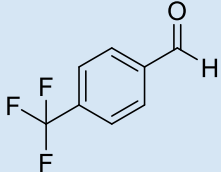
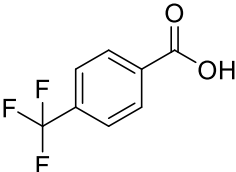
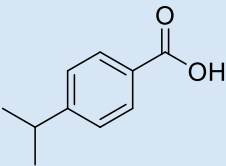
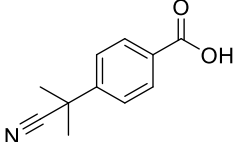


Figure 2.29 – Structure of 5 compounds shown to significantly reduce seizure recovery time (first 5) and 3 others which may have anticonvulsant activity

Table 2.5 - Structures and selected properties of compounds which show potential anticonvulsant activity from the first generation of compounds. Only those with variation in the group para relative to the acid/aldehyde were found to have any anticonvulsant effect.

Compound RAB	Structure	Molecular weight	Volume (Å <sup>3</sup> )	pKa	cLogP	LogD (pH 7.4)	Recovery time reduction
102	<chem>CC(C)(C)c1ccc(cc1)C=O</chem>	162.2	155.2	N/A	3.32	N/A	43%

103		178.2	162.1	4.40	3.71	0.22	18%
113		152.1	114.8	4.25	2.02	-1.39	66%
118		198.2	151.2	4.25	4.251	0.23	27%
130		174.1	111.2	N/A	2.59	N/A	25%
131		190.1	118.1	3.95	2.94	-0.56	15%
132		164.2	144.7	4.35	3.31	-0.45	60%
135		189.2	158.4	4.10	2.02	-0.63	31%

Comparison of the structures of the active compounds shown above, indicates that changes to the central ring structure or acid/aldehyde region abolishes compound activity. Conversely, compounds that only have variation in the lipophilic *para* region of the molecule all retained activity, apart from RAB120 and RAB133. This suggests a polar group *para* to a lipophilic region is crucial for activity. Additionally, RAB113 and RAB135 contain hydrogen bond acceptors which may also contribute. The fluorine containing molecules may also benefit from similar dipole-dipole interactions due to the polarity of the C-F bond. RAB113 showed the largest reduction in recovery time, but the size of the dataset was limited (N = 12) when compared to most other compounds tested (N = 24).

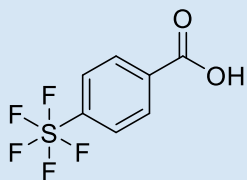
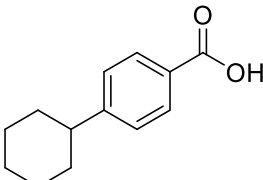
Overall, the first generation of screening found that all active compounds possessed an acid/aldehyde directly bonded to a benzene ring, with a requirement for a group in the *para* position

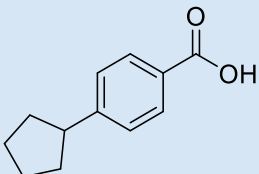
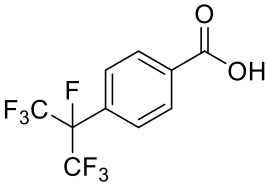
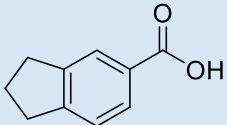
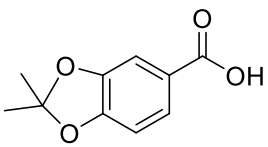
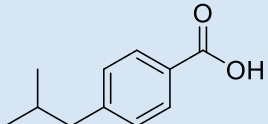
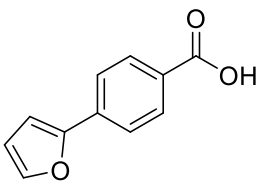
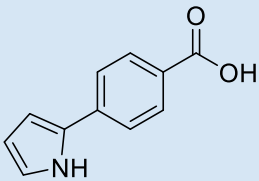
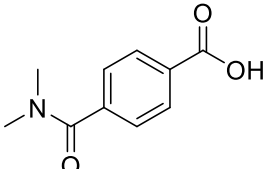
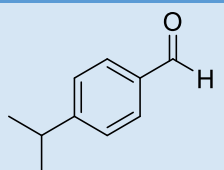
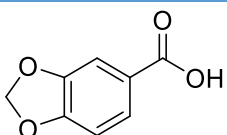
relative to the benzene ring. Changes to the central ring structure or relative position of the 2 groups, made compounds inactive. Compounds with both polar and lipophilic groups in the *para* position were found to be active. These results were used to create a structure activity relationship, which formed the basis for the design of the second generation compounds.

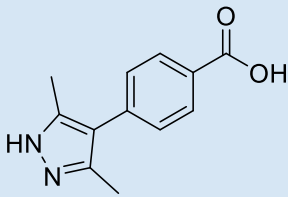
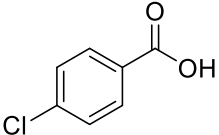
#### 2.2.4 Design of Generation 2 Compounds

Using the data from the first round of compounds, a second generation library was designed. All contained a polar acid / aldehyde group *para* to a lipophilic group, with some forming a fused ring structure to the carbon in the *meta* position. Most of the variation in this second generation of compounds comes from the *para* lipophilic region, as the first screen suggested any other variations to the acid/aldehyde in position 1 reduced efficacy. Additionally, any variations to the ring structure were also found to reduce efficacy. However, in order to increase the chemical space explored, some analogues with fused rings (RAB206, RAB207, RAB217) and one ring variant (RAB203) were included. Some analogues also contain a conventional hydrogen bond donor/acceptor (RAB211, RAB213 and RAB216) or fluorine atoms (RAB201, RAB 205) to test for additional electrostatic interactions. The structures and properties of the generation 2 compounds are shown in Table 2.6.

**Table 2.6 - Structure and physical properties for the second generation of compounds. Structure shown is the major form of the compound at physiological pH (7.4).**

Compound # (RAB)	Structure	MW (g/mol)	cLogP	Polar surface area Å <sup>2</sup>	pKa	Purchased/ synthesised/ Synthesis unsuccessful
201		248.0	3.12	37.30	3.8	Purchased Apollo Scientific
202		204.1	4.51	37.30	4.3	Purchased Fluorochem

204		190.1	3.95	37.30	4.3	Purchased
205		290.0	3.56	37.30	3.0	Purchased
206		162.1	2.90	37.30	4.1	Purchased Fluorochem
207		194.05	2.61	55.76	3.9	Purchased Fluorochem
208		178.1	-3.84	37.30	4.2	Purchased Merck
210		188.0	3.16	46.53	4.3	Purchased Merck
211		187.1	2.64	49.33	4.4	Synthesised
212		193.1	0.61	57.61	4.2	Synthesised
213		148.1	2.92	17.07	None	Purchased Fluorochem
215		166.0	1.97	55.76	3.8	Purchased Fluorochem

216		216.2	1.92	61.7	4.0	Synthesised
217		156.6	2.70	37.3	4.0	Purchased

RAB201 contains a pentafluorosulfanyl group ( $\text{SF}_5$ ) in the *para*-position relative to the acid.  $\text{SF}_5$  has been shown to be chemically and thermally stable and has also been deemed inert under physiological conditions (Altomonte *et al.*, 2014a). Interestingly, this group is highly electronegative, due to the 5 fluorine atoms, yet relatively lipophilic. This is highlighted in a comparison between RAB201 and another highly active compound from the first screen, RAB132. RAB132 contains the lipophilic isopropyl group in the 4 position and has a cLogP of 3.31, compared to 3.12 for RAB201, highlighting the cLogP of a group is comparable to that of groups which are considered lipophilic.  $\text{SF}_5$  is also more lipophilic than the  $\text{CF}_3$  group seen in RAB131, a common electronegative isostere for the *tert*-butyl group. Additionally, it is also more electronegative than the  $\text{CF}_3$  group with electronegativities measured at 3.65 for  $\text{SF}_5$  and 3.36 for  $\text{CF}_3$  (Sheppard, 1962). Despite  $\text{SF}_5$  first being incorporated into organic molecules in the 1960s (Sheppard, 1962), use of this group in pharmaceuticals has been limited. This is mainly due to its lack of synthetic accessibility; however, more recently new routes have been discovered, including methods that allow the synthesis of alkyl substituted  $\text{SF}_5$  groups (see review (Altomonte and Zanda, 2012)). Studies have shown the  $\text{SF}_5$  group to be potential isosteres for  $\text{CF}_3$ , *tert*-butyl,  $\text{NO}_2$  and halogen groups (Stump *et al.*, 2009; Wipf *et al.*, 2009; Altomonte *et al.*, 2014b; Hendriks *et al.*, 2015).

RAB202 and RAB204 contain saturated carbon rings in the 4 position. These were designed based on the benzene analogue being found to be active in the first round of testing, which suggests the putative binding pocket being able to tolerate large lipophilic groups in this region. The surface areas of cyclohexane ( $263 \text{ \AA}^2$ ), cyclopentane ( $244 \text{ \AA}^2$ ) and benzene ( $234 \text{ \AA}^2$ ) are all relatively similar according to the calculated Connolly accessible area, as calculated using Chem3D. However, the structure of benzene is quite different to cyclohexane due to its aromaticity, which makes benzene planar.

Heterocycle analogues, RAB210, RAB211 and RAB216, were also designed with the activity of the benzene analogue in mind. These groups are all similar in size to benzene, with no deviation of the Connolly accessible area larger than 20%. Additionally, these rings all contain at least one hydrogen

bond acceptor, which the first screen suggested is beneficial for activity. RAB211 and RAB216 also contain a hydrogen bond donor group (NH) which was not tested at this position in the previous set of compounds.

RAB205 and RAB208 are more related structurally to the most potent compound from the first screen; RAB132. RAB208 has one additional carbon compared to RAB132, that takes the isopropyl group further from the benzene ring. RAB205 combines the structure of RAB132 with fluorine analogues, which were generally more potent than the related non-fluorinated compounds. This is possibly due to additional interactions from the C-F bond polarity or increased metabolic stability. Fluorine containing groups in the *ortho* or *para* positions withdraw electron density from acid groups stabilising the negative charge and lowering the pKa (DiMagno and Sun, 2006). The fluorinated isopropyl group has a profound effect on the predicted pKa, lowering it from 4.2 in RAB132 to 3.0. In comparison, RAB131 and RAB201 both contain fluorinated groups in this position and have pKa of 3.9 and 3.8, respectively.

RAB206, RAB207 and RAB215 contain fused rings which connect to the central ring through the *para* and *meta* positions. These were designed in order to provide an alternative way of adding appropriate groups to this position, whilst increasing the amount of chemical space investigated. RAB205 possesses a lipophilic cyclopentane group in this position which was designed to be similar in electronic structure to RAB132. RAB207 and RAB215 both contain the methylenedioxyphenyl group, with RAB207 also having 2 extra methyl groups. These analogues were included for 2 reasons. Firstly, the oxygen atoms in this ring system can act as hydrogen bond acceptors which featured in the active compounds from screen one. This includes RAB113, which effectively contains half of the methylenedioxy group in position 4. Secondly, the methylenedioxyphenyl group features in CNS active compounds including 3,4-methylenedioxy-methamphetamine (MDMA) and the anticonvulsant stiripentol, meaning it may be beneficial in the crossing of the BBB (Murray, 2000). The 2 methylene groups in RAB207 were included to increase lipophilicity and to replicate the isopropyl group seen in RAB132.

The remaining analogues were selected to be structural mimetics of the current lead compounds, whilst adding variability to the screen. RAB212 was designed to probe for potential hydrogen bonding interactions in this region, suggested from the first screen. Both the oxygen and nitrogen centres here have the potential to act as hydrogen bond acceptors (Böhm *et al.*, 1996). The 2 methyl groups were added to increase lipophilicity and to mimic the structure of RAB132. Table 2.6 shows the addition of these 2 heteroatoms has a large effect on the cLogP, due to the relatively small size of these compounds. RAB213 was added to the screen in order to compare the effectiveness of the

aldehyde and acid. The acid group is generally preferred to aldehydes due to their better stability and safety profile (Ahmed Laskar and Younus, 2019a). However, if the aldehyde analogue is found to be more efficacious than the acid alternative, other active compounds can be screened with an aldehyde in this position to compare activity. Due to their small size and relative simplicity some of the analogues could be purchased commercially, however other analogues had to be synthesised.

### 2.2.5 Synthesis of generation 2 compounds

The first compound synthesised was the pyrazole analogue RAB216. The synthesis begins with an Ullman like reaction known as a Hurtley reaction, which utilises copper for cross coupling reactions of C-H acid derivatives with aryl halides, to form C-C bonds. Typically, Ullman reactions require high temperatures in order to proceed, which can limit both the efficiency and scope of the reaction (Fanta, 1974). However, by using bidentate, N/O/S containing ligands, the required reaction temperature is radically reduced from 200 °C to as low as 40 °C (Zhang, Zhang and Liebeskind, 1997; Lu and Twieg, 2005; Ma and Jiang, 2007). The ligands employed include 1,3-diketones, Schiff bases and amino acids, although the ligand of choice is dependent on the type of coupling (Jiang *et al.*, 2013). For the coupling with acetylacetone, shown in Figure 2.30, the amino acid proline has been proven to be an effective choice of ligand (Jiang *et al.*, 2005).

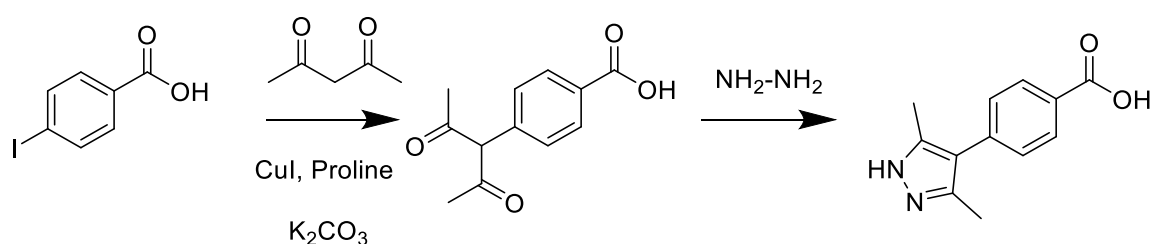


**Figure 2.30 - Reaction scheme for the synthesis of RAB216. The first step is an Ullmann-like cross coupling reaction, utilising copper iodide and proline as catalysts and the enolate of acetylacetone as the nucleophile (yield 72%). The second step is a Knorr pyrazole synthesis which gave the desired product (RAB216) in a very good yield of 85%.**

Evidence from calculations and kinetic studies shows that, in most cases, the mechanism of these reactions proceeds *via* a 2 electron Cu(I)/Cu(III) pathway (Zhang *et al.*, 2007; Casitas and Ribas, 2013). However, there is evidence to suggest that in other Ullmann-like couplings that form C-heteroatom bonds, a single electron Cu(I)/Cu(II) involving radicals, can occur (Creutz *et al.*, 2012). For the Cu(I)/Cu(III) pathway, the exact mechanism is not clear, particularly the ordering of the oxidative addition/substitution steps as shown in Figure 2.31 (Beletskaya and Cheprakov, 2004). In

the case of this reaction evidence from reaction monitoring by Ribas and co-workers, suggests that the mechanism follows route A in Figure 2.31 with the full mechanism shown in Figure 2.32. The cycle begins with the oxidative addition of the aryl iodide across the Cu(I) centre to give Cu(III). A substitution step then occurs with the iodide being replaced by the enolate of acetylacetone, which is followed by a reductive elimination step to give the desired product and regenerates the active Cu(I) catalyst. By using 0.1 eq CuI with 0.2 eq proline the reaction reached completion in 24h. The product was taken forward to the second step crude, as the product and remaining starting material co-eluted in all solvent systems tested.

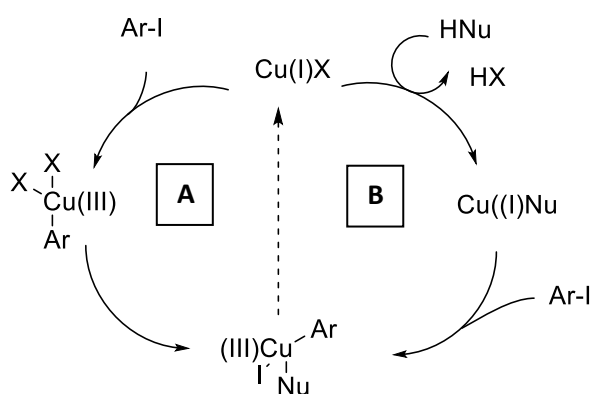


**Figure 2.31- Possible routes for the mechanism of Ullmann couplings that proceed via the 2 electron Cu(I)/Cu(III) pathway. In route A, the oxidative addition occurs before the substitution, whereas in B, the substitution occurs first.**

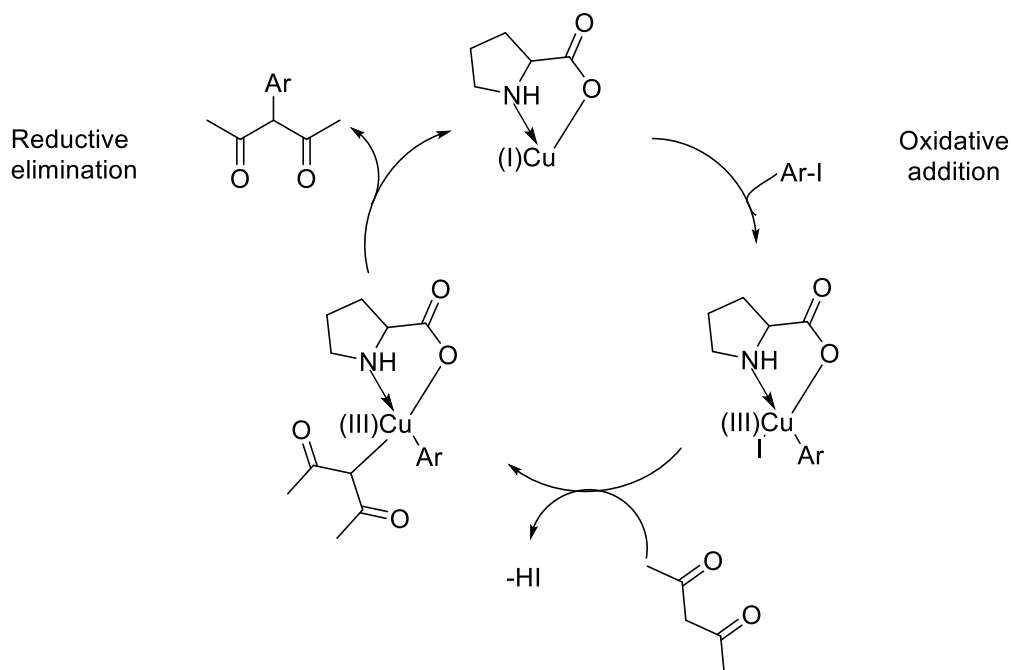


**Figure 2.32- Catalytic cycle of copper in the Hurtley reaction, the first step in the synthesis of RAB216. The cycle begins with the oxidative addition of the aryl iodide on to the Cu(I) centre to give Cu(III). The iodide is then substituted with the deprotonated acetylacetone before the reductive elimination step occurs, yielding the desired substituted aryl and the Cu(I) catalyst.**

The second step in the synthesis of RAB216, was a Knorr pyrazole synthesis. This reaction combines a 1,3-diketone with hydrazine, using an acid catalyst to give the pyrazole ring. The mechanism begins with a nucleophilic attack of one of the carbonyl groups by hydrazine, leading to the formation of an imine followed by the elimination of water. The second nitrogen of the hydrazine then attacks the other carbonyl group, forming a second imine. Finally, the  $sp^3$  hybridised carbon is deprotonated, allowing the formation of the aromatic pyrazole. The mechanism is shown in Figure 2.33. The reaction proceeded first time, with a yield of 35% over 2 steps following purification by column chromatography.

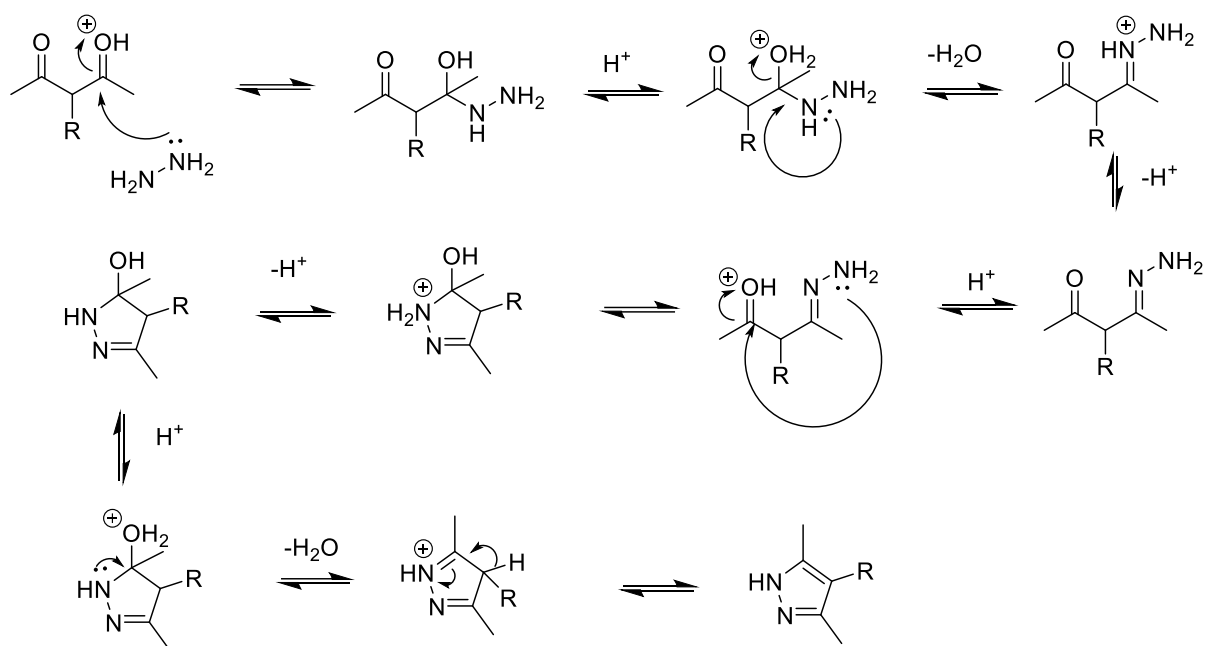


**Figure 2.33 - Mechanism of the Knorr pyrazole synthesis, use to make RAB 216.** The nucleophilic hydrazine attacks one carbonyl group, followed by elimination of water to give an imine. The free nitrogen of the imine attacks the other carbonyl eliminating another water molecule. After a tautomerisation the final pyrazole product is formed.

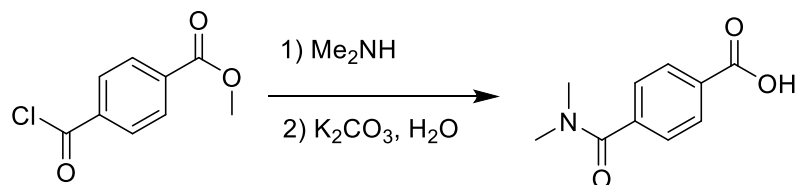


**Figure 2.34 - Scheme for the synthesis of RAB212.** The first step is an addition-elimination reaction with dimethylamine and an acid chloride. This is followed by hydrolysis of the ester in the presence of base.

RAB212 was made *via* a 2-step synthesis (Figure 2.34), starting with the formation of an amide by the reaction of an acid chloride with an amine. The lone pair of the dimethylamine nitrogen attacks the carbonyl carbon of the acid chloride, eliminating HCl to give the amide. The product was used directly in the next step following extraction with ethyl acetate and a wash with dilute HCl. The second step was an ester hydrolysis using potassium carbonate and water as the source of the hydroxide ion. After purification with column chromatography, RAB212 was isolated in a yield of 61% over 2 steps.

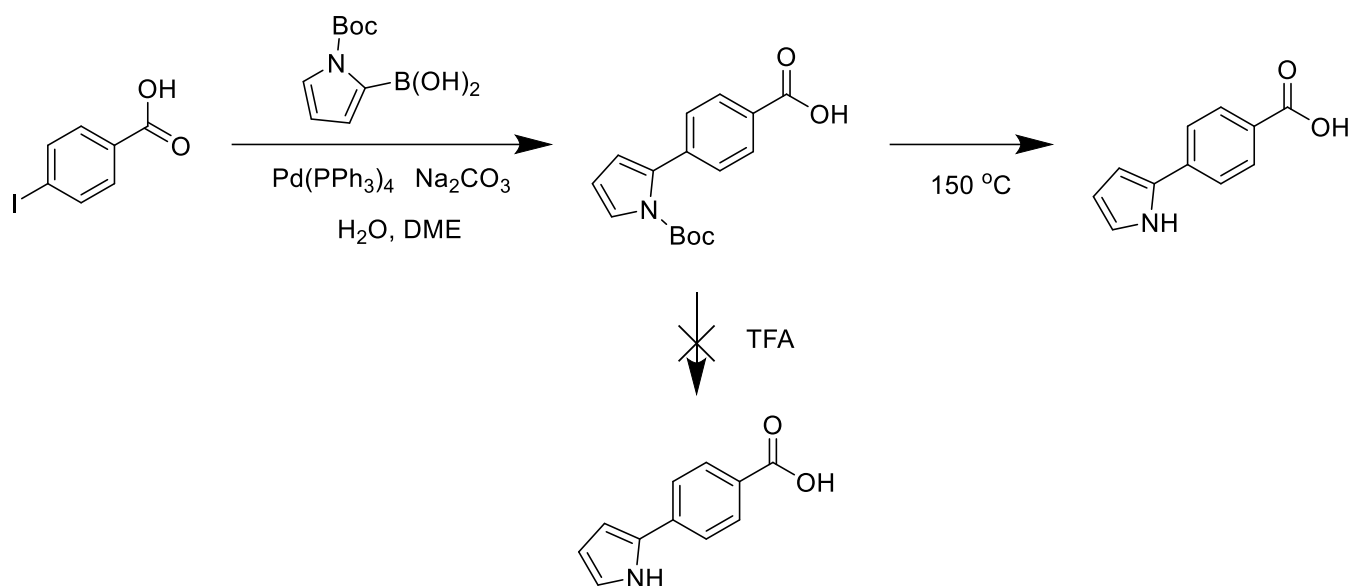


**Figure 2.35 - Synthesis of RAB211.** The first step is a Suzuki coupling with a Boc protected pyrrole and 4-iodobenzoic acid. The first attempt at the boc removal using trifluoroacetic acid did not result in any product formation. A thermal deprotection method was used by heating the compound to 150 °C which resulted in the formation of product.

The final compound synthesised in the second generation was the pyrrole analogue RAB211. The first step of the synthesis was a Suzuki coupling (Maeda *et al.*, 2011). Suzuki reactions are palladium catalysed cross-coupling reactions, where the coupling partners are a boronic acid and an organohalide. The pyrrole boronic acid reagent was protected using a Boc group, to prevent the pyrrole nitrogen coordinating to the palladium catalyst. The catalytic cycle for this reaction is similar to that seen for the copper catalysed reaction, but also includes a transmetalation step.

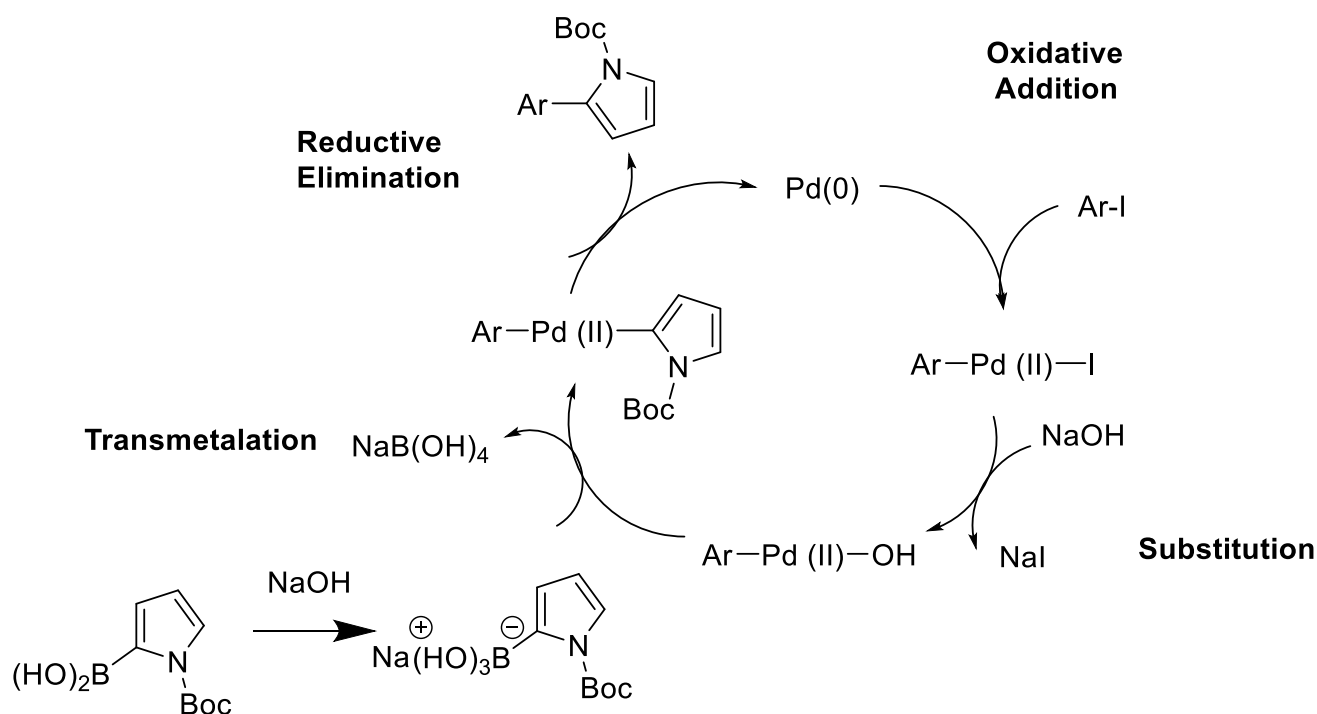
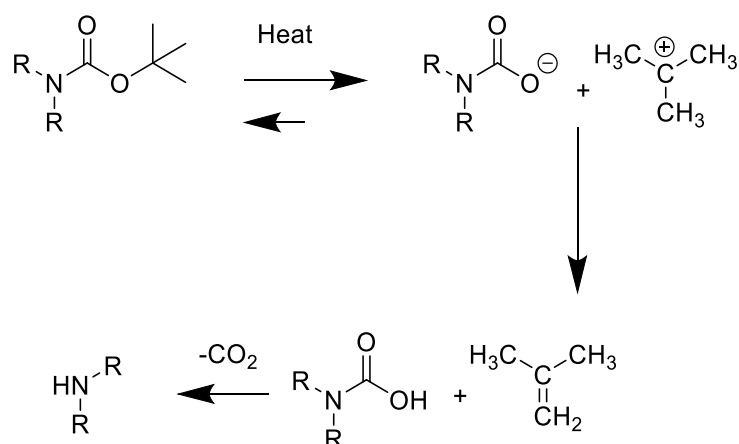


Figure 2.36 - Mechanism of the Suzuki coupling used to make RAB212. The  $\text{Pd}(0)$  is converted to  $\text{Pd(II)}$  by oxidative addition, as it enters between the iodine aryl bond. The iodine is substituted for a hydroxyl before the transmetalation step, whereby the hydroxyl group transfers to the boron centre, allowing the pyrrole to bind to  $\text{Pd(II)}$ . The final step is a reductive elimination, resulting in the formation of an aryl-pyrrole bond and regeneration of the  $\text{Pd}(0)$  catalyst.

The reaction, shown in figure 2.36, begins with the oxidative addition of the aryl iodide across the palladium centre, changing its oxidation state from 0 to +2. Palladium catalysts must have an oxidation state of 0 in order to facilitate this step of the reaction. The hydroxide ion formed through the aqueous carbonate solution substitutes for the iodide before the transmetalation step. This step involves the transfer of the pyrrole ligand from the boron centre onto the palladium. The aryl group and pyrrole then form a bond *via* reductive elimination to give the cross-coupled product and free  $\text{Pd}(0)$ , which can then participate in another catalytic cycle. This first step of the synthesis reached completion after 1 h and was taken to the next step without further purification.

The final step was the deprotection of the pyrrole by removal of the Boc group. Boc groups are sensitive to strong acid and therefore reaction with trifluoroacetic acid (TFA) is the most common way to remove it (Blondelle & Houghten, 1993). However, when this was attempted in this synthesis, it resulted in an unidentifiable mixture of products. Pyrrole rings have previously been shown to react with TFA which may be responsible for this mixture of products (Imuro and Hanafusa, 1976). Instead, a thermal Boc deprotection was used (Figure 2.37), by heating the product to  $150\text{ }^{\circ}\text{C}$  to give RAB211. The *tert*-butyl ester fragments to give a carbamic acid and the relatively stable *tert*-butyl carbocation. The resulting carbamic acid then undergoes a decarboxylation to give the desired unprotected amine.



**Figure 2.37 - Mechanism for a thermal Boc deprotection.** Due to the relative stability of the tert-butyl cation, heat induces an equilibrium between the ester and the carboxylate/ cation. The carboxylate acts as a base to form the carboxylic acid and 1-butene. The carbamic acid undergoes a decarboxylation to give the unprotected pyrrole.

Because Boc groups are sensitive to acid, they are prone to cleavage during LCMS analysis that use acidified eluents (Tom *et al.*, 2004). Therefore, Boc deprotections can be difficult to analyse *via* this method. The  $^1\text{H}$  NMR spectrum in Figure 2.38 shows the pyrrole ring is present and the boc group has been removed.  $^1\text{H}$  NMR data to support this is the peak with a chemical shift of 11.5, which corresponds to the NH group. Secondly, the 3 peaks each with an integration of  $^1\text{H}$  indicate the presence of the pyrrole group. Lastly, there is no peak with an integration of 9H in the alkyl region of the spectrum, which indicates the Boc group is not present. Following purification by column chromatography, the final product was isolated in a yield of 47% over 2 steps.

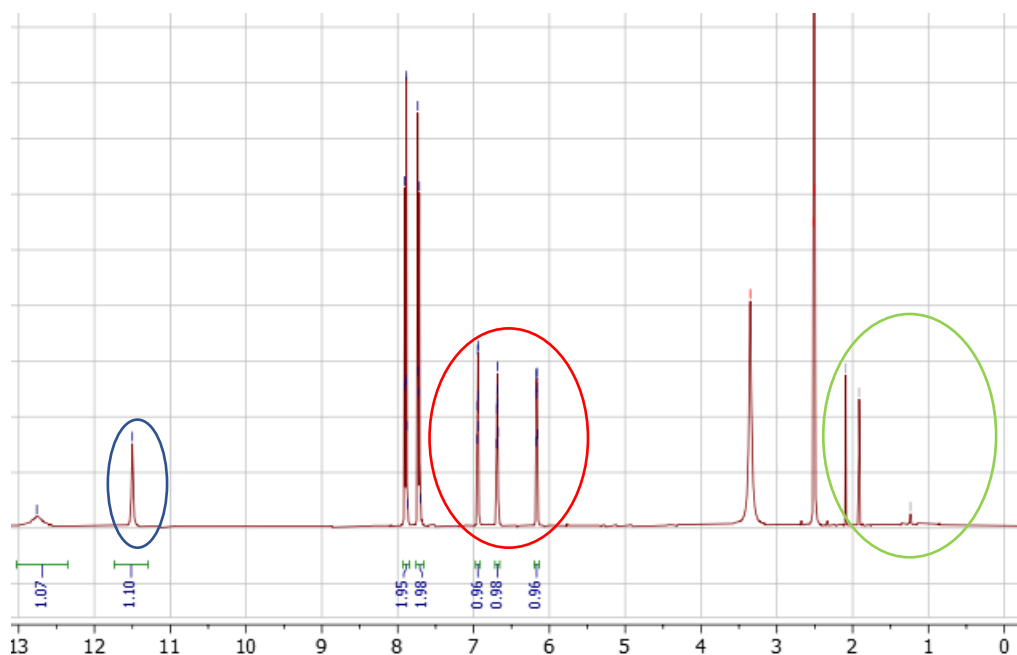


**Figure 2.38–  $^1\text{H}$  NMR spectrum of RAB 211. Blue circle - peak representing pyrrole NH. Red circle - peaks representing pyrrole CHs. Green circle- area where Boc tert-butyl group peak would be, which is not present.**

## 2.2.6 Screening of Generation 2 Compounds

Once the second generation of compounds were available, they were screened *via* the same electroshock assay as the first generation. Again, each compound was independently screened by 2 UG project students (Thomas Humphreys and Ceri Hughes) to accommodate for the variability seen with this behavioural assay. All of the compounds shown in Table 2.6 were screened, aside from RAB209 and RAB214 which were not synthesised successfully due to time constraints. This screen also includes RAB109 from generation 1 which was missing from the first screen due to a lack of material. The results of the initial generation 2 screen are shown in Figure 2.39.

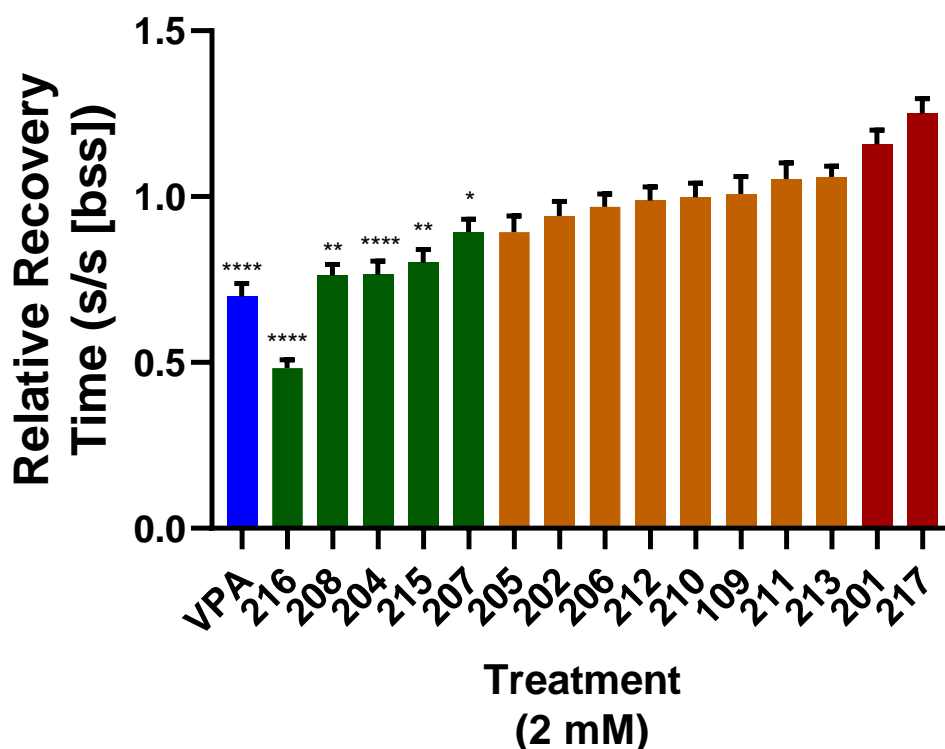


Figure 2.39 - Initial L3 seizure assay screen of generation 2 RAB compounds. Relative recovery time was calculated as a ratio of the treatment group recovery time compared to the corresponding untreated *para*<sup>bss</sup> group from that week of screening. Green denotes a significant reduction in recovery time, orange denotes no change and red denotes a significant increase. Sodium valproate (VPA), in blue, was included as a positive control. N= 24, refers to number of larvae shocked. Results were analysed via a one-way ANOVA [ $F(15, 617) = 20.35$   $P < 0.0001$ ] with correction for multiple comparison (Dunnett's). Values given are mean  $\pm$  SEM. \* =  $p < 0.05$ , \*\* =  $p < 0.01$ , \*\*\* =  $p < 0.001$ , \*\*\*\* =  $p < 0.0001$ .

Of the 15 RAB compounds screened, 5 were found to significantly reduce seizure duration as evidenced by a reduced recovery time (green), 2 significantly increased it (red) and 8 were found to have no effect (orange). Valproate, included as the positive control, was also found to significantly reduce recovery time. The generation 1 compound, RAB109 (structure shown in Figure 2.40), was found to be ineffective in this assay, further suggesting that any changes to the acid group eradicated activity.

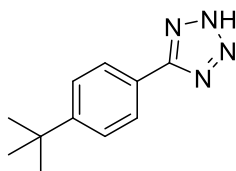
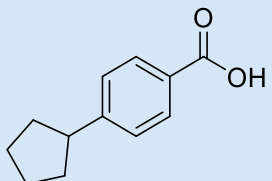
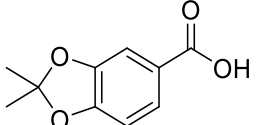


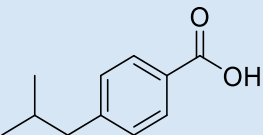
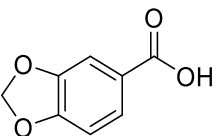
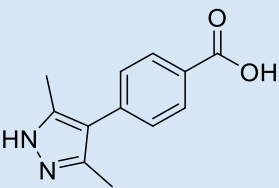
Figure 2.40 - Structure of generation 1 compound RAB109 which was included in the second screen, due to lack of material for the first round of screening. This analogue features a tetrazole ring in the place of the carboxylic acid group. This analogue was found to have no effect on the recovery time in the *e*-shock assay, further suggesting that any changes to the carboxylic acid group eradicates anticonvulsant activity.

The 5 compounds that were found to be active are shown in Table 2.7. Aside from RAB215, the size of the active compounds shows little variability, with an average of 160.95 Å<sup>3</sup> and values ranging from 147.1 – 172.3 Å<sup>3</sup>. Larger compounds, such as the C(CF<sub>3</sub>)<sub>3</sub> analogue RAB205 (187.2 Å<sup>3</sup>), may be too large to be tolerated by the putative binding target, particularly as similar, but smaller fluorine containing analogues, were found to be active in the first screen. Cyclohexyl analogue RAB202 was found to be inactive, despite being closely related to the active cyclopentyl analogue RAB204. This could be due to the difference in size, as with a volume of 184.3 Å<sup>3</sup> it is larger than any of the active compounds from either screen. Additionally, RAB202 has a CLogP of 4.51, which is higher than any other compounds found to be active in the other screens.

Three of the 5 active compounds contain 2 hydrogen bond acceptors in the modified group, with RAB216 also containing an N-H hydrogen bond donor. Results from the first screen showed that hydrogen bond acceptors can be tolerated, as nitrile analogue RAB135 proved to be active. Additionally, fluorine analogues also performed well in the first screen, which can form intramolecular dipole interactions similar, yet weaker, to hydrogen bonds (DiMagno and Sun, 2006). Therefore, it was predicted that the inclusion of electronegative atoms in the varied region of the compound may increase potency. Only one of the compounds featured 2 hydrogen bond acceptors, the amide analogue RAB212, which showed no anticonvulsant activity. This is likely due to either the low CLogP affecting the distribution of the compound *in vivo* or a lack of lipophilic bulk in the varied region, which has been present in all other active compounds. Compounds that feature hydrogen bond acceptors in this region may show increased potency due to improvements in solubility or the formation of additional interactions through hydrogen bonding.

**Table 2.7- Structure and selected properties of active compounds from the generation 2 screen.**

Compound RAB	Structure	Molecular weight	Volume (Å <sup>3</sup> )	pKa	cLogP
204		190.2	166.5	4.30	3.95
207		194.19	147.1	3.95	2.61

208		178.23	157.9	4.25	3.84
215		166.13	112.2	3.82	1.97
216		216.24	172.3	3.98	1.92

From comparison of the physical properties of the active compounds from this second screen, it seems that certain characteristics increase the chance of the compound being active. No compound with a cLogP above 4 or a solvent excluded volume over 180 Å<sup>3</sup> was found to be active. Additionally, compounds which feature 2 or more hydrogen bond acceptors in the modified region are more likely to be active, with 3 out of 4 of these compounds showing anticonvulsant activity. From the data RAB216 was the most active analogue, however, due to the variability expected with behavioural assays, it was decided that the best way to validate the most active compounds would be to continually reduce compound dose until only a suitable number of compounds are left to be taken forward to mammalian testing.

#### 2.2.7 Establishment of Lead Compounds

Once the second generation compounds had been screened, the next step was to screen the 11 compounds found to active in the 2 screens, at lower concentrations (Note: concentration refers to the amount in fly food and does not take into account differences in absorption or access to the fly nervous system). The aim of these experiments was to establish 2-3 lead compounds to take forward to mammalian testing, reducing the number of mice required. An initial concentration of 0.4 mM was chosen as this was the highest concentration RAB102 had been tested where no anticonvulsant activity was observed. Additionally, RAB132 had been found to be active at this concentration, meaning any compounds with increased potency should reduce recovery times at this concentration. The results of this screen are shown in Figure 2.41.

### L3 Seizure Assay 3: Compound Ranking

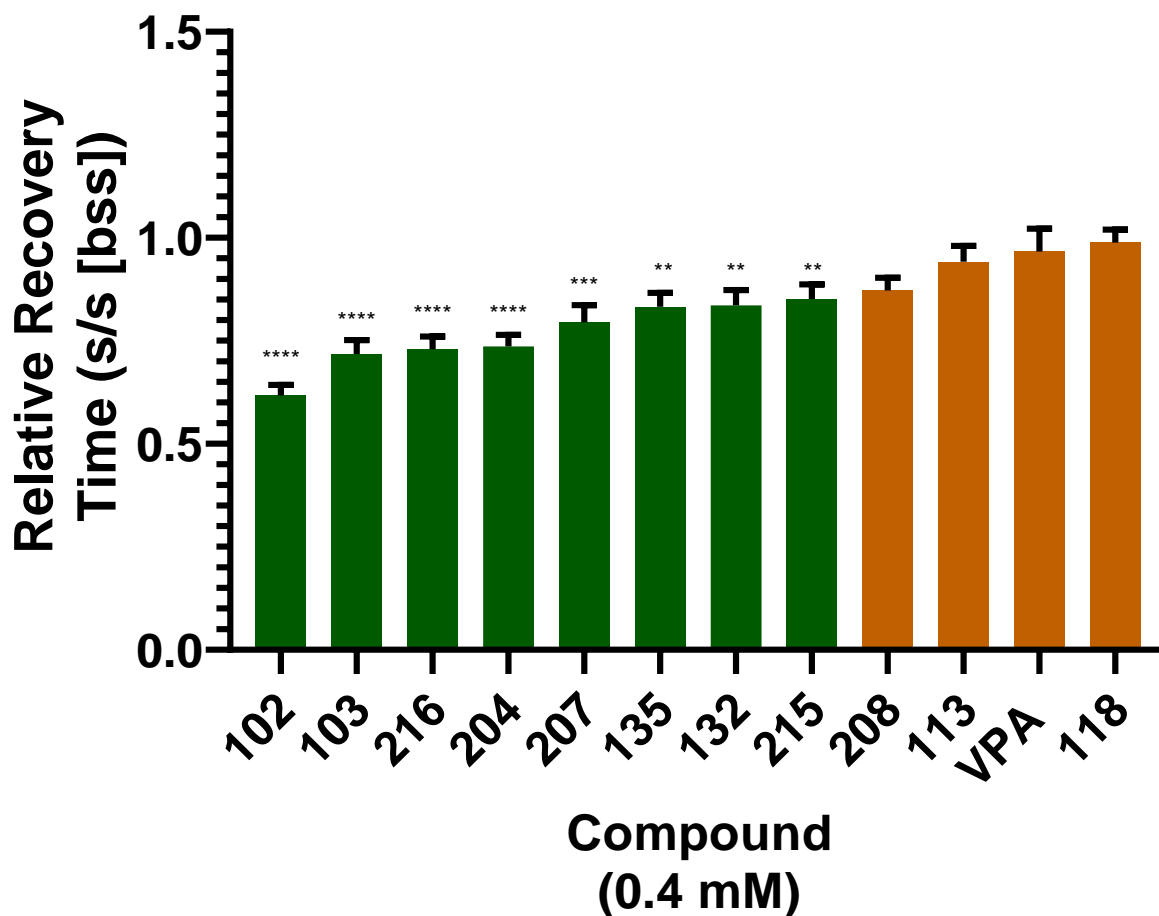


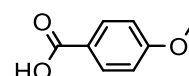
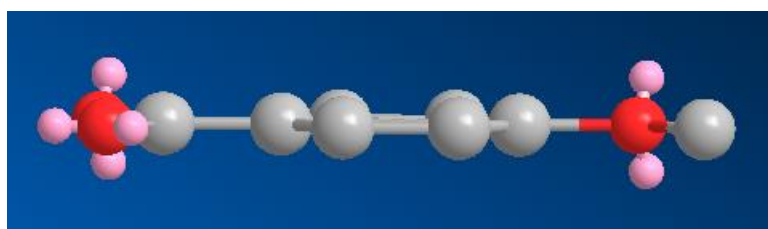
*Figure 2.41 - Second L3 seizure assay screen of active RAB compounds. Relative recovery time was calculated as a ratio of the treatment group recovery time compared to the corresponding untreated bss group from that week of screening. Green denotes a significant reduction in recovery time, orange denotes no change. Sodium valproate (VPA) was included as a positive control but was not found to be active at this concentration N= 24, refers to number of larvae shocked. Results were analysed via a one-way ANOVA [ $F(11, 454) = 9.810$   $P < 0.0001$ ] with correction for multiple comparison (Dunnett's). Values given are mean  $\pm$  SEM. \* =  $p < 0.05$ , \*\* =  $p < 0.01$ , \*\*\* =  $p < 0.001$ , \*\*\*\* =  $p < 0.0001$*

Of the 11 analogues tested, 8 were found to significantly reduce recovery time at a reduced level (in food) of 0.4mM. Additionally, the clinically active antiepileptic valproate was found to be inactive at this concentration. The 2 compounds that were not active were the methoxy analogue RAB113 and the benzene analogue RAB118. These 2 compounds possess very different groups in the *para* position, but one characteristic they each share is a lack of 3D structure, having a planar carbon skeleton. Furthermore, all of the compounds that were active do have a 3D structure, suggesting that it may be important.

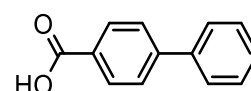
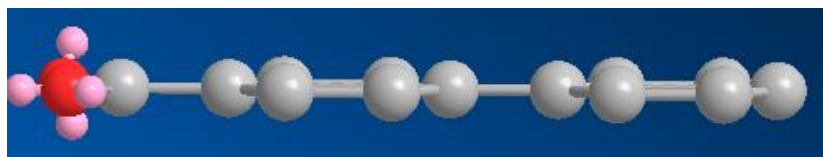
Other planar analogues such as RAB211 and RAB210 have been screened previously and found to be inactive, further supporting the idea that a lack of 3D structure is undesirable for target binding.

Both RAB210 and RAB211 contain 5 membered aromatic heterocycles, similar to RAB216. However,

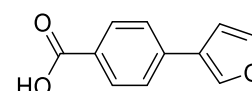
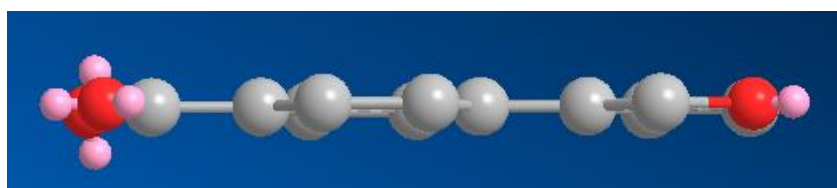
the presence of the 2 methyl groups on the pyrazole ring causes it to be twisted relative to the benzene ring, as highlighted in Figure 2.42. This is a result of the steric hindrance caused by the methyl group hydrogen atoms clashing with the hydrogens of the benzene ring. It is therefore energetically favourable for the lowest energy conformation to have a twist in the pyrazole of approximately  $18^\circ$ .



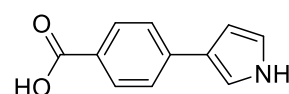
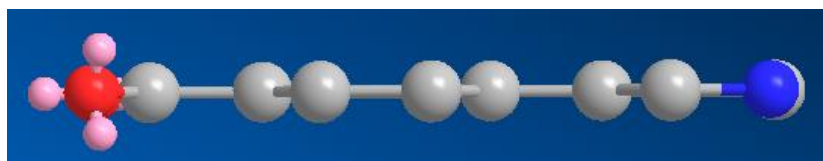
A



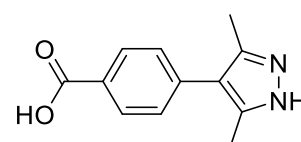
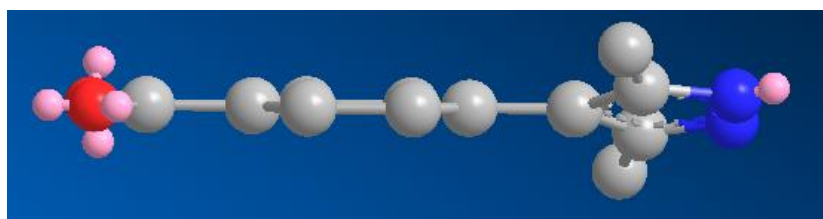
B



C



D



E

**Figure 2.42- 3D structures of A) RAB113, B) RAB118, C) RAB210, D) RAB211, E) RAB216 in their lowest energy conformation where Red = O, grey = C, blue = N and pink = lone pairs. Relative to the plane of the benzene ring, the pyrazole group of RAB 216 is twisted at an angle of approximately  $18^\circ$ , whereas all the other molecules shown possess no 3D structure in their carbon skeletons. Models were created and calculations were done using Chem3D software.**

To recap, 8 compounds were found to be active at the concentration of 0.4 mM. Therefore, in order to reduce the number of compounds taken forward for further study, another round of screening at a lower concentration was required. The next concentration used was 0.1 mM (in flyfood) and the results are shown in Figure 2.43.

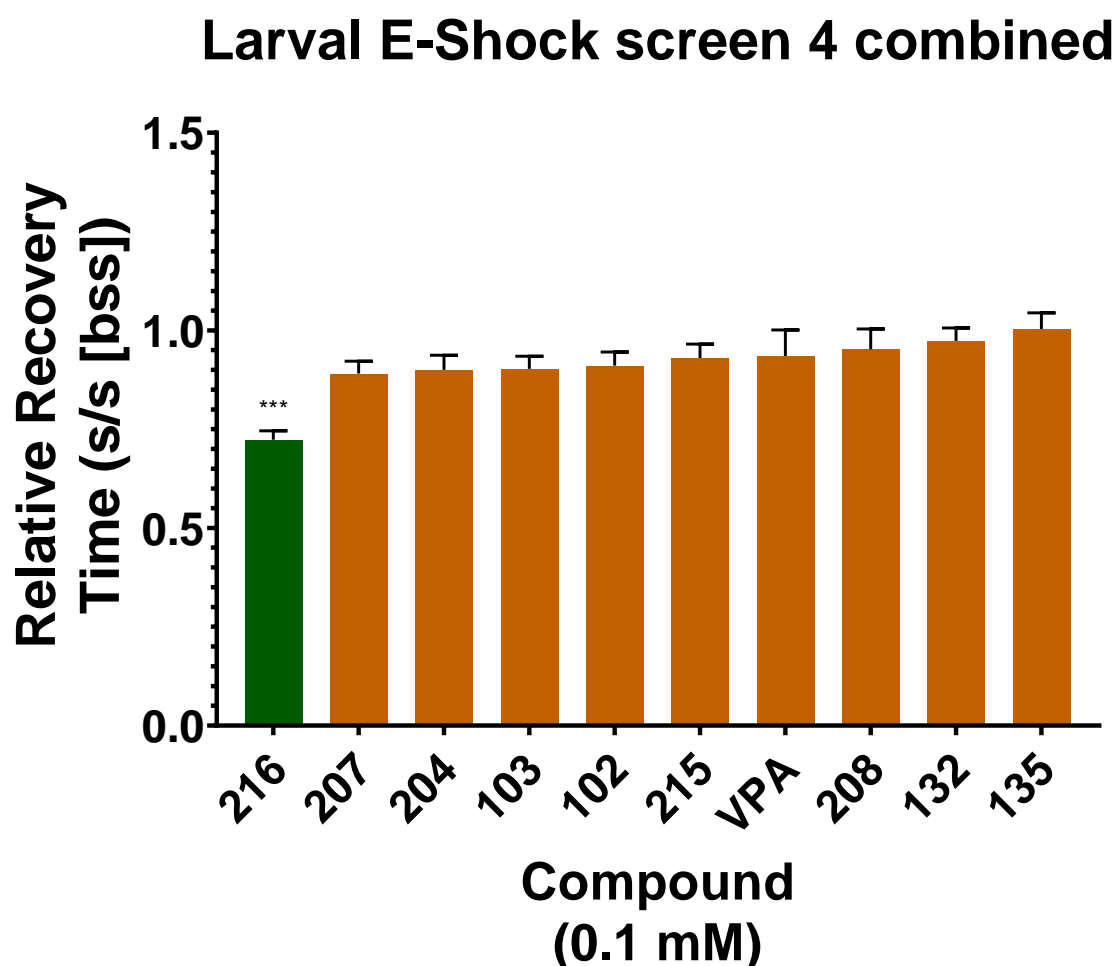


*Figure 2.43 – L3 seizure assay of compounds found to be active in screen 3. RAB216 was the only compound found to be active at this concentration and was therefore taken forward for further investigation. Green denotes a significant reduction in recovery time, orange denotes no change. Sodium valproate (VPA) was included as a positive control but was not found to be active at this concentration. N= 24, refers to number of larvae shocked. Results were analysed via a one-way ANOVA [ $F(9, 294) = 4.813$   $P < 0.0001$ ] with correction for multiple comparison (Dunnnett's). Values given are mean  $\pm$  SEM. \* =  $p < 0.05$ , \*\* =  $p < 0.01$ , \*\*\* =  $p < 0.001$ , \*\*\*\* =  $p < 0.0001$*

At a concentration of 0.1 mM, RAB216 was the only compound found to be significantly active, reducing the mean recovery time by 28% compared to untreated *para<sup>bss</sup>* mutants. Valproate was not active at this concentration, which was also the case in the 0.4 mM screen. Whilst this shows that RAB216 is likely to be more potent than valproate in this model, further studies in a variety of models would be required to compare their overall effectiveness.

### 2.2.8 Screening of Lead Analogues

In medicinal chemistry, to establish an effective SAR one small change is made to each analogue in order to find the physical and structural features that make compounds more potent. To identify which structural features of RAB216 are important for its potency, 2 more analogues (Figure 2.44) were screened with minor changes in the structure of the pyrazole ring.

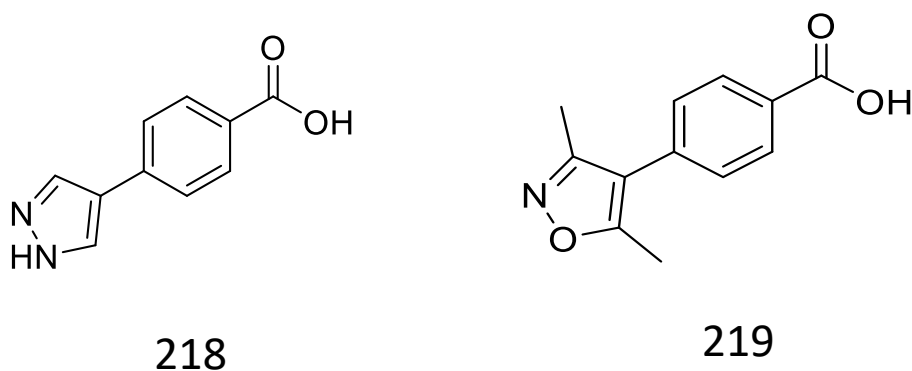


*Figure 2.44 – Structures of 2 analogues based on the structure of lead compound RAB216. RAB218 has the pyrazole ring seen in RAB216 but without the 2 methyl groups, meaning it lacks lipophilic bulk in this region and doesn't have the twist described in Figure 2.42. RAB219 has the two methyl groups seen in RAB216 but has an oxygen in place of the NH and therefore lacks the hydrogen bond donor, whilst retaining similar electronic properties.*

RAB 218 has the same pyrazole ring as RAB 216 but lacks the 2 methyl groups on the free carbons. As a result, the compound would have a reduced lipophilic bulk in this region and lacks the  $\sim 18^\circ$  twist of the pyrazole relative to the benzene ring. RAB 219 still possesses the 2 methyl groups present in RAB 216 but, additionally, has an oxygen atom in place of the NH group, meaning the ring is an isoxazole instead of a pyrazole. As a result, RAB 219 doesn't possess a H-bond donor. The 2 groups have a similar electronic structure although there are differences. Figure 2.45 shows the relative electron densities of each atom within the rings of the 2 analogues. Although the electron density is more evenly spread across the isoxazole, the 2 heteroatoms within the ring have opposing relative charges in both groups. One has a partial positive charge and the other having a partial negative charge. As a result, these heteroatom pairs within the 2 heterocycles should be able to form similar electrostatic interactions, aside from the H-bond provided by the N-H. This allows the importance of the H-bond on potency to be studied.

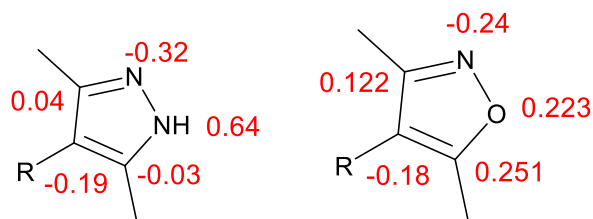


Figure 2.45 - Relative charge densities of the 5 atoms within the pyrazole ring (left) and isoxazole (right) calculated via the extended Hückel method using Chem3D software. The spread of charge is similar, although it is more evenly spread around the ring in the isoxazole when compared to the pyrazole. Both were calculated using the structures of RAB 216 and RAB 219.

## L3 Seizure Assay: RAB 216 Analogue Screening

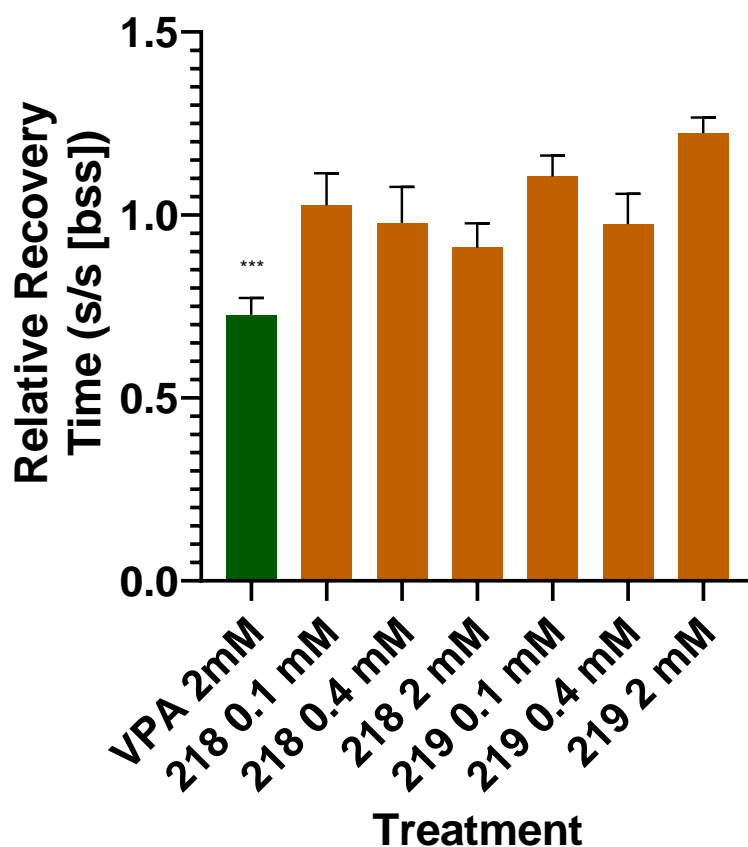
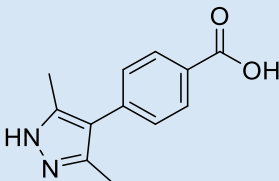
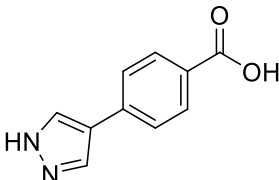
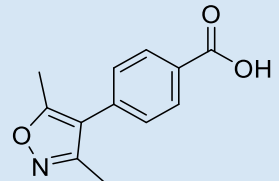


Figure 2.46 - L3 seizure assay of RAB 216 analogues RAB218 and RAB219. Sodium valproate (2mM) was used as positive control and reduced recovery times significantly. RAB218 and RAB219 had no significant effect on recovery time at any of the concentrations tested.  $N=24$ , refers to number of larvae shocked. Results were analysed via a one-way ANOVA [ $F(6, 74) = 5.412$   $P < 0.0001$ ] with correction for multiple comparison (Dunnett's). Values given are mean  $\pm$  SEM. \* =  $p < 0.05$ , \*\* =  $p < 0.01$ , \*\*\* =  $p < 0.001$ , \*\*\*\* =  $p < 0.0001$

The 2 analogues of RAB216, RAB218 and RAB219 were screened at the 3 concentrations used for the previous screens. VPA was also included as a positive control. The results of this screen are shown in Figure 2.46. Interestingly, neither analogue had any effect on seizure recovery time at all the concentrations tested (0.1, 0.4 and 2mM). This suggests that both the N-H hydrogen bond donor and the methyl groups, present in 216, are integral to efficacy. The key physiochemical properties of the 3 compounds are shown in Table 2.7. Overall, there is little difference in the listed properties for the 3 compounds. The only difference between RAB216 and the other 2 analogues could potentially be the slightly lower cLogP for RAB 219 of 1.78. This may be important for the compound's distribution, especially considering CNS active drugs typically have a higher cLogP.

*Table 2.7 - Structure of RAB 216 and analogues RAB218 and RAB219, which were designed to investigate the importance of certain RAB216 features. Structures shown with selected physiochemical properties.*

Compound Name	Structure	CLogP	MW	TPSA	pKa	Source	Recovery time reduction (2mM)
RAB216		1.92	216.2	61.69	3.97	Synthesised	52%
RAB218		1.98	188.1	61.69	4.02	Purchased Fluorochem	9%
RAB219		1.78	217.2	58.89	3.83	Purchased Fluorochem	N/A

Whilst the physiochemical properties of RAB216 and RAB218 shown in Table 2.7 are almost identical, there are significant differences in the structure. The 2 methyl groups in RAB216 provide extra lipophilic bulk in a region of the molecule that many of the previous hits exhibited lipophilicity. Analogues such as RAB102, RAB132 and RAB135 were all active in the 0.4 mM screen and all possessed at least 2 methyl groups on the carbon adjacent to the benzene ring. As a result, all these

analogues, similar to RAB216, have a 3D lipophilic group in this region, suggesting this may be a key factor for compound potency.

## 2.3 Discussion

By utilising the *Drosophila para<sup>bss</sup>* seizure mutant, a previously identified lead anticonvulsive compound, avobenzene, has been significantly improved, both in terms of optimal drug-like physicochemical properties and potency. Avobenzene would not make a suitable drug, *in vivo*, mainly because of the toxic side products it forms when undergoing lysis reactions. Additionally, a cLogP of 4.7 is relatively high and could cause issues with the distribution and solubility of the compound *in vivo*. Due to the ease with which avobenzene undergoes photolysis, it was hypothesized that the active product was in fact a product of its photolysis. Some possible photolytic products were screened before this project to design of analogues began and identified the benzaldehyde analogue, RAB102. This was the starting point for my project.

Whilst RAB102 exhibits more drug-like properties than avobenzene, it has similar issues in terms of stability and potential toxicity. In solution, when exposed to air, some aldehydes readily convert to the acid *via* a free radical mechanism (Larkin, 1990). The rate of this reaction varies depending on conditions such as temperature, solvent, and oxygen concentration, as well as the presence of other solutes that either act to promote or inhibit radical initiation. Additionally, aldehydes are converted into different groups (usually acids) by a multitude of different enzymes including aldehyde oxidases and CYP450 (Marelja *et al.*, 2014; Ahmed Laskar and Younus, 2019b). These enzymes act as a detoxifying system, converting the highly reactive electrophilic centre of aldehydes to a less reactive carboxylic acid or alcohol group. Both of these groups also lead to an increase in the compound's aqueous solubility, aiding excretion from the body (Olsson *et al.*, 2011). In addition, the aldehyde group of RAB102 is reactive towards nucleophiles, and therefore could potentially form a covalent adduct with for example some amino acid side chains (Kumalo, Bhakat and Soliman, 2015). The purity of RAB102 was tested regularly and batches were replaced if there was any noticeable crystal formation, indicative of aldehyde oxidation. However, it is difficult to know how much of the active product was in the aldehyde form after the compound has been in fly food for a few days and also the amount metabolised following ingestion by *Drosophila* larvae.

Previous experiments, where investigators have attempted to detect metabolites in *Drosophila*, have required radiolabelling or a stable isotope labelled standard (Büscher *et al.*, 2009). Even when one of these standards is readily available, analysis can also be difficult due to matrix effects (Coelho

*et al.*, 2015). However, this may improve with advances such as capillary electrophoresis mass spectrometry, which allows the concentration of molecules as small as GABA to be analysed within a sample of 30 adult *Drosophila* heads (Phan *et al.*, 2013).

Testing the stability of a compound within the food may be an easier experiment to conduct as the concentration would be higher in food compared to a larval CNS. Moreover, the LCMS trace would likely be less noisy than an extract from a *Drosophila* head. This experiment would still require a stable isotope labelled standard in order to calculate the final concentration and extraction efficiency, however it may be possible to conduct a qualitative experiment without an internal standard. Despite *Drosophila* feeding experiments being common, there have been few studies on the stability of compounds within food. Most functional groups are likely to be stable under the conditions that *Drosophila* are kept in, but less stable groups, such as aldehydes and esters, could be affected. Standard fly food contains yeast, which is known to possess alcohol dehydrogenase, an enzyme that converts aromatic aldehydes (such as RAB102) to carboxylic acids. Experiments studying the stability of compounds within fly food could affect the design of feeding experiments in the future, either by limiting what compounds can be studied by this method, or the introduction of additives which promote compound stability, such as dithiothreitol to prevent oxidation.

Due to the instability and reactivity of aldehydes, for example RAB102, it was decided to test its corresponding acid analogue, RAB103. As well as being the product of aldehyde oxidation, the carboxylic acid is also one of the major breakdown products of avobenzene photolysis. The pre-screen undertaken before this project began discovered that both avobenzene exposed to UV and RAB102 were equally effective at reducing seizure recovery time when compared to avobenzene alone. The carboxylic acid of RAB102 was not tested in this screen and therefore was the first compound tested when the project began. RAB103 was found to be just as effective at reducing recovery times when compared to RAB102. Without further investigation, it is not possible to know what the active product is of each treatment group. It is possible that RAB103 is in fact the active product of avobenzene and RAB102 treatment groups, especially when they were all found to be equally potent at the 2 mM concentration. Additionally, the aldehyde RAB130 had very similar activity to its acid analogue RAB131. However, there is evidence to suggest a difference in potency between the aldehyde and acid analogues. Whilst RAB132 was found to be active at 2mM and 0.4 mM, its corresponding aldehyde RAB213, had no effect at these concentrations. even if they were, it would be problematic having a library of aldehydes due to the strong chance of toxicity, especially with long term exposure. There are very few examples of aldehydes in drugs and even drugs that are metabolised to aldehydes can cause toxicity issues (Paludetto *et al.*, 2019). It was therefore decided

to focus on carboxylic acids when designing compounds, testing the corresponding aldehyde analogue where it was commercially available.

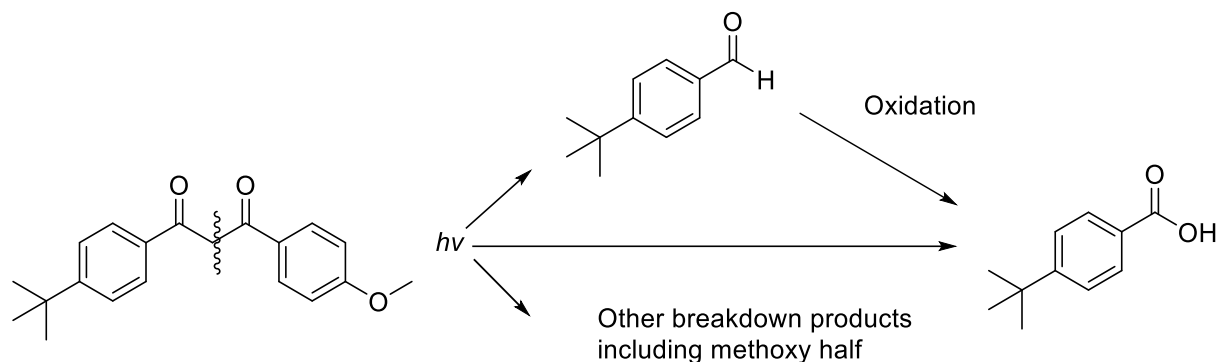


Figure 2.47 - Potential scheme of avobenzone photolysis leading to the formation of RAB103. RAB103 is one of the major breakdown products of avobenzone photolysis. Its corresponding aldehyde is also a major breakdown product of avobenzone photolysis.

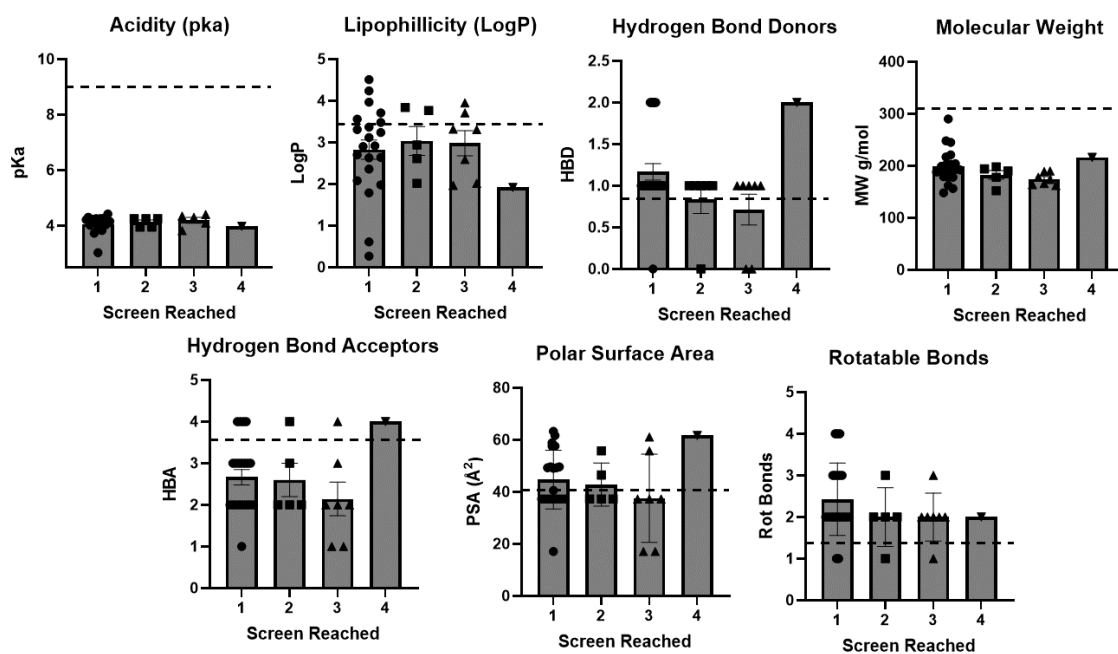


Figure 2.48 - Selected properties of all compounds screened compared to the mean value of CNS acting drugs, represented by the dotted line of each graph. Screen reached represents the screen in which the compound was eliminated. Group 4 represents RAB216 only. Data on averages taken from (Doan et al., 2002).

*Table 2.8 - Comparison of the properties of RAB216 with CNS and non-CNS drugs. The asterisks represent properties where there is a significant difference between CNS and non-CNS properties. Data on CNS and non-CNS averages were taken from (Doan et al., 2002). 48 CNS and 43 non-CNS drugs were analysed. Selection was based on molecular weight 150-800 and stability/state (gasses and solids excluded).*

Physical Chemical Properties	CNS	Non-CNS	RAB216
Molecular weight	319	330	216.2
cLogP	3.43*	2.78*	1.92
clogD	2.08	1.07	-1.23
PSA	40.5	56.1	61.7
Hydrogen bond donors	0.85*	1.56*	2
Hydrogen bond acceptors	3.56	4.51	3
Flexibility (rotatable bonds)	1.27*	2.18*	2

One way of potentially rationalising why certain compounds were more potent than others, is by comparing their physiochemical properties to each other and marketed drugs. Drugs that need to enter the CNS to reach their target have different mean values for certain physiochemical properties. Those that are statistically different are marked with an asterisk in Table 2.8. The main reason for this difference in the necessity of crossing the BBB which generally requires higher lipophilicity and appears to be aided by reduced molecular flexibility. The difference in H-bond donors is linked to lipophilicity. H-bond donors are polar bonds between a heteroatom and a hydrogen atom and therefore an increased number of H-bond donors results in lower cLogP. This effect is enhanced in smaller molecules, as the polar atoms make up a larger proportion of the molecule.

To study the effects of physiochemical properties on compound potency, the compounds were sorted into 4 categories, depending on the lowest concentration at which they were active. Compounds which had no effect on recovery time were placed in the first group and RAB216 alone was placed in the 4th group. There is no clear trend in the data that suggests any particular physiochemical property had an integral effect on compound potency. There is no observable difference between the compounds that showed activity at 0.4 mM and those that were ineffective at any concentration. For certain properties, such as mol weight, there was only a small range explored by the library, reducing the chance of finding any meaningful trend. However, for other properties including PSA and cLogP a larger range was explored, but still no obvious differences were observed. The chemical space explored was limited by the structural aspects of the compound

required for potency, particularly after the first screen. This is reflected on the graphs in Figure 2.48, which shows the range in each physiochemical property was generally larger for the compounds eliminated in the first screen.

The main observation from the first screen was that any changes to either the central ring structure or the acid/aldehyde group resulted in loss of activity. Therefore, the entire second generation of compounds varied only in a specific region of the molecule. Exploring additional chemical space is important, particularly in the early stages of a drug discovery project with no ligand binding model (Hughes *et al.*, 2011). There are an almost infinite number of changes that can be made to a molecule and without computational modelling by docking compounds to the target (structure of receptor(s) not available for this project), there is no way of accurately knowing which changes will have a positive effect on potency. However, with a limited library size, a more focussed library was required for this project.

The graphs in Figure 2.48 also feature the mean value for each physiochemical chemical property of CNS active molecules taken from an analysis of 48 CNS drugs, which are also shown in Table 2.8 (Doan *et al.*, 2002). The library was designed with these parameters in mind, so for a majority of the properties analysed, the compounds in the library do not deviate much from the mean. The 2 largest differences come from the mol weight and pKa. In early stage drug development it is advantageous to start with a library of lower mol weight compounds, because this leaves space to add to the compound when making future analogues (Hughes *et al.*, 2011). Additionally, other analysis has shown that lower mol weight compounds (<300) are more likely to have desirable absorption, distribution, metabolism, excretion and toxicity (ADMET) properties, especially when combined with a cLogP between 1-3 (Gleeson *et al.*, 2011).

The difference in pKa between the compounds screened for this project and marketed CNS drugs is due to the inclusion of a carboxylic acid group. Carboxylic acids are not typically found in CNS drugs because they are negatively charged at physiological pH. Anions have poor penetration of the BBB via passive diffusion, due to charge repulsion at the BBB surface, which itself is negatively charged (Walter *et al.*, 2021). However, there are numerous cases of anions crossing the BBB, usually via active transport (Gao *et al.*, 2000; Kikuchi *et al.*, 2003; Tohyama, Kusuhara and Sugiyama, 2004). This includes sodium valproate, which is carried into the brain by a medium-chain fatty acid transporter (Adkison and Shen, 1996). Another group of transporters relevant to carboxylic acids, is the monocarboxylate transporters (MCTs). These proteins are responsible for the transport of endogenous acids such as lactate, pyruvate and  $\beta$ -hydroxybutyrate (Figure 2.49), as well as certain amino acids, across the BBB (Vijay and Morris, 2014). They have also shown to be responsible for a

number of drugs crossing the BBB, including 4-phenylbutyrate, ketoprofen and benzoic acid (Choi, Jin and Han, 2005). All the compounds mentioned share physical features with the compounds screened in this project, particularly benzoic acid as every compound found to be active across the screens featured benzoic acid or benzaldehyde within the structure. Additionally, the other MCT substrates mentioned, also possess a single carboxylic acid, a benzene ring and have a relatively low mol weight. The fact that ketoprofen is a substrate also shows that slightly larger compounds, featuring additional functional groups can also interact with MCTs. Therefore, whilst the inclusion of an acid group in the lead compound makes passive diffusion difficult, there is a chance it may be actively transported across the BBB *via* an MCT transporter.

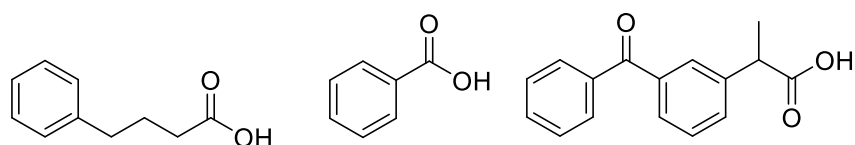


*Figure 2.49 - Structures of 4-phenylbutyrate, ketoprofen and benzoic acid (left to right). All possess a carboxylic acid group and are substrates of monocarboxylate transporters (MCTs). The lead compound (RAB216) shares features with these compounds, such as a single carboxylic acid group and a benzene ring. The structure is particularly similar to benzoic acid, which was used as part of the scaffold when designing compounds.*

Whilst the brain organisation of *Drosophila* is different to mammals, they do both possess MCTs and a membrane barrier between the CNS and circulatory system (Gonzalez-Gutierrez *et al.*, 2019). Insects have an open circulatory system where molecules are dissolved in a fluid called haemolymph that bathes organs. This is separated from the CNS by a thin layer of epithelial cells derived from glia (Treherne and Pichon, 1972). The insect CNS barrier is therefore less complex topologically; however, they do share many features on a cellular level. The sub-perineural glia forms pleated septate junctions, that create a tight barrier to paracellular diffusion, in a similar manner to the endothelial cells that form tight junctions in vertebrates. Additionally, the *Drosophila* proteins that make up the septate junctions are nearly identical to those found in the tight junctions of the vertebrate BBB (Banerjee, Sousa and Bhat, 2006).

In both insects and vertebrates, the barrier has evolved to prevent xenobiotics from entering the CNS, whilst allowing the transport of key nutrients. A mutation to the gene *moody* prevents the barrier from functioning properly, increasing the sensitivity of *Drosophila* to nicotine and cocaine (Bainton *et al.*, 2005). This highlights the role of the barrier in preventing drugs reaching the CNS. MCTs have been identified in *Drosophila*, including *chaski* which transports lactate and pyruvate to the CNS, and *silnoon*, which is required for butyrate induced apoptosis (Delgado *et al.*, 2018). Interestingly, the drug gamma-hydroxybutyric acid (GHB) has been shown to have an effect on the *Drosophila* CNS. In vertebrates MCTs are required for the transport of GHB across the BBB. In the case of GHB and the acid compounds in this screen, it is hard to know whether these compounds

reach the CNS through active transport or because the CNS barrier in *Drosophila* larvae is less selective. Little is known about the comparative selectivity between the 2 barrier systems, but to improve drug screens in *Drosophila* going forward, it would be interesting to investigate. Crossing the BBB is one of the biggest hurdles for a CNS drug discovery project and is also the cause of side effects for many drugs which do not act on the CNS. If the selectivity of the *Drosophila* CNS is comparable to that of vertebrates, this would make them a useful tool for investigating compound permeability *in vivo* before screening them in more complex organisms.

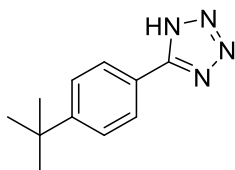
The aim of these screens was to use SAR and the principles of drug discovery to design a library of compounds to improve potency when compared to the parent compound RAB102. Results suggest that the lead RAB216 is at least 4 times more potent in comparison to RAB102 and is also more drug-like due to the lack of the aldehyde present in RAB102. Screening compounds in *Drosophila*, before taking them forward to more complex organisms, means less protected animals need to be used, which has benefits in terms of time, cost, and ethics. However, there are clearly more differences in terms of physiology and genetics between humans and *Drosophila* when compared to humans and rodents. Therefore, the most potent compound RAB216 is to be taken forward to mouse along with the original parent compound, RAB102. These experiments are intended to not only validate the compound's activity, but also the *Drosophila* model used in this screen.

## 2.4 Materials and Methods

### 2.4.1 Chemistry

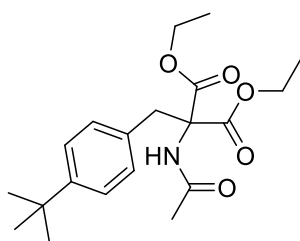
All solvents, deuterated solvents and common reagents were purchased from Sigma–Aldrich, Alfa-Aesar, Fisher Scientific or Fluorochem. Chemicals used for screening were purchased from where stated in Tables 2.2, 2.3, 2.4 and 2.6. Chemicals used in synthesis were purchased from where stated in synthesis methods.  $^1\text{H}$  and  $^{13}\text{C}$  NMR spectra were recorded on a Bruker Avance 400 or 300 MHz spectrometer. Chemical shifts ( $\delta$ ) are defined in parts per million (ppm) referenced to residual solvent peak. ESI and APCI mass spectrometry was carried out on a Waters Acquity UPLC system connected to a Waters SQD2 mass spectrometer. Molecular ion peaks are defined as mass/charge ( $m/z$ ) ratios. Melting points were measured using a Stuart SMP10 melting point apparatus. Solvent evaporation was conducted on a Büchi Rotavapor R-200. Analytical thin-layer chromatography was performed using silica gel 60 on aluminium sheets coated with F254 indicator. Spots were visualised with ultraviolet light using a MV Mineralight lamp (254/365) UVGL-58.

### 5-(4-(*tert*-Butyl)phenyl)-1*H*-tetrazole (RAB109)



4-(*tert*-Butyl)benzonitrile (Fluorochem) (0.75 mL, 5 mmol), sodium azide (359 mg, 5 mmol) and ammonium chloride (Alfa-Aesar) (295 mg 5mmol) were added to DMF (10 mL) and heated to 100 °C for 24h. The mixture was quenched with 0.1 M HCl (10 mL) and the resultant precipitate was collected by filtration to give 5-(4-(*tert*-butyl)phenyl)-1*H*-tetrazole. Yield 0.18 g (20%). <sup>1</sup>H NMR (300 MHz, Chloroform-*d*) δ 7.98 (d, *J* = 8.2 Hz, 2H), 7.48 (d, *J* = 8.2 Hz, 2H), 5.24 (s, 1H, NH), 1.29 (s, 9H). <sup>13</sup>C (DMSO-*d*<sub>6</sub>, 126 MHz) δ 152.8, 150.3, 125.7, 125.1, 120.2, 34.3, 30.5. MS (ES<sup>+</sup>, *m/z*) 202.1. Calc 201.1

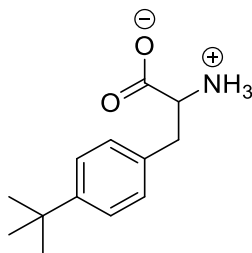
### Diethyl acetamido(4-(2-methyl-2-propanyl)benzyl)malonate



Diethyl acetamidomalonate (Merck) (1.56 g, 7 mmol) was added to a solution of sodium ethoxide (0.55 g, 8 mmol) in ethanol (30 mL) which was then heated at reflux for 30 min. The solution was cooled to room temperature before 4-*tert*-butylbenzyl chloride (Fluorochem) (1.25 mL, 7 mmol) was added dropwise and the mixture was heated at reflux overnight. The reaction mixture was then poured into a flask containing a 0.05 M KHSO<sub>4</sub> solution (60 mL) and *n*-hexane (30 mL) cooled to 0 °C with vigorous stirring. This was left for 30 mins before the precipitate was filtered and washed with cold *n*-hexane to give diethyl acetamido[4-(2-methyl-2-propanyl)benzyl]malonate. Yield 2.40 g

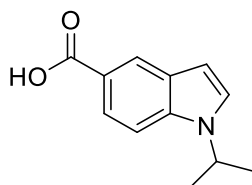
(76%).  $^1\text{H}$  NMR (300 MHz, DMSO)  $\delta$  8.11 (s, 1H, NH), 7.29 (d,  $J$  = 8.2 Hz, 2H), 6.90 (d,  $J$  = 8.2 Hz, 2H), 4.15 (q,  $J$  = 7.1 Hz, 4H), 3.34 (s, 2H), 1.95 (s, 3H), 1.25 (s, 9H), 1.17 (t,  $J$  = 7.1 Hz, 6H).  $^{13}\text{C}$  NMR (126 MHz, DMSO)  $\delta$  169.87, 167.51, 149.57, 132.58, 130.09, 125.41, 67.51, 62.18, 37.52, 34.59, 31.61, 22.63, 14.32. MS ( $\text{ES}^+$ ,  $m/z$ ) 364.2. Calc 363.45

## 2-Amino-3-(4-(*tert*-butyl)phenyl)propanoic acid (RAB106)



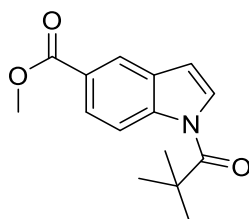
Diethyl 2-acetamido-2-(4-(*tert*-butyl)benzyl)malonate) (1.5 g, 4 mmol) was added to a solution of NaOH (1.4 g) in water (10 mL) and ethanol (25 mL). This was heated at reflux for 4h before HCl was added until pH 2. The solvent was removed through evaporation and ethanol was added. The mixture was filtered, before the solvent was removed *in vacuo* to give a mixture of 2-acetamido-2-(4-(*tert*-butyl)benzyl)malonic acid and 2-amino-3-(4-(*tert*-butyl)phenyl)propanoic acid as a crude mixture. This was carried through crude as 2-amino-3-(4-(*tert*-butyl)phenyl)propanoic acid was the desired final product. 6 M HCl (100 mL) was added to the solid which was then heated at reflux overnight. Once cooled approximately half of the solvent was removed through evaporation. The solution was cooled to 0 °C and after 2 h the resultant precipitate was filtered. The solid was triturated with cold diethyl ether to give 2-amino-3-(4-(*tert*-butyl)phenyl)propanoic acid. Yield 0.23 g (26%).  $^1\text{H}$  NMR (300 MHz, DMSO- $d_6$ )  $\delta$  8.52 – 8.25 (m, 3H,  $\text{NH}_3^+$ ), 7.35 (d,  $J$  = 8.1 Hz, 2H), 7.20 (d,  $J$  = 8.1 Hz, 2H), 4.16 (t,  $J$  = 6.2 Hz, 1H), 3.09 (d,  $J$  = 6.2 Hz, 2H), 1.27 (s, 9H).  $^{13}\text{C}$  NMR (126 MHz, DMSO- $d_6$ )  $\delta$  170.83, 149.89, 132.28, 129.66, 125.78, 53.57, 35.67, 34.66, 31.60. MS ( $\text{ES}^+$ ,  $m/z$ ) 223.3. Calc 222.1

## 1-isopropyl-1*H*-indole-5-carboxylic acid (RAB136)



Methyl 1*H*-indole-5-carboxylate (Fluorochem) (400 mg, 2.2 mmol) was added to a solution of sodium hydride (60 % NaH with mineral oil, 110 mg, 2.6 mmol) in anhydrous DMF (10 mL) under an inert atmosphere. This was left to stir at room temperature for 30 mins, before 2-iodopropane (Merck) (0.25 mL, 2.6 mmol) was added dropwise and the mixture was stirred at 50 °C for 6 hours. The solution was concentrated in vacuo to give the crude product, which was used directly in the next step without further purification. The crude material was dissolved in a 50:50 methanol water mix (15 mL) and sodium hydroxide (2 g) was added. The mixture was left to stir at room temperature overnight. The solution was diluted with a 2 M sodium hydroxide solution and washed with DCM (3 x 25 mL). The pH was adjusted to <4 using 2 M HCl and the organics were extracted into DCM (3 x 25 mL), dried over MgSO<sub>4</sub> and concentrated in vacuo. The crude product was purified using silica gel chromatography (10-40% EtOAc in hexanes) to give 1-isopropyl-1*H*-indole-5-carboxylic acid (yield 123 mg, 28% over 2 steps). <sup>1</sup>H NMR (400 MHz, CDCl<sub>3</sub>) δ 8.43 (d, *J* = 1.7 Hz, 1H), 7.91 (dd, *J* = 8.8, 1.7 Hz, 1H), 7.34 (d, *J* = 8.8 Hz, 1H), 7.23 (d, *J* = 6.2 Hz, 1H), 6.58 (d, *J* = 6.2 Hz, 1H), 4.65 (Sept, *J* = 6.7 Hz, 1H), 1.48 (d, *J* = 6.7 Hz, 6H). <sup>13</sup>C NMR (101 MHz, CDCl<sub>3</sub>) δ 173.18, 138.41, 128.13, 125.16, 125.01, 123.13, 120.34, 109.13, 103.15, 47.47, 22.79. MS (ES<sup>+</sup>, *m/z*) 203.2. 202.1

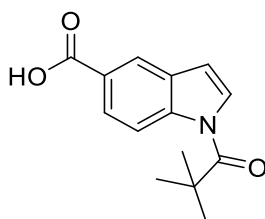
## Methyl 1-pivaloyl-1*H*-indole-5-carboxylate



Methyl 1*H*-indole-5-carboxylate (Fluorochem) (1g, 5.5 mmol) was added to a solution of sodium hydride (60 % NaH with mineral oil, 275 mg, 6.5 mmol) in anhydrous DMF (10 mL) under an inert atmosphere. This was left to stir at room temperature for 30 mins, before 2,2-dimethylpropanoyl chloride (Merck) (1.1 mL, 6.0 mmol) was added dropwise, and the mixture was stirred at 30 °C for 2

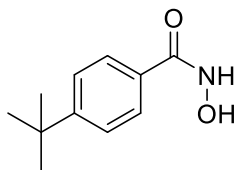
hours. The solution was concentrated *in vacuo* and to give methyl 1-pivaloyl-1*H*-indole-5-carboxylate (1.3 g, 4.83 mmol, yield 88%), <sup>1</sup>H NMR (400 MHz, CDCl<sub>3</sub>) δ 8.46 (d, *J* = 8.8 Hz, 1H), 8.21 (s, 1H), 7.97 (d, *J* = 8.9 Hz, 1H), 7.73 (d, *J* = 3.8 Hz, 1H), 6.62 (d, *J* = 3.8 Hz, 1H), 3.87 (s, 3H), 1.45 (s, 9H). <sup>13</sup>C NMR (101 MHz, CDCl<sub>3</sub>) δ 177.19, 167.42, 139.41, 129.18, 126.89, 126.36, 125.39, 122.73, 116.95, 108.62, 52.12, 41.37, 28.61.

### 1-Pivaloyl-1*H*-indole-5-carboxylic acid (RAB137)



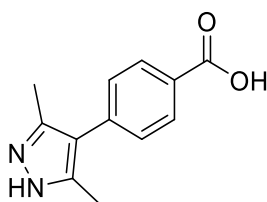
*N,N*-Dimethylaniline (2.3 mL, 18.5 mmol) was added to a solution of methyl 1-pivaloyl-1*H*-indole-5-carboxylate (1 g, 3.7 mmol) and aluminium chloride (1.48 g, 11.1 mmol in DCM (20 mL) under an inert atmosphere. This was left to stir for 2 h at room temperature before the mixture was diluted with 0.5 M hydrochloric acid. The organics were extracted with DCM (3 x 20 mL) which was then washed with 0.5 M hydrochloric acid (20 mL). The organic extracts were dried over MgSO<sub>4</sub> and concentrated *in vacuo*. The resulting crude solid was then purified through flash column chromatography (hexane, 20% ethyl acetate, 1% acetic acid) to give 1-pivaloyl-1*H*-indole-5-carboxylic acid (0.36 g, 1.5 mmol, yield 40%), <sup>1</sup>H NMR (400 MHz, CDCl<sub>3</sub>) δ 8.60 (d, *J* = 8.8 Hz, 1H), 8.41 (s, 1H), 8.15 (d, *J* = 8.8 Hz, 1H), 7.85 (d, *J* = 3.8 Hz, 1H), 6.75 (d, *J* = 3.8 Hz, 1H), 1.56 (s, 9H). MS (ES<sup>+</sup>, *m/z*) 245.1. Calc 244.1

#### 4-(*tert*-Butyl)-N-hydroxybenzamide (RAB116)



4-*tert*-Butylbenzoic acid (Fluorochem) (1 g, 5.6 mmol) was added to ethanol (20 mL) and refluxed for 16 h. The mixture was diluted with a 2 M NaOH solution and the product extracted with ethyl acetate (3 x 25 mL). The organic layer was concentrated *in vacuo* to give ethyl 4-(*tert*-butyl)benzoate (0.95 g, 4.5 mmol, 82 % yield) which was taken forward to the next step without any further purification. Hydroxylamine hydrochloride (Fluorochem) (0.834 g, 12 mmol) was added to a solution of NaOH (0.72 g, 18 mmol) in methanol (20 mL) and stirred for 30 mins at 0 °C. The resultant precipitate was filtered off and ethyl 4-(*tert*-butyl)benzoate (0.5 g, 2.4 mmol) was added. The solution was stirred at room temperature for 2 h before being diluted with water. The organics were extracted with ethyl acetate (3 x 25 mL) and concentrated *in vacuo*. The product was purified by silica gel chromatography (10-50% EtOAc in hexane) to give 4-(*tert*-butyl)-N-hydroxybenzamide (yield 0.13 g, 29%). <sup>1</sup>H NMR (400 MHz, CDCl<sub>3</sub>) δ 7.66 (d, J = 8.0 Hz, 2H), 7.50 (br s, 1H), 7.34 (d, J = 8.0 Hz, 2H), 1.24 (s, 9H). <sup>13</sup>C NMR (101 MHz, CDCl<sub>3</sub>) δ 156.09, 126.91, 125.79, 123.31, 119.61, 35.03, 31.09. MS (ES<sup>-</sup>) (M-H) 191.11. Calc 192.1

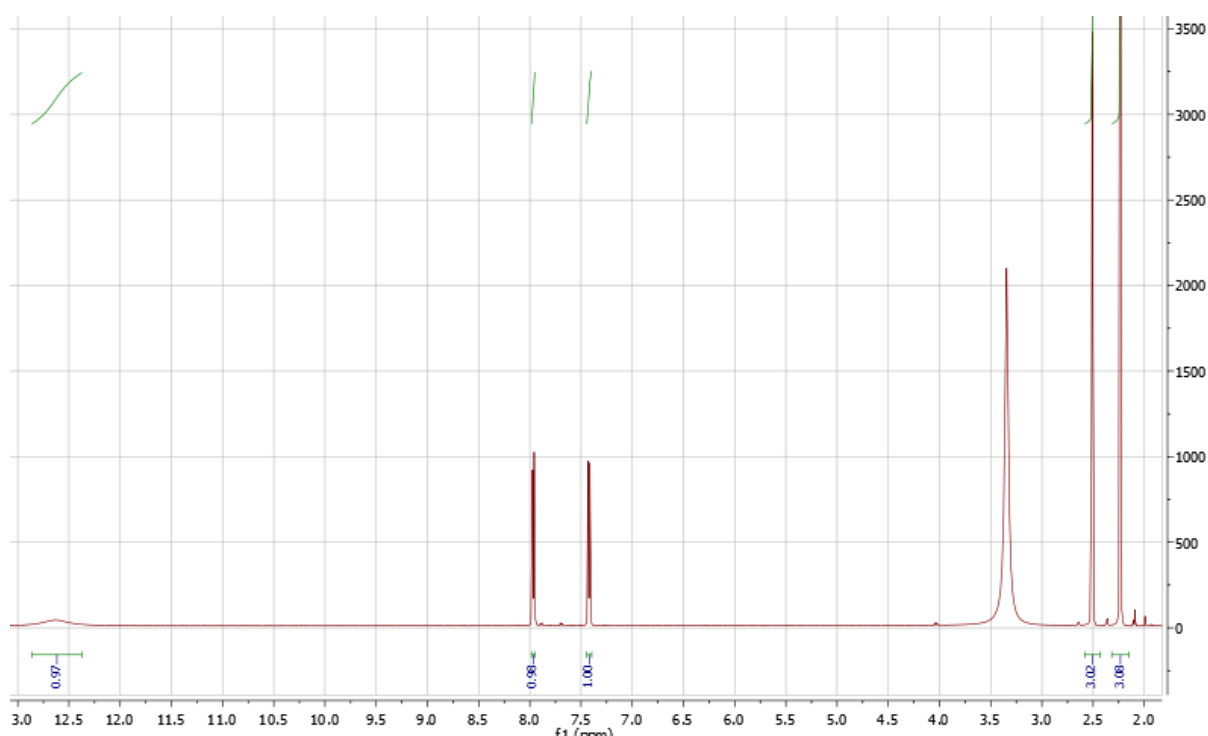
#### 4-(3,5-Dimethyl-1H-pyrazol-4-yl)benzoic acid (RAB216)



4-Iodobenzoic acid (Merck) (4.46 g, 20 mmol), copper(I) iodide (0.381 g, 2 mmol), L-proline (0.460 g, 4 mmol) and K<sub>2</sub>CO<sub>3</sub> (11.10 g, 80 mmol) were suspended in dry dimethyl sulfoxide (100 mL) under an argon atmosphere and stirred for 10 minutes at room temperature. 2,4-Pentanedione (Merck) (6.2 mL, 60 mmol) was added dropwise to this mixture, which was heated to 90 °C and stirred for 24 hours. After cooling to room temperature, the mixture was transferred slowly and with stirring into hydrochloric acid (3 M, 250 mL). An additional 150 mL of water was added, and the mixture was

cooled in an ice bath causing a precipitate to form. After filtration and washing with ice-cooled water (3x 100 mL) the filter cake was dried in an oven to give 3-(4-carboxyphenyl)-2,4-pentanedione (3.60 g) as a crude product. The compound was taken forward to the next step without purification due to co-elution seen by TLC.

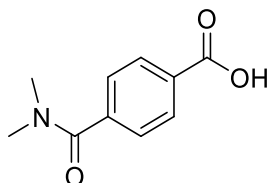
A solution of crude 3-(4-carboxyphenyl)-2,4-pentanedione (3.24 g, 15 mmol) in ethanol (40 mL) was added dropwise to a solution of hydrazine monohydrate (1.75 g, 20 mmol) in ethanol (10 mL) while stirring. Upon complete addition the combined solution was then heated at reflux for 1 h. After cooling to room temperature, the solvent was removed under reduced pressure to give the crude product. The product was purified by silica gel chromatography (85% EtOAc in hexane) to give 4-(3,5-Dimethyl-1H-pyrazol-4-yl)benzoic acid  $^1\text{H}$  NMR (500 MHz, DMSO- $d_6$ )  $\delta$  12.63 (s, 1H, COOH), 12.63 (s, 1H, NH), 7.96 (d,  $J$ = 8.5 2H), 7.42 (d,  $J$ = 8.5, 2H), 2.24 (s, 6H).  $^{13}\text{C}$  NMR (126 MHz, DMSO- $d_6$ ):  $\delta$  11.6; 127-130; 138.8; 167.5. MS ( $\text{ES}^+$ ,  $m/z$ ) 217.1. calc 216.2



NMR spectrum of RAB 216, the singular synthesised compound taken forward to rodent models.

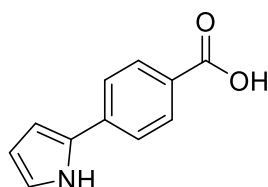
NMR spectrum highlights high purity with negligible peaks, aside from those assigned to the protons within the molecule.

#### 4-(Dimethylcarbamoyl)benzoic acid (RAB212)



Methyl 4-chlorocarbonylbenzoate (Fluorochem) (1 g, 5 mmol), was dissolved in DCM (20 mL) and a solution of dimethyl ammonium chloride (Merck) (0.61 g, 7.5 mmol) and triethylamine (1.05 mL, 7.5 mmol) was added slowly with stirring. The reaction was left for 1 h and the product was extracted with DCM (3 x 25 mL) and then washed with water (3 x 20 mL). The solvent was removed *in vacuo* to give methyl 4-(dimethylcarbamoyl)benzoate as a crude product. The crude product was taken forward to the next step without further purification. Crude methyl 4-(dimethylcarbamoyl)benzoate was dissolved in THF (50 mL) and a solution of LiOH (1 g) in water (50 mL) was added and the solution was stirred at room temperature for 16 h. HCl was added to the solution with stirring until the solution reached pH 3. The product was extracted with ethyl acetate (3 x 50 mL) and washed with 0.1 M HCl (3 x 30 mL) before the solvent was removed *in vacuo* to give 4-(dimethylcarbamoyl)benzoic acid (0.80 g, yield 83% over 2 steps)  $^1\text{H}$  NMR (400 MHz, DMSO- $d_6$ )  $\delta$  7.86 (d,  $J$  = 7.7 Hz, 2H), 7.27 (d,  $J$  = 7.7 Hz, 2H), 2.97 (s, 3H), 2.90 (s, 3H). MS ( $\text{ES}^+$ ,  $m/z$ ) 194.08. Calc 193.1

#### 4-(1H-Pyrrol-2-yl)benzoic acid (RAB211)



A solution of  $\text{Na}_2\text{CO}_3$  (1.83 g, 17.3 mmol) in water (10 mL) was added to 1-*tert*-butoxycarbonylpyrrole-2-boronic acid (1.04 g, 4.88 mmol), 4-carboxyiodobenzene (Fluorochem) (1g, 4.04 mmol), and tetrakis(triphenylphosphine)palladium(0) (Merck) (0.30 g, 0.257 mmol) in THF (60 mL) under argon. The mixture was heated at 45 °C for 2 h and cooled to room temperature. 2 M HCl was added until the solution reached pH 3. The product was extracted with ethyl acetate (3 x 50 mL)

and washed with 0.1 M HCl (3 x 20 mL). The solution was dried over MgSO<sub>4</sub> and the solvent was removed *in vacuo* to give 4-(1-(*tert*-butoxycarbonyl)-1H-pyrrol-2-yl)benzoic acid, which was dissolved in DMSO (20 mL) and heated to 150 °C for 30 min. The solution was cooled to room temperature and 0.1 M HCl (50 mL) was added. The product was extracted with ethyl acetate (3 x 100 mL) and washed with 0.1 M HCl (3 x 30 mL). The solution was dried over MgSO<sub>4</sub> and the solvent was removed *in vacuo*. The product was purified by silica gel chromatography (6% MeOH/CH<sub>2</sub>Cl<sub>2</sub>) to give 4-(1H-pyrrol-2-yl)benzoic acid (0.53 g, yield 70%) <sup>1</sup>H NMR (400 MHz, DMSO-d<sub>6</sub>) δ 12.76 (s, 1H), 11.50 (s, 1H), 7.90 (d, J = 8.7 Hz, 2H), 7.72 (d, J = 8.7 Hz, 2H), 6.94 (td, J = 3.5, 2.7, 1.4 Hz, 1H), 6.69 (ddd, J = 3.9, 2.5, 1.5 Hz, 1H), 6.17 (dt, J = 3.5, 2.3 Hz, 1H). MS (ES<sup>+</sup>, *m/z*) 188.05. Calc 187.1

#### 2.4.2 Fly Stocks

The wild type Canton-S line was maintained by the Baines lab. *para*<sup>bss</sup> is detailed in (Parker et al., no date) and was obtained from Dr Kevin O'Dell (Institute of Molecular, Cell and Systems Biology, University of Glasgow, UK). This fly carries a gain-of-function mutation in the sole voltage-gated Na<sup>+</sup> channel in *Drosophila* (termed *paralytic*). Flies were maintained on standard cornmeal medium at 25 °C.

#### 2.4.3 Larval Seizure Electroshock Assay

Larvae that leave food and climb the walls of the tube are deemed to have reached the wandering stage (L3), which represents a 10hr window prior to pupation that all larvae must go through. Thus all larvae tested were 60 ± 10hrs of age. L3 were transferred to water to wash them and then carefully dried on tissue paper. They were then placed on a plastic plate and allowed time to resume typical peristaltic crawling behaviour. Once this was observed, an electro-stimulator, made from 2 tungsten wires (0.1 mm diameter and approx. 1-2 mm apart), was placed on the anterior-dorsal surface of the larvae (over the CNS). A DC pulse (2.5 V) generated by a constant current simulator (DS2A, Digitimer, UK) was applied for 2 s. This caused larvae to exhibit a seizure-like behaviour characterised by complete cessation of mobility (see Marley and Baines, 2011). The time taken (termed Recovery Time, RT) for larvae to resume normal peristaltic crawling behaviour was recorded. Normal behaviour was defined as consistent waves of contraction across the whole body, whereby the larva is again in control of its movement and moving forward. Investigators were blinded to the treatment group when experiments were performed.

## 2.5 Bibliography

- Adkison, K.D. and Shen, D.D. (1996) 'Uptake of valproic acid into rat brain is mediated by a medium-chain fatty acid transporter.', *Journal of Pharmacology and Experimental Therapeutics*, 276(3), pp. 1189–1200.
- Ahmed Laskar, A. and Younus, H. (2019a) 'Aldehyde toxicity and metabolism: the role of aldehyde dehydrogenases in detoxification, drug resistance and carcinogenesis', *Drug metabolism reviews*, 51(1), pp. 42–64.
- Ahmed Laskar, A. and Younus, H. (2019b) 'Aldehyde toxicity and metabolism: the role of aldehyde dehydrogenases in detoxification, drug resistance and carcinogenesis', *Drug metabolism reviews*, 51(1), pp. 42–64.
- Altomonte, S. *et al.* (2014a) 'The pentafluorosulfonyl group in cannabinoid receptor ligands: synthesis and comparison with trifluoromethyl and tert-butyl analogues', *RSC Advances*, 4(39), pp. 20164–20176.
- Altomonte, S. *et al.* (2014b) 'The pentafluorosulfonyl group in cannabinoid receptor ligands: synthesis and comparison with trifluoromethyl and tert-butyl analogues', *RSC Advances*, 4(39), pp. 20164–20176.
- Altomonte, S. and Zanda, M. (2012) 'Synthetic chemistry and biological activity of pentafluorosulfonyl (SF<sub>5</sub>) organic molecules', *Journal of Fluorine Chemistry*, 143, pp. 57–93.
- Alves, F.R. de S. and Fraga, E.J.B. and C.A.M. (2009) 'From Nature to Drug Discovery: The Indole Scaffold as a Privileged Structure', *Mini-Reviews in Medicinal Chemistry*, pp. 782–793. Available at: <https://doi.org/http://dx.doi.org/10.2174/138955709788452649>.
- Bach, R.D., Badger, R.C. and Lang, T.J. (1979) 'Theoretical studies on E2 elimination reactions. Evidence that syn elimination is accompanied by inversion of configuration at the carbanionic center', *Journal of the American Chemical Society*, 101(11), pp. 2845–2848.
- Bainton, R.J. *et al.* (2005) 'moody encodes two GPCRs that regulate cocaine behaviors and blood-brain barrier permeability in *Drosophila*', *Cell*, 123(1), pp. 145–156.
- Banerjee, S., Sousa, A.D. and Bhat, M.A. (2006) 'Organization and function of septate junctions', *Cell biochemistry and biophysics*, 46(1), pp. 65–77.
- Beletskaya, I.P. and Cheprakov, A. V (2004) 'Copper in cross-coupling reactions: the post-Ullmann chemistry', *Coordination chemistry reviews*, 248(21), pp. 2337–2364.
- BLONDELLE, S.E. and HOUGHTEN, R.A. (1993) 'Comparison of 55% TFA/CH<sub>2</sub>Cl<sub>2</sub> and 100% TFA for Boc group removal during solid-phase peptide synthesis', *International Journal of Peptide and Protein Research*, 41(6), pp. 522–527.
- Böhm, H. *et al.* (1996) 'Oxygen and nitrogen in competitive situations: which is the hydrogen-bond acceptor?', *Chemistry—A European Journal*, 2(12), pp. 1509–1513.
- Brown, B.R. (1951) 'The mechanism of thermal decarboxylation', *Quarterly Reviews, Chemical Society*, 5(2), pp. 131–146. Available at: <https://doi.org/10.1039/QR9510500131>.

- Büscher, J.M. *et al.* (2009) 'Cross-platform comparison of methods for quantitative metabolomics of primary metabolism', *Analytical chemistry*, 81(6), pp. 2135–2143.
- Byun, K., Mo, Y. and Gao, J. (2001) 'New Insight on the Origin of the Unusual Acidity of Meldrum's Acid from ab Initio and Combined QM/MM Simulation Study', *Journal of the American Chemical Society*, 123(17), pp. 3974–3979. Available at: <https://doi.org/10.1021/ja001369r>.
- Casitas, A. and Ribas, X. (2013) 'The role of organometallic copper (III) complexes in homogeneous catalysis', *Chemical Science*, 4(6), pp. 2301–2318.
- Choi, J.-S., Jin, M.J. and Han, H.-K. (2005) 'Role of monocarboxylic acid transporters in the cellular uptake of NSAIDs', *Journal of Pharmacy and Pharmacology*, 57(9), pp. 1185–1189.
- Coelho, A. *et al.* (2015) 'Cytochrome P450-dependent metabolism of caffeine in *Drosophila melanogaster*', *PLoS One*, 10(2), p. e0117328.
- Creutz, S.E. *et al.* (2012) 'Photoinduced Ullmann C–N coupling: demonstrating the viability of a radical pathway', *Science*, 338(6107), pp. 647–651.
- Delgado, M.G. *et al.* (2018) 'Chaski, a novel *Drosophila* lactate/pyruvate transporter required in glia cells for survival under nutritional stress', *Scientific reports*, 8(1), pp. 1–13.
- DiMaggio, S.G. and Sun, H. (2006) 'The strength of weak interactions: aromatic fluorine in drug design', *Current Topics in Medicinal Chemistry*, 6(14), pp. 1473–1482.
- Doan, K.M.M. *et al.* (2002) 'Passive permeability and P-glycoprotein-mediated efflux differentiate central nervous system (CNS) and non-CNS marketed drugs', *Journal of Pharmacology and Experimental Therapeutics*, 303(3), pp. 1029–1037.
- Fanta, P.E. (1974) 'The Ullmann synthesis of biaryls', *Synthesis*, 1974(01), pp. 9–21.
- Fringuelli, F., Pizzo, F. and Vaccaro, L. (2001) 'AlCl<sub>3</sub> as an efficient Lewis acid catalyst in water', *Tetrahedron Letters*, 42(6), pp. 1131–1133.
- Gao, B. *et al.* (2000) 'Organic anion-transporting polypeptides mediate transport of opioid peptides across blood-brain barrier', *Journal of Pharmacology and Experimental Therapeutics*, 294(1), pp. 73–79.
- Gleeson, M.P. *et al.* (2011) 'Probing the links between in vitro potency, ADMET and physicochemical parameters', *Nature reviews Drug discovery*, 10(3), pp. 197–208.
- Gonzalez-Gutierrez, A. *et al.* (2019) 'Monocarboxylate transport in *Drosophila* larval brain during low and high neuronal activity', *bioRxiv*, p. 610196.
- Hardee, D.J., Kovalchuk, L. and Lambert, T.H. (2010) 'Nucleophilic acyl substitution via aromatic cation activation of carboxylic acids: rapid generation of acid chlorides under mild conditions', *Journal of the American Chemical Society*, 132(14), pp. 5002–5003.
- Hay, R.W. and Bond, M.A. (1967) 'Kinetics of the Decarboxylation of Acetoacetic acid', *Australian Journal of Chemistry*, 20(9), pp. 1823–1828. Available at: <https://doi.org/10.1071/CH9671823>.
- Hempel, A. *et al.* (1999) 'A Schiff base formed from sulfanilic acid and dimethylformamide', *Acta Crystallographica Section C: Crystal Structure Communications*, 55(4), pp. 697–698.

- Hendriks, C.M.M. *et al.* (2015) 'Pentafluorosulfanyl-containing flufenamic acid analogs: Syntheses, properties and biological activities', *Bioorganic & medicinal chemistry letters*, 25(20), pp. 4437–4440.
- Himo, F. *et al.* (2002) 'Mechanisms of Tetrazole Formation by Addition of Azide to Nitriles', *Journal of the American Chemical Society*, 124(41), pp. 12210–12216. Available at: <https://doi.org/10.1021/ja0206644>.
- Hughes, J.P. *et al.* (2011) 'Principles of early drug discovery', *British journal of pharmacology*, 162(6), pp. 1239–1249.
- Imuro, K. and Hanafusa, T. (1976) 'Trifluoroacetylation at the 3 Position of 1-(2-Aminophenyl)-2, 5-dimethylpyrrole in Trifluoroacetic Acid. Possible Remote Control of an Amino Group in Electrophilic Substitution', *Bulletin of the Chemical Society of Japan*, 49(5), pp. 1363–1365.
- Jiang, Y. *et al.* (2005) 'An efficient and mild CuI/l-proline-catalyzed arylation of acetylacetone or ethyl cyanoacetate', *Synlett*, 2005(18), pp. 2731–2734.
- Jiang, Y. *et al.* (2013) 'Cu-catalyzed Ullmann-type C–heteroatom bond formation: the key role of dinucleating ancillary ligands', in *CH and CX Bond Functionalization*, pp. 1–45.
- Kageyama, T. *et al.* (2000) 'The 4F2hc/LAT1 complex transports L-DOPA across the blood–brain barrier', *Brain Research*, 879(1), pp. 115–121. Available at: [https://doi.org/https://doi.org/10.1016/S0006-8993\(00\)02758-X](https://doi.org/https://doi.org/10.1016/S0006-8993(00)02758-X).
- Karlsson, I. *et al.* (2009) 'Photodegradation of Dibenzoylmethanes: Potential Cause of Photocontact Allergy to Sunscreens', *Chemical Research in Toxicology*, 22(11), pp. 1881–1892. Available at: <https://doi.org/10.1021/tx900284e>.
- Kemnitz, C.R. and Loewen, M.J. (2007) "'Amide resonance" correlates with a breadth of C– N rotation barriers', *Journal of the American Chemical Society*, 129(9), pp. 2521–2528.
- Kienzle, G.J., Reischl, G. and Machulla, H.-J. (2005) 'Electrochemical radiofluorination. 3. Direct labeling of phenylalanine derivatives with [<sup>18</sup>F]fluoride after anodic oxidation', *Journal of Labelled Compounds and Radiopharmaceuticals*, 48(4), pp. 259–273. Available at: <https://doi.org/10.1002/jlcr.918>.
- Kikuchi, R. *et al.* (2003) 'Contribution of organic anion transporter 3 (Slc22a8) to the elimination of p-aminohippuric acid and benzylpenicillin across the blood-brain barrier', *Journal of Pharmacology and Experimental Therapeutics*, 306(1), pp. 51–58.
- Kumalo, H.M., Bhakat, S. and Soliman, M.E.S. (2015) 'Theory and applications of covalent docking in drug discovery: merits and pitfalls', *Molecules*, 20(2), pp. 1984–2000.
- Kunde, P.D. *et al.* (2021) 'On the use of electronegativity and electron affinity based pseudo-molecular field descriptors in developing correlations for quantitative structure-activity relationship modeling of drug activities', *Chemical Biology & Drug Design*, 98(2), pp. 258–269.
- Larkin, D.R. (1990) 'The role of catalysts in the air oxidation of aliphatic aldehydes', *The Journal of Organic Chemistry*, 55(5), pp. 1563–1568.
- Lipinski, C.A. *et al.* (2001) 'Experimental and computational approaches to estimate solubility and permeability in drug discovery and development settings<sup>1</sup>', *Advanced Drug Delivery Reviews*, 46(1–3), pp. 3–26. Available at: [https://doi.org/http://dx.doi.org/10.1016/S0169-409X\(00\)00129-0](https://doi.org/http://dx.doi.org/10.1016/S0169-409X(00)00129-0).

- Lipinski, C.A. (2016) 'Rule of five in 2015 and beyond: Target and ligand structural limitations, ligand chemistry structure and drug discovery project decisions', *Advanced drug delivery reviews*, 101, pp. 34–41.
- Lu, Z. and Twieg, R.J. (2005) 'A mild and practical copper catalyzed amination of halothiophenes', *Tetrahedron*, 61(4), pp. 903–918.
- Ma, H.-C. and Jiang, X.-Z. (2007) 'N-Hydroxyimides as efficient ligands for the copper-catalyzed N-arylation of pyrrole, imidazole, and indole', *The Journal of Organic Chemistry*, 72(23), pp. 8943–8946.
- Mac, M. and Nałęcz, K.A. (2003) 'Expression of monocarboxylic acid transporters (MCT) in brain cells: Implication for branched chain  $\alpha$ -ketoacids transport in neurons', *Neurochemistry International*, 43(4), pp. 305–309. Available at: [https://doi.org/https://doi.org/10.1016/S0197-0186\(03\)00016-0](https://doi.org/https://doi.org/10.1016/S0197-0186(03)00016-0).
- Maeda, H. *et al.* (2011) 'Self-sorting self-complementary assemblies of  $\pi$ -conjugated acyclic anion receptors', *Chemical Communications*, 47(29), pp. 8241–8243.
- Manallack, D.T. (2007) 'The pKa distribution of drugs: application to drug discovery', *Perspectives in medicinal chemistry*, 1, p. 25.
- Marcelin, G. and Brooks, P.R. (1975) 'Steric hindrance in potassium atom-oriented molecule reactions. Methyl iodide and tert-butyl iodide', *Journal of The American Chemical Society*, 97(7), pp. 1710–1715.
- Marelja, Z. *et al.* (2014) 'The four aldehyde oxidases of *Drosophila melanogaster* have different gene expression patterns and enzyme substrate specificities', *The Journal of Experimental Biology*, 217(12), pp. 2201–2211. Available at: <https://doi.org/10.1242/jeb.102129>.
- Meanwell, N.A. (2011) 'Improving Drug Candidates by Design: A Focus on Physicochemical Properties As a Means of Improving Compound Disposition and Safety', *Chemical Research in Toxicology*, 24(9), pp. 1420–1456. Available at: <https://doi.org/10.1021/tx200211v>.
- Moxon, L.N. *et al.* (1985) 'Purification and molecular properties of alcohol dehydrogenase from *Drosophila melanogaster*: Evidence from NMR and kinetic studies for function as an aldehyde dehydrogenase', *Comparative Biochemistry and Physiology Part B: Comparative Biochemistry*, 80(3), pp. 525–535.
- Mudhar, H. and Witty, A. (2010) 'One-pot conversion of alkyl aldehydes into substituted propanoic acids via Knoevenagel condensation with Meldrum's acid', *Tetrahedron Letters*, 51(38), pp. 4972–4974.
- Murray, M. (2000) 'Mechanisms of inhibitory and regulatory effects of methylenedioxyphenyl compounds on cytochrome P450-dependent drug oxidation', *Current drug metabolism*, 1(1), pp. 67–84.
- Nakamura, S., Hirao, H. and Ohwada, T. (2004) 'Rationale for the Acidity of Meldrum's Acid. Consistent Relation of C–H Acidities to the Properties of Localized Reactive Orbital', *The Journal of organic chemistry*, 69(13), pp. 4309–4316.
- Nguyen, T. V and Bekensir, A. (2014) 'Aromatic cation activation: Nucleophilic substitution of alcohols and carboxylic acids', *Organic letters*, 16(6), pp. 1720–1723.
- Olsson, B. *et al.* (2011) 'Pulmonary drug metabolism, clearance, and absorption', in *Controlled pulmonary drug delivery*. Springer, pp. 21–50.

- Pajouhesh, H. and Lenz, G.R. (2005) 'Medicinal Chemical Properties of Successful Central Nervous System Drugs', *NeuroRx*, 2(4), pp. 541–553.
- Palling, D. and Jencks, W.P. (1984) 'Nucleophilic reactivity toward acetyl chloride in water', *Journal of the American Chemical Society*, 106(17), pp. 4869–4876.
- Paludetto, M.-N. *et al.* (2019) 'Involvement of pazopanib and sunitinib aldehyde reactive metabolites in toxicity and drug–drug interactions in vitro and in patient samples', *Chemical research in toxicology*, 33(1), pp. 181–190.
- Parker, L. *et al.* (2011a) 'Drosophila as a model for epilepsy: bss is a gain-of-function mutation in the para sodium channel gene that leads to seizures', *Genetics*, 187(2), pp. 523–534.
- Parker, L. *et al.* (2011b) 'Drosophila as a model for epilepsy: bss is a gain-of-function mutation in the para sodium channel gene that leads to seizures', *Genetics*, 187(2), pp. 523–534. Available at: <https://doi.org/10.1534/genetics.110.123299>.
- Phan, N.T.N. *et al.* (2013) 'Capillary electrophoresis–mass spectrometry-based detection of drugs and neurotransmitters in Drosophila brain', *Analytical chemistry*, 85(17), pp. 8448–8454.
- Posner, G.H. and O'Neill, P.M. (2004) 'Knowledge of the Proposed Chemical Mechanism of Action and Cytochrome P450 Metabolism of Antimalarial Trioxanes Like Artemisinin Allows Rational Design of New Antimalarial Peroxides', *Accounts of Chemical Research*, 37(6), pp. 397–404. Available at: <https://doi.org/10.1021/ar020227u>.
- Rahimi, M. and Fattahi, A. (2021) 'Acidity enhancement of  $\alpha$ -carbon of beta diketones via hydroxyl substituents: A density functional theory study', *Journal of Physical Organic Chemistry*, 34(3), p. e4157.
- Sheppard, W.A. (1962) 'Arylsulfur pentafluorides', *Journal of the American Chemical Society*, 84(16), pp. 3064–3072.
- Singh, N. and Ecker, G.F. (2018) 'Insights into the structure, function, and ligand discovery of the large neutral amino acid transporter 1, LAT1', *International journal of molecular sciences*, 19(5), p. 1278.
- Stump, B. *et al.* (2009) 'Pentafluorosulfanyl as a novel building block for enzyme inhibitors: trypanothione reductase inhibition and antiprotozoal activities of diarylamines', *ChemBioChem*, 10(1), pp. 79–83.
- Tohyama, K., Kusuvara, H. and Sugiyama, Y. (2004) 'Involvement of multispecific organic anion transporter, Oatp14 (Slc21a14), in the transport of thyroxine across the blood-brain barrier', *Endocrinology*, 145(9), pp. 4384–4391.
- Tom, N.J. *et al.* (2004) 'Deprotection of a primary Boc group under basic conditions', *Tetrahedron letters*, 45(5), pp. 905–906.
- Treherne, J.E. and Pichon, Y. (1972) 'The insect blood—brain barrier', in *Advances in insect physiology*. Elsevier, pp. 257–313.
- Varnavas, A. *et al.* (2005) 'Anthranilic acid based CCK1 receptor antagonists: preliminary investigation on their second "touch point"', *European Journal of Medicinal Chemistry*, 40(6), pp. 563–581. Available at: <https://doi.org/https://doi.org/10.1016/j.ejmech.2005.01.002>.

- Vijay, N. and Morris, M.E. (2014) 'Role of monocarboxylate transporters in drug delivery to the brain', *Current pharmaceutical design*, 20(10), pp. 1487–1498.
- Vuignier, K. *et al.* (2010) 'Drug–protein binding: a critical review of analytical tools', *Analytical and bioanalytical chemistry*, 398(1), pp. 53–66.
- Wager, T.T. *et al.* (2010) 'Defining Desirable Central Nervous System Drug Space through the Alignment of Molecular Properties, in Vitro ADME, and Safety Attributes', *ACS Chem. Neurosci*, 1, pp. 420–434. Available at: <https://doi.org/10.1021/cn100007x>.
- Walter, F.R. *et al.* (2021) 'Surface charge, glycocalyx, and blood-brain barrier function', *Tissue Barriers*, 9(3), p. 1904773.
- Westphal, M. V *et al.* (2015) 'Evaluation of tert-Butyl Isosteres: Case Studies of Physicochemical and Pharmacokinetic Properties, Efficacies, and Activities', *ChemMedChem*, 10(3), pp. 461–469.
- Wipf, P. *et al.* (2009) 'Synthesis and biological evaluation of the first pentafluorosulfanyl analogs of mefloquine', *Organic & biomolecular chemistry*, 7(20), pp. 4163–4165.
- Zhang, S., Zhang, D. and Liebeskind, L.S. (1997) 'Ambient temperature, Ullmann-like reductive coupling of aryl, heteroaryl, and alkenyl halides', *The Journal of Organic Chemistry*, 62(8), pp. 2312–2313.
- Zhang, S.-L. *et al.* (2007) 'Theoretical study on Copper (I)-catalyzed cross-coupling between aryl halides and amides', *Organometallics*, 26(18), pp. 4546–4554.

## 3.0 Chapter 3- Biological Characterisation of Lead Compounds

### 3.1 Introduction

Once a lead compound had been established through the L3 seizure assay and structure-activity study (previous chapter), the next step was to determine the mode-of-action for this class of compound and how broad effects may be in terms of treating different forms of epilepsy. Additionally, mammalian seizure studies with RAB216 were required to establish whether RAB216 maintains its efficacy in a model that better reflects the human system.

One of the main advantages of using *Drosophila* as a model is genetic tractability. Genome editing experiments are significantly simpler when compared to mammalian organisms and by using the GAL4-UAS expression system, genes can be expressed or silenced in specific locations, down to individual neurons (Klueg *et al.*, 2002). By utilising GAL4-UAS, changes in gene expression can be studied *in vivo* at a relatively high throughput. This system also allows additional genes to be expressed to provide experimental tools such as optogenetics (proteins that respond to light) and fluorescent labelling (Honjo, Hwang and Tracey, 2012). The *Gal4* gene encodes a yeast transcription activator, which when downstream to a promoter of interest will be co-expressed each time that gene promoter is activated. GAL4 binds to the upstream activation system (UAS), an enhancer which can activate reporter gene transcription. By design, the UAS-reporter gene is expressed in all cells, however nothing is expressed without the presence of GAL4, the expression of which can be cell, and time-specific. Therefore, in the case of GFP, only locations that express both the gene of interest and UAS-GFP will show as fluorescent.

Another use of the GAL4-UAS system comes in the form of a luciferase reporter gene. Luciferase is an enzyme that catalyses the breakdown of its substrate luciferin, resulting in the generation of luminescence (Gould and Subramani, 1988). A common form of this gene is taken from fireflies, which uses this reaction to generate their luminescence. This tool can be particularly useful for tracking changes in gene expression as by utilising the GAL4 system. Any expression changes can be investigated by measuring the concentration of luciferase, which itself can be measured through the addition of luciferin and recording the luminescence generated. The main advantage of luminescence assays for studying expression changes compared to western blots is the increased throughput. One example of this can be seen from the large FDA drug screen conducted by Lin, Giachello and Baines which investigated the changes in *pum* expression in cells following treatment with 785 different drugs (Lin *et al.*, 2017). In the context of *Pum* in *Drosophila* this method is particularly useful as there are no antibodies that reliably bind to *dpum*.

*Drosophila* are a useful research tool due to their genetic tractability, ease of handling and fast reproduction rate, which allows for high-throughput studies relative to other *in vivo* models. However, they do have major differences to mammals which may change how efficacious compounds are. Firstly, their circulatory system is different. *Drosophila*, have an open circulatory system whereby haemolymph bathes organs and provides nutrients, hormones, and other metabolites directly (Fessler, Nelson and Fessler, 1994). Therefore, any drugs consumed would be distributed around the body in a completely different way to vertebrates, who rely on the blood to distribute compounds via a closed circulatory system.

Secondly, the barrier protecting the *Drosophila* CNS is different from the blood-brain barrier in vertebrates (Hindle and Bainton, 2014). Whilst both share some of the same features that prevent molecules from reaching the CNS, there are clear differences which could mean that drugs that are able to reach the *Drosophila* CNS are not capable of crossing a mammalian BBB. Lack of brain penetration is one of the most common reasons CNS drugs fail in their development phases (Pardridge, 1998). Therefore, acquiring data that demonstrates the compound crosses the BBB is integral if the compound is to be taken any further through development.

Finally, *Drosophila* only have one form of the Pumilio protein, whereas humans and other mammals have two variants: Pum1 and Pum2. These two proteins show high homology and overlap in their target mRNAs, however they each have some specific functions. For example, in embryonic stem cells Pum1 promotes differentiation, whereas Pum2 promotes self-renewal (Uyhazi *et al.*, 2020). Whilst this difference between the two proteins may not be relevant to Pum's neurological function, it does show that they are not fully redundant and thus may have slightly distinct functions in the CNS. Therefore, how the drug affects the expression of each variant individually requires investigation. Furthermore, relevant targets of Pum, such as sodium channels, are also expressed differently. Mammals possess nine genes that encode for functional Na<sub>v</sub>s (*SCN1-5A*, *8-11A*), whereas *Drosophila* only encode *para*. *Drosophila* do have variety in the characteristics of their Na<sub>v</sub>s, but this comes via different splice forms, of which there are predicted to be at least 60 (Lin *et al.*, 2009). Whilst it is known that *para* mRNA is regulated by dPum, the relationship between mammalian Na<sub>v</sub>s and Pum may be more complex. Whilst most Na<sub>v</sub> transcripts contain one or more Pumilio-response elements (PRE), indicating they are capable of binding with Pum, evidence suggests only Na<sub>v</sub> 1.1, Na<sub>v</sub> 1.2 and Na<sub>v</sub> 1.6 expression are affected by changes in Pum activity (Vessey *et al.*, 2010; Driscoll *et al.*, 2013; Bohn *et al.*, 2018). Whilst *Drosophila* are a useful tool for modelling seizures and drug screening, there are significant differences between the way Pum regulates genes between *Drosophila* and mammals. Therefore, to confirm the antiseizure effects of the lead compounds are translatable, testing in mice is also required.

There are a wide range of methods available to model seizures in mice, ranging from acute models that rely on pharmaceuticals or electrical stimulation, to chronic models such as kindling and those of a genetic nature (Wilcox, West and Metcalf, 2020). Pharmaceutical models utilise proconvulsants such as picrotoxin (PTX), pentylenetetrazol (PTZ) or kainic acid (KA) to induce acute seizures within minutes of injection. PTX and PTZ increase excitatory transmission through GABA inhibition, whereas KA acts as an excitatory neurotransmitter, binding to kainate receptors, a type of glutamate receptor (Jensen and Petersen, 1983; Lévesque and Avoli, 2013). Treatments are injected prior to the administration of a proconvulsant, and its effectiveness can be measured by how delayed the onset of seizures are or by their severity. The timing of the treatment injection can vary depending on the compound's mechanism of action. For example, in this project's experiments, it is planned that RAB216 will be injected once per day for 3 days before PTZ administration, whereas sodium valproate would only need to be administered 30 mins prior to PTZ injection.

Acute pharmaceutical models are one of the oldest forms of rodent seizure models and have been integral to the development of established AEDs such as succinimides (Teschendorf and Kretzschmar, 1985). The maximal electric shock (MES) model has also been adopted in published rodent seizure screens. This method induces synchronous neural discharges throughout the brain via artificial current input (Fischer and Müller, 1988). These two models were integral for the development of most current AEDs on the market and have been adopted as the standards by the antiseizure screening project, a programme set up to test AEDs in a standardised, consistent manner that made important contributions to the development of several AEDs (Wilcox, West and Metcalf, 2020). The two models are often used in parallel as they better reflect different forms of epilepsy. For example, the sodium channel blocker phenytoin was originally discovered via the MES model but was found to be ineffective at alleviating seizures induced by PTZ (Smith, Wilcox and White, 2007). Conversely trimethadione, an AED used to treat absence seizures, was more effective in the PTZ model. This is consistent with phenytoin's lack of efficacy against absence seizures.

Another model later adopted by the antiseizure screening project is the 6 Hz psychomotor seizure model. This method induces seizures by applying a low frequency, long duration (~3 s) electrical stimulation to induce psychomotor seizures, similar to those seen in human patients with complex partial seizures. Despite being developed nearly 70 years ago (BROWN et al. 1953). it was rarely used until more recently because phenytoin, one of the few AEDs available at the time, was not active. However, Barton and colleagues observed that the AED levetiracetam effectively protected against seizures in this model, despite being inactive in the MES model (Barton *et al.*, 2001). As a result, it has now been repurposed as a tool for the discovery of AEDs that are effective against drug resistant epilepsy. By screening the lead compounds in both a pharmacological model and the 6 Hz seizure

model, more can be learnt about which types of seizure they may be 'more' effective against. Furthermore, when combined with screening in various *Drosophila* seizure mutants, it can be observed whether drugs that act through Pum have the potential to be wide acting AEDs that reduce the severity of multiple forms of seizure.

When choosing a model to study disease, there is usually a trade-off between the time, cost and ease with which experiments can be conducted and how closely the model represents the human system. The genetic tractability and high reproduction rates allow *Drosophila* to be a versatile and high throughput model, and can be advantageous over cell models, as it allows for experiments to be conducted *in vivo*. One of the aims from this project was to demonstrate the effectiveness of *Drosophila* as a drug screening tool, which can reduce the number of mammals required for drug screening. Results from chapter 1 demonstrate that *Drosophila* are a viable model for the screening of AEDs, emphasised by the fact that marketed AEDs are effective at alleviating seizure-like behaviour. However, to validate the potential effectiveness of RAB216 as an AED, experiments in a model that better reflects the human system are required.

### 3.2 Results

To assess whether RAB216 is effective on a variety of epilepsy, it was screened in other *Drosophila* seizure assays, using different bang sensitive mutants. The *slamdance* (*sda*) bang sensitive phenotype is due to a mutation in the *Julius seizure* (*jus*) gene (Dean *et al.*, 2018). This gene was discovered relatively recently, and its function is currently not well characterised. *Easily Shocked* (*eas*) mutants are defective in the gene for ethanolamine kinase, which is necessary for the synthesis of phosphatidylethanolamine (Pavlidis, Ramaswami and Tanouye, 1994). As a result, *eas* mutants have an altered membrane phospholipid composition, leading to an increase in excitability.

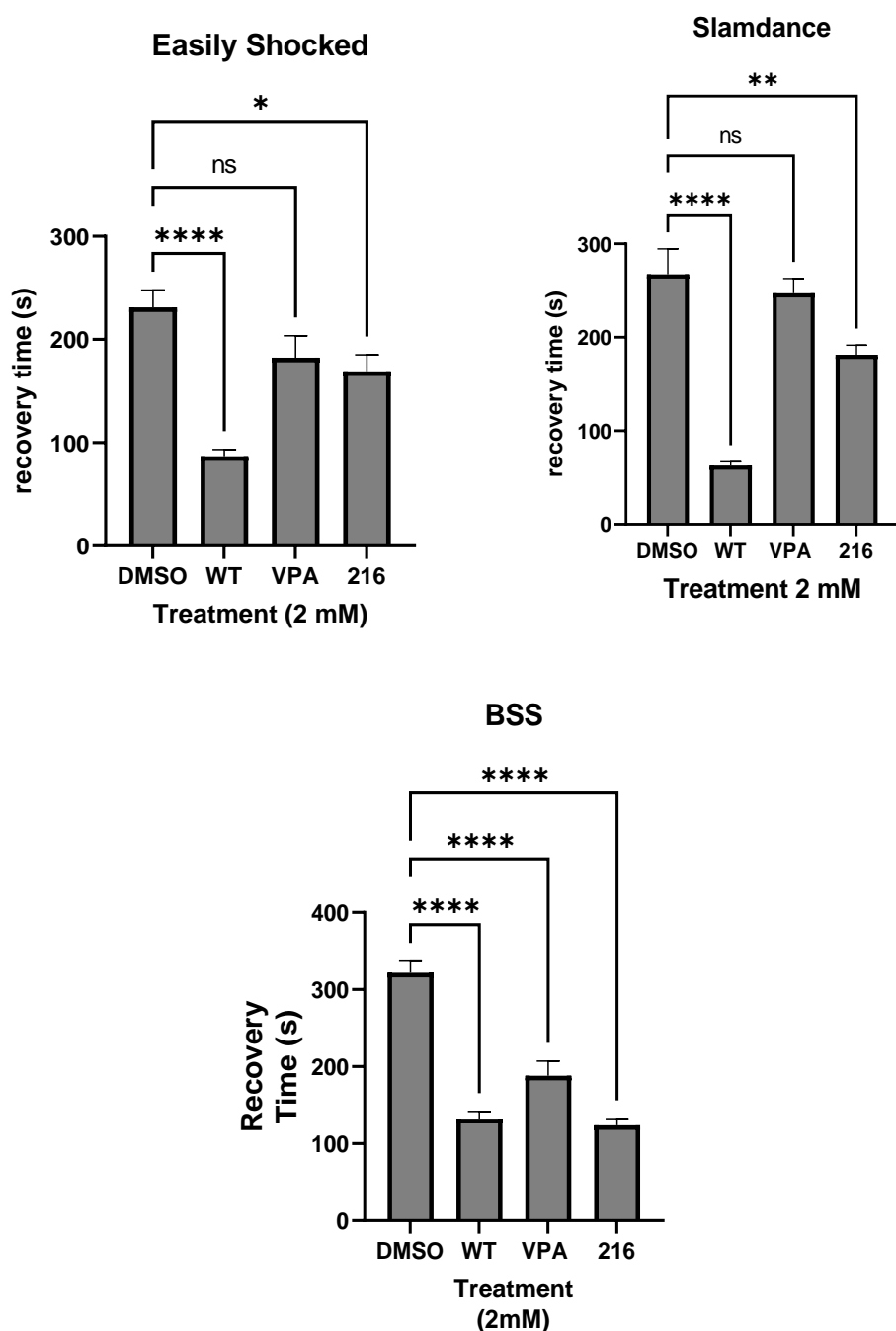


Figure 3.1 - L3 seizure assay of lead compound RAB216 and sodium valproate. The compounds were screened in two different seizure mutants, *slamdance* (*sda*) and *easily shocked* (*eas*). RAB216 significantly reduced recovery times in both mutants, but VPA had no effect in either. Results were analysed via a one-way ANOVA [*Easily shocked*  $F(3, 56) = 13.94$ ] [*Slamdance*  $F(3, 56) = 30.44$ ] [*BSS*  $F(3, 70) = 41.46$ ] with correction for multiple comparison (Dunnett's). Values given are mean  $\pm$  SEM. \* =  $p < 0.05$ , \*\* =  $p < 0.01$ , \*\*\* =  $p < 0.001$ , \*\*\*\* =  $p < 0.0001$

The results from Figure 3.1 show that RAB216 is effective at reducing seizure severity in both seizure mutants, in addition to *para*<sup>bss</sup> which has already been shown in the previous chapter. However,

valproate did not have a significant effect on the recovery time of either mutant, but does tend towards significance in the easily shocked mutant ( $p = 0.90$ ). Previous studies have shown that valproate reduces the likelihood of seizures in *sda* adult *Drosophila* in a dose dependent manner (Kuebler and Tanouye, 2002), but the effect has never been shown in larvae. Valproate has also previously been tested on adult *eas* mutants but had no significant effect on seizure like behaviour (Song *et al.*, 2008). This same study also found that valproate significantly alleviated seizure like behaviour in adult *para<sup>bss</sup>* mutant, which is in agreement with our data.

In the same way that certain AEDs work better for particular types of epilepsy, the response to AEDs varies with different *Drosophila* bang-sensitive mutants. An AED that works on a wide range of bang-sensitive mutants could be indicative of an AED that would work on a variety of different types of human epilepsies. Validation of this theory would be to find disease causing mutations in epilepsy patients and express them in *Drosophila*, taking advantage of their genetic tractability. It could then be seen whether the effect of AEDs in *Drosophila* is representative of their effect on the homologous human condition. This would only be representative of a small percentage of epilepsy cases, as most epilepsies in human are idiopathic, but could be a useful insight into the treatment of specific conditions and the quality of *Drosophila* as a model for screening AEDs.

As an example, *ATP6VOC* was recently identified as a gene that can cause epilepsy with intellectual disability (Ittiwut *et al.*, 2021). It encodes a membrane-bound subunit of vacuolar ATPase (V-ATPase), an enzyme responsible for the acidification of various intracellular organelles. Exome sequencing and PCR analysis revealed a *de novo* heterozygous mutation resulting in the RNA levels being reduced to around half, suggesting the pathology was caused by haploinsufficiency. A number of epilepsy patients have been found with mutations in *ATP6VOC* and the most common effective treatments appear to be levetiracetam, lamotrigine and topiramate (Prof Sid Banka, 2021, personal communication). The *ATP6VOC* knockdown line increases recovery time in *Drosophila* (Figure 3.2), indicating that loss of *ATP6VOC* causes seizure like behaviour in this model. To evaluate whether the effectiveness of these treatments transfer into the *Drosophila* model, a variety of AEDs, including RAB216, were screened in an *ATP6VOC* RNAi line.

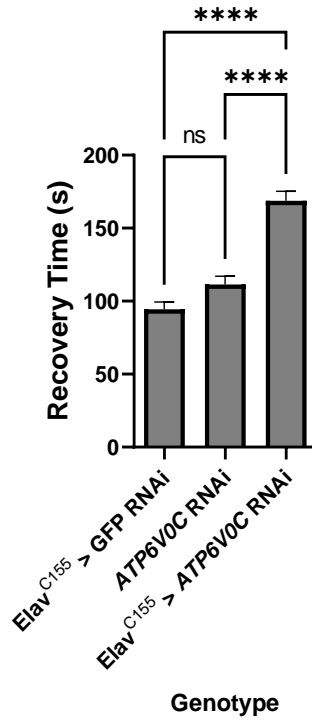


**Figure 3.2 – L3 seizure assay of ATP6V0C RNAi line.** Seizure recovery time was significantly increased in the ATP6V0C line when with the Elav driver, in comparison to both controls. This indicates that knockdown of ATP6V0C in proconvulsant in drosophila larvae. N= 24, refers to number of larvae shocked. Results were analysed via a one-way ANOVA [ $F(4, 109) = 34.50$   $P < 0.0001$ ] with correction for multiple comparison (Dunnett's). Values given are mean  $\pm$  SEM. \* =  $p < 0.05$ , \*\* =  $p < 0.01$ , \*\*\* =  $p < 0.001$ , \*\*\*\* =  $p < 0.0001$ .

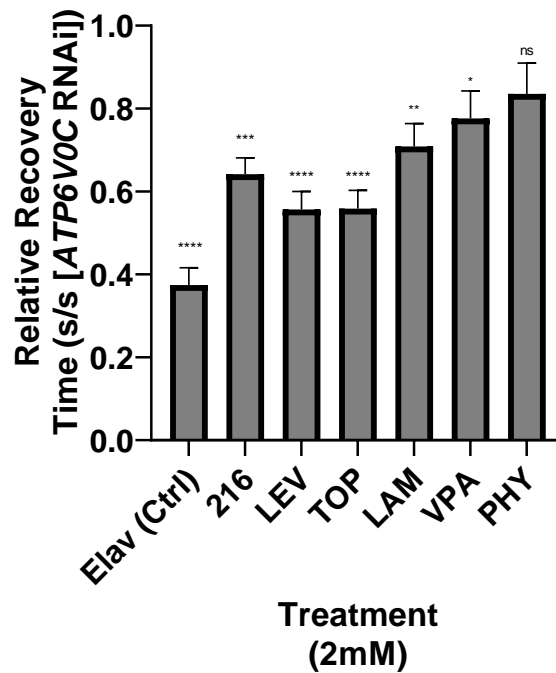


*Figure 3.3 - L3 seizure assay in v-ATPase RNAi line. Values shown are relative to the VATPase RNAi line recordings, which were done alongside those listed. The drugs screened were RAB216 and the AEDs levetiracetam (LEV), topiramate (TOP), lamotrigine (LAM) sodium valproate (VPA) and phenytoin (PHY). The uncrossed Elav line was included as a positive control. Phenytoin was the only AED screened which did not significantly reduce recovery time. Levetiracetam and topiramate were significantly more effective at reducing recovery times than sodium valproate, with  $p$  values of 0.0354 and 0.0378, respectively. Results were analysed via a one-way ANOVA [ $F(6, 113) = 7.497$   $P < 0.0001$ ] with correction for multiple comparison (Dunnett's). Values given are mean  $\pm$  SEM. \* =  $p < 0.05$ , \*\* =  $p < 0.01$ , \*\*\* =  $p < 0.001$ , \*\*\*\* =  $p < 0.0001$*

The results in Figure 3.3 show that levetiracetam and topiramate were the most effective treatments, whereas phenytoin was the only treatment tested that did not significantly reduce recovery times. Although sodium valproate was found to significantly reduce recovery times, levetiracetam and topiramate were found to be significantly more potent than sodium valproate at this concentration with a  $P$  value of 0.0354 and 0.0378, respectively. Lamotrigine also reduced recovery times, with a potency between that of sodium valproate and the two more effective treatments.

Whilst these results are not conclusive, they do suggest that the treatments that are most effective in human patients are also the most effective in this *Drosophila* model. Additionally, RAB216 was also found to significantly reduce the recovery time of *ATP6VOC* mutants, further indicating that it has the potential to be a wide-acting AED.

The above results suggest that the approach of finding epilepsy causing human genes and expressing them in flies has the potential to be a useful tool in discovering the most appropriate treatment for specific epilepsy conditions. To validate this approach, it would require the screening of a range of AEDs, against other lines possessing mutations characterised in humans, ideally at a variety of concentrations, which can then be compared to the AEDs most effective in epilepsy patients. This approach could also be applied to mammalian studies to both further validate the *Drosophila* model and provide insights that may provide a high-throughput route to researching more personalised medicine for specific epilepsy conditions.

### 3.2.1 Mechanism of Action Studies

Once RAB216 had been established as the lead compound (chapter 2) and shown to be a potentially wide-acting AED, the next step was to confirm that the compound still acts through Pumilio. Previous experiments in both mice (Figure 3.5) and *Drosophila* (Figure 3.6) showed that RAB102 significantly increase levels of Pumilio protein (Wei-Hsiang Lin and R. Baines, unpublished). In mice, the changes in concentration of both Pum1 and Pum2 were measured by Western blot, whereas the data from *Drosophila* was acquired using a luciferase reporter. By using the GAL4/UAS system and a luciferase reporter, the rate of transcription can be measured as a function of luminescence. To achieve this the *dpum* promoter was inserted upstream of GAL4 such that when the *dpum* promoter is activated, transcription of GAL4 occurs. GAL4 protein then binds to UAS -luciferase, activating the transcription of luciferase, an enzyme that reacts with luciferin to produce luminescence. With this construct therefore, the rate of *pum* transcription can be measured by homogenising *Drosophila*, adding luciferin, and recording the amount of luminescence produced. A graphical representation of this construct is shown in Figure 3.4.

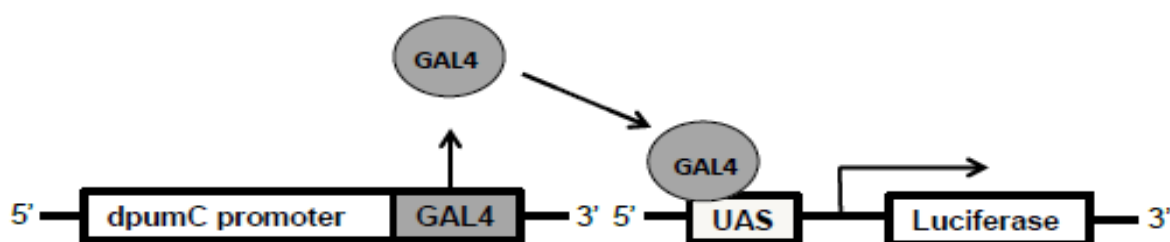


*Figure 3.4 - Graphical representation of the genetic construct used for the luciferase reporter assay. When the *dpumC* promoter is activated for transcription, GAL4 protein is also synthesised. This then binds to UAS initiating transcription of luciferase protein. Therefore, concentration of luciferase directly correlates to *dpumC* concentration.*

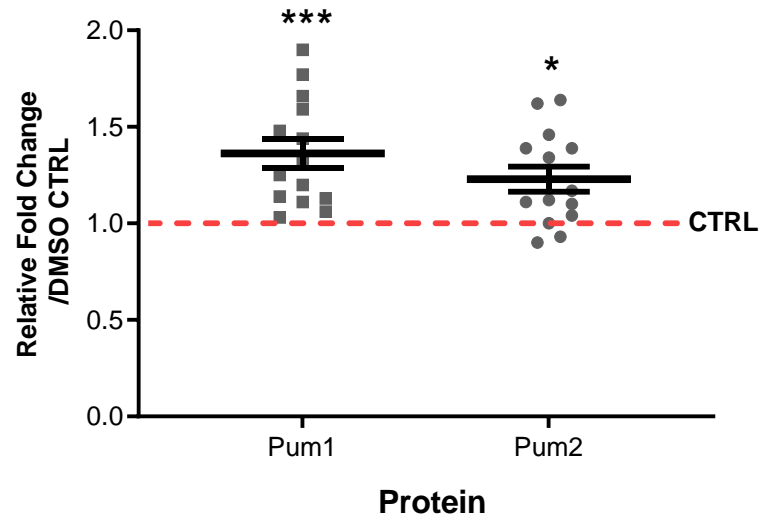


Figure 3.5 - Western blot analysis of the changes to Pum1 and Pum2 concentration in the mouse brain, following 3 days of RAB102 400 mg/g) injection. Changes compared to a vehicle control group, also injected for 3 consecutive days prior to analysis. The concentration of both Pum1 and Pum2 were significantly increased after RAB102 treatment. Data collected by Wei-Hsiang Lin and R. Baines, unpublished. Results were analysed via multiple unpaired t tests. Values given are mean  $\pm$  SEM. \* =  $p < 0.05$ , \*\* =  $p < 0.01$ , \*\*\* =  $p < 0.001$ , \*\*\*\* =  $p < 0.0001$

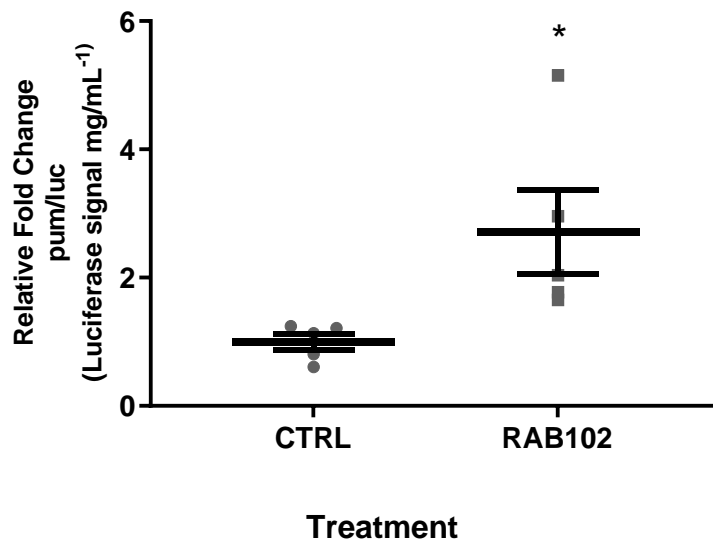
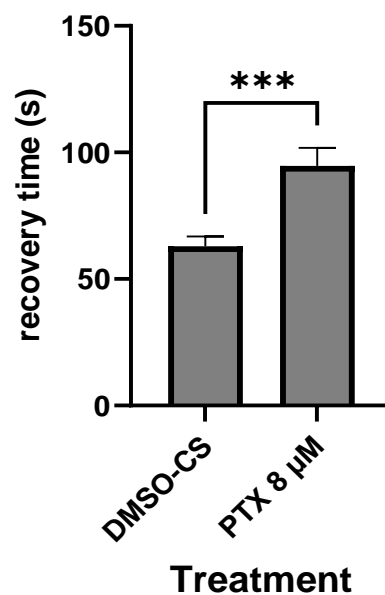
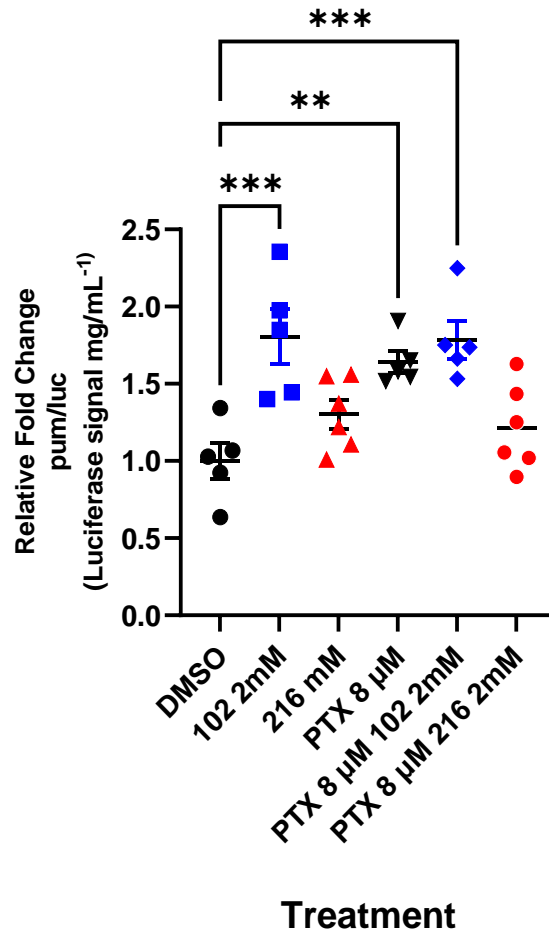


Figure 3.6- Luciferase reporter assay investigating the changes in transcription of pum in Drosophila following treatment with RAB102. Drosophila larvae raised on food containing RAB102 had a significantly higher rate of transcription compared to the control. Results were analysed via an unpaired t-test. Values given are mean  $\pm$  SEM. \* =  $p < 0.05$ , \*\* =  $p < 0.01$ , \*\*\* =  $p < 0.001$ , \*\*\*\* =  $p < 0.0001$

In order to test whether RAB216 has the same mechanism of action as RAB102 it was tested in the same luciferase reporter assay as shown in Figure 3.6. The proconvulsant PTX was included as a positive control, as previous screens had shown it increases *dpum* transcription. This may be due to a homeostatic mechanism aimed at reducing overall excitability. This supports a model of *pum* expression in *Drosophila*, which predicts Pum protein levels to increase in response to elevated CNS activity. PTX is a GABA antagonist and therefore will increase overall activity in the CNS through reduced inhibition. Although both RAB102 and PTX increase *pum* expression, behavioural experiments show that they have opposing effects on seizure like activity in *Drosophila*. RAB102 has been shown to reduce recovery times of seizure mutants in previous experiments. However, the data in Figure 3.7 highlights that PTX increases recovery times of wild type larvae. The combination of PTX with other compounds was also tested to see how they affect the increase in *pum* expression seen with PTX. The results are shown in Figure 3.7.



**Figure 3.7 - L3 seizure assay of wild type CS flies with and without PTX. Larvae fed with PTX had a significantly increased recovery time. This highlights that despite their similar effects on *pum* expression, they have opposing effects on seizure like activity. N= 24, refers to number of larvae shocked Results were analysed via an unpaired t-test. Values given are mean ± SEM. \* =  $p < 0.05$ , \*\* =  $p < 0.01$ , \*\*\* =  $p < 0.001$ , \*\*\*\* =  $p < 0.0001$**



**Figure 3.8 - Luciferase reporter assay investigating the changes in *dpumC* expression when *drosophila* larvae are treated with RAB102, RAB216 and PTX. Two groups were administered with a combination of PTX and either RAB102 or RAB216. Treatment with RAB102 alone significantly increased *pumC* expression, whereas RAB216 had no significant effect. Treatment with the proconvulsant PTX significantly increased *dpumC* expression, likely due a compensatory mechanism aimed at reducing excitability. Combination of PTX treatment with RAB102 resulted in an increase in *dpumC* expression, whereas raising larvae on a combination of PTX with RAB216 resulted in no significant change. Results were analysed via a one-way ANOVA [ $F(5, 26) = 7.676$   $P=0.0002$ ]. Values given are mean  $\pm$  SEM. \* =  $p < 0.05$ , \*\* =  $p < 0.01$ , \*\*\* =  $p < 0.001$ , \*\*\*\* =  $p < 0.0001$**

The results in Figure 3.8 show that, as seen previously, RAB102 significantly increased *dpum* expression. Additionally, PTX increased *dpum* expression as predicted. The combination of RAB102 and PTX resulted in an increase similar to that seen for both individual treatments. Interestingly, whilst RAB216 had no effect on *dpum* expression, it did prevent the increase seen with PTX treatment.

These results suggest that the two compounds may have different mechanisms of action. Whilst RAB102 seems to lower excitability by increasing the rate of transcription of *pum*, treatment with RAB216 prevents the need for the intrinsic homeostatic system to respond to PTX. It seems likely therefore, that RAB216 affects neuronal homeostasis through an alternative, and currently unknown, mode of action. However, the half-life of luciferase catalytic activity is approximately 3 hours, meaning that luciferase reporter assays reflect a snapshot of the current rate of transcription, rather than the overall concentration of Pum protein. In the case of Pum, this distinction is even more important, as the protein regulates its own transcript. Therefore, larger increases in transcription may not directly translate into higher protein concentrations. Furthermore, the rate of *pum* transcription is increased in response to elevated CNS activity, so it may be that an initial increase in Pum protein concentration lowers excitability to the point where *pum* transcription is reduced. Due to these complications, a Western blot analysis of protein concentration may better reflect how these compounds truly affect *pum* expression. Currently, there are no antibodies compatible with *Drosophila* Pum, therefore Western blot analysis had to be reserved for mammalian experiments.

In order to establish whether RAB compounds require the presence of Pum to exert their function, the compounds were screened in a *Drosophila* seizure mutant that also had the *pum* gene knocked down (Figure 3.9). By using the Elav Gal4 driver, Pum RNAi can be expressed in all neurons specifically, reducing the amount of *pum* RNA produced. The AED phenytoin was also screened in this line as a control (should not be dependent on Pum for activity). Phenytoin was chosen over valproate as its mechanism of action is better understood and more specific. Whilst both compounds have effects on gene expression, it is thought that valproate exerts some of its antiepileptic effect through histone-deacetylase inhibition. This ultimately leads to changes in the expression of a range of genes involved in epilepsy, including brain-derived neurotrophic factor (BDNF) and Glial cell-derived neurotrophic factor (GDNF) (Wu *et al.*, 2008; McNamara and Scharfman, 2012; Paolone *et al.*, 2019). Conversely, phenytoin works through blockade of sodium channels (Yaari, Selzer and Pincus, 1986), which is less likely to affect changes in expression caused by *pum* knockdown.

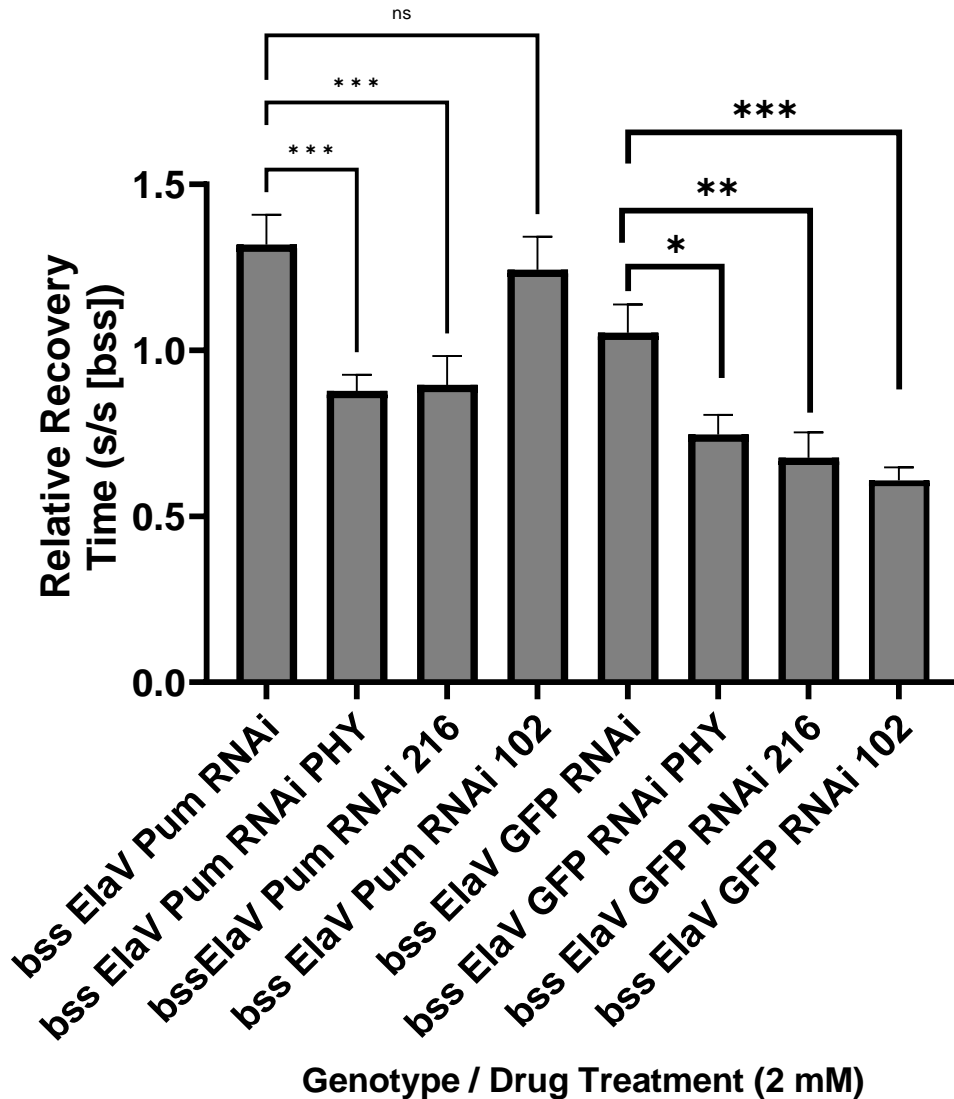


**Figure 3.9- L3 seizure assay of RAB216, RAB102 and phenytoin in *bss* seizure mutants with *pum* RNAi or GFP RNAi.** In the *pum* RNAi line, phenytoin and RAB216 significantly reduced recovery times, whereas RAB102 had no effect. In the GFP RNAi line all three compounds significantly reduced recovery times including RAB102. The *pum* RNAi line had a longer recovery time than the GFP RNAi line, but the difference was not significant ( $p = 0.080$ ).  $N = 24$ , refers to number of larvae shocked. Results were analysed via a one-way ANOVA [ $F(7, 112) = 11.58$   $P < 0.0001$ ] with correction for multiple comparison (Dunnett's). Values given are mean  $\pm$  SEM. \* =  $p < 0.05$ , \*\* =  $p < 0.01$ , \*\*\* =  $p < 0.001$ , \*\*\*\* =  $p < 0.0001$

The *pum* RNAi line had an increased recovery time when compared to the GFP RNAi group, but the difference was not significant ( $p = 0.080$ ). Whilst RAB216 and phenytoin significantly reduced recovery times in the *pum* RNAi line, RAB102 had no effect under these same conditions. Additionally, all three compounds had a significant effect in the GFP RNAi line. These results suggest that whilst RAB102 requires the presence of *pum* for function, RAB216 does not. This further supports the evidence from the luciferase reporter assay (see above) that suggested RAB216 has a

different mechanism of action to RAB102. Alternatively, it may be the case that RAB216 still exerts part of its function through Pum, but also has an additional mechanism of action.

To further investigate the mechanism of action for the two RAB compounds, and the antiepileptic effect of increased *pum* expression, both were screened in a *para<sup>bss</sup>* *Drosophila* line overexpressing *pum*. Previous experiments have shown *pum* overexpression to be anticonvulsant in these mutants (Lin et al., 2017), but the combination of over-expression with AEDs has not been tested.

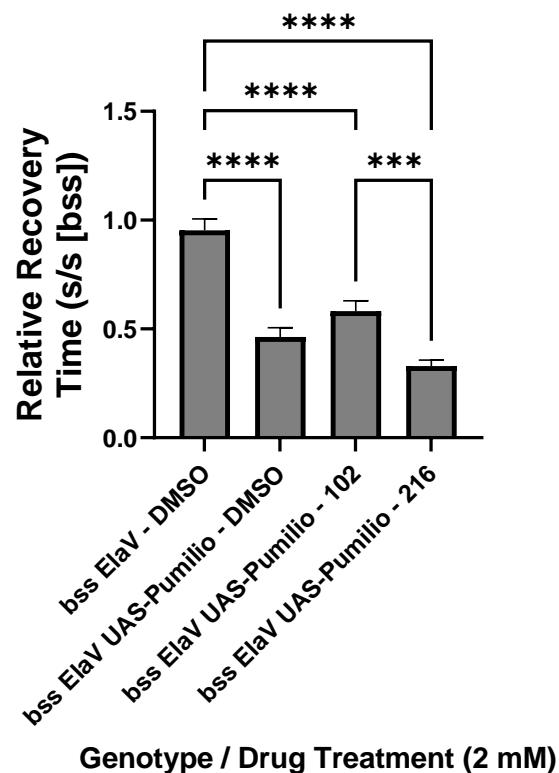


**Figure 3.10- L3 seizure assay of RAB102 and RAB216 in *bss* mutants overexpressing *pum*.** The *bss ElaV* genotype was included as a control. Overexpression of *pum* in *bss* mutants is significantly anticonvulsant. When overexpression was combined with drug treatment there were no significant differences. However, the RAB216 treatment group had a significantly lower recovery time than the RAB102 group. All results are normalised to the recovery times of *bss* seizure mutants, recorded at the same time. N= 24, refers to number of larvae shocked. Results were analysed via a one-way ANOVA [ $F(3, 56) = 37.93$   $P < 0.0001$ ] with correction for multiple comparison (Dunnnett's). Values given are mean  $\pm$  SEM. \* =  $p < 0.05$ , \*\* =  $p < 0.01$ , \*\*\* =  $p < 0.001$ , \*\*\*\* =  $p < 0.0001$

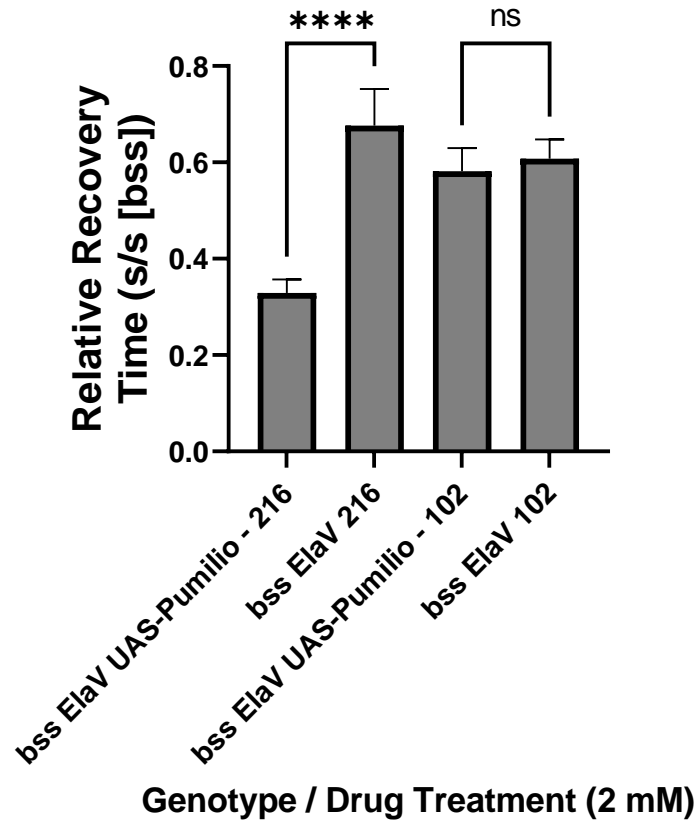


**Figure 3.11 - L3 seizure assay of RAB216 and RAB102 in drosophila seizure mutants with and without overexpression of *pum*.** Whilst there was no difference between the recovery times of the two RAB102 treatment groups, RAB216 + *pum* overexpression had a significantly lower recovery time when compared to *pum* overexpression alone. All results are normalised to the recovery times of *bss* seizure mutants, recorded at the same time. N= 24, refers to number of larvae shocked. Results were analysed via a one-way ANOVA [ $F(3, 56) = 8.844$   $P < 0.0001$ ] with correction for multiple comparison (Dunnett's). Values given are mean  $\pm$  SEM. \* =  $p < 0.05$ , \*\* =  $p < 0.01$ , \*\*\* =  $p < 0.001$ , \*\*\*\* =  $p < 0.0001$

The results in Figure 3.10 highlight the anticonvulsant effect of increased *pum* expression, which reduced recovery times of the *para*<sup>bss</sup> mutant by over 50 %. When combined with *pum* overexpression, drug treatment had no additional significant effect on recovery time. However, there was, again, a significant difference between the RAB102 and RAB216 treatment groups, Furthermore, when RAB102 is fed to seizure mutants overexpressing *pum*, recovery time is not significantly changed as compared to the same seizure mutants fed RAB102 but without overexpressing *pum*. Conversely, when *Drosophila* seizure mutants overexpressing *pum* were fed RAB216 (Figure 3.11), recovery time was found to be significantly lower than the seizure mutants fed RAB216 but not overexpressing *pum*. This may indicate that in the *pum* overexpression line, RAB102 has no effect because its effect is already being replicated genetically by increased *pum* expression and thus has reached saturation. It would also indicate that RAB216 has a mechanism that does not involve, or in addition to, an increase in *pum* expression.

Data from multiple *Drosophila* experiments suggest that RAB216 has a different mechanism of action to RAB102. Data from the *pum* overexpression and knockdown experiments show that RAB102 requires the presence of *pum* for activity and has no additional effect in seizure mutants overexpressing *pum*, indicating a saturation effect. Conversely, RAB216 reduced recovery times in both *pum* knockdown and *pum* overexpression seizure mutants. The luciferase reporter assay also supported these findings. Whilst RAB102 was found to significantly increase *pum* transcription, RAB216 had no effect. However, RAB216 did prevent the increase in *pum* transcription seen with PTX treatment, which may indicate a protective effect against the proconvulsant.

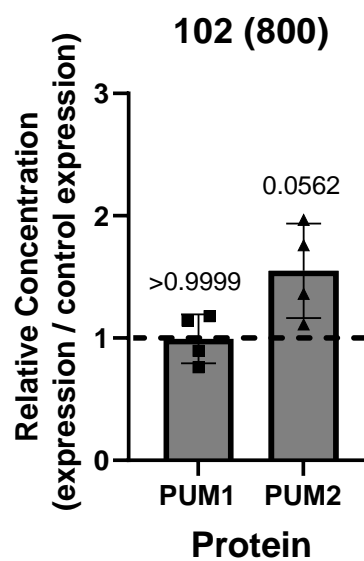
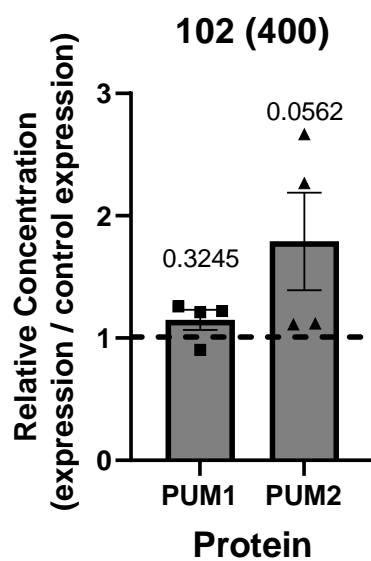
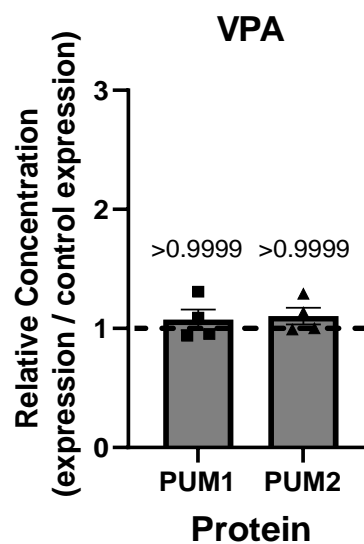
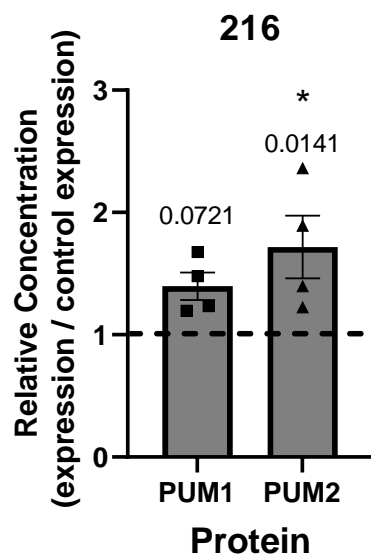
Due to their genetic tractability, high reproduction rate and lack of ethical concerns, *Drosophila* are a useful tool in the study of seizures and how they are affected by AEDs. It provides an opportunity to investigate the effect of drugs *in vivo*, taking into account effects such as toxicity and metabolism, in a time and cost-effective manner when compared to models such as mice. However, screening drugs in mammalian models is likely to be more reflective of how drugs may behave in human, particularly in terms of toxicity and efficacy. Furthermore, in the case of CNS drugs it is important to know whether a drug is capable of crossing the BBB. Whilst *Drosophila* do have such a barrier protecting the CNS, they do not have the same type of circulatory system and it is unknown whether a mammalian BBB and the *Drosophila* system are similar in terms of selectivity. *Drosophila* also only has one *Pum* protein whereas, like humans, mice possess *Pum1* and *Pum2*.

The mammalian studies part of this project had two main aims. Firstly, to test the effect of RAB216 and RAB102 on expression of *Pum* protein (all variants), which was investigated by Western blot in mice. Secondly, the drugs were tested for their anticonvulsant efficacy in two models: proconvulsant PTZ and the 6 Hz model of psychomotor seizures.

In order to confirm whether RAB216 has effect on *pum* expression, a Western blot experiment was undertaken. Due to the short functional half-life of the luciferase protein, the reporter assay reflects a snapshot of recent transcription, whereas Western blots report the total change in protein concentration. *Pum* works through a homeostatic mechanism, whereby increased neuronal activity leads to increased *pum* expression and a reduction in neuronal excitability. Therefore, if neuronal excitability had been sufficiently reduced by RAB216 any effects on *pum* expression could be missed.

Mice were injected with drug once per day for 3 successive days before brains were removed (4hr after final injection) and analysed for changes in *pum* expression. This experiment was also used as a

pre-screen to check for potential issues with toxicity before the compounds were screened using a larger set of animals. As a result, the sample size for this experiment is low (n = 4).



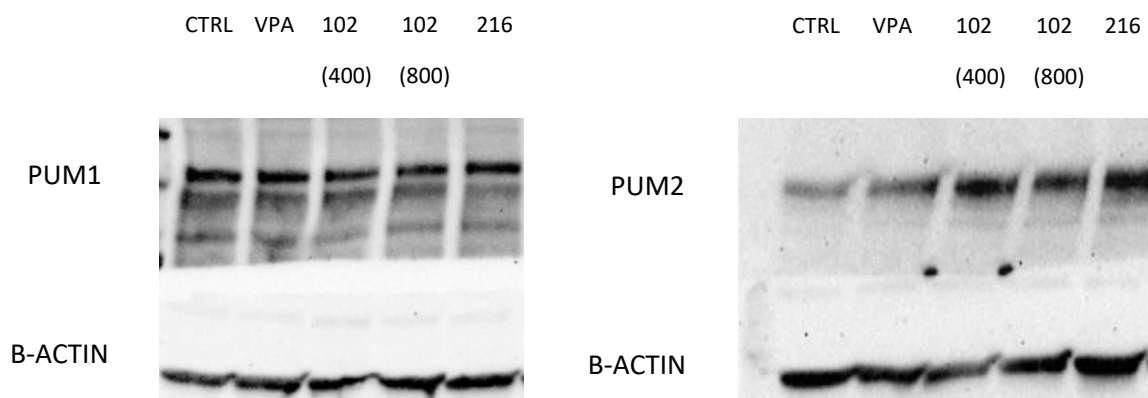


**Figure 3.12 - Western blot quantification of mouse brain samples following 3 days of injection with sodium valproate (400 mg/kg), sodium salt of RAB216 (200 mg/kg) and RAB102 (400 and 800 mg/kg). The only statistically significant result was the pum2 concentration in the RAB216 treatment group. Representative image from 1 mouse brain sample shown. N=4, refers to number of different mouse brain samples analysed. Results were analysed via a t-test. Values given are mean  $\pm$  SEM. \* =  $p < 0.05$ , \*\* =  $p < 0.01$ , \*\*\* =  $p < 0.001$ , \*\*\*\* =  $p < 0.0001$**

The quantification of the Western blot experiment is shown in Figure 3.12. The only statistically significant result across all treatment groups was the increase seen in pum2 expression for the RAB216 group. However, 3 additional groups were found to be close to significance. The increase in Pum1 expression in the RAB216 treatment group ( $p = 0.0721$ ) and the increase in pum2 expression for both RAB102 treatment groups (RAB102 (400)  $p = 0.0562$  and RAB102 (800)  $p = 0.0562$ ). These results likely suffer from the low N number, but they do suggest that it is likely that both RAB216 and RAB102 increase pum expression.

### 3.2.2 Rodent Seizure Models

Once both compounds had been tested for safety on a small set of mice and their effect on Pum expression established, the next stage was to investigate their efficacy at reducing seizures in rodent models. Results from the *Drosophila* screening suggested that RAB216 may be effective at reducing recovery times across a range of different seizure types. In order to see whether this effect translates into rodent models, RAB216 was screened using two different methods. The first was a pharmacological model using the proconvulsant PTX, which is categorised as a model of generalised seizure (Mackenzie *et al.*, 2002). The second was the 6 Hz psychomotor seizure model, a model which better represents partial seizures (Bankstahl, Bankstahl and Löscher, 2013). Interestingly, the marketed AED phenytoin is effective in the PTZ model but shows no activity in the 6 Hz model (Löscher, 2017). However, the opposite is true for levetiracetam, another marketed AED (Barton *et al.*, 2001). This highlights the need for testing compounds in multiple models, as a drug being

inactive in one model does not mean it is not a viable treatment for other forms of epilepsy. Furthermore, if a drug is found to be effective in multiple models, it may mean it has the potential to be a wide acting AED that is effective against various forms of epilepsy.

The results of the PTZ screen are shown in Figure 3.13. The dose of RAB216 was set at 200 mg/kg for two reasons. Firstly, according to the results from the *Drosophila* screen (chapter 2), the compound should be more efficacious than RAB102 (by ~4x). Therefore, the dose was set at 200 mg/kg, compared to 800mg / kg for RAB102. Mice were given 1 dose of drug per day for 3 successive days and the PTZ dose was given 4 hours after the third dose.

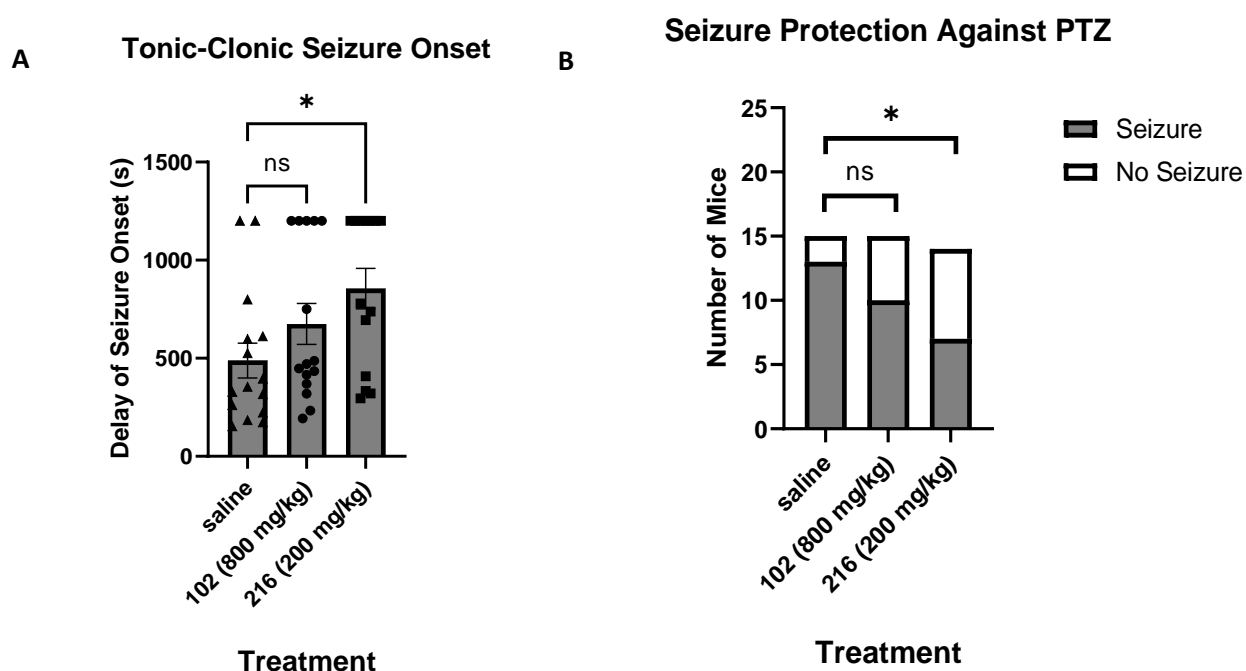


**Figure 3.13 – Data from the PTZ mouse seizure assay.** A) RAB216 significantly delayed the onset of seizures when compared to the control. RAB102 did not increase the tonic-clonic seizure onset time significantly ( $p = 0.2622$ ). Results were analysed using a Kruskal-Wallis test. Values given are mean  $\pm$  SEM. \* =  $p < 0.05$ , \*\* =  $p < 0.01$ , \*\*\* =  $p < 0.001$ , \*\*\*\* =  $p < 0.0001$ . B) Analysis of seizing vs non-seizing animals. In the control group, 13/15 animals went into full tonic-clonic seizure. In the RAB216 group 7/14 went into a full tonic-clonic seizure, a significant decrease when compared to the control. In the RAB102 group 10/15 experienced a tonic-clonic seizure with no significant difference from the control. Results were analysed using a chi-squared test. \* =  $p < 0.05$ , \*\* =  $p < 0.01$ , \*\*\* =  $p < 0.001$ , \*\*\*\* =  $p < 0.0001$ .

The results from Figure 3.13 show that whilst RAB216 effectively reduces seizure severity in mice, RAB102 has no significant effect at the dose tested. RAB216 treatment increased the average time of seizure onset from 488 s to 855 s. Furthermore, it increased the number of mice that did not reach the full tonic-clonic seizure threshold from 2/15 to 7/14. Whilst RAB102 increased both the average

time of onset and the number of mice that did not exhibit full seizures, neither of these changes were statistically significant. In the control group, 13/15 mice reached the full tonic-clonic seizure stage. This is approximately what would be expected for injections at this dose and is in line with previously published studies (Van Erum, Van Dam and De Deyn, 2019).

Overall, the results from the PTZ screen suggest that RAB216 provides protection against generalised seizure. However, to ascertain whether RAB216 has the potential to treat a wider range of seizure types, screening in additional models of seizure was required. RAB216 was screened in the 6 Hz model of psychomotor focal seizure. The results are shown in Figure 3.14 (which was done in collaboration with Prof Ilse Smolders and Dr Najat Aourz, Vrije Universiteit Brussel).

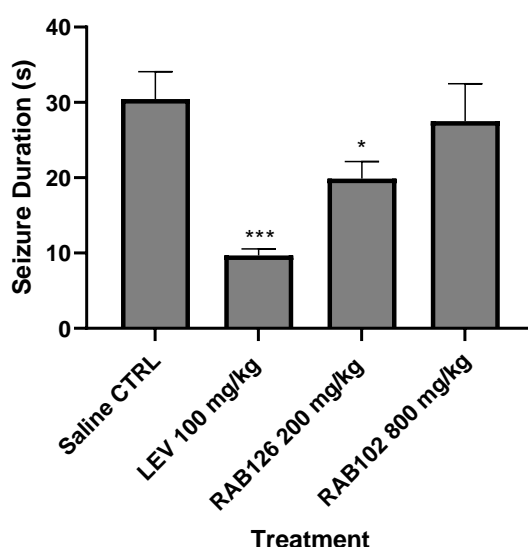


**Figure 3.14 -The effect of RAB216 on seizure duration as measured by the 6 Hz seizure model. Levetiracetam was also included as a positive control. RAB216 was found to significantly reduce seizure duration by 35 %. Levetiracetam was also found to significantly reduce seizure duration. N=9, refers to number of mice tested. Results were analysed via a one-way ANOVA [ $F(3, 31) = 8.558$   $P=0.0003$ ] with correction for multiple comparison (Dunnett's). Values given are mean ± SEM. \* =  $p < 0.05$ , \*\* =  $p < 0.01$ , \*\*\* =  $p < 0.001$ , \*\*\*\* =  $p < 0.0001$**

The results from Figure 3.14 show that RAB216 effectively provides protection against psychomotor focal seizures in this model. Treatment with RAB216 lowered seizure duration by a third and was significantly shorter than the vehicle control. Levetiracetam was used as a positive control and reduced seizure duration significantly. The reduction in seizure duration from levetiracetam treatment is similar to results reported in previous similar experiments (Walrave *et al.*, 2015).

RAB102 was also screened but had no significant effect on seizure duration. In the 6 Hz seizure model experiments NMRI mice were used whereas for the PTZ seizure experiments, compounds were screened in C57BL/6Jax. Interestingly, the death rate of mice administered RAB102 seemed to be higher in the NMRI mice. In a previous 6 Hz model experiment (data unpublished), 3 of the 14

mice treated with RAB102 died before the PTZ injection stage of the experiment. There are genetic differences between mouse strains which may cause them to react differently to substances. For example, the rate of enzymatic reactions varies from strain to strain, which could have significant effects on the metabolism of drugs (Guo *et al.*, 2007). The causes of RAB102's apparent toxicity is unknown, but it may be linked to the presence of the aldehyde group. Aldehydes are highly reactive and will readily form covalent bonds with any nucleophilic residues *in vivo*. They are usually rapidly metabolised and converted into carboxylic acids to aid with excretion, therefore any changes to the hepatic system from genetic variance, could have a significant effect on toxicity.

### 3.3 Discussion

When screening drugs in any model of disease, it is always beneficial to use a variety of models. No one model is perfect and using a variety decreases the chances that any positive or negative effects will be missed. This is particularly true for epilepsy, due to the variation in the causes, symptoms, and effective treatment choices of different epilepsy types. The results from the screening of RAB216 suggest that it is effective in every model tested so far. In the *Drosophila* electric shock model, all 3 seizure mutants tested had a reduced seizure recovery time when treated with RAB216. Additionally, the luciferase reporter experiment suggested that RAB216 prevented the increase in excitation seen in *Drosophila* raised on PTX. In mouse models, treatment with RAB216 delayed seizure onset in both the PTX and 6 Hz seizure models. In the PTX model RAB216 also prevented full tonic-clonic seizure in 50% of the animals tested, compared to 13% in the control group. Furthermore, Western blot analysis showed that RAB216 significantly increased the concentration of Pum2 protein in the brain, whilst Pum1 concentration was also higher, this was found to be just short of significance ( $p = 0.0721$ ).

RAB102, the starting point for the structure-activity studies, failed to have a significant effect on seizure onset or severity in this set of experiments. It also had no significant effect on the concentration of Pum1 or Pum2 within mouse brain, although the increase in Pum2 concentration was close to reaching significance at both doses of 400 mg/kg ( $p = 0.562$ ) and 800 mg/kg ( $p = 0.0562$ ). This is in contrast with previously obtained data, which showed that Pum1 and Pum2 concentration significantly increased after treatment with RAB102, even at the lower dose of 400 mg/kg. In the experiment shown in Figure 3.3, mouse brains were recovered following 3 days of treatment with RAB102 or saline control and 20 mins after PTZ treatment, whereas results from the

more recent study in Figure 3.12, were obtained following injection of the drug treatments alone with no PTZ. In theory, this difference should be accounted for as any changes in protein concentration are measured against a control that was treated the same way. However, it may be the case that RAB102 changes the way mouse brain responds to PTZ. In terms of changes to protein expression, the 20 mins following PTZ injection is a short amount of time for any significant changes to occur. However, there are examples of PTZ having effects on gene expression over similar time frames. For example, c-fos transcription is significantly increased just 15 mins following injection of PTZ (Yount, Ponsalle and White, 1994). Results from the VPA treated mice suggest this change in Pum expression is not an effect that is general to AEDs and that these compounds possess a novel mechanism of action.

The N number for the original experiment which showed RAB102 to have a significant effect to Pum expression was higher at 15 mice, compared to 5 mice in this most recent study, which could partially explain the difference in results. The brains of the mice used in the PTZ study from Figure 3.12 were not analysed via Western blot, as a full iTRAQ (isobaric tags for relative and absolute Quantification) proteomics study was planned, which would have revealed any changes in Pum protein concentrations.

Compounds were initially screened using the *Drosophila para<sup>bss</sup>* mutant line. This line possesses a gain of function mutation in their singular Na<sub>v</sub> (*para*) and most closely resembles pharmacologically resistant epilepsies caused by mutations in the human Na<sub>v</sub> SCN1A (Parker *et al.*, 2011c). This group of conditions are amongst the more severe forms of epilepsy, which aligns with *para<sup>bss</sup>* having the longest recovery time of all recorded BS mutants (Baines, Giachello and Lin, 2017). The other two seizure mutants tested (*eas* and *sda*) have a less severe phenotype and the exact cause of their seizure-like behaviour is less clear. The *sda* phenotype was linked to a mutation in aminopeptidase N (Zhang *et al.*, 2002), but has since been attributed to the gene *julius seizure*, which encodes for an uncharacterised protein (Dean *et al.*, 2018). The fact these models have not been correlated with a specific form of human epilepsy does not mean they are any less representative of the condition. Approximately 75% of epilepsy cases are idiopathic and are likely often the result of multiple genetic and environmental risk factors (Walsh *et al.*, 2017). Characterisation of mutants such as *eas* and *sda* could lead to further understanding of some of the genetic risk factors that lead to seizures and epileptogenesis. An example of this can be seen with the *easily shocked* mutant, which is null for ethanolamine kinase (Pavlidis, Ramaswami and Tanouye, 1994), which is integral in the biosynthetic pathway of phosphatidylethanolamine, one of the most abundant phospholipids in many animal cell types (Kliman *et al.*, 2010). It was not fully understood how this produced an epileptic phenotype,

until recently it was discovered that deletion of a key enzyme in this pathway lead to a complex hereditary spastic paraplegia with seizures (Vaz *et al.*, 2019).

Despite the mechanism of increased excitability in some of these mutants not being fully understood, the antiseizure effect of RAB216 in these models still indicates that it has the potential to be an AED that is effective against different form of epilepsy. Further characterisation of these mutants and similar experiments where AEDs are screened in specific mutants may reveal more about some of the mechanisms underlying genetic risk factors, as well as which classes of AEDs are most effective at treating them.

In the V-ATPase screen, the opposite approach was taken, whereby a null mutation linked to epilepsy was discovered in human patients and the corresponding RNAi line was made in *Drosophila* in order to make a model the condition. Recent studies have discovered a novel condition caused by 16p13.3 microdeletion that results in seizures, microcephaly, and neurodevelopmental disorders (Mucha *et al.*, 2019). Further investigation revealed that the condition may be caused by haploinsufficiency of *ATP6VOC*, a gene encoding for a component of V-ATPase (Tinker *et al.*, 2021). V-ATPase is responsible for the acidification of intracellular organelles and is present in synaptic vesicles, lysosomes, endosomes, and the Golgi complex (Bayascas *et al.*, 2008). In zebrafish embryos, it has been found that *ATP6VOC* facilitates neurotransmitter storage and has a neuron specific expression at presynaptic vesicles, which possibly underlies the seizure phenotype seen with these mutants (Tinker *et al.*, 2021). An unpublished communication (Siddharth Banka 2021) suggested the most effective treatments for patients with this mutation were levetiracetam, lamotrigine and topiramate. These drugs were screened against the *Drosophila* RNAi line targeting *ATP6VOC*, and were found to be the most effective treatments, as was RAB216. This result further supports the proposal that RAB216 has the potential to be a wide acting AED, as it continued to be effective in every model of seizures in which it was screened. Additionally, this study highlights the potential strength of the *Drosophila* seizure model. The same treatments that were effective in human patients were also found to be the most effective in this animal, which suggests this model may be an effective way of testing AEDs against specific epilepsy causing mutations found in human patients.

A similar approach was taken by Baraban and colleagues in zebrafish, whereby they screened a list of FDA-approved drugs in a model of Dravet syndrome (Baraban, Dinday and Hortopan, 2013; Griffin *et al.*, 2017). Through this screen they discovered that clemizole was potentially an effective treatment and as the drug had already been FDA approved, they were able to move on to trialling the treatment in human. The treatment had some success at treating Dravet syndrome patients,

which is typically seen as one of the hardest epilepsy syndromes to manage. Additionally, this investigation discovered a potentially effective new AED target in serotonin receptors. This result also highlights the power of the so called 'Bench to Bedside' technique, whereby results from drug screens can be taken from smaller organisms such as zebrafish and *Drosophila*, before the results are applied to treating human. In the case of RAB216 the situation is different as it has not had any legal approval. However, this provides evidence that results from screens in simpler organisms can be translated to mammals and could thus be a useful tool in future as medicine becomes more personalised to genetics.

Overall, the results from this chapter support our conviction that RAB216 has the potential to be an effective and wide-acting AED. It was found to be active in every screen tested and whilst results from the luciferase reporter assay and PUM KD experiment indicate that it might have additional mechanism(s) of action, the Western blot experiment revealed that it likely acts through Pum for at least part of its effect. To better understand its mechanism of action, additional studies looking at the changes in expression of Pum targets, such as Na<sub>v</sub>s and GABARs, through Western blot or iTRAQ could reveal more about how the drug works. Additionally, screening in further rodent models such as genetic and/or kindling models would also reveal more about how effective the compound is overall and potentially which forms of epilepsy it is best suited to treat.

### 3.4 Experimental/Methods

#### 3.4.1 Fly Stocks

The wild type Canton-S line, *easily shocked* (detailed here: (Pavlidis, Ramaswami and Tanouye, 1994)) and *slamdance* (detailed here: (Zhang *et al.*, 2002)) were maintained by the Baines lab. *para<sup>bss</sup>* is detailed in (Parker *et al.*, 2011c) and was obtained from Dr Kevin O'Dell (Institute of Molecular, Cell and Systems Biology, University of Glasgow, UK). This fly carries a gain-of-function mutation in the sole voltage-gated Na<sup>+</sup> channel in *Drosophila* (termed *paralytic*). vATPase was knocked-down using pan-neuronal (elav-GAL4) expression of a gene-specific RNAi construct (102067), provided by the Vienna Drosophila Resource Center. Flies were maintained on standard cornmeal medium at 25 °C.

#### 3.4.2 L3 Seizure Electroshock Assay

Larvae climbing the walls of the tube are deemed to have reached the wandering stage (L3), which represents a 10hr window prior to pupation that all larvae must go through. Thus, all larvae tested were  $60 \pm 10$  hrs of age. L3 were transferred to water to wash them and then carefully dried on tissue paper. They were then placed on a plastic plate and allowed time to ensure that typical, peristaltic crawling behaviour was observed. Once observed, an electro-stimulator, made from two tungsten wires (0.1 mm diameter and approx. 1-2 mm apart), was placed on the anterior-dorsal surface of the larvae (over the CNS). A DC pulse (2.5 V) generated by a constant current simulator (DS2A, Digitimer, UK) was applied for 2 s. This caused larvae to exhibit a seizure-like behaviour characterised by complete cessation of mobility (see Marley and Baines, 2011). The time taken (termed Recovery Time, RT) for larvae to resume normal peristaltic crawling behaviour was recorded. Normal behaviour was defined as consistent waves of contraction across the whole body, whereby it seems the larva is in control of its movement and moving forward. Investigators were blinded to the treatment group when experiments were performed.

### 3.4.3 Western Blot

Whole brain was homogenised in ice-cold buffer (150 mM NaCl, 50 mM Tris-HCl, 1% Nonidet P-40, 0.5% sodium deoxycholate and 0.1% SDS) containing protease inhibitors (Promega, Madison, USA) and centrifuged at  $10,000 \times g$  (30 min at  $4^{\circ}\text{C}$ ). Supernatant was stored in ice. Antibodies were: anti-Pum 1 (1:1000, #12322, Cell Signaling, MA, USA), anti-Pum 2 (1:1000, ab10361, Abcam, Cambridge, UK) and anti- $\beta$ -Actin (1:5000, ab8227, Abcam). Samples (25  $\mu\text{g}$  of protein) were separated by SDS page, and protein transferred to a polyvinylidene difluoride membrane (GE Healthcare). After blocking (0.5 % BSA and 0.05% TWEEN-20 in Tris-buffered saline, TBS-T), membrane was incubated overnight ( $4^{\circ}\text{C}$ ) in primary antibody diluted in 0.5% BSA in TBS-T. Membranes were incubated with HRP conjugated secondary antibodies (1:2500, #7074, Cell Signaling) in 0.3% BSA in TBS-T and blots developed with an Enhanced Chemiluminescent Detection Kit (Pierce, Rockford, USA). Protein band density was measured using Image J (NIH, USA).

A dpum promoter-GAL4 line was crossed to attP24 UAS-luciferase flies 35. Flies carrying the UAS-luciferase transgene alone were used for background controls. Adult flies were allowed to lay eggs in vials containing food with added compound (or vehicle, DMSO) and to develop to L3. Ten L3 CNSs, of either sex, were placed in 100  $\mu\text{l}$  Promega Glo Lysis buffer for each sample, and 5 independent samples collected. CNSs were homogenized, incubated at room temperature (10 min), centrifuged (5 min), and supernatant transferred to a new tube. 30  $\mu\text{l}$  of each sample was then transferred to a well of a white-walled 96-well plate at room temperature, 30  $\mu\text{l}$  Promega Luciferase reagent was

added to each well and plates incubated in the dark (10 min). Luminescence was measured with a GENios plate reader (TECAN, Reading, UK). Values were normalized to total protein concentration, measured using the Bradford protein assay (Bio-Rad, Watford, UK).

#### 3.4.4 PTZ Seizure-Induction

Mice (male, C57BL/6J, 12-15 weeks, 23-30 g,) were injected subcutaneously (sc.) with 0.1 ml of compound (in NaCl, 0.9% w/v saline) or saline vehicle, once per day for 3 days. Four hours after the last injection on day 3, a single dose of PTZ (60 mg/kg/sc. in saline) was injected. Each mouse was placed into a separate clear plastic arena and videoed for 20 min. After the observation period, mice were anesthetized with isoflurane (3-4% in 20% O<sub>2</sub> and 50% N<sub>2</sub>O, 0.5 l/min), transcardially perfused with 0.9% saline and brains removed and stored at -80°C. Seizure scoring was carried out from videos, independently scored by two experimenters blinded to the experimental groups until full analysis was complete.

#### 3.4.5 6 Hz Seizure-Induction

NMRI mice (35–45g, male, Charles River, Chatillon-sur-Chalaronne, France) were used. Prior to the electrical stimulation, 0.5% xylocaine was applied to the cornea to induce local anaesthesia and ensure good conductivity. Corneal stimulation (46 mA, 0.2 ms duration pulses at 6 Hz for 3 s) was administered by a constant current device (ECT Unit 57800; Ugo Basile, Comerio, Italy). Acutely evoked 6 Hz seizures were characterized by stun, forelimb clonus, twitching of vibrissae, and/or Straub-tail. For each animal, the total seizure duration was manually recorded. Ip administration of levetiracetam (LEV, 100mg/kg) 1 h before seizure induction was used as a positive control. Seizure scoring was carried out live during the experiment. The entire experiment was also video recorded. The researcher was blinded to the experimental groups until full analysis was complete.

### 3.5 Bibliography

- Baines, R.A., Giachello, C.N.G. and Lin, W.-H. (2017) 'Drosophila', in *Models of Seizures and Epilepsy*. Elsevier, pp. 345–358. Available at: <https://doi.org/10.1016/B978-0-12-804066-9.00024-9>.
- Bankstahl, M., Bankstahl, J.P. and Löscher, W. (2013) 'Pilocarpine-induced epilepsy in mice alters seizure thresholds and the efficacy of antiepileptic drugs in the 6-Hertz psychomotor seizure model', *Epilepsy Research*, 107(3), pp. 205–216. Available at: <https://doi.org/10.1016/j.eplepsyres.2013.09.014>.
- Baraban, S.C., Dinday, M.T. and Hortopan, G.A. (2013) 'Drug screening in Scn1a zebrafish mutant identifies clemizole as a potential Dravet syndrome treatment', *Nature Communications*, 4, p. 2410. Available at: <https://doi.org/10.1038/ncomms3410>.
- Barton, M.E. et al. (2001) 'Pharmacological characterization of the 6 Hz psychomotor seizure model of partial epilepsy', *Epilepsy Research*, 47(3), pp. 217–227. Available at: [https://doi.org/10.1016/S0920-1211\(01\)00302-3](https://doi.org/10.1016/S0920-1211(01)00302-3).
- Bayascas, J.R. et al. (2008) 'Mutation of the PDK1 PH domain inhibits protein kinase B/Akt, leading to small size and insulin resistance', *Molecular and cellular biology*, 28(10), pp. 3258–3272.
- Bohn, J.A. et al. (2018) 'Identification of diverse target RNAs that are functionally regulated by human Pumilio proteins', *Nucleic acids research*, 46(1), pp. 362–386.
- BROWN, W.C. et al. (1953) 'Comparative assay of an antiepileptic drugs by psychomotor seizure test and minimal electroshock threshold test', *The Journal of pharmacology and experimental therapeutics*, 107(3), pp. 273–283.
- Dean, D. et al. (2018) 'Extending julius seizure, a bang-sensitive gene, as a model for studying epileptogenesis: Cold shock, and a new insertional mutation', *Fly*, 12(1), pp. 55–61.
- Driscoll, H.E. et al. (2013) 'Pumilio-2 Regulates Translation of Nav1.6 to Mediate Homeostasis of Membrane Excitability', *Journal of Neuroscience*, 33(23), pp. 9644–9654. Available at: <https://doi.org/10.1523/JNEUROSCI.0921-13.2013>.
- Van Erum, J., Van Dam, D. and De Deyn, P.P. (2019) 'PTZ-induced seizures in mice require a revised Racine scale', *Epilepsy & Behavior*, 95, pp. 51–55.
- Fessler, L.I., Nelson, R.E. and Fessler, J.H. (1994) 'Drosophila extracellular matrix', in *Methods in Enzymology*. Elsevier, pp. 271–294. Available at: [https://doi.org/10.1016/0076-6879\(94\)45016-1](https://doi.org/10.1016/0076-6879(94)45016-1).
- Fischer, W. and Müller, M. (1988) 'Pharmacological modulation of central monoaminergic systems and influence on the anticonvulsant effectiveness of standard antiepileptics in maximal electroshock seizure.', *Biomedica biochimica acta*, 47(7), pp. 631–645.
- Gould, S.J. and Subramani, S. (1988) 'Firefly luciferase as a tool in molecular and cell biology', *Analytical biochemistry*, 175(1), pp. 5–13.
- Griffin, A. et al. (2017) 'Clemizole and modulators of serotonin signalling suppress seizures in Dravet syndrome', *Brain*, 140(3), p. aww342. Available at: <https://doi.org/10.1093/brain/aww342>.
- Guo, Y. et al. (2007) 'In silico and in vitro pharmacogenetic analysis in mice', *Proceedings of the National Academy of Sciences*, 104(45), pp. 17735–17740.

- Hindle, S.J. and Bainton, R.J. (2014) 'Barrier mechanisms in the *Drosophila* blood-brain barrier', *Frontiers in neuroscience*, 8, p. 414.
- Honjo, K., Hwang, R.Y. and Tracey, W.D. (2012) 'Optogenetic manipulation of neural circuits and behavior in *Drosophila* larvae', *Nature protocols*, 7(8), pp. 1470–1478.
- Ittiwut, C. *et al.* (2021) 'Novel de novo mutation substantiates ATP6V0C as a gene causing epilepsy with intellectual disability', *Brain and Development*, 43(3), pp. 490–494.
- Jensen, L.H. and Petersen, E.N. (1983) 'Bidirectional effects of benzodiazepine receptor ligands against picrotoxin-and pentylentetrazol-induced seizures', *Journal of neural transmission*, 58(3), pp. 183–191.
- Kliman, M. *et al.* (2010) 'Structural mass spectrometry analysis of lipid changes in a *Drosophila* epilepsy model brain', *Molecular BioSystems*, 6(6), pp. 958–966. Available at: <https://doi.org/10.1039/b927494d>.
- Klueg, K.M. *et al.* (2002) 'Creation of a GAL4/UAS-coupled inducible gene expression system for use in *Drosophila* cultured cell lines', *genesis*, 34(1-2), pp. 119–122.
- Kuebler, D. and Tanouye, M. (2002) 'Anticonvulsant valproate reduces seizure-susceptibility in mutant *Drosophila*.', *Brain research*, 958(1), pp. 36–42.
- Lévesque, M. and Avoli, M. (2013) 'The kainic acid model of temporal lobe epilepsy', *Neuroscience & Biobehavioral Reviews*, 37(10), pp. 2887–2899.
- Lin, W.-H. *et al.* (2009) 'Alternative splicing in the voltage-gated sodium channel DmNav regulates activation, inactivation, and persistent current', *Journal of neurophysiology*, 102(3), pp. 1994–2006.
- Lin, W.-H., Giachello, C.N.G. and Baines, R.A. (2017a) 'Seizure control through genetic and pharmacological manipulation of Pumilio in *Drosophila*: a key component of neuronal homeostasis.', *Disease models & mechanisms*, 10(2), pp. 141–150. Available at: <https://doi.org/10.1242/dmm.027045>.
- Lin, W.-H., Giachello, C.N.G. and Baines, R.A. (2017b) 'Seizure control through genetic and pharmacological manipulation of Pumilio in *Drosophila*: a key component of neuronal homeostasis', *Disease Models & Mechanisms*, 10(2), pp. 141 LP – 150.
- Löscher, W. (2017) 'Animal models of seizures and epilepsy: past, present, and future role for the discovery of antiseizure drugs', *Neurochemical research*, 42(7), pp. 1873–1888.
- Mackenzie, L. *et al.* (2002) 'Picrotoxin-induced generalised convulsive seizure in rat: Changes in regional distribution and frequency of the power of electroencephalogram rhythms', *Clinical Neurophysiology*, 113(4), pp. 586–596. Available at: [https://doi.org/10.1016/S1388-2457\(02\)00040-8](https://doi.org/10.1016/S1388-2457(02)00040-8).
- McNamara, J.O. and Scharfman, H.E. (2012) 'Temporal Lobe Epilepsy and the BDNF Receptor, TrkB'. National Center for Biotechnology Information (US), Bethesda (MD). Available at: <http://europepmc.org/abstract/MED/22787630>.
- Mucha, B.E. *et al.* (2019) 'A new microdeletion syndrome involving TBC1D24, ATP6V0C, and PDPK1 causes epilepsy, microcephaly, and developmental delay', *Genetics in Medicine*, 21(5), pp. 1058–1064.

Paolone, G. *et al.* (2019) 'Long-term, targeted delivery of GDNF from encapsulated cells is neuroprotective and reduces seizures in the pilocarpine model of epilepsy', *Journal of Neuroscience*, 39(11), pp. 2144–2156.

Pardridge, W.M. (1998) 'CNS Drug Design Based on Principles of Blood-Brain Barrier Transport', *Journal of Neurochemistry*, 70(5), pp. 1781–1792. Available at: <https://doi.org/https://doi.org/10.1046/j.1471-4159.1998.70051781.x>.

Parker, L. *et al.* (2011) 'Drosophila as a model for epilepsy: bss is a gain-of-function mutation in the para sodium channel gene that leads to seizures', *Genetics*, 187(2), pp. 523–534. Available at: <https://doi.org/10.1534/genetics.110.123299>.

Pavlidis, P., Ramaswami, M. and Tanouye, M.A. (1994) 'The Drosophila easily shocked gene: A mutation in a phospholipid synthetic pathway causes seizure, neuronal failure, and paralysis', *Cell*, 79(1), pp. 23–33. Available at: [https://doi.org/10.1016/0092-8674\(94\)90397-2](https://doi.org/10.1016/0092-8674(94)90397-2).

Smith, M., Wilcox, K.S. and White, H.S. (2007) 'Discovery of antiepileptic drugs', *Neurotherapeutics*, 4(1), pp. 12–17.

Song, J. *et al.* (2008) 'DNA topoisomerase I inhibitors ameliorate seizure-like behaviors and paralysis in a Drosophila model of epilepsy', *Neuroscience*, 156(3), pp. 722–728.

Teschendorf, H.J. and Kretzschmar, R. (1985) 'Succinimides', in *Antiepileptic drugs*. Springer, pp. 557–574.

Tinker, R.J. *et al.* (2021) 'Haploinsufficiency of ATP6V0C possibly underlies 16p13.3 deletions that cause microcephaly, seizures, and neurodevelopmental disorder', *American Journal of Medical Genetics, Part A*, 185(1), pp. 196–202. Available at: <https://doi.org/10.1002/ajmg.a.61905>.

Uyhazi, K.E. *et al.* (2020) 'Pumilio proteins utilize distinct regulatory mechanisms to achieve complementary functions required for pluripotency and embryogenesis', *Proceedings of the National Academy of Sciences*, 117(14), pp. 7851–7862.

Vaz, F.M. *et al.* (2019) 'Mutations in PCYT2 disrupt etherlipid biosynthesis and cause a complex hereditary spastic paraplegia', *Brain*, 142(11), pp. 3382–3397.

Vessey, J.P. *et al.* (2010) 'Mammalian Pumilio 2 regulates dendrite morphogenesis and synaptic function', *Proceedings of the National Academy of Sciences*, 107(7), pp. 3222–3227.

Walrave, L. *et al.* (2015) 'Validation of the 6 Hz refractory seizure mouse model for intracerebroventricularly administered compounds', *Epilepsy research*, 115, pp. 67–72.

Walsh, S. *et al.* (2017) 'A systematic review of the risks factors associated with the onset and natural progression of epilepsy', *Neurotoxicology*, 61, pp. 64–77.

Wilcox, K.S., West, P.J. and Metcalf, C.S. (2020) 'The current approach of the Epilepsy Therapy Screening Program contract site for identifying improved therapies for the treatment of pharmacoresistant seizures in epilepsy', *Neuropharmacology*, 166, p. 107811.

Wu, X. *et al.* (2008) 'Histone deacetylase inhibitors up-regulate astrocyte GDNF and BDNF gene transcription and protect dopaminergic neurons', *International Journal of Neuropsychopharmacology*, 11(8), pp. 1123–1134. Available at: <https://doi.org/10.1017/S1461145708009024>.

Yaari, Y., Selzer, M.E. and Pincus, J.H. (1986) 'Phenytoin: mechanisms of its anticonvulsant action', *Annals of Neurology: Official Journal of the American Neurological Association and the Child Neurology Society*, 20(2), pp. 171–184.

Yount, G.L., Ponsalle, P. and White, J.D. (1994) 'Pentylentetrazole-induced seizures stimulate transcription of early and late response genes', *Molecular brain research*, 21(3–4), pp. 219–224.

Zhang, H.G. *et al.* (2002) 'The *Drosophila* slamdance gene: A mutation in an aminopeptidase can cause seizure, paralysis and neuronal failure', *Genetics*, 162(3), pp. 1283–1299. Available at: <https://doi.org/10.1093/genetics/162.3.1283>.

## 4.0 Chapter 4- Discussion

The main aims of this project were to develop a drug-like molecule with increased activity based on the structure of avobenzene and test it in a variety of models to show it has the potential to be an effective, wide acting AED. Avobenzene could not be considered a drug-like molecule due to its instability and tendency to break down into toxic by-products (Mturi and Martincigh, 2008). Early results suggested that one of its breakdown products, which possesses more drug-like properties, was equally as effective at reducing recovery times in *Drosophila* seizure mutants. Therefore, it was decided that RAB102 would be the structure the library was designed based upon. Screening and the application of SAR lead to the discovery of RAB 216, a compound that was found to be approximately 4x more potent than RAB 102 in the initial screen. Further testing suggested that RAB216 has the potential to be an effective and wide acting AED, as it reduced the severity or onset time in all the models it was tested in. Whilst evidence from experiments measuring gene expression, suggest the compound act though PUM, the exact mechanism of how RAB 216 works is unknown and requires further investigation.

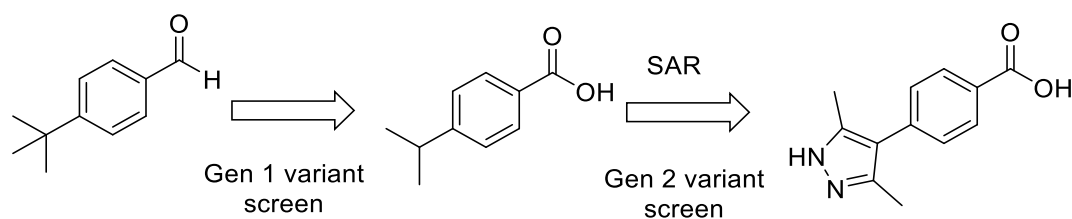


**Figure 4.1- Progression of lead compounds across the project. When it began, RAB102 had been identified as the active part of avobenzene, which has been shown to be active previously (Lin et al., 2015). The first generation of compound design was based on the structure of RAB102, using principles of design to create more drug-like compounds. The second generation used the same principles as well as the results of the first screen to create an SAR, with aim of increasing potency.**

The first generation of compound design was based on the structure of RAB102 and aimed to create a library that was more drug-like, whilst varying the structure in 1 way with each compound, in order to find changes that increase potency. The compound was split into 3 sections, the polar group, the central ring structure and the group *para* to the polar group. The first thing investigated was whether the aldehyde seen in RAB102 could be changed to a carboxylic acid. Due to their reactivity, aldehydes are generally undesirable groups to have in pharmaceuticals (Ahmed Laskar and Younus, 2019a). Furthermore, they are often rapidly metabolised to carboxylic acids in both *Drosophila* and mammals (Henehan, Chang and Oppenheimer, 1995; Srivastava *et al.*, 1999), so it is possible that the carboxylic acid is already the active metabolite of RAB102. Carboxylic acids do not have the same toxicity profile as aldehydes and are generally much less reactive, however they are rarely found in

CNS active drugs due to anionic state at physiological pH, which makes it difficult to cross the negatively charged BBB (Pardridge, 1998). There are examples of carboxylic acids that do cross the BBB, which usually occurs with the aid of a transporter such as MCTs (Vijay and Morris, 2014).

The generation 2 compounds were designed using the results from the first drug screen which suggested that any changes to the central ring structure or acid/aldehyde group, caused the compound to be inactive. Therefore, most of the design was focussed on the third portion of the molecule, the group *para* to the acid/aldehyde group. Results from the first drug screen found RAB 132 to be the most efficacious, but also suggested that larger groups and groups containing electronegative atoms could also be tolerated in this position. With this in mind, the generation 2 compounds had more variety in this position when compared to generation 1, including RAB216, which was found to be the most potent compound of all those tested. Although the drug does contain a carboxylic acid group, it was found to be active in every model of seizures in which it was tested. It is therefore likely the drug is able to cross the BBB, but more investigation would be required to ascertain, how it crosses and how much is able to penetrate into the brain.

Epilepsy is one of the most common neurological conditions, but despite this 30% of cases cannot be controlled with the current treatment options available. It has been stated that one of the reasons for this may be because current treatment options focus on downstream targets, which can increase the likelihood of drug resistance (Boison, Masino and Geiger, 2011). Electrophysiological recordings of hippocampal slices from pharmacoresistant epilepsy patients, revealed that carbamazepine no longer demonstrated use-dependent block of Na<sup>+</sup> channels (Jandová *et al.*, 2006). Changes in the pharmacodynamics of GABA<sub>A</sub> receptors have also been found in a rat model of drug resistant temporal lobe epilepsy, which resulted in a resistance to phenobarbital (Bethmann *et al.*, 2008). These findings are further supported by other studies, which linked changes in GABA<sub>A</sub> receptor composition to benzodiazepine resistance (Chen and Wasterlain, 2006).

In modern drug design the aim is generally to produce a compound that acts specifically, in order to reduce the likelihood of side effects. As well as target specificity, this also means selecting targets as far downstream as possible. By only targeting a specific signal transduction pathway, the likelihood of drug resistance is increased as these targets are prone to compensatory reactions that may contribute to pharmacoresistance (Boison, Masino and Geiger, 2011). Conversely, targeting a homeostatic regulator, like PUM allows a drug to effect entire networks on multiple different pathways. Both GABARs and Na<sub>v</sub>s are downstream targets of Pum and both possess individual mechanisms of pharmacoresistance (Sperk *et al.*, 2004; Kwan *et al.*, 2008), but if both are targeted at

the same time through an overarching homeostatic mechanism, the chance of pharmacoresistance is reduced.

Whilst there are currently no marketed drugs that directly target neuronal homeostasis, there are emerging areas of research that suggest it is a viable strategy for controlling epilepsy. One of these targets includes the neuronal adenosine system. Adenosine is a vital molecule in the life of any cell and contributes to genetic, redox and energy regulation (Cunha, 2019). Studies have found that controlled release of adenosine has potent antiseizure effects, with no overt side effects (Wilz *et al.*, 2008). Furthermore, there is evidence to suggest that adenosine is a key contributor to the anti-seizure effects observed with the ketogenic diet (Kawamura, Ruskin and Masino, 2010). Similar to targeting Pum, targeting adenosine aims to circumvent pharmacoresistance by making use of an endogenous agent and by providing upstream control of complex network regulation (Boison, Masino and Geiger, 2011). Despite an abundance of new epilepsy drugs released within the last 30 years, the rate of pharmacoresistance has changed very little. Whilst targeting endogenous agents further upstream does have the potential to lead to a higher number of side-effects, this method also has the potential to treat pharmacoresistant epilepsy by indirectly interacting with a multitude of the current targets, through control of the overarching network. However, when it comes to Pum specifically, there is the potential for side effects as both PUM1 and PUM2 are expressed widely and have been linked to the development of certain cancers (Silva, Kohata and Shigunov, 2022). Whilst we saw no safety issues with RAB216 in our studies, more research into the long-term exposure of the compound would be required.

Whilst evidence from the results presented in this thesis indicate that RAB 216 increases the concentration of Pum, little is known of how it achieves this. Results from the luciferase reporter assay in *Drosophila* suggested that the rate of Pum transcription wasn't increased by treatment with RAB216. However, it did prevent the increase seen in the PTX (a proconvulsant) control group and lower recover times in *Drosophila* raised on PTX, meaning it is likely the drug was exerting an anticonvulsant effect.

There is little research into what alters the concentration of Pum and therefore we can only speculate as to how RAB216 exerts its effect. However, one area that has been linked to Pum concentration is DNA damage. A cell culture study found that when human cells were exposed to DNA damaging agents, the levels of PUM1 and PUM2 decreased (Yamada *et al.*, 2020). In this study they found the level of PUM1/2 transcripts was also increased, yet results from this project's luciferase studies in *Drosophila*, suggest that the increase in Pum protein may be separate from transcription rates so. It is therefore likely the increase in Pum proteins seen in our studies, is

separate from the mechanism involved following DNA damage. A potential target that regulates Pum but doesn't affect transcription is Rbfox1 (Carreira-Rosario *et al.*, 2016). This protein has been shown to repress translation of *pum* mRNA in *Drosophila* (Carreira-Rosario *et al.*, 2016) and has been linked to epilepsy in numerous studies (Gehman *et al.*, 2011; Lal *et al.*, 2013). Interestingly, whilst *PUM1/2* is downregulated in models of intractable epilepsy (Wu *et al.*, 2015b), *RBFOX1* is upregulated (Wen *et al.*, 2015). Further studies would be required to know if these two were directly linked, but it is plausible that disrupting the interaction between Rbfox1 and *PUM1/2* RNA, could increase concentration of Pum proteins.

In order for neurons to homeostatically alter their activity, they require a way of monitoring their firing rate. Work from the Baines lab has identified the histone acetyltransferase P300 (referred to as Nej in *Drosophila*) as protein involved in reacting to changes in neuron activity, which also interacts with Pum (Lin and Baines, 2019). P300 forms a complex with Mef2, but in *Drosophila* as synaptic polarisation increases, levels of P300 are reduced, releasing Mef2. Once released, Mef2 transactivates *pum* gene transcription by binding the *pum* promoter. In mammals however, MEF2 expression is instead directly related to neuronal activity, increasing with depolarisation (Flavell *et al.*, 2006). Analysis of human and mouse *PUM2* promoters shows they contain multiple MEF2 binding-motifs (Lin and Baines, 2019). In mammals, whilst P300 (known as EP300 in mammals) is also reported to regulate MEF2, how this protein reacts to changes in synaptic depolarisation has not been described. Additionally, in mammals MEF2 is also known to increase expression microRNAs, including mir-134, which has been found to downregulate expression of *PUM2* (Fiore *et al.*, 2014) and blocking mir-134 with an antagomir is anticonvulsant in rodents (Reschke *et al.*, 2017). The regulatory mechanisms involved in Pum related neuronal homeostasis are complex and it is conceivable that RAB216 acts at any point along one of these pathways. With better understanding of Pum and function and that of its upstream regulators, there is the potential to create a new target for controlling seizures by altering the neuron's intrinsic homeostatic mechanisms. Identification of the binding site for these compounds would also aid in creating more potent analogues through the development of ligand binding assays.

The next stages of this project would be to elucidate how RAB 216 increases Pum levels, identify the binding target and produce more potent analogues based on the structure of the binding pocket. Currently, there are no known compounds that affect the expression or activity of Pum proteins. In order to find evidence of how this may work with RAB 216, an experiment using Isobaric tags for relative and absolute quantitation (iTRAQ) was originally planned, but not performed due to time constraints. iTRAQ is a technique that uses isotopic labelling and mass spectrometry to determine the amount of protein from various sources in a single experiment (Zieske 2006). It was planned to

use this technique to analyse the proteome of rodent brains that had been exposed to RAB 216 and others that had their Pum levels increased through genetic methods. By comparing the changes in the proteome between these 2 groups it may be possible to identify proteins upstream of the Pum neuronal homeostasis pathway, that are differently expressed between the 2 groups. This could narrow the search for the potential binding target of RAB 216 that eventually leads to increased levels of Pum proteins. Once the potential number of binding targets has been narrowed, there are various techniques available that could help to identify it, including *in silico* methods, knockdown experiments and drug affinity responsive target stability (DARTS) (Lomenick et al. 2009). With a binding target identified, *in vitro* assays could be designed to screen compounds that are both higher throughput and more precise. Furthermore, computational chemistry methods could aid the design of compounds, through modelling the shape of the binding pocket and any potential interactions.

Overall, this study has demonstrated the first proof that targeting neuronal homeostasis provides a possible route to suppressing seizures and has the potential to be a suitable treatment for treating patients that do not respond to current medication. 30% of epilepsy cases are drug refractory and the discovery of new druggable targets is required to reduce this number. Through the screening of 2 different generations of compounds based on the structure of the initial lead RAB102, RAB216 was discovered and found to be approximately 4x more potent in the *Drosophila* model and significantly more effective in both the PTZ and 6 Hz models of seizures in mice. Whilst there are potential concerns with the long-term safety of targeting Pum and much work to be done before compounds could enter clinical trials, the identification of a potentially druggable neuronal homeostatic pathway offers an interesting route of developing treatments to control epilepsy through a completely novel target.

## 4.1 Bibliography

- Ahmed Laskar, Amaj, and Hina Younus. 2019. "Aldehyde Toxicity and Metabolism: The Role of Aldehyde Dehydrogenases in Detoxification, Drug Resistance and Carcinogenesis." *Drug Metabolism Reviews* 51 (1): 42–64.
- Bethmann, Kerstin, Jean-Marc Fritschy, Claudia Brandt, and Wolfgang Löscher. 2008. "Antiepileptic Drug Resistant Rats Differ from Drug Responsive Rats in GABAA Receptor Subunit Expression in a Model of Temporal Lobe Epilepsy." *Neurobiology of Disease* 31 (2): 169–87.
- Boison, Detlev, Susan A Masino, and Jonathan D Geiger. 2011. "Homeostatic Bioenergetic Network Regulation: A Novel Concept to Avoid Pharmacoresistance in Epilepsy." *Expert Opinion on Drug Discovery* 6 (7): 713–24.

- Carreira-Rosario, Arnaldo, Varsha Bhargava, Jens Hillebrand, Rahul K. Kollipara, Mani Ramaswami, and Michael Buszczak. 2016. "Repression of Pumilio Protein Expression by Rbfox1 Promotes Germ Cell Differentiation." *Developmental Cell* 36 (5): 562–71. <https://doi.org/https://doi.org/10.1016/j.devcel.2016.02.010>.
- Chen, James W.Y., and Claude G. Wasterlain. 2006. "Status Epilepticus: Pathophysiology and Management in Adults." *Lancet Neurology* 5 (3): 246–56. [https://doi.org/10.1016/S1474-4422\(06\)70374-X](https://doi.org/10.1016/S1474-4422(06)70374-X).
- Cunha, Rodrigo A. 2019. "Signaling by Adenosine Receptors—Homeostatic or Allostatic Control?" *PLoS Biology* 17 (4): e3000213.
- Fiore, Roberto, Marek Rajman, Chrysovalandis Schwale, Silvia Bicker, Anna Antoniou, Claus Bruehl, Andreas Draguhn, and Gerhard Schratt. 2014. "MiR-134-dependent Regulation of Pumilio-2 Is Necessary for Homeostatic Synaptic Depression." *The EMBO Journal* 33 (19): 2231 LP – 2246.
- Flavell, Steven W, Christopher W Cowan, Tae-Kyung Kim, Paul L Greer, Yingxi Lin, Suzanne Paradis, Eric C Griffith, Linda S Hu, Chinfei Chen, and Michael E Greenberg. 2006. "Activity-Dependent Regulation of MEF2 Transcription Factors Suppresses Excitatory Synapse Number." *Science* 311 (5763): 1008–12. <https://doi.org/10.1126/science.1122511>.
- Gehman, Lauren T, Peter Stoilov, Jamie Maguire, Andrey Damianov, Chia-Ho Lin, Lily Shiue, Manuel Ares, Istvan Mody, and Douglas L Black. 2011. "The Splicing Regulator Rbfox1 (A2BP1) Controls Neuronal Excitation in the Mammalian Brain." *Nature Genetics* 43 (7): 706–11.
- Henehan, Gary T M, Simon H Chang, and Norman J Oppenheimer. 1995. "Aldehyde Dehydrogenase Activity of Drosophila Melanogaster Alcohol Dehydrogenase: Burst Kinetics at High PH and Aldehyde Dismutase Activity at Physiological PH." *Biochemistry* 34 (38): 12294–301.
- Jandová, Katerina, Dennis Päsler, Leandro Leite Antonio, Claudia Raue, Shengbo Ji, Marleisje Njunting, Oliver Kann, et al. 2006. "Carbamazepine-Resistance in the Epileptic Dentate Gyrus of Human Hippocampal Slices." *Brain* 129 (12): 3290–3306. <https://doi.org/10.1093/brain/awl218>.
- Kawamura, Masahito, David N Ruskin, and Susan A Masino. 2010. "Metabolic Autocrine Regulation of Neurons Involves Cooperation among Pannexin Hemichannels, Adenosine Receptors, and KATP Channels." *Journal of Neuroscience* 30 (11): 3886–95.
- Kwan, Patrick, Wai Sang Poon, Ho-Keung Ng, David E Kang, Virginia Wong, Ping Wing Ng, Colin H T Lui, Ngai Chuen Sin, Ka S Wong, and Larry Baum. 2008. "Multidrug Resistance in Epilepsy and Polymorphisms in the Voltage-Gated Sodium Channel Genes SCN1A, SCN2A, and SCN3A: Correlation among Phenotype, Genotype, and MRNA Expression." *Pharmacogenetics and Genomics* 18 (11): 989–98.
- Lal, Dennis, Eva M Reinthaler, Janine Altmüller, Mohammad R Toliat, Holger Thiele, Peter Nürnberg, Holger Lerche, Andreas Hahn, Rikke S Møller, and Hiltrud Muhle. 2013. "RBFox1 and RBFox3 Mutations in Rolandic Epilepsy." *PloS One* 8 (9): e73323.
- Lin, Wei-Hsiang, and Richard A Baines. 2019. "Myocyte Enhancer Factor-2 and P300 Interact to Regulate the Expression of Homeostatic Regulator Pumilio in Drosophila." *European Journal of Neuroscience* 50 (1): 1727–40. <https://doi.org/https://doi.org/10.1111/ejn.14357>.
- Lin, Wei-Hsiang, Miaomiao He, and Richard A. Baines. 2015. "Seizure Suppression through Manipulating Splicing of a Voltage-Gated Sodium Channel." *Brain* 138 (4): 891–901. <https://doi.org/10.1093/brain/awv012>.

- Lomenick, Brett, Rui Hao, Nao Jonai, Randall M Chin, Mariam Aghajan, Sarah Warburton, Jianing Wang, Raymond P Wu, Fernando Gomez, and Joseph A Loo. 2009. "Target Identification Using Drug Affinity Responsive Target Stability (DARTS)." *Proceedings of the National Academy of Sciences* 106 (51): 21984–89.
- Mturi, Georges J., and Bice S. Martincigh. 2008. "Photostability of the Sunscreening Agent 4-Tert-Butyl-4'-Methoxydibenzoylmethane (Avobenzone) in Solvents of Different Polarity and Proticity." *Journal of Photochemistry and Photobiology A: Chemistry* 200 (2–3): 410–20.  
<https://doi.org/10.1016/J.JPHOTOCHEM.2008.09.007>.
- Pardridge, William M. 1998. "CNS Drug Design Based on Principles of Blood-Brain Barrier Transport." *Journal of Neurochemistry* 70 (5): 1781–92. <https://doi.org/https://doi.org/10.1046/j.1471-4159.1998.70051781.x>.
- Reschke, Cristina R, Luiz F Almeida Silva, Braxton A Norwood, Ketharini Senthilkumar, Gareth Morris, Amaya Sanz-Rodriguez, Ronán M Conroy, et al. 2017. "Potent Anti-Seizure Effects of Locked Nucleic Acid Antagomirs Targeting MiR-134 in Multiple Mouse and Rat Models of Epilepsy." *Molecular Therapy - Nucleic Acids* 6: 45–56. <https://doi.org/https://doi.org/10.1016/j.omtn.2016.11.002>.
- Silva, Isabelle Leticia Zaboroski, Arissa Andreina Kohata, and Patrícia Shigunov. 2022. "Modulation and Function of Pumilio Proteins in Cancer." *Seminars in Cancer Biology* 86: 298–309.  
<https://doi.org/https://doi.org/10.1016/j.semcancer.2022.03.010>.
- Sperk, Günther, Sabine Furtinger, Christoph Schwarzer, and Susanne Pirker. 2004. "GABA and Its Receptors in Epilepsy." *Recent Advances in Epilepsy Research*, 92–103.
- Srivastava, Sanjay, Stanley J Watowich, J Mark Petrash, Satish K Srivastava, and Aruni Bhatnagar. 1999. "Structural and Kinetic Determinants of Aldehyde Reduction by Aldose Reductase." *Biochemistry* 38 (1): 42–54.
- Vijay, Nisha, and Marilyn E Morris. 2014. "Role of Monocarboxylate Transporters in Drug Delivery to the Brain." *Current Pharmaceutical Design* 20 (10): 1487–98.
- Wen, Ming, Yong Yan, Ning Yan, Xiao Shan Chen, Shi Yong Liu, and Zhan Hui Feng. 2015. "Upregulation of RBFOX1 in the Malformed Cortex of Patients with Intractable Epilepsy and in Cultured Rat Neurons." *International Journal of Molecular Medicine* 35 (3): 597–606.
- Wilz, Andrew, Eleanor M Pritchard, Tianfu Li, Jing-Quan Lan, David L Kaplan, and Detlev Boison. 2008. "Silk Polymer-Based Adenosine Release: Therapeutic Potential for Epilepsy." *Biomaterials* 29 (26): 3609–16.
- Wu, Xu-Ling, Hao Huang, Yun-Yi Huang, Jin-Xian Yuan, Xin Zhou, and Yang-Mei Chen. 2015. "Reduced Pumilio-2 Expression in Patients with Temporal Lobe Epilepsy and in the Lithium–Pilocarpine Induced Epilepsy Rat Model." *Epilepsy & Behavior* 50: 31–39.  
<https://doi.org/https://doi.org/10.1016/j.yebeh.2015.05.017>.
- Yamada, Toshimichi, Naoto Imamachi, Katsutoshi Imamura, Kenzui Taniue, Takeshi Kawamura, Yutaka Suzuki, Masami Nagahama, and Nobuyoshi Akimitsu. 2020. "Systematic Analysis of Targets of Pumilio-Mediated mRNA Decay Reveals That PUM1 Repression by DNA Damage Activates Translesion Synthesis." *Cell Reports* 31 (5): 107542.  
<https://doi.org/https://doi.org/10.1016/j.celrep.2020.107542>.

Zieske, Lynn R. 2006. "A Perspective on the Use of ITRAQ™ Reagent Technology for Protein Complex and Profiling Studies." *Journal of Experimental Botany* 57 (7): 1501–8.